# List of ABSTRACTS

## Section I - Trends in Remote Sensing applications

| | |
|---|---|
| Markéta Potůčková, Jana Albrechtová, Katharina Anders, Lucie Červená, Jakub Dvořák, Krzysztof Gryguc, Bernhard Höfle, Lucie Kupková, Zuzana Lhotáková, Adriana Marcinkowska-Ochtyra, Andreas Mayr, Eva Neuwirthová, Adrian Ochtyra, Martin Rutzinger, Alex Šrollerů | E-LEARNING ON TIME SERIES ANALYSIS IN REMOTE SENSING: THE WAY TOWARDS COLLABORATIVE COURSE DEVELOPMENT |
| Roman Johannis Hiby, Claudia Lindner, Fabian Meyer-Heß, Andreas Rienow | MOON AND REMOTE SENSING IN EDUCATION – A CONCEPT FOR IMPLEMENTING REMOTELY-SENSED LUNAR TOPICS INTO THE SCHOOL CURRICULUM |
| Jochem Verrelst, David Kovács, Pablo Reyes-Muñoz, Matias Salinero-Delgado, Viktor Ixio Mészáros, Katja Berger | GLOBAL CLOUD-FREE MAPS OF ESSENTIAL VEGETATION TRAITS PROCESSED FROM THE TOA SENTINEL-3 OLCI CATALOGUE IN GOOGLE EARTH ENGINE |
| Katja Berger, Lammert Kooistra, Lukas Valentin Graf, Benjamin Brede, Clement Atzberger, Pablo Reyes Munoz, Jochem Verrelst | A REVIEW OF REMOTE SENSING TIME SERIES ANALYSIS FOR VEGETATION PRODUCTIVITY MONITORING |
| Cozmin Lucau Danila, Yann Chemin, Yannick Curnel, Julien Morel, Mattia Rossi, Viviane Planchon | BENCHMARKING OF GRASSLAND DYNAMIC MODELS COUPLED WITH SENTINEL-2 TO MONITOR GRASSLANDS GROWTH OVER WALLONIA REGION (BELGIUM) |

## Section II - Earth Observation applied in forest hazards management

| | |
|---|---|
| Andreas Müterthies, Sebastian Mader, Nils Wolf | MONITORING OF DROUGHT-INDUCED FOREST DAMAGES IN GERMANY |
| Chunyan Xu, Michael Förster, Birgit Kleinschmit | MODELLING VITALITY LOSS OF EUROPEAN BEECH (FAGUS SYLVATICA L.) USING RANDOM FOREST REGRESSION |
| Debora Voltolina, Daniela Stroppiana, Simone Sterlacchini, Matteo Sali, Bachisio Arca, Mariano García, Michele Salis, Emilio Chuvieco | IMPLEMENTATION OF A FUEL TYPE CLASSIFICATION SYSTEM FOR SARDINIA, ITALY, WITH THE INTEGRATION OF REMOTELY SENSED DATA |
| Daniela Stroppiana, Lorenzo Parigi, Giulio Tellina, Claudia Giardino, Monica Pinardi, Rossana Caroni, Mariano Bresciani | THE IMPACT OF WILDFIRES ON WATER QUALITY USING CCI EO PRODUCTS: LAKE BAIKAL CASE STUDY |

## Section III - Remote sensing applications for environment

| | |
|---|---|
| Mahmoud Saber Kenawi, Tor Haakon Bakken | QUANTIFICATION OF NET CARBON STOCK CHANGE DUE TO THE NORWEGIAN RESERVOIRS DEVELOPMENT |
| Stefanie Steinbach, Anna Bartels, Martin W. Chege, Niels Dedring, Wisdom Kipkemboi, Simon W. Muthee, Andrew Nelson, Kuria B. Thiong'o, Sander J. Zwart, Andreas Rienow | INTEGRATING LOW-COST SENSORS AND REMOTE SENSING TO MONITOR SMALL RESERVOIRS IN KENYAN WETLANDS |
| Andrei Toma, Ionut Sandric | MONITORING MINING OPERATIONS IN THE ROVINARI AREA USING RADAR INTERFEROMETRY |
| Maxim Shoshany, Sofia Mozhaeva | CLIMATE VERSUS VEGETATION INDICES REGRESSION MODELS CLASSIFICATION ACROSS DESERT-FRINGE ECOSYSTEM |
| Alex Šrollerů, Eva Štefanová, Markéta Potůčková | MULTISOURCE POINT CLOUD FUSION FOR FOREST AND POST-FIRE POREST MAPPING: CASE STUDY FROM THE BOHEMIAN SWITZERLAND NATIONAL PARK |

## Section IV - Land cover mapping and monitoring for supporting decisions in agriculture

| | |
|---|---|
| Hugo do Nascimento Bendini, Leila Maria Garcia Fonseca, Luiz Mario Lustosa Pascoal, Philippe Rufin, Caio Augusto Bertolini, Tharles de Sousa Andrade, Ravi Fernandes Mariano, Renato Gomes Silvério, Pedro Lacerda Santos, Daniel Assumpção Costa Ferreira, Thiago Henriques Fontenelle | METHODOLOGICAL PROPOSAL FOR OPERATIONAL MONITORING OF AGRICULTURAL DYNAMICS IN CENTER PIVOTS IRRIGATION AREAS IN BRAZIL USING SENTINEL 2 IMAGERY |
| Ursula Gessner, Sarah Asam, Andreas Hirner, Jennifer Kriese, Jonas Meier, Sophie Reinermann, Martina Wenzl | PRODUCTS FOR MONITORING OF AGRICULTURE FROM EARTH OBSERVATION TIME SERIES AND VERY HIGH RESOLUTION DATA |
| Stelios Neophytides, Thanasis Drivas, Christiana Papoutsa, Charalambos Kontoes, Diofantos Hadjimitsis | THE DATA CUBE OF ERATOSTHENES CENTRE OF EXCELLENCE TO EMPOWER ENVIRONMENTAL MONITORING IN EMMENA REGION |
| Stefanie Steinhauser, Matthias Wocher, Andrej Halabuk , Svetlana Košánová , Tobias Hank | QUANTIFICATION AND MAPPING OF NON-PHOTOSYNTHETIC CROPLAND BIOMASS USING LABORATORY HYPERSPECTRAL DATA AND MACHINE LEARNING |

## Section V - Monitoring and mapping multi-hazards under climate change

| | |
|---|---|
| Tuyen Ha Van, Juliane Huth, Soner Uereyen, Claudia Kuenzer | SPATIOTEMPORAL CHARACTERISTICS OF DROUGHT AND THEIR IMPACTS ON CROPLAND VEGETATION OVER THE LOWER MEKONG BASIN USING SATELLITE-BASED TIME-SERIES OBSERVATIONS |
| Marina Vîrghileanu, Bogdan-Andrei Mihai, Ionuț Săvulescu | MAPPING SOIL EROSION INTENSITY BASED ON MULTITEMPORAL SENTINEL-1 SAR AND SENTINEL-2 MSI SATELLITE IMAGERY. AN INTER-COMPARISON APPROACH USING IN-SITU MEASUREMENTS |
| Niels Dedring, Valerie Graw, Andreas Rienow | HEC-RAS SIMULATION OF A GLACIAL LAKE OUTBURST FLOOD TO DETERMINE POTENTIAL IMPACTS USING THE EXAMPLE OF CHAMLANG NORTH TSHO (LAKE 464) IN THE HONGU VALLEY, NEPAL |
| Valerie Graw, Torben Dedring, Roman Hiby, Jose Jara-Alvear, Pablo Guzman, Carsten Juergens, Andreas Rienow | EVALUATION OF SENTINEL-1-BASED CHANGE DETECTION APPROACHES FOR REGRESSIVE EROSION ALONG THE COCA RIVER, ECUADOR |
| Gurcan Buyuksalih, Cem Gazioglu, Karsten Jacobsen | POTENTIAL OF PLANET'S SKYSAT COLLECT IMAGES FOR TOPOGRAPHIC MAPPING |

## Section VI - New methods and algorithms in EO for agriculture

| | |
|---|---|
| Chenglong Zhang, Joao Valente, Wensheng Wang, Leifeng Guo, Lammert Kooistra | APPLE FRUIT LOAD ESTIMATION IN MULTI-TEMPORAL HIGHRESOLUTION UAV IMAGERY BY DEEP LEARNING |
| Spyridon E. Detsikas, George P. Petropoulos, Rahul Raj | LEVERAGING PIXXEL'S HYPERSPECTRAL IMAGERY FOR LAND USE AND LAND COVER MAPPING IN AN AGRICULTURAL REGION OF NORTHEAST AUSTRALIA |
| Marcel Schwieder, Felix Lobert, Arnab Muhuri, Natascha Oppelt, Sarah Asam, Sophie Reinermann, Julien Morel, Mattia Rossi, Dominique Weber, Filippo Sarvia, Samuele De Petris, Enrico Borgogno-Mondino, Oliver Buck, Stefan Ernst, Patrick Hostert, Silvia Valero, Anatol Garioud, Ann-Kathrin Holtgrave, Clément Mallet, Mathilde De Vroey, | MOWING DETECTION INTERCOMPARISON EXERCISE (MODCIX): A CROSS-EUROPEAN EVALUATION OF MOWING DETECTION ALGORITHMS |

| | |
|---|---|
| Andreas Schaumberger, Iason Tsardanidis, Ruth Sonnenschein, Stefan Erasmi | |
| Stefan Popa, George Feldioreanu, Kamal Marandskiy, Mihai Ivanovici | CONVOLUTIONAL NEURAL NETWORK HARDWARE IMPLEMENTATION FOR SOIL ROUGHNESS ESTIMATION |
| Paolo Dal Lago, Nikos Vavlas, Lammert Kooistra, Gerlinde De Deyn | QUANTIFICATION OF NITROGEN UPTAKE IN COVER CROPS FROM UAVBASED MULTISPECTRAL IMAGES |

## Section VII - Remote sensing solutions for a sustainable forest management

| | |
|---|---|
| Marcin Kluczek, Bogdan Zagajewski, Tomasz Zwijacz-Kozica | SENTINEL-2, PLANETSCOPE 2 AND AIRBORNE HYSPEX HYPERSPECTRAL IMAGERY FOR MOUNTAIN WOODY SPECIES MAPPING |
| Karimon Nesha, Martin Herold, Veronique De Sy, Sytze De Bruin, Arnan Araza, Natalia Málaga, Javier GP Gamarra, Kristell Hergoualc'h, Anssi Pekkarinen, Carla Ramirez, David MoralesHidalgo, Rebecca Tavani | EXPLORING CHARACTERISTICS OF NATIONAL FOREST INVENTORIES FOR INTEGRATION WITH GLOBAL SPACE-BASED FOREST BIOMASS DATA |
| Mirela Beloiu, Nataliia Rehush, Verena Griess, Stefan Erasmi | AUTOMATIC DETECTION OF TREE SPECIES IN HETEROGENEOUS FORESTS USING RGB IMAGERY AND DEEP LEARNING |
| Constantin-Cosmin Loghin, Flaviu Popescu, Florin Achim, Ionel Ban, Mihai Furdui, Robert-Ştefan Ciobanu, Razvan Raducu, Virgil Zamfira, Aurelian Vladoiu | IDENTIFICATION, MAPPING AND ASSESSMENT OF WINDTHROW EFFECTS USING REMOTE SENSING METHODS |

## Section VIII - Risk detection and management in agriculture - climate

| | |
|---|---|
| Stelios Neophytides, Marinos Eliades, Georgios Papadavid, Christiana Papoutsa, Diofantos Hadjimitsis | A WEB TOOL FOR IRRIGATION MANAGEMENT TO SUPPORT LOCAL AUTHORITIES AND FARMERS IN CYPRUS FROM ERATOSTHENES CENTRE OF EXCELLENCE |
| Tomáš Rusňák | AGRICULTURAL DROUGHT MONITORING IN THE DANUBIAN LOWLAND USING VEGETATIONS INDICES DERIVED FROM MODIS TIME SERIES |
| Mohana Priya Logakrishnan, Jesko Zimmermann, Stuart Green | EVALUATING SENTINEL-1'S ABILITY TO IDENTIFY BARE SOIL ON TILLAGE PARCELS IN WINTER IN THE REPUBLIC OF IRELAND USING RANDOM FOREST MODEL |
| Quanxing Wan, Magdalena Smigaj, Benjamin Brede, Lammert Kooistra | FROM THE LAB TO THE FARM: QUANTIFYING FACTORS INFLUENCING TEMPERATURE MEASUREMENTS FROM MINIATURIZED THERMAL CAMERAS TO BENEFIT CROP WATER STRESS DETECTION AT DIFFERENT CROP GROWTH STAGES |
| Enrico Chiesa, Samuele De Petris, Alessandro Farbo, Filippo Sarvia, Enrico Borgogno-Mondino | COMPARING MULTISPECTRAL RPAS AND SATELLITE DATA FOR RICE CROP MULTITEMPORAL CHARACTERISATION |

## Section IX - Recent Earth Observation technology applications in natural hazards research

| | |
|---|---|
| Ales Létal, Ionuţ Şandric, Jan Klimes | AUTOMATIC MAPPING OF LANDSLIDES BY DEEP LEARNING AND HIGH-RESOLUTION LIDAR PRODUCTS |
| Claudiu-Valeriu Angearu, Anişoara Irimescu, Denis Mihăilescu, Irina Onțel, Argentina Nerțan, Vasile Crăciunescu | SATELLITE ANALYSIS OF THE IMPACT OF SEVERE METEOROLOGICAL PHENOMENA ON THE VULNERABLE SANDY LANDS OF THE BARAGAN PLAIN |

| | |
|---|---|
| Ionut Sandric, Viorel Ilinca, Zenaida Chitu, Radu Irimia | MAPPING ACTIVE SLOW-MOVING LANDSLIDES USING PERSISTENT SCATTERS INTERFEROMETRY IN ROMANIA |
| Mohammad Amin Khalili, Luigi Guerriero, Domenico Calcaterra, Diego Di Martire | ENHANCING LANDSLIDE DEFORMATION PREDICTION IN SOUTHERN ITALY USING A CNN-LSTM ALGORITHM WITH SPATIO-TEMPORAL DEPENDENCY |
| Martin W. Chege, Angeline Asangire Oprong | DESERTIFICATION MITIGATION POLICIES IN THE FACE OF CLIMATE CHANGE IN KENYA: EXPLORING THE POTENTIAL OF REMOTE SENSING FOR SUPPORTING STAKEHOLDER INVOLVEMENT |

## Section X - Risk detection and management in agriculture - pests and weeds

| | |
|---|---|
| Magdalena Smigaj, Harm Bartholomeus, Lammert Kooistra | LEVERAGING MULTIMODALITY FOR DISEASE DETECTION IN SEED POTATOES |
| Diana Petre, Ionuț Șandric, Diana Vizitiu, Ionela Sărdărescu, Marian Dârdală, Cristian Ioniță | MAPPING VINEYARDS PATHOGENS USING CONVOLUTIONAL NEURAL NETWORKS |
| Karolina Barbara Zdunek, Marcin Kluczek, Bogdan Zagajewski | SENTINEL-2 AND PLANETSCOPE DATA FOR ALIEN INVASIVE SPECIES OF GOLDENROD (SOLIDAGO SPP.) MAPPING |
| Coraline Wyard, Florian Bueno, Benjamin Beaumont, Yasmina Loozen, Eric Hallot | SPATIALIZATION OF JAPANESE KNOTWEED COLONIES: FROM LOCAL DRONE SCALE TO REGIONAL AIRBORNE APPLICATION |
| Luka Mamic, Francesco Pirotti | ASSESSING THE IMPACT OF OZONE ON CROP HEALTH AND PRODUCTIVITY USING OPEN-SOURCE REMOTE SENSING DATA AND MACHINE LEARNING |

## Section XI - Land use and land cover - remote sensing

| | |
|---|---|
| Marcin Kluczek, Bogdan Zagajewski, Edwin Raczko, Marlena Kycko, Anca Dabija, Ahmed H. Al-Sulttani, Anna Tardà, Lydia Pineda, Jordi Corbera | COMPARISON OF MACHINE LEARNING ALGORITHMS FOR LAND COVER MAPPING ACCORDING TO CORINE LAND COVER NOMENCLATURE |
| Adam Waśniewski, Agata Hościło, Linda Aune-Lundberg | CAN WE IMPROVE THE ACCURACY OF THE LAND COVER CLASSIFICATION BY PRE-SELECTION OF THE REFERENCE SAMPLES AND APPLYING DEM IN THE MOUNTAIN AREA IN NORWAY? |
| Tomáš Bouček, Martin Landa, Lukáš Brodský, Lena Halounová, Ondřej Pešek | ST_LUCAS: EASY ACCESS SYSTEM FOR HARMONIZED LUCAS DATASET |
| Jan-Philipp Langenkamp, Andreas Rienow | EXPLORING THE USE OF ORTHOPHOTOS IN GOOGLE EARTH ENGINE FOR HIGH-RESOLUTION MAPPING OF IMPERVIOUS SURFACES: A DATA FUSION APPROACH IN WUPPERTAL, GERMANY |
| Andreas Rienow | REGIONAL MODELING OF FUTURE URBAN GROWTH BASED ON GLOBAL SETTLEMENT PRODUCTS – COMPARING THE PERFORMANCES OF OSM WITH THE GLOBAL HUMAN SETTLEMENT LAYER AND THE WORLD SETTLEMENT FOOTPRINT |

## Section XII - Urban climate and green infrastructure applications with remote sensing

| | |
|---|---|
| Stefanos Georganos, Sabine Vanhuysse, Angela Abascal, Jon Wang, Monika Kuffer | INVESTIGATING EXTREME TEMPERATURE VARIABILITIES IN DEPRIVED URBAN AREAS IN SUB-SAHARAN AFRICAN CITIES |
| Sunhui Sim | COMPARATIVE STUDY OF URBAN HEAT AND ITS VULNERABILITY IN NASHVILLE AND PORTLAND, USA |
| Irada Ismayilova, Sabine Timpf | SEMANTIC IDENTIFICATION OF URBAN GREEN SPACES: URBAN GARDENS |
| Ana-Maria Popa, Diana-Andreea Onose, Ionut-Cosmin Sandic, Evangelos Dosiadis , George Petropoulos, Athanasios-Alexandru Gavrilidis, Antigoni Faka | USING GEOBIA AND VEGETATION INDICES TO ASSESS SMALL URBAN GREEN AREAS IN TWO CLIMATIC REGIONS |
| Marian Puie, Bogdan-Andrei Mihai, Ionuț Șandric | MONITORING URBAN TRAFFIC IMPACT IN URBAN ENVIRONMENTS USING YOLO7 |

## Section XIII - Hyperspectral and multispectral applications of remote sensing

| | |
|---|---|
| Gabriela Ifimov, Raymond Soffer, Raphaël Mabit, Simon Belanger | ASSESSMENT OF THE NOVEL WATERSAT IMAGING SPECTROMETER ENHANCED (WISE) SENSOR FOR THE MAPPING OF OPTICALLY SHALLOW INLAND AND COASTAL WATERS |
| Agnieszka Soszynska, Thomas Groen, Harald van der Werff | DETECTION OF GEOTHERMAL ANOMALIES USING PRE-DAWN THERMAL REMOTE SENSING DATA FROM ECOSTRESS SENSOR |
| Bringfried Pflug, Jérôme Louis, Avi Putri Pertiwi, Raquel de los Reyes, Francesco C. Pignatale, Silvia Enache, Rosario Quirino Iannone, Valentina Boccia, Ferran Gascon | INITIAL VALIDATION OF SENTINEL-2 COLLECTION-1 L2A-PRODUCTS |
| Juan Manuel Sánchez, Joan Miquel Galve, Alejandro Martín SimónSánchez, José González-Piqueras, Ramón López-Urrea | MONITORING HIGH-RESOLUTION LST IN WOODY CROPS FROM THE SYNERGY OF SENTINEL-2 AND SENTINEL-3 |
| Elias Symeonakis, Christina Karakizi, Eva Arnau, Antonis Korkofigkas | ASSESSMENT OF FRACTIONAL WOODY VEGETATION COVER CHANGE IN AN AFRICAN SAVANNAH REGION |

## Section XIV - Using UAS for natural hazards and environmental studies

| | |
|---|---|
| Karsten Jacobsen | SELF-CALIBRATION STILL AN UNDERESTIMATED TOOL |
| Sarah Pflüger, Mario Blersch, Maike Petersen, Alexander Siegmund | GEO-MONITORING OF TREE SPECIES, VITALITY AND MAINTENANCE CONDITION OF FRUIT TREES IN MEADOW ORCHARDS USING UAV TECHNOLOGY |
| Razvan Mateescu, Liliana Rusu, Elena Vlasceanu, Dragos Niculescu | THE SUPPORT OF THE UAV IMAGERY IN COMPLEMENTARITY OF THE SATELLITE HIGH RESOLUTION REMOTE SENSING IMAGERY FOR THE ROMANIAN SHORE MONITORING |
| Alexandru-Bogdan Cucu, Gheorghe Raul Radu, Ştefan Petrea, Tibor Şerban | THE RELATION BETWEEN TREE ABOVE-GROUND BIOMASS AND CROWN HEIGHT MODEL USING A HIGH-RESOLUTION CAMERA ON UAV: A CASE STUDY IN SESSILE OAK STAND |
| Adrian Lorent, Marius Petrila, Bogdan Apostol, Florinel Capalb, Cristiana Marcu, Ovidiu Badea | IDENTIFICATION OF THE DRIVING FACTORS FOR THE OCCURRENCE OF FOREST FIRES AND THE ZONING OF FOREST FIRE HAZARD THROUGH LOGISTIC REGRESSION AND RANDOM FOREST IN ROMANIA FIRE HAZARD THROUGH LOGISTIC REGRESSION AND RANDOM FOREST IN ROMANIA |

## POSTERS:POSTERS:

## Crop dynamics monitoring using earth observation

| | |
|---|---|
| Hugo do Nascimento Bendini, Rémy Fieuzal, Pierre Carrere, Aubin Allies, Aurélie Galvani, Éric Ceschia | EXPLORING SENTINEL-2 DENSE IMAGE TIME SERIES TO IDENTIFY COVER CROP EMERGENCE AND DESTRUCTION DATES IN FRANCE: TOWARDS THE DEVELOPMENT OF AN APPROACH FOR BIOMASS ESTIMATION |
| Felix Lobert, Johannes Löw, Marcel Schwieder, Alexander Gocht, Michael Schlund, Patrick Hostert, Stefan Erasmi | DERIVING WINTER WHEAT PHENOLOGY FROM COMBINED OPTICAL AND SAR TIME SERIES WITH DEEP LEARNING |
| Karlmarx Thangamani, Tanja Riedel, Jennifer McLelland, Markus Moeller, Heike Gerighausen | DERIVATION OF CROP PARAMETERS USING SENTINEL-1 SAR DATA: A CASE STUDY FOR WINTER WHEAT IN NORTHERN GERMANY |
| Alejandro Martín Simón-Sánchez, José González-Piqueras, Luis de la Ossa, Juan Manuel Sánchez | MONITORING IRRIGATED AREAS BY APPLYING CONVOLUTIONAL NEURAL NETWORKS TO SENTINEL-2 AND METEOROLOGICAL TIME SERIES |

## Trends in Remote Sensing applications

| | |
|---|---|
| Lorenzo Parigi, Mirco Boschetti, Francesco Nutini, Filippo Bussotti, Martina Pollastrini, Daniela Stroppiana | ESTIMATING PHENOLOGY METRICS FROM SENTINEL-2 TIME SERIES IN FOREST SITES |
| Martin W. Chege, Kuria B. Thiong'o, Arthur W. Sichangi , Stefanie Steinbach, Andreas Rienow | DEVELOPMENT OF A GEOSPATIAL TELEMETRIC WATER QUALITY MONITORING SYSTEM. |

## Integrated remote sensing methods for improving agricultural practices

| | |
|---|---|
| Sarathchandrakumar Thottuchirayil Sasidharan, Daniele Latini, Mihai Ivanovici, Giovanni Schiavon, Kathiravan Thangavel, Fabio Del Frate | ON-BOARD DATA PROCESSING FOR REAL TIME INFERENCE USING EDGE-AI: AN APPLICATION ON WEED DETECTION. |
| Katarzyna Kubiak, Jan Kotlarz | FERTILIZATION OF MAIZE CROPS USING REMOTE SENSORS OF AN AUTONOMOUS FIELD ROBOT |
| Julianne Oliveira, Julien Morel, Junxiang Peng, Bengt-Ove Rustas, David Parsons | ASSESSMENT OF GRASSLAND FORAGE QUALITY IN THE CONTEXT OF NORTHERN EUROPE AGRICULTURE USING SENTINEL-2 |
| François Godechal, Emilie Beriaux, Alban Jago, Adrien Cassiers, Cozmin Lucau-Danila, Yannick Curnel, Viviane Planchon | MOWING DETECTION BASED ON SENTINEL-1 & -2 DATA FOR SUPPORTING CAP IN WALLONIA |
| Jennifer Kriese, Sarah Asam, Mariel Dirscherl, Michael Stellmach, Kirstel Kerler, Johanna Buchner, Ursula Gessner | MAPPING AND CHARACTERIZATION OF HEDGES IN AGRICULTURAL LANDSCAPES FOR ECOLOGICAL ASSESSMENTS IN BAVARIA, GERMANY |

## Remote sensing applications for natural hazards

| | |
|---|---|
| Radu Irimia, Ionut Sandric, Viorel Ilinca, Zenaida Chitu, Ion Gheuca | A SEMIAUTOMATED MAPPING OF LANDSLIDE VOLUME DISPLACEMENTS USING UAV AERIAL IMAGERY |
| George P. Petropoulos, Vassilia Karathanassi, Ionut Sandric, Dimitris Sykas, Marko Scholtze, Łukasz Kubowicz, Giuseppe Di Carpio, Juha Lemmetyinen, Massimiliano Chersich, Manfred Krischke, Spyridon E. Detsikas | EO-PERSIST: A CLOUD-BASED REMOTE SENSING DATA SYSTEM FOR PROMOTING RESEARCH AND SOCIOECONOMIC STUDIES IN ARCTIC ENVIRONMENTS |
| Krystyna Michałowska, Ewa Głowienka, Tomasz Pirowsk | INTEGRATION OF MULTI-SENSOR REMOTE SENSING DATA FOR MONITORING ILLEGAL OPEN PIT MINES |

## Section I - Trends in Remote Sensing applications

EARSeL Bucharest 2023

Abstract

Corresponding Author:

marketa.potuckova@natur.cuni.cz

# E-learning on time series analysis in remote sensing: the way towards collaborative course development

Markéta Potůčková[1], Jana Albrechtová[1], Katharina Anders[2], Lucie Červená[1], Jakub Dvořák[1], Krzysztof Gryguc[3], Bernhard Höfle[2], Lucie Kupková[1], Zuzana Lhotáková[1], Adriana Marcinkowska-Ochtyra[3], Andreas Mayr[4], Eva Neuwirthová[1], Adrian Ochtyra[3], Martin Rutzinger[4], Alex Šrollerů[1]

[1]Charles University, Faculty Of Science, Czech Republic
[2]Heidelberg University, Institute Of Geography, 3dgeo Research Group, Germany
[3]University Of Warsaw, Department Of Geoinformatics, Cartography And Remote Sensing, Poland
[4]University Of Innsbruck, Institute Of Geography, Remote Sensing & Topographic Lidar Research Group, Austria

**Keywords:** remote sensing, time series analysis, e-learning, 3D point cloud, multispectral data, hyperspectral data

## Abstract

Earth observation programmes run by space agencies provide datasets comprising, among others, multispectral and SAR imagery, enabling monitoring of the Earth´s surface and its resources on various scales (from global to national) and in different time spans. On the national level, aerial images and LiDAR point clouds are acquired annually or over e.g., a 2- to 5-year period to update topographic databases. In addition, selected areas are regularly monitored within environmental, geoscience and other research activities. In these cases, numerous in-situ datasets are also collected, including 3D time series using terrestrial and UAV-borne LiDAR or photogrammetry. Current open data policies have opened up new possibilities in both research and practice. They have been followed by tools suited for processing large datasets with minimal hardware and software requirements on the client side. Along with this and in accordance with the UN Sustainable Development Goal 4 ("Quality Education"), advanced, up-to-date, and quality learning materials must be made available so that both the young generation/future experts and current practitioners can fully benefit from these innovations.

Processing time series of remote sensing (RS) data is challenging when considering various time and spatial scales, the combination of heterogeneous and multimodal data sources, reliability and quality of the results obtained by different processing methods. To provide high-quality learning materials that examine time series in RS from various perspectives, we decided to follow up on our previous collaboration within the 4EU+ Alliance. Joining the specific expertise and knowledge of each involved research group, we developed an e-learning course on Time Series Analysis in RS for Understanding Human-Environment Interactions (E-TRAINEE). There are four main modules in the course. The first one provides a general overview of methods for RS time series analysis, and the other three focus on specific processing steps connected to different types of data:

Module 1: Methods of Time Series Analysis in RS

Module 2: Satellite Multispectral Images Time Series Analysis

Module 3: 3D/4D Geographic Point Cloud Time Series Analysis

Module 4: Airborne Imaging Spectroscopy Time Series Analysis

Each module consists of several themes (see Figure 1) containing a theoretical part, a self-evaluation quiz, and exercises. Moreover, modules 2-4 include two or three case studies with a deeper look into selected research problems. In addition, there is Module 0 summarising basic knowledge in RS, statistics, and programming necessary to follow the course; links to available learning materials are provided.

Datasets and methodologies presented in Modules 1-4 are connected to the past or ongoing research projects of the involved institutions, and are related to the applications of RS in environmental studies, specifically monitoring of vegetation (forest disturbances like drought, bark beetle attacks, or air pollution; changes of relict arctic-alpine tundra vegetation as a possible indicator of climate change) and monitoring of geomorphological features (e.g., landslides, mountain and continental glaciers, sandstone rocks, coastal environments). The practical exercises are based on open software tools such as QGIS, CloudCompare, EnMAP-Box, Google Earth Engine, or scripting in Python or R. The datasets used are either already open (e.g., Copernicus, Landsat programmes) or will be released under a Creative Commons license (LiDAR point clouds, UAV hyperspectral images, laboratory and in-situ spectroradiometer measurements). The whole course is being developed in a git repository allowing for easy and fluent collaborative work on each module, versioning, and sustainable maintenance of the course in the future.

The course is developed and funded within the Erasmus+ Strategic partnership programme (2020-1-CZ01-KA203-078308, 2020-2023). It is currently in the process of finalising the learning materials, fixing overlaps and gaps between the modules, and testing the course with groups of MSc and PhD students. The goal is to fully implement the course in the MSc curricula in geography/geoinformatics of the partner universities (Charles University, Heidelberg University, University of Innsbruck, and University of Warsaw) from the academic year 2023/24 onwards. The first release of the course will also be open to the public starting in August 2023 (for details, visit http://web.natur.cuni.cz/gis/etrainee/). The international collaboration allowed for the creation of rich, research-oriented course content. It enriched the knowledge and experience of all involved partners. The course materials will be continuously updated as all four institutions will actively use the course, and new releases will be made available for public use. Moreover, the course provides a base for online discussions and seminars across the universities that will increase the attractiveness and quality of education.

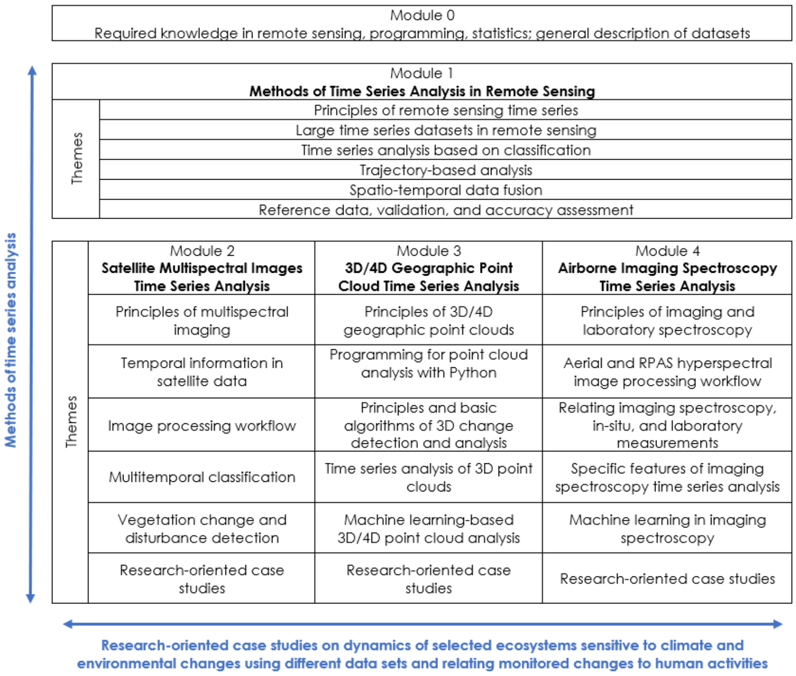

| Module 0<br>Required knowledge in remote sensing, programming, statistics; general description of datasets |
|---|

| | Module 1<br>**Methods of Time Series Analysis in Remote Sensing** |
|---|---|
| Themes | Principles of remote sensing time series |
| | Large time series datasets in remote sensing |
| | Time series analysis based on classification |
| | Trajectory-based analysis |
| | Spatio-temporal data fusion |
| | Reference data, validation, and accuracy assessment |

| | Module 2<br>**Satellite Multispectral Images Time Series Analysis** | Module 3<br>**3D/4D Geographic Point Cloud Time Series Analysis** | Module 4<br>**Airborne Imaging Spectroscopy Time Series Analysis** |
|---|---|---|---|
| Themes | Principles of multispectral imaging | Principles of 3D/4D geographic point clouds | Principles of imaging and laboratory spectroscopy |
| | Temporal information in satellite data | Programming for point cloud analysis with Python | Aerial and RPAS hyperspectral image processing workflow |
| | Image processing workflow | Principles and basic algorithms of 3D change detection and analysis | Relating imaging spectroscopy, in-situ, and laboratory measurements |
| | Multitemporal classification | Time series analysis of 3D point clouds | Specific features of imaging spectroscopy time series analysis |
| | Vegetation change and disturbance detection | Machine learning-based 3D/4D point cloud analysis | Machine learning in imaging spectroscopy |
| | Research-oriented case studies | Research-oriented case studies | Research-oriented case studies |

**Figure 1.** The course structure and content of the modules. All modules relate to methods of time series analysis. They are applied to different datasets and demonstrated on specific case studies.

EARSeL Bucharest 2023
Abstract

Corresponding Author:
roman.hiby@rub.de

# Moon and Remote Sensing in Education – A Concept for Implementing Remotely-Sensed Lunar Topics into the School Curriculum

Roman Hiby[1], Claudia Lindner[1], Fabian Meyer-Heß[1], Andreas Rienow[1]

[1]Ruhr-University Bochum, Institute Of Geography, Germany

**Keywords:** Moon, Remote Sensing, Lunaserv, Augmented Reality, Education

## Abstract

The education of the general public regarding the advantages and capabilities of remote sensing is becoming increasingly crucial as awareness of the technology's impact on everyday life remains low. As the quantity and quality of data collected from space increases, remote sensing has the potential to fundamentally alter our understanding of the planet. One approach to increase general knowledge of remote sensing principles is to incorporate it more regularly into the school curriculum. As an interdisciplinary field of both application and research, remote sensing is well-suited to serve as an educational tool that can facilitate examination of STEM-related subjects.

Remote sensing is not only a powerful tool for scientific analysis on Earth, but also on the Moon. The overarching goal of this concept is to inspire students and teachers about the topic of space exploration and to reveal the Moon as a worthwhile research project with a focus on socially, ecologically, economically and culturally sustainable development on Earth. The Moon should be perceived not only as the "dead" neighbour of the living Earth, but also as an accessible and tangible field of natural science research and profession with high innovation potential within the Earth-Moon system.

The purpose of this educational concept is to introduce teachers and students into the topic of the Moon and the Earth-Moon system with the help of remote sensing techniques in the school subjects of physics and geography. This will be achieved through the use of three instructional strategies. The guiding questions for these instructions are:

1) What is the geological composition of Earth and Moon and what does it tell us about the origin of the Moon?
2) Are the given environmental factors on the Moon conducive to human habitation when compared to those on Earth?
3) How do gravitational forces affect the Earth and the Moon in the past, present and future? What is the significance of the Moon in relation to human life on Earth?

The students shall be able to describe, comprehend and analyse the various lunar topics and their interconnection as derived from the guiding questions, through the use of scientific background information including remote sensing products related to the moon as well as the Earth-Moon system. A remote sensing tool to be employed in this instruction is the Web Map Service (WMS) Lunaserv,

which has been developed based on the Lunar Reconnaissance Orbiter Camera (LROC) of Arizona State University. Similar to the Earth, the Moon is constantly observed and analysed through various satellites in orbit. These data can be accessed through Lunaserv, are accurately geo-referenced and make the Moon more tangible as a celestial body. The Web Map Service can be operated through QGIS, providing teachers and students with an insight into utilization of satellite-based lunar observation data as well as additional scientific background information pertaining to lunar topics such as geology, topography, crustal thickness, gravity and more.

In addition to Lunaserv, the implementation of lunar satellite data for an Augmented Reality application will also be presented. This will enable teachers and students to experience complex sets of data from lunar observation missions on their own devices, in accordance with the “Bring Your Own Device”-principle. Augmented Reality content can be flexibly incorporated into the curriculum as needed. A meta-study of the learning effects of Augmented Reality has shown, that the effectiveness of learning and the cognitive abilities of students can be improved through the usage of AR content. Additionally, teachers emphasise, that AR content brings much more motivation and readiness for learning from students than traditional learning methods. Because of that, the utilization of lunar Augmented Reality content is highly suitable for the given educational purposes, particularly when the link to Lunaserv products is given.

The presentation will explain and emphasise the relevance of lunar topics with the help of satellite based moon observation for teachers, students and education in general. It will show the content that already has been carried out as well as the road ahead.

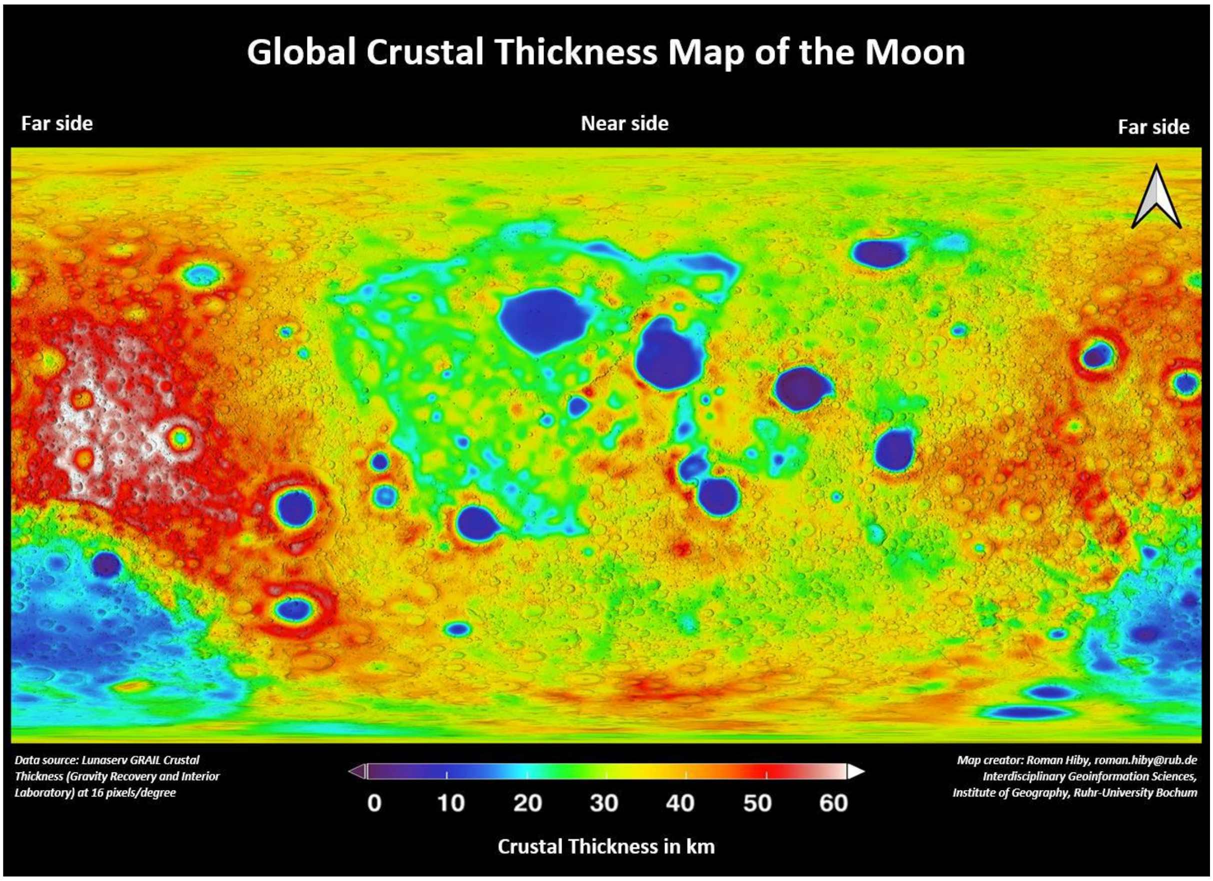

**Figure 2.** Global Crustal Thickness Map with the help of Lunaserv GRAIL Crustal Thickness

# Global cloud-free maps of essential vegetation traits processed from the TOA Sentinel-3 OLCI catalogue in Google Earth Engine

EARSeL Bucharest 2023

Abstract

Corresponding Author:

katber@uv.es

Jochem Verrelst[1], Dávid D.Kovács[1], Pablo Reyes-Muñoz[1], Matías Salinero-Delgado[1], Viktor Ixion Mészáros[1], Katja Berger[1,2]

[1] Image Processing Laboratory (IPL), University of Valencia, C/Catedratico José Beltran 2, Paterna, 46980 Valencia, Spain
[2] Mantle Labs GmbH, Grünentorgasse 19/4, 1090 Vienna, Austria

**Keywords:** Google Earth Engine, Sentinel-3, Gaussian Process Regression, Temporal reconstruction, Whittaker, Essential Vegetation Traits, machine learning, TOA radiance, time series, FAPAR, LAI, FVC, LCC

## Abstract

In support of the upcoming Fluorescence Explorer mission (FLEX), we present a cloud-computing processing chain for the spatiotemporally-continuous retrieval of four Essential Climate Variables (ECVs) at a global scale: (1) fraction of photosynthetically active radiation (FAPAR), (2) leaf area index (LAI) and two additional biochemical/biophysical variables; (3) fractional vegetation cover (FVC) and (4) leaf chlorophyll content (LCC).

For each variable, we first simulated top-of-atmosphere (TOA) radiance data by coupling SCOPE-6SV radiative transfer models. Subsequently, the synthetic data set was used to train a Gaussian Processes Regression (GPR) model, therefore applying a hybrid retrieval strategy. These models were implemented using Sentinel-3 Ocean and Land Colour Instrument (OLCI) Level-1B data for the global mapping.

We used the Whittaker smoother (WS) for temporal reconstruction, thus obtaining continuous data streams for the four traits. Cloud-free maps were inferred at 5 km spatial resolution at 10-day temporal composites for the year 2019. The consistency of the obtained product maps was evaluated by direct validation using interpolated in situ data from the VALERI network over European sites in seven different countries. Also, by per-pixel intra-annually correlating against corresponding Copernicus Global Land Service (CGLS) and MODIS vegetation products global Pearson correlation maps were produced. The most consistent global variable was LAI, which showed correlations with an average Pearson correlation coefficient (R) of 0.57 against the CGLS LAI product. Error metrics were also calculated locally against reference products over four radically distinct vegetated land covers, namely evergreen broadleaf, deciduous broadleaf, agricultural fields (consisting mainly of rice and wheat) and sparsely vegetated areas. Through the land cover analysis, the most consistently responding variable was FVC over deciduous broadleaf forests at the Monongahela National Park in Western USA, with an R of 0.98 also against the CGLS product. The land covers with pronounced phenology fluctuations led to high correlations between our (S3-TOA-GPR-1.0-WS) and reference products. In contrast, sparsely vegetated fields as well as areas near the Equator showing lower yearly seasonality presented lower R values.

Despite a few limitations, we conclude that our retrieval chain for inferring global gap-free maps of the ECVs and other variables was consistent. Moreover, the direct validation of our models against VALERI estimates showed good retrieval performance. Thanks to Google Earth Engine (GEE), the entire OLCI L1B

catalogue can be processed easily into cloud-free ECV products on a global scale. Additionally, GEE facilitates the workflow to be operationally applicable and easily accessible to the broader community.

# A Review of Remote Sensing Time Series Analysis for Vegetation Productivity Monitoring

EARSeL Bucharest 2023
Abstract
Corresponding Author:
katber@uv.es

Katja Berger[1,2], Lammert Kooistra[3], Lukas Valentin Graf[4,5], Benjamin Brede[6], Clement Atzberger[7], Pablo Reyes Munoz[1], Jochem Verrelst[1]

[1] Image Processing Laboratory (IPL), University of Valencia, C/Catedratico José Beltran 2, Paterna, 46980 Valencia, Spain

[2] Mantle Labs GmbH, Grünentorgasse 19/4, 1090 Vienna, Austria

[3] Wageningen University & Research, Laboratory of Geo-Information Science and Remote Sensing, Droevendaalsesteeg 3, 6708 PB Wageningen, the Netherlands

[4] Earth Observation of Agroecosystems Team, Division Agroecology and Environment, Agroscope, Zurich, Switzerland

[5] Institute of Agricultural Science, Crop Science, ETH Zürich, Zurich, Switzerland

[6] Helmholtz Center Potsdam GFZ German Research Centre for Geosciences, Section 1.4 Remote Sensing and Geoinformatics, Telegrafenberg, Potsdam, 14473, Germany

[7] Institute of Geomatics, University of Natural Resources and Life Sciences, Vienna (BOKU), Peter JordanStraße 82, 1190 Vienna, Austria

**Keywords:** Time Series, satellite platforms, GPP, process modelling, agriculture, forests

## Abstract

Vegetation productivity plays a vital role in the health of global ecosystems, and it is constantly affected by climate change and human activities. As such, monitoring vegetation productivity is crucial in assessing the overall well-being of our planet. A wide range of sensing platforms, from ground-based to airborne and satellite, provide us with valuable information on the status of terrestrial vegetation. Earth observation (EO) data is usually acquired at high frequencies, and this allows the derivation of vegetation metrics reflecting seasonal patterns, trends, and dynamics that are unequivocally related to vegetation productivity. In this paper, we systematically reviewed time series (TS) literature for assessing the state-of-the-art EO-based vegetation productivity monitoring approaches for different ecosystems based on optical data. Vegetation productivity is commonly defined in three measures: gross primary productivity (GPP), net primary productivity (NPP), and net ecosystem productivity (NEP). Our review identified several methods for inferring vegetation productivity, or GPP, from EO data. These include (i) TS of vegetation indices as direct indicators, (ii) trend analysis and anomaly detection, (iii) TS-derived metrics of land surface phenology, and finally, integration and assimilation of TS-derived metrics into (iv-a) simple (semi-) empirical models, and (iv-b) process-based dynamic vegetation models (DVM). In view of DVMs, three distinct strategies were proposed to integrate remotely sensed TS with process-based models, as depicted in Fig. 1. The first strategy, known as model forcing, involves forcing the process model to follow the trajectory of a state variable (e.g., leaf area index) obtained from remotely sensed imagery. In contrast, the second strategy, model recalibration, also referred to as `data assimilation,' utilizes remotely sensed state variables to readjust inputs to the DVM whenever new observations become available. The first two strategies rely on inverse modelling to obtain the remotely sensed state variables. The third strategy, coupled forward modelling, integrates a DVM with a radiative transfer model (RTM) to simulate

vegetation optical properties, which are then compared to remotely sensed data. The key benefit of this last approach is the avoidance of inverse modelling, which is typically not only ill-posed but also computationally intensive. We also identified that the validation of EO-data derived productivity can be categorized into three methods: (1) direct, using in situ measured data, such as crop yield, (2) sensor networks as the most common method, referring to a network of distinct sensors including spectra radiometers, flux towers, or phenocams, and (3) inter-comparison of different productivity products or models. In conclusion, we address current challenges in vegetation productivity monitoring and propose a conceptual framework that employs fully integrated process models and RTMs capable of simulating the full range of spectral measurements over time. This framework meets the requirements of a digital twin of multiple ecosystems, enabling a better understanding of vegetation dynamics and enhancing the accuracy of vegetation productivity monitoring. Overall, our review highlights the importance of monitoring vegetation productivity in assessing ecosystem health and the availability of various sensing platforms and methods to do so. It is crucial that we continue to develop and refine these methods to ensure that we can better understand the changing dynamics of our planet and mitigate any negative impacts of climate change and human activities.

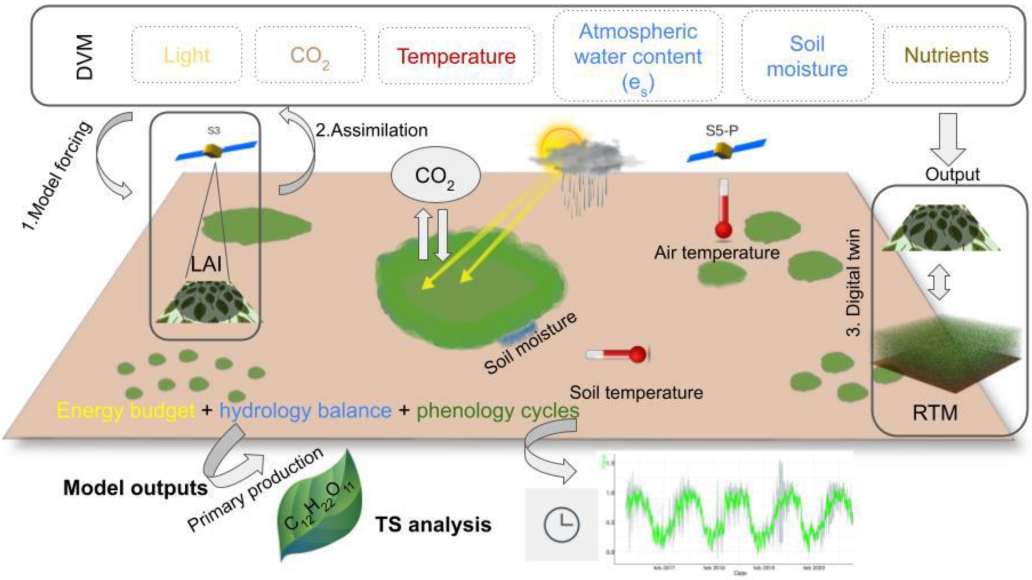

**Figure 3.** The three strategies to combine remotely sensed time series with process-based dynamic vegetation models (DVM): (1) model forcing; (2) model recalibration, and (3) coupled forward modelling of DMV and radiative transfer models (RTM).

EARSeL Bucharest 2023

Abstract

Corresponding Author:

c.lucau-danila@cra.wallonie.be

# Benchmarking of grassland dynamic models coupled with Sentinel-2 to monitor grasslands growth over Wallonia region (Belgium)

Cozmin Lucau-Danila[1], Yann Chemin[2], Yannick Curnel[1], Julien Morel[2], Mattia Rossi[2], Viviane Planchon[1]

[1]Walloon Agricultural Research Centre (Cra-W), Belgium
[2]Eu Joint Research Centre (Jrc), Italy

**Keywords:**
Grasslands, Lingra, ModVege, grassland yield, yield forecasting, Sentinel-2, recalibration

## Abstract

Grasslands play an important role in Europe's/Word's biodiversity and climate related services such as soil erosion prevention or carbon and water storage, while at the same time being a key source of feed for livestock.

In Wallonia (Belgium), grasslands cover 367,200 ha and represent the dominant land cover class (47% of Utilized Agricultural Area (UAA), 43 % for permanent grasslands and 4% for temporary grasslands). In comparison, at EU level, permanent grasslands represent 34% of the UAA (5,497,800 ha).

The proportion of grasslands in the different Walloon pedoclimatic regions is however quite variable, from 18.6% up to 94.3% of the UAA. Grassland yields are quite fluctuating according to different factors such as the pedoclimatic region, the floristic composition, the intensification level (e.g. rest period length, stocking density or fertilization level), the parcel (e.g. exposition or slope) as well as management (e.g. cutting height).

The management of grasslands fields is therefore rather complex and a great challenge in a changing climate. In the case of grazed parcels, it requires farmers to regularly adjust their practices depending on the spatial and temporal distribution of available feed biomass. This information is usually estimated from time-consuming in-situ observations or measurements (with e.g. a rising plate meter).

Remote sensing data could be used to help farmers to adapt their practices. Satellite-mounted optical sensors provide region-scale objective and spatial information on the status of vegetation and could easily be used to map within-field heterogeneity. However, the efficiency of the system can be hampered by cloud cover, and remotely-sensed data cannot be used to predict the status of vegetation. On the other hand, process-based dynamic crop models, relying on sets of ecophysiological-related mathematical equations, can predict potential productivity of crops using weather forecasts, but due to their formalism, do not account for every factor that can affect plant growth. Moreover, crop models provide field-wise information, whereas in the case of grazing, paddock-wise information is required.

Coupling remote sensing data with crop models[10.1016/j.jag.2006.05.003] can provide an accurate tool to both estimate and predict the growth of grasslands at field and paddock-scale. In this study the coupled use of two dynamic grassland models (Lingra and ModVege) and Copernicus Sentinel-2 MSI satellite data has been evaluated to estimate and predict the dry matter yield of grassland field.

This study is designed as a benchmarking exercise to monitor grasslands productivity at European scale. Here, we focused on Wallonia (Belgium), where grasslands represent the dominant land cover class,). Field data were collected over 32 fields from 2019 to 2022 located in three different pedoclimatic regions (fig.1): fifteen (G1-G15) in the Loamy region, eleven (L1-L11) in the Ardenne region and six (M1-M6) in the Jurassic region. Areas of fields are between 0.3ha (M6) and 2.4 ha (G5). The field measurements have been carried out between 2019 and 2022 from march-april to october-november and consists of : geolocalized compressed sward height on a weekly basis measured using electronic rising plates meter, fresh and dried biomass monthly.

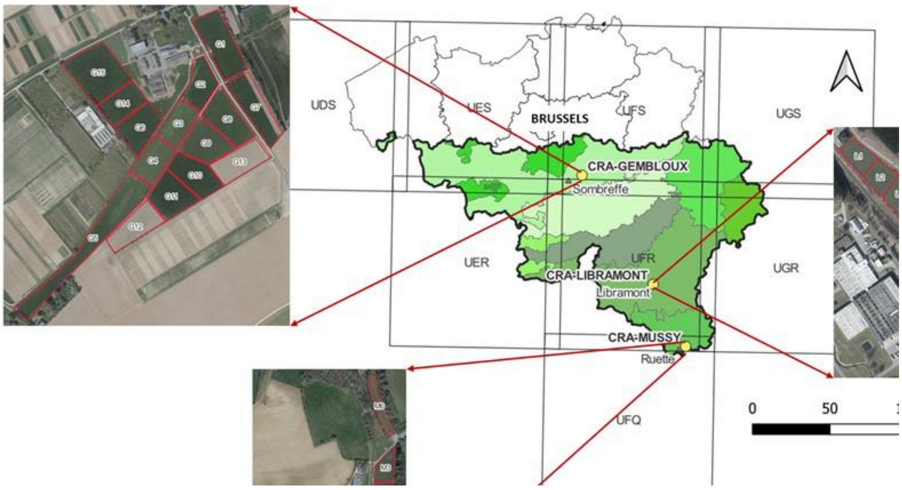

**Figure 4.** Map of the locations of the monitored fields (yellow dots) and corresponding weather stations (red triangles), namely Sombreffe (Gembloux), Libramont (Libramont) and Ruette (Mussy). The different pedoclimatic regions from Wallonia and Sentinel 2 orbites are presented.

The models used in this study to estimate the grass growth of monitored fields are Lingra [10.1016/S1161-0301(98)00027-6] and ModVege [10.3390/agronomy12102468]. These models are dynamic and process- based, and simulate on a daily time step the growth of a homogeneous field of grass based on soil and plant traits, farming practices and weather data.

Bottom of atmosphere (Level 2A) optical remote sensing data were obtained from the Copernicus Sentinel-2 constellation, which provide open-access 10 meter resolution multispectral images with a high revisit frequency (approximately 2.5 days for Belgium). The number of cloud free images available over monitored fields is between 42 and 50 per year (32-44 covering the period march-october). The Leaf Area Index (LAI) values per field were calculated for all cloud free available S2 images.

A recalibration coupling approach was used to minimize the differences between satellite-derived crop information and its model-simulated counterpart through a cost function. The performances of each model will be assessed before and after recalibration, using randomly sampled test and validation subsets.

### Perspectives

Limitations of the proposed approach has been identified, and strategies to move toward an operational system will be discussed. A particular attention has been paid to the detection of mowing events, which is a bottleneck for accurate simulation of grassland growth dynamics. Conclusions drawn from this test site will be analysed with a view to extend the method to EU scale.

## Section II - Earth Observation applied in forest hazards management

# Monitoring of drought-induced forest damages in Germany

EARSeL Bucharest 2023
Abstract

Corresponding Author:
andreas.mueterthies@eftas.com

Andreas Müterthies [1], Nils Wolf[1], Sebastian Mader [1]

[1] EFTAS Fernerkundung Technologietransfer GmbH, Germany

**Keywords:** forest damages, drought, bark beetle, Copernicus, Sentinel-2, Planet Dove, neural networks, in-situ data collection, forest timber volume

## Abstract

With a forest area of 11.4 million hectares (around 32 percent of the area of the country), Germany is one of the most densely forested countries in Europe. Forests make an invaluable contribution to Germany: economically, ecologically and in climate protection. The annual carbon sequestration effect of these forests and long-lived wood products amounts to around 62 million tonnes of CO2. This means that forests in Germany compensate for about 7% of the German annual CO2 emissions. However, climate change is putting a strain on the forests and is manifesting itself in Germany by persistent drought and extreme weather conditions.

Since 2018 droughts in combination with drought induced insect calamities in Germany and in several other European countries lead to severe forest damages and a loss of timber volume. Forest agencies in Germany requested a continuous monitoring of forest damages. Moreover the timber industry asked for a calculation of the remaining timber volume. Therefore AI-based remote sensing methods have been developed to monitor the intensity of damages and to quantify the reaming timber volume. Copernicus Sentinel-2 and Planet dove data were combined with reference data from forest agencies using neural networks. However for certain classes reference data was unavailable and had to be collected by field campaigns. To reduce efforts, the collection of in-situ data was supported by GeoIT-application including a real time monitoring of data collection of the field teams, which was developed originally for the LUCAS field campaings by EFTAS.

The methods have been applied with different monitoring frequencies to several German states including North Rhine-Westphalia. According to the major impact of droughts and insect damages special focus was given to damage monitoring of spruce forests whereas timber volume was calculated for the major tree species used in the timber industry. The results for NRW are published on the webportal "Waldinfo.NRW" of the Ministry of Agriculture and Consumer Protection of the Federal State of North Rhine-Westphalia (see figure).

Developments supported by the ForstCARe-project will contribute to future forest damage monitoring campaigns.

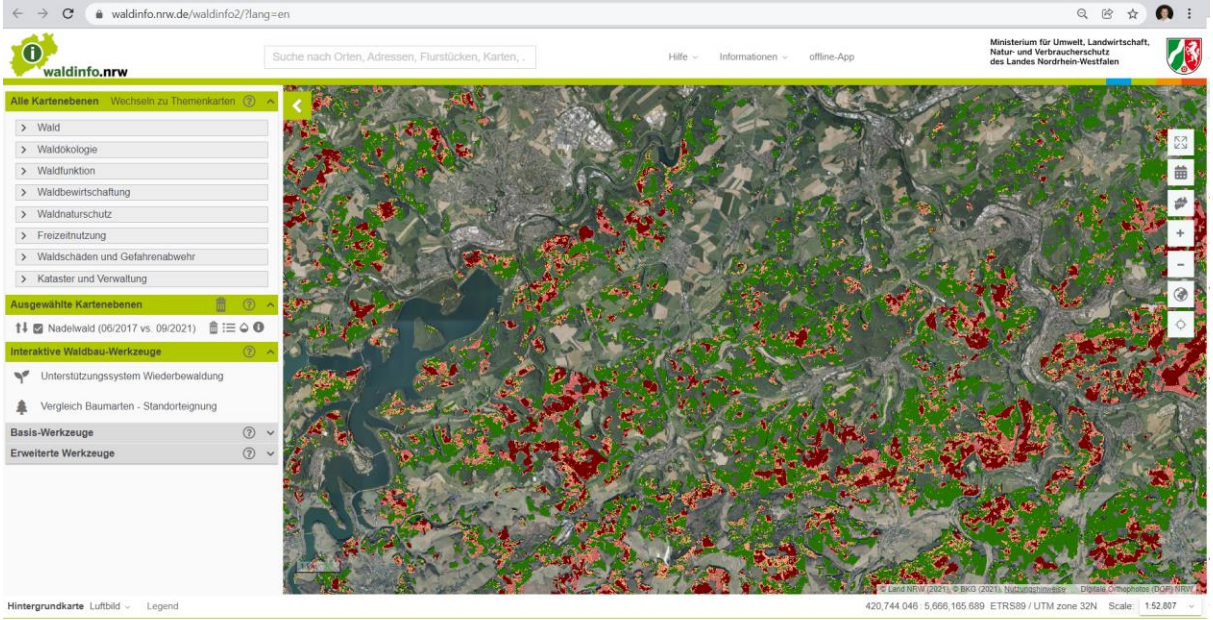

**Figure 5.** Forest information system of the Ministry of Agriculture and Consumer Protection of the Federal State of North Rhine-Westphalia, based on remote sensing data (Source: EFTAS, data basis Copernicus and Planet Labs)

# Modelling Vitality Loss of European Beech (*Fagus sylvatica* L.) using Random Forest Regression

EARSeL Bucharest 2023
Abstract
Chunyan Xu
c.xu@tu-berlin.de

Chunyan Xu[1], Michael Förster[1], Birgit Kleinschmit[1]

[1] Technical University of Berlin, Geoinformation in Environmental Planning Lab, Germany

**Keywords:** forest mortality, drought monitor, leaf loss, European deciduous forest, Sentinel-2, Random Forest Regression, vegetation indices, National Forest Condition survey, climate condition

## Abstract

Climate conditions influence the structure and function of forest ecosystems, leaving an impact on forest health. By impairing photosynthesis and directly triggering mortality through hydraulic failure, drought has been regarded as a destructive factor in forest disturbances. Severe droughts since 2018 hit large parts of central Europe, which has led to premature leaf senescence in European beech (*Fagus sylvatica* L.), the most important and widespread broadleaved tree in Europe. This tree species is known for its sensitivity to drought and its distribution could be thus threatened by continuous heat waves. However, the relationships between hydrologic drought stress as well as other geo-ecological factors (such as tree age, location, climate conditions) and vitality loss of European beech (*Fagus sylvatica* L.) are not yet fully understood, especially with a perspective of remote sensing. Many studies are traditionally implemented during field surveys which are laborious and limited in time and scales. When the frequency of severe droughts becomes higher, more European beech (*Fagus sylvatica* L.) forests would be affected and obtaining timely information of beech health conditions at large scales becomes increasingly necessary. Remotely sensed data could compensate for the limitation, which would make it possible to identify the locations of damaged beech trees and conduct large-scale monitoring. The vegetation indices (VIs) of Sentinel-2 could capture valuable information of chlorophyll and cell structure of leaves and provide temporally and spatially continuous data on forest conditions. Therefore, we utilised VIs such as the Disease Water Stress Index (DWSI), Plant Senescence Reflectance Index (PSRI), Normalised Difference Vegetation Index (NDVI) and Normalised Difference Red-Edge (NDRE) derived from Sentinel-2 time series for analysing their temporal changes over the drought years from 2016 to 2022 in Lower Saxony, federal state of Germany. We adopted the yearly field observed data of the National Forest Condition Survey, which is part of the National Forest Inventory (NFI). We further revealed the correlations of vitality loss to the used VIs and other factors by using the Random Forest Regression (RFR), where the soil moisture, Diameter at Breast Height (DBH), exposure, precipitation, temperature, height above mean sea level and VIs were used for predicting the percentage of beech leaf loss. Because leaf loss is believed to be directly related to impairment of physiological conditions of beech trees. In our study, 70% of the samples were used for training and 30% were used for validation. The preliminary results showed that the RFR model produced rather accurate percentages of leaf loss, when compared to the measured leaf loss from the NFI. In terms of the importance in our modelling, the NDRE and DWSI contributed more than the other VIs. However, other geo factors such as precipitation and DBH showed rather higher importance than VIs. Our study still demonstrated the possibility of Sentinel-2 time series in predicting vitality loss of beech stands, and hence highlighted the perspective of using remotely sensed data and additional geo factors to gain a better understanding of the response of *Fagus Sylvatica* to drought stress. Thus, our findings will improve climate adapted forest management of European beech (*Fagus sylvatica* L.) stands.

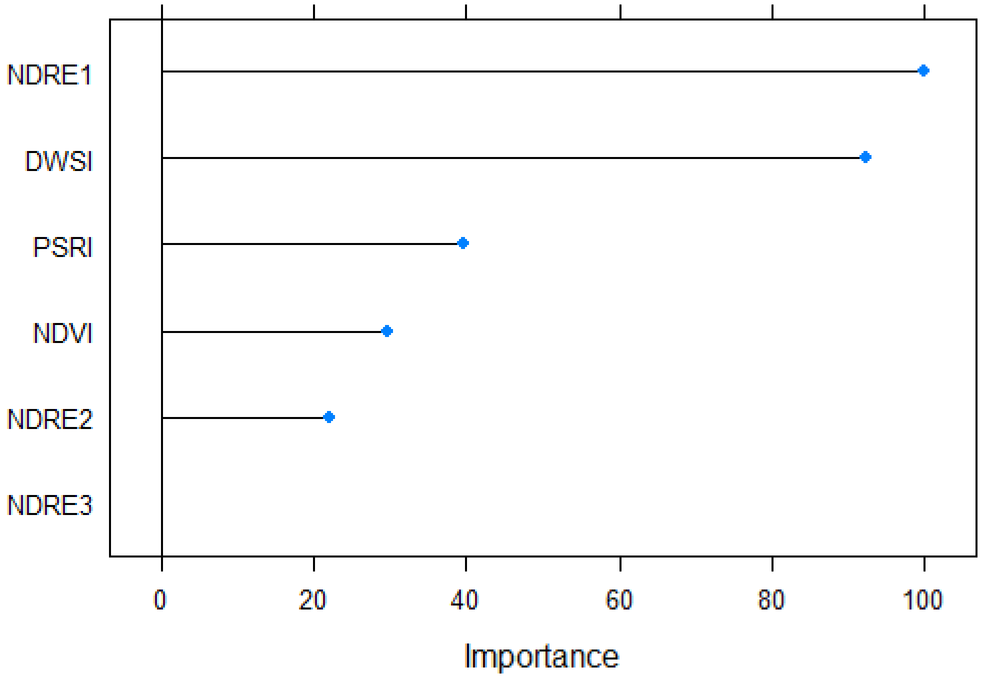

**Figure 6.** Selected variance importance of VIs for RFR in our study

# Implementation of a fuel type classification system for Sardinia, Italy, with the integration of remotely sensed data

EARSeL Bucharest 2023
Abstract

Corresponding Author:
debora.voltolina@igag.cnr.it

Debora Voltolina[1], Daniela Stroppiana[2], Simone Sterlacchini[1], Matteo Sali[2], Bachisio Arca[3], Mariano García[4], Michele Salis[3], and Emilio Chuvieco[4]

[1] National Research Council, Institute of Environmental Geology and Geoengineering, Milano Unit, Italy
[2] National Research Council, Institute for Electromagnetic Sensing of the Environment, Milano Unit, Italy
[3] National Research Council, Institute of BioEconomy, Sassari Unit, Italy
[4] Universidad de Alcalá, Department of Geology, Geography, and Environment Science, Spain

**Keywords:** fuel model mapping, fire behaviour, Sardinia, Sentinel-2, FirEUrisk

## Abstract

Forest fires are a keystone ecosystem process in the evolution and maintenance of the Mediterranean biome. However, the expected increase in fire activity under future climate projections poses a growing ecological and socio-economic threat to the Euro-Mediterranean region. The dynamic mapping of fuel types and models assumes relevance to wildland fire risk prevention and management across multiple spatial and temporal scales due to the tight dependence of fire ignition, spread, and growth on vegetation characteristics. Thematic maps of fuel types and models already exist at a global and continental scale, but the spatiotemporal variability of fuel characteristics in the Euro-Mediterranean region highlight the need for further improvements in the identification of techniques and methodologies based on the integration of field observations with remotely sensed data that allow for a periodic update of high resolution thematic maps.

This research proposes a methodology for generating a fuel type map for a pilot site located in Sardinia, Italy, compliant with the first level scheme of the hierarchical classification system recently proposed within the context of the EU project FirEUrisk; the classification system has been chosen for its adaptability to different scales of investigation and to different geographical contexts in the Euro-Mediterranean regions.

The adopted methodology applies supervised learning algorithms for the fuel type classification from time series of multispectral images of the Sentinel-2 (S2) missions of the Copernicus program. The classification methodology is applied to S2 time series of spectral indices for the period 2020-2021 after preliminary cloud cover masking and compositing. Remotely sensed information is integrated with auxiliary information derived from institutional datasets available on a continental scale, such as the CORINE Land Cover system, and on a local scale, such as the digital elevation model and the mosaic of high resolution orthophotos for the year 2018. Due to the lack of field data uniformly distributed in the pilot site, an ad hoc dataset is generated by photointerpretation for the supervised classification model training and testing. To this aim, a web application is designed and developed to support a consistent data collection within 1 ha regions of interest (ROIs). The application allows the labelling of each 10x10 meter S2 pixel within each ROI selected with a stratified random sampling strategy. A gradient boosting ensemble model is trained for a pixel-level classification that integrates spectral metrics, textural metrics, and other geo-environmental descriptive metrics. Finally, the classifier is applied to derive a 10 m resolution thematic fuel type map for the pilot site in Sardinia (Figure 1). Preliminary results show an overall

accuracy greater than 0.9 and calculated as the number of pixels correctly classified by the model out of the total number of pixels included in the different cross-validation datasets. The classification specificity is greater than 0.7 for most of the fuel type classes.

Future activities will be focused on a robust validation of the thematic fuel type map by selecting suitable sites based on the possibility of carrying out ad hoc field surveys. If the preliminary results are confirmed, the methodology could be extended to other pilot sites in the Euro-Mediterranean basin and the obtained thematic fuel type map could be processed to obtain a fuel model map to be used for fire management purposes, such as the simulation of fire spread and growth using simulators based on the Rothermel mathematical model.

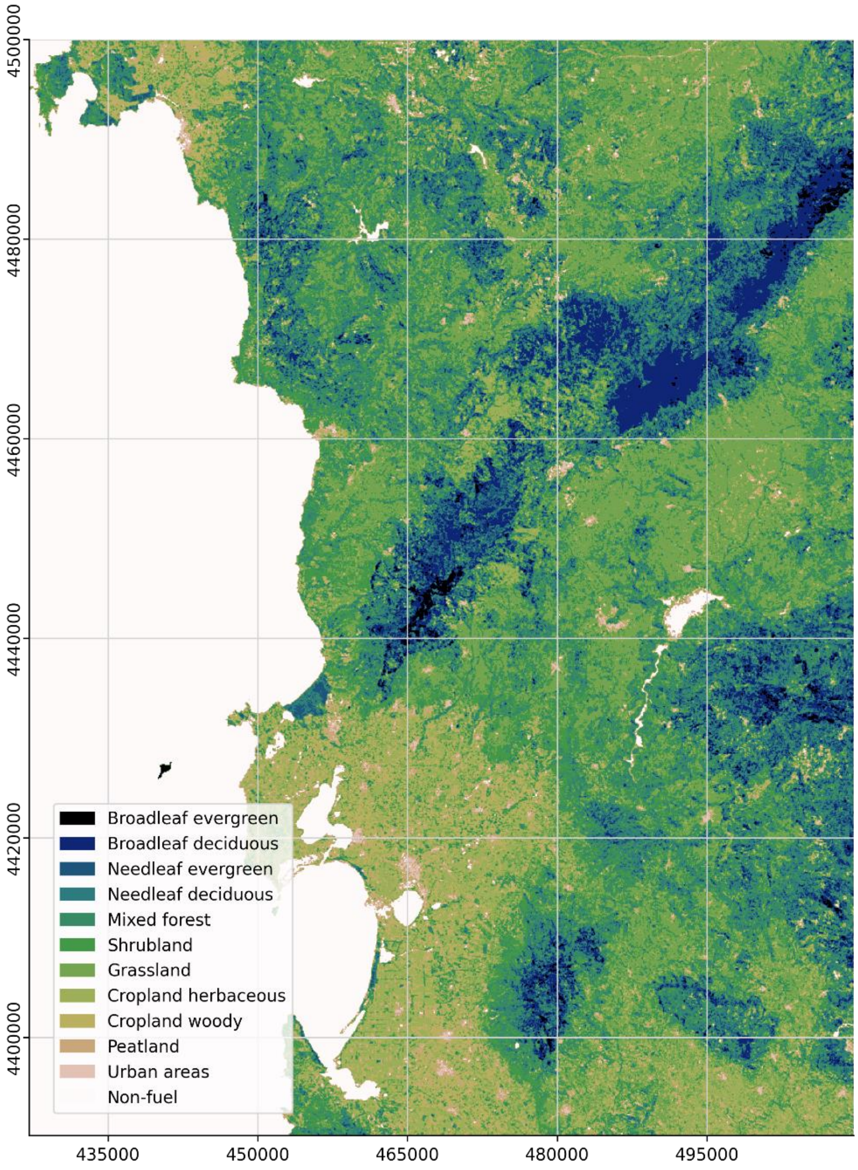

**Figure 1** Fuel type map for the pilot site in Sardinia, Italy.

# The impact of wildfires on water quality using CCI EO products: Lake Baikal case study

EARSeL Bucharest 2023
Abstract
Daniela Stroppiana
stroppiana.d@irea.cnr.it

Daniela Stroppiana[1], Lorenzo Parigi[1], Giulio Tellina[1], Claudia Giardino[1], Monica Pinardi[1], Rossana Caroni[1], Mariano Bresciani[1]

[1] Institute for Electromagnetic Sensing of the Environment, National Research Council, Milan, 20133, Italy

**KEYWORDS:** BOREAL REGIONS, ESA CCI, TIME SERIES

## Abstract

Fires have numerous and complex effects on geological, hydrological, ecological, and economic systems. In many areas of the world, the frequency and intensity of wildfire have increased in recent years and are projected to escalate with predicted climatic and land use changes.

Lakes provide crucial ecosystem services for human society and they are sentinels, integrators and regulators of climate. Climate change is generating complex responses in aquatic ecosystems that vary according to their geographic distribution, magnitude, and timing across the global landscape (Williamson et al., 2009). Fires play a crucial role in the process of global climate change, by reducing forest cover and emitting greenhouse gases. In landscapes exposed to fires, water quality of streams, rivers and lakes can significantly be affected due to both transport process through the atmosphere and the hydrological network. Worldwide boreal regions represent a sensitive biome where wildfires are the major source of climate-driven impacts.

In this context, satellites in the past five decades have continuously observed the Earth surface to provide data for monitoring the state of the natural environment. The European Space Agency (ESA) has undertaken the Climate Change Initiative (CCI) programme to support monitoring activities and policies with long-term global products mainly derived from Earth Observation data and programs.

In this work, we rely on ESA CCI global products depicting fire occurrence and lake water quality to investigate the relationship between fires and water quality in the boreal regions of Lake Baikal (Siberia). We mainly focused on hydrological processes of sediments transport and deposition. Lake Baikal, the deepest and largest lake (by volume) on Earth, currently in oligotrophic state, is recognized as one of the most vulnerable areas in Russia where deforestation rapidly increased in the last decade and fires contributed to the degradation of both terrestrial and aquatic ecosystems.

We exploited time series of Burned Area (BA) and Chlorophyll-a (Chl-a) and Turbidity extracted from CCI global products for the period 2003-2020 to investigate the potential relationship between wildfires and meteo-climatic data through hydrological processes. Lake water parameters were extracted from the CCI datasets for the ice free summer months and averaged over Regions Of Interest (ROIs) in correspondence of the inflow of the three major tributaries of Lake Baikal (Angara, Barguzin and Selenga); the FireCCI51 BA dataset was aggregated over the catchments of the three tributaries (total burned area). All values were also aggregated to weekly average and total values for the lake and fire parameters, respectively.

We analysed time series of weekly values to highlight anomalies in Chl-a and turbidity (Z-score) corresponding or being related to extreme fire conditions and eventually attributable to significant rainfall events. Since the Chl-a and turbidity products have a time gap of four years (2012-2015), the analyses were presented separately for the two time periods 2003-2011 (p1) and 2016-2020 (p2).

We also investigated the correlation between input variables with a NonParametric Multiplicative Regression (NPMR) (McCune, 2006a) to estimate the response of the Chl-a and Turbidity to the variables fire and rainfall. Results for all the regression models, in three catchments by two time periods (p1, p2), showed that temporal variability (seasonal and annual) was the main predictor of Chl-a and Turbidity concentrations. Additional parameters included in the models were found significant at different levels depending on the considered catchment. In the Angara catchment (the northernmost one), cumulative burned area and rainfall amount resulted important factors especially during p2. In the southern Selenga sub-basin, fires and southerly winds (v wind component) were found significant factors for both chlorophyll-a and turbidity concentrations. Finally, for the Barguzin catchment, fires and easterly winds were the most significant factors affecting Chl-a and turbidity, pointing out a potential effect of burned material from fires occurring in the eastern regions of the lake and being transported directly by winds to the recipient lake. In general, the observed response of lake water quality (Chl-a and turbidity) to fires was found to be weak and to vary for the three catchments.

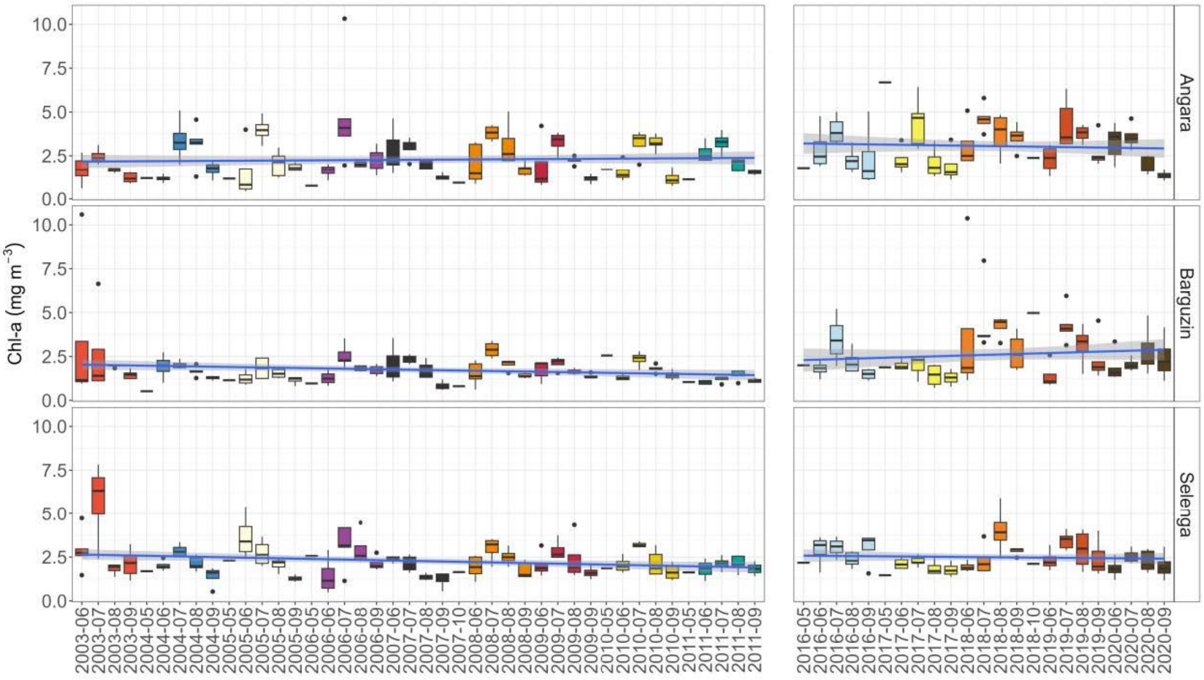

**Figure 1.** Boxplots of daily Chlorophyll-a (Chl-a; mg m$^{-3}$) values showing monthly statistics (median, quartiles, range and outliers) split for the two periods: 2003-2011 (p1) and 2016-2020 (p2) for the three catchments.

## Section III - Remote sensing applications for environment

# Quantification Of Net Carbon Stock Change Due To The Norwegian Reservoirs Development

EARSeL Bucharest 2023
Abstract
Corresponding Author:
mahmoud.s.kenawi@ntnu.no

Mahmoud Saber Kenawi[1], Tor Haakon Bakken[1]

[1]Norwegian University Of Science And Technology, Norway

**Keywords:** LULLC, GIS, hydropower, carbon sequestration, OBIA

## Abstract

Hydropower is widely recognized as a renewable source of energy that is efficiently being implemented and included in all climate change mitigation scenarios and the reduction of fossil fuels dependency. The flexible way of production gives an advantage over other renewable energy sources that suffer from the variability as it can be a clean efficient source of energy in addition to balancing other renewable energy sources. Hydropower is currently involved in all climate mitigation scenarios and a backbone for the green transition in European Union energy policies.

However, a lot of controversy is associated with hydropower construction and operation due to the environmental and social issues to the surrounding ecosystem during the construction and operation phases. Such issues can vary from the impact on the riverine ecosystem to and alteration of the river morphology or the social pressure it can cause mainly due to large projects that can cause resettlement problems and increase the pressure on the land by increasing the access to isolated lands or raise the level of competitiveness due to this resettlement problems.

A major environmental concern is the GHG emissions from the reservoirs as reservoirs can act as a source of methane depending on the size, location, and the age of reservoir. Yet, such accusations have been criticized due to overestimating and ignoring the status of GHG emissions prior to the reservoir development. Additionally, recent studies show that reservoirs can also work as carbon sinks and have positive effects sequestering carbon and burying it within the sediment inside the reservoir. Such studies created a debate on how to correctly associate and monitor the net GHGs emissions that can occur due to reservoir and hydropower development

The uncertainty and limitation gaps in understanding the net emissions of GHGs and reservoir characteristics motivate us further to investigate this relation. In Norway where it contains more than 50% of the total European reservoir capacity. Hydropower development has been going on since the 50ties onwards. Such a period can help us model the net GHGs emission by these reservoirs throughout their lifetime and when they can reach neutrality.

By understanding the land composition that existed prior to the hydropower development and comparing it to the post-impoundment state we can associate the change in the carbon cycle in the catchment area that contains the reservoir and using the available remote sensing data can help us reach this goal.

The goal of this work is to monitor the alteration in the carbon cycle due to reservoir development and associate it with reservoir characteristics. We classified historical aerial images with monochromatic bands to identify the land systems prior to the development of 40 hydropower systems in Norway counting 105 reservoirs with different construction types and compared them with the recent images representing the same land.

We identified the change in the land mainly in a level land classification system. We also identified the inundated land due to this development. We found that 63% of the total reservoir areas were already existing water bodies while 9% of the vegetation land was used for this development. We also found that 84% of the reservoirs were built on existing lakes or lakes that were expanded due to hydropower developments.

Afterward, we compared different carbon budgeting tools that associate the change in the land with different carbon emission factors to identify the change in the carbon cycle. Results show the variability based on reservoir size and construction type which supports the huge variability of hydropower development.

The results of this work contribute to the fairly limited picture of how the interaction between the land and the development of Norwegian hydropower in this era and contributes to monitoring the associated net GHGs by reservoir development. It also shows the contrast between the widespread perception that huge land is lost to inundation due to the construction of dams.

# Integrating Low-cost Sensors and Remote Sensing to Monitor Small Reservoirs in Kenyan Wetlands

EARSeL Bucharest 2023
Abstract

Corresponding Author:
stefanie.steinbach@rub.de
s.steinbach@utwente.nl

Stefanie Steinbach[1,2], Anna Bartels[1], Martin W. Chege[3], Niels Dedring[1], Wisdom Kipkemboi[3], Simon Muthee[3], Andrew Nelson[2], Kuria B. Thiong'o[3], Sander J. Zwart[4], Andreas Rienow[1]

[1] Department of Geography, Ruhr University Bochum, Germany
[2] Faculty of Geo-Information Science and Earth Observation (ITC), University of Twente, The Netherlands
[3] Institute of Geomatics, GIS and Remote Sensing (IGGReS), Dedan Kimathi University of Technology, Kenya
[4] Integrated Water Management Institute (IWMI), Accra, Ghana

**Keywords:** Sentinel-2, turbidity, Arduino, citizen science

## Abstract

Low costs, simplicity, and adaptability to local conditions have led to the construction of thousands of small dams across the African continent. Despite their relatively short lifespans, they can support smallholder agriculture and farmer-led irrigation development. In Nyeri county, Kenya, as in other parts of East Africa, several small reservoirs are located in wetlands where they are used for irrigation, fishing, and aquaculture, and thus contribute to livelihoods and food security. They are owned by the user communities and managed under local Water Resource Users Associations (WRUA). Wetland use plays a significant role in water quality in small reservoirs. Likewise, water quality critically impacts the status and functioning of wetlands. Yet, small reservoirs are insufficiently understood and their impact on water resources and wetland ecology is poorly documented, in particular in lower latitudes.

Water quality monitoring networks often neglect small dams due to the time and cost in relation to limited and localized impact. Traditional monitoring methods require physical access and do not produce spatially continuous data. Remote sensing technology is a cost-efficient alternative for spatially and temporally continuous water quality monitoring. Satellite observations can be matched with ground reference to derive different water quality parameters. Turbidity measures water clarity and refers to suspension load. It can indicate water pollution and soil erosion, allowing for inferences about land management. The launch of satellites providing high spatial resolution imagery, such as Sentinel-2, has stimulated a growing body of studies of small water bodies. Yet, model calibration and validation require in-situ information, which is a bottleneck. Low-cost sensors may serve as a possibility for water parameter retrieval where measuring networks are sparse. The aim of this study is therefore to increase knowledge of small tropical reservoirs and to address the challenge of water quality monitoring using Sentinel-2 optical imagery and in-situ data from low-cost turbidity sensors.

We collected data during the transition from the short rains to the dry season in January 2023. We sampled water in ten small reservoirs between 0.5 and 5 ha simultaneously with five Sentinel-2 overpasses. Turbidity was measured with a Lovibond TB 211 IR turbidimeter in Nephelometric Turbidity Units (NTU), and by immersing two low-cost sensor setups into the water for a minute, resulting in about 30 measurements. The setups consisted of three off-the-shelf turbidity sensors, the SEN-0189 for Setup A and the TSW-10 for Setup B, connected to an Arduino Nano microcontroller where passing infrared light was recorded in voltage. Turbidity, pH, and temperature were measured at the inflow, in the center location, and at the outflow as shown in Figure 1a). In addition, we recorded bathymetry using a Garmin GPS-enabled sonar.

The performance of the low-cost sensors was assessed by comparing value range and variance per setup and across setups. The accuracy was verified against the measurements conducted with the turbidimeter. Different spectral indices were calculated to set up the remote sensing-based turbidity model, and value matching with the turbidity measurements in the center locations was performed. Feature selection served to reduce the dataset to relevant variables. Models were set up and tested with turbidity and low-cost setup measurements.

The results reflect different functions that the water bodies have in the landscape, attributable to how they are built and how water and land resources are used. Turbidity ranged from 5.2 to 145 NTU across reservoirs, with a median of 13.3 NTU. The maximum reported depths were all significantly larger than the recorded ones. None of the reservoirs exceeded 4 m. This points to a problem with siltation entailing the risk of eventually drying up. The performance assessment of the low-cost turbidity sensor setups showed acceptable results for Setup A (cf. Figure 1b)) and a significantly higher variance for Setup B with one sensor failing altogether. Consequently, only data from the turbidimeter and Setup A were used for the turbidity model, where shorter wavelengths were of higher importance.

We conclude that a combination of low-cost turbidity sensors and remote sensing observations can serve as a resource-efficient option for small reservoir monitoring. Yet, low-cost sensor capabilities, failure, degradation, and high variance must be considered. It is recommended to average across sensors to improve the result, despite the higher total cost. The approach is not adapted to test for water safety and there is considerable noise in the lower value spectrum. However, the turbidity parameter can serve as a surrogate indicator for monitoring and could provide insights into wetland-water quality interactions. The approach can also serve to engage the user communities in water quality monitoring.

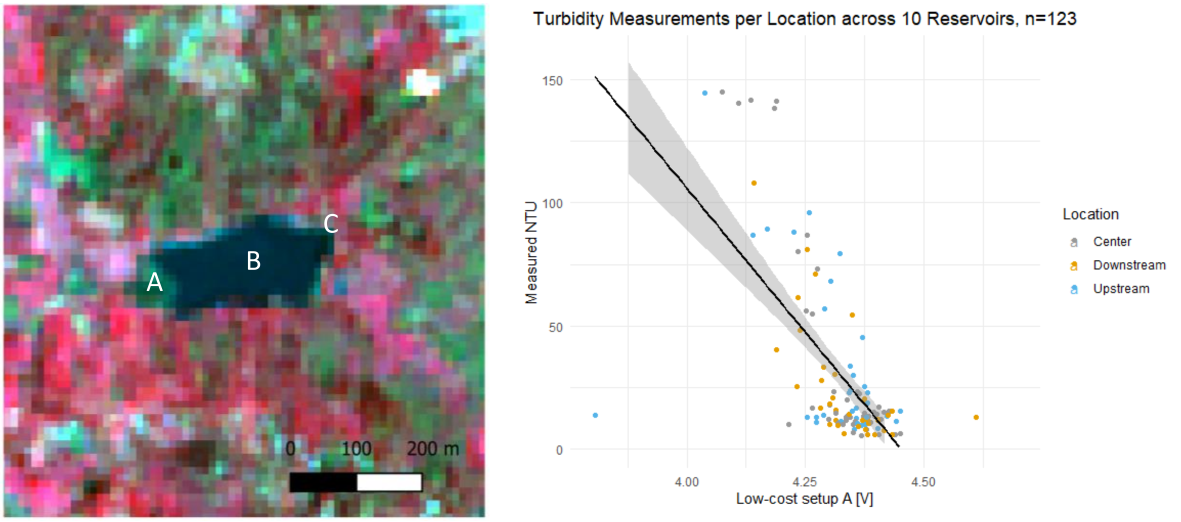

**Figure 7.** (a) Sentinel-2 false-color image (NIR-R-G) of Njeng'u Dam with sampling locations at the A-inflow, B-center, and C-outflow and (b) comparison of turbidity measured with low-cost sensor Setup A and a commercial turbidimeter for all reservoirs and locations.

# Monitoring mining operations in the Rovinari area using radar interferometry

EARSeL Bucharest 2023
Abstract
Coresponding Author:
Andrei Toma
andrei.toma3@s.unibuc.ro

Andrei Toma[1], Ionut Sandric[1]

[1]University of Bucharest, Faculty of Geography, Romania

**Keywords:** Sentinel-1; SAR; PSI; ground deformation

## Abstract

The current research focuses on mapping investigated ground surface deformation's spatial and temporal patterns in the Rovinari areas from Jiu Valley, a region with intense mining activities that have been affecting the local topography for decades, by means of Persistent Scatterer Interferometry (PSI). PSI, a powerful tool for monitoring ground surface deformation in urban and rural areas, is a remote sensing technique that utilizes synthetic aperture radar (SAR) data to measure changes in the ground surface over short and long periods. The PSI technique relies on the coherent scattering of radar signals by persistent scatterers (PS), which are usually man-made features rather than natural ones that have stable and coherent radar reflectivity over time. The PSI algorithm calculates the phase difference between pairs of SAR images and converts it into ground deformation data.

For Rovinari analysis was used a dataset consisting of 355 ASC and 281 DSC Synthetic Aperture Radar (SAR) images, free of charge, acquired by the European Copernicus Sentinel-1 A/B satellites between 2016 and 2022. The SAR images were processed using a powerful and advanced workflow developed by SARscape to generate deformation data which was later imported into ArcGIS Pro for further analysis and cartographic representation.

The results of the PSI analysis revealed significant ground surface deformation in the Rovinari area. The deformation rates ranged from about -9.19 mm/yr to 19.50mm/yr. The deformation patterns showed a clear correlation with the mining activities, with the most significant deformation rates occurring in the areas with active and abandoned mines. The time-series analysis of the PSI results revealed that the deformation rates were not constant over time. Instead, they varied, and some areas exhibited periodic patterns of deformation.

The PSI study conducted in the Rovinari area provided valuable insights into ground surface deformation's spatial and temporal patterns in a region with intense known mining activities. The analysis showed that the PSI technique is a powerful tool for monitoring ground surface deformation and identifying the most affected areas. The results of the current study can be used by local authorities and mining companies to assess the impact of mining activities and to develop mitigation strategies to reduce ground surface deformation.

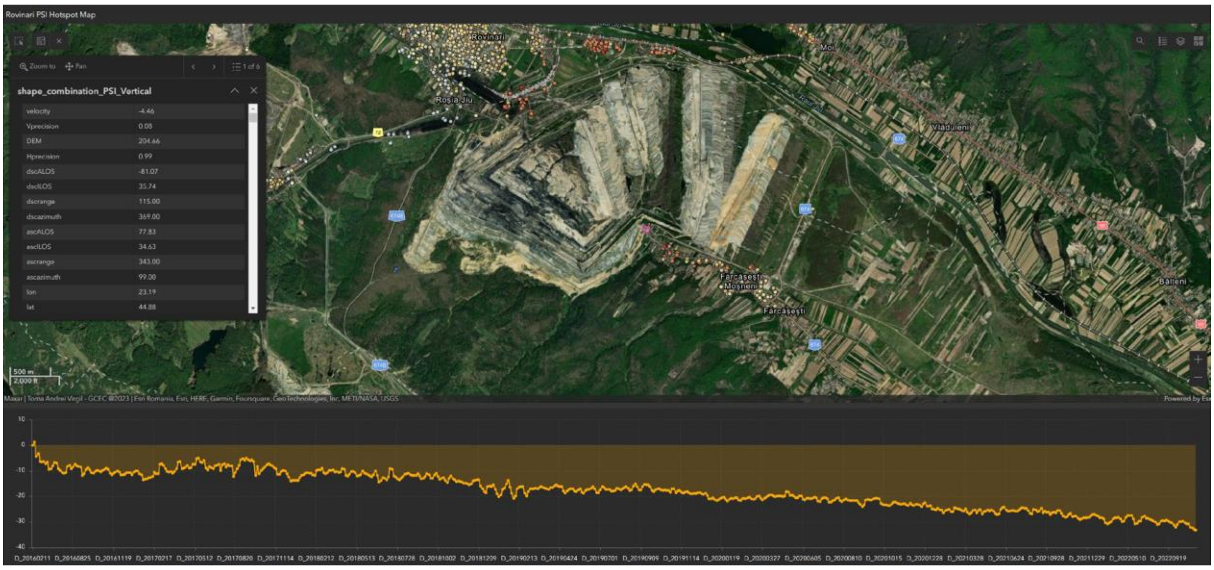
Rovinari PSI Hotspot Map

shape_combination_PSI_Vertical

| | |
|---|---|
| velocity | -4.46 |
| Vprecision | 0.08 |
| DEM | 204.66 |
| Hprecision | 0.99 |
| dscALOS | -81.07 |
| dsclLOS | 35.74 |
| dscrange | 115.00 |
| dscazimuth | 369.00 |
| ascALOS | 77.83 |
| asclLOS | 34.63 |
| ascrange | 343.00 |
| ascazimuth | 99.00 |
| lon | 23.19 |
| lat | 44.88 |

Maxar | Toma Andrei Virgil - GCFC ©2023 | Esri Romania, Esri, HERE, Garmin, Foursquare, GeoTechnologies, Inc, METI/NASA, USGS

**Figure 1.** Plotted ground deformatin for the whole scene

# Climate versus Vegetation Indices Regression Models Classification across desert-fringe ecosystem

EARSeL Bucharest 2023
Abstract
Corresponding Author:
maximsh@technion.ac.il

Maxim Shoshany[1], Sofia Mozhaeva[1]

[1] Technion, Department of Civil &Environmental Engineering, IL

**Keywords:** Vegetation Indices, Climatic Parameters, Regression, Unsupervised Classification

## Abstract

Understanding ecosystems response to climate condition change is fundamental for developing methods for wide range monitoring and mapping climate change effects on desert fringe ecosystems. Spectral vegetation indices were found in numerous earlier studies to represent water content in the terrain boundary zone. However, plants and soil moisture across desert fringes highly vary at different temporal and spatial scales due to the heterogeneity of plants, soil and rock compositions in response to changes in rainfall, evapotranspiration, lithology and disturbance regimes. Here we utilized regression between spectral vegetation indices and climatic parameters at pixel level of summer and winter Sentinel II images (25) between 2016 and 2018 representing years of high, low and average rainfall. Slope and intercept coefficients of the per pixel regression were classified utilizing ISODATA unsupervised tool for exploring temporal and spatial patterns of Vegetation Indices versus climatic parameters for a transition between Mediterranean (450mm/year) and arid ecosystems (<200 mm/year) in the south-eastern Mediterranean basin. Natural ecosystems vary from dense Mediterranean shrublands with Quercus calliprinos, Pistacia lentiscus, Ceratonia siliqua, and Rhamnus palaestinus as dominant species, to open shrublands with the same species mixed with dwarf shrubs (primarily Sarcopoterium spinosum) and winter herbaceous growth, to desert fringe Batha (steppe shrublands) dominated by Sarcopoterium spinosum and Thymelaea hirsuta and arid ecosystems characterized by moderate and low cover of Sarcopoterium spinosum with Phlomis brachyodon, Echinops polyceras, Artemisia sieberi, Thymelaea hirsute, and Noaea mucronate. Soils vary from brown Rendzina (developed on calcareous rocks) and desert lithosols.

Mapping monthly rainfall and Potential evapotranspiration (PET) for 2016, 2017 and 2018 allowed systematic assessment of accumulated rainfall and PET for between 1 and 6 month and their corresponding relationships with 16 vegetation indices representing VIS, NIR and SWIR spectral bands. The regression models were implemented for the 2 month accumulation spans with 4 climatic parameters: Rainfall, PET, Aridity Index and Water Deficit. Experimenting with different number of clusters (classification categories) allowed us to assess expressions to vegetation, soil and rock patterns. Patterns formed by the ISODATA were assessed visually in comparison to RGB orthophotographs of the region prepared and published annually by the Survey of Israel (SOI).

Figure 1 presents the regression slope and intercept information and the ISODAT map obtained for NDVI coefficients. The gray shades of slope and intercept show different gradients of change between high vegetation cover with light gray and eroded/bare surfaces with dark gray shades. The clusters' color map defined by the ISODATA provide expression for the degraded areas represented by contiguous green patches with sharp boundary (desert border?!) with adjacent semi-arid surfaces represented by purple extensions. Redish colors are associated with areas of high vegetation cover: shrubs and planted forests. Combinations of regression slope and intercepts which show sensitivity to spatial variations of vegetation, soil and rock patterns indicate their potential sensitivity to future impacts of climate change.

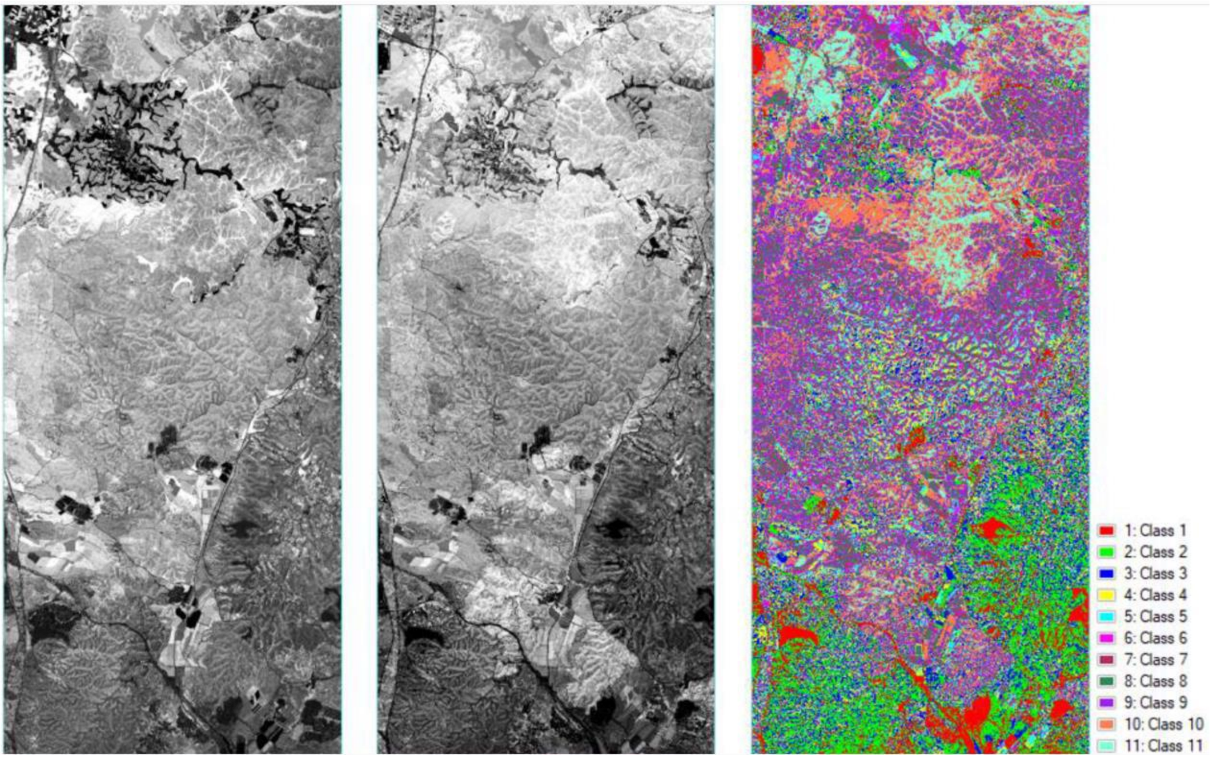

**Figure 1.** Gray shades of the regression slope coefficients (left); of the intercepts (centre) and the ISODATA clusters (right).

# Multisource point cloud fusion for forest and post-fire forest mapping: Case study from the Bohemian Switzerland National Park

EARSeL Bucharest 2023
Abstract
Corresponding Author:
marketa.potuckova@natur.cuni.cz

Alex Šrollerů[1], Eva Štefanová[1], Markéta Potůčková[1]

[1]Charles University, Faculty of Science, Department of Applied Geoinformatics and Cartography, Czech Republic

**Keywords:** point cloud, LiDAR, SfM, handheld scanner, point cloud fusion, forest, terrain, mapping

## Abstract

Airborne and RPAS laser scanning and photogrammetry are well established techniques for forest mapping and monitoring. Nevertheless, they face challenges in complex, rugged terrain consisting of e.g., steep valleys or rock formations. Due to occlusion and canopy cover, LiDAR pulses do not reach the bare earth with sufficient density to reliably model the terrain and canopy height. Mobile, handheld terrestrial laser scanners can help to overcome this problem, though, from a practical point of view, they are best suited for smaller areas.

Our study is focused on the comparison and fusion of point clouds acquired with RPAS LiDAR, photogrammetry, and a handheld laser scanner. The collected dataset is quite unique in that it covers a relatively deep and narrow valley in a sandstone area that was originally forested but has now been significantly altered due to a recent forest fire. The main objective is to evaluate the suitability of each method for forest and terrain mapping in this specific area with respect to point cloud quality. In particular, the goals are to 1) assess absolute spatial accuracy of the point clouds based on check points, 2) evaluate relative accuracy/alignment between the point clouds, 3) test existing methods (ICP, local plains) for point cloud fusion to achieve the best possible dataset for terrain and forest modelling.

The area of interest, the Deep Valley (Hluboký důl, 50.8775N, 14.3355E), is located in the Bohemian Switzerland National Park, Czechia. The scanned area captured with all three technologies covers approximately 0,1 km$^2$ and ranges from 290 to 380 m.a.s.l. It comprises steep slopes with numerous sandstone outcrops. The dominating Norway spruce forest was destroyed or considerably damaged during the fire that affected a large area of the National Park between July 22nd and August 12th, 2022. At the time of scanning, there were several standing burned spruce trunks/stumps and logs on the ground. Edges of the valley were surrounded by still surviving or not damaged patches of both deciduous (beech, birch) and coniferous (spruce, pine) forest.

The RPAS data acquisition was carried out on October 13th, 2022, i.e., at the end of the vegetation season but still during the leaf-on period. The LiDAR point cloud was acquired with a Riegl miniVUX-1 UAV laser scanner equipped with the APX-15 UAV GNSS/IMU and mounted on a hexacopter, the DJI M600. The PosPac and RiPROCESS software packages were used for trajectory postprocessing and computing the point cloud, respectively. The RGB images were collected with a DJI Phantom Pro+. The point cloud was created using Structure from Motion (SfM)/Multiview stereo in the Agisoft Metashape software package. Due to remaining trees, narrowness, and steepness of the valley, both flights could not be performed at a constant height above the terrain, which caused uneven point density/pixel size. A GeoSLAM Zeb Horizon mobile scanner was used to collect the third point cloud on November 30th, 2022. The range of the scanner was 100 m. 360° panoramic 4K images were captured with a panoramic camera Zeb Vision to colour the point cloud. In addition to that, 11 ground control points (GCP) and 10 check points (CP) were signalised on stones and stumps and measured with a GNSS/RTK receiver on October 6th, 2022, to evaluate the absolute positional accuracy of each of the acquired point clouds. Due to limited sky openings in some parts of the valley, the accuracy of the RTK measurements varied between 0.02 m and 0.10 m.

The comparison with CP revealed $RMSE_{XY}$ of 0.05 m and 0.02 m and $RMSE_Z$ of 0.09 m and 0.05 m for the SfM and GeoSLAM point clouds, respectively. The CP on the LiDAR point cloud could be evaluated only with respect to height with a resulting $RMSE_Z$ of 0.07 m. The LiDAR point cloud was collected with the lowest point density of 166 points/$m^2$, while the SfM and GeoSLAM point clouds achieved densities of 2287 (587) and 3744 (1752) points/$m^2$, respectively (in the parenthesis, there is the density after point cloud filtering/thinning). Relative comparison between the point clouds was carried out in the Cloud Compare software package. The computation of cloud-to-cloud distance on well-defined surfaces (after excluding trees) showed a very good alignment between the point clouds with mean distance of 0.10 m and 0.08 m and standard deviation of 0.09 m and 0.10 m between the LiDAR and SfM and GeoSLAM and SfM point clouds, respectively, and a mean distance of 0.10 m and standard deviation of 0.09 m between the LiDAR and GeoSLAM point clouds (see also histograms in Figure 1). Further tests with point cloud fusion methods will be evaluated, nevertheless, considerable improvement in point cloud alignment is not expected. Visual inspection of individual point clouds and their superimposition revealed that the GeoSLAM's added value was in better capturing burned tree trunks, tree crowns, and steep, nearly vertical slopes, and sandstone outcrops occluded in both SfM and LiDAR point clouds. It also aided in the identification of logs. In comparison to SfM, the LiDAR point cloud better describe the structure of tree canopy (where applicable). In comparison to GeoSLAM, very few LiDAR echoes corresponded to standing burned trunks and burned logs with low reflectivity, due to the longer measurement range and lower pulse repetition frequency.

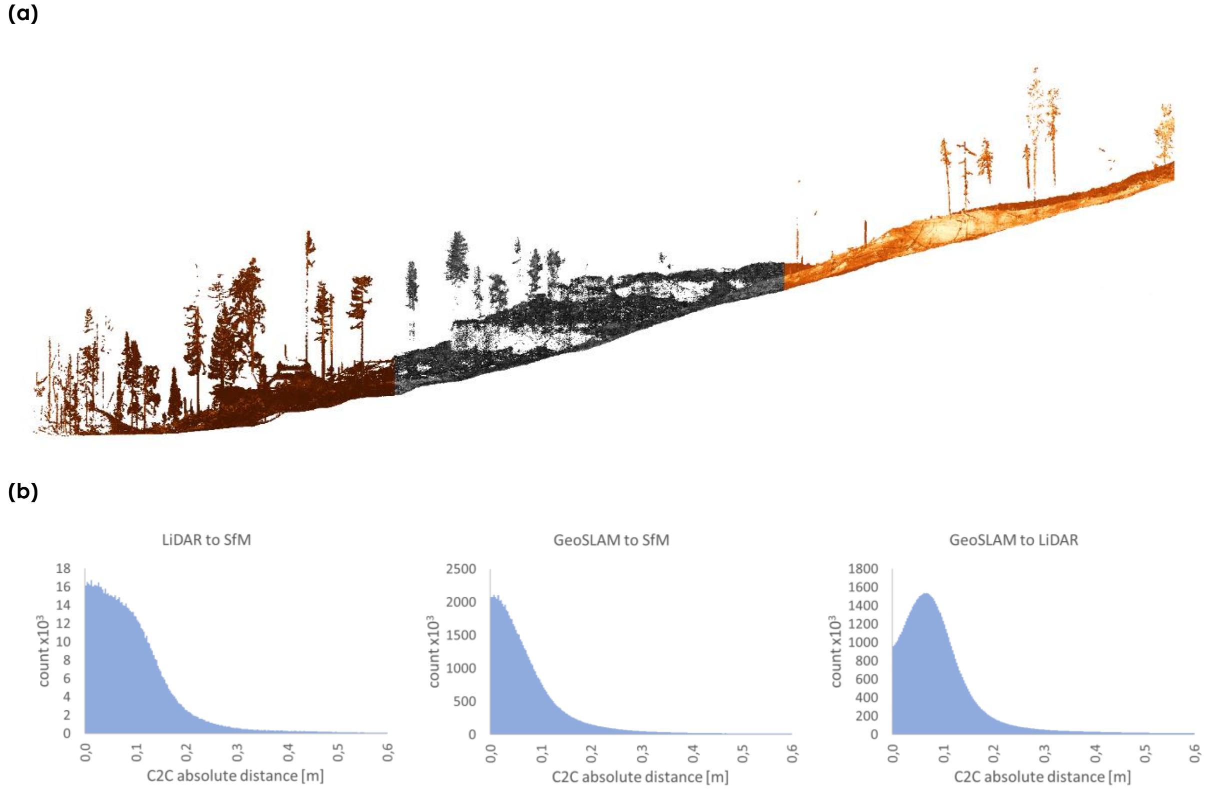

**Figure 8.** (a) a profile of captured point clouds: from left to right GeoSLAM, LiDAR, SfM and (b) histograms of cloud-to-cloud absolute distances

## Section IV - Land cover mapping and monitoring for supporting decisions in agriculture

# METHODOLOGICAL PROPOSAL FOR OPERATIONAL MONITORING OF AGRICULTURAL DYNAMICS IN CENTER PIVOTS IRRIGATION AREAS IN BRAZIL USING SENTINEL 2 IMAGERY

EARSeL Bucharest 2023
Abstract

Corresponding Author:
hugo.bendini@inpe.br

Hugo do Nascimento Bendini[1], Leila M. G. Fonseca[1], Luiz M. L. Pascoal[1], Philippe Rufin[3,4], Caio A. Bertolini[1], Tharles S. Andrade[1], Ravi F. Mariano[1], Renato G. Silvério[1], Pedro L. Santos[1], Daniel A. C. Ferreira[2], Thiago H. Fontenelle[2]

[1] National Institute for Space Research (INPE), Department of Earth Observation, Brazil
[2] National Water and Sanitation Agency (ANA), Brazil
[3] Humboldt-Universität zu Berlin, Geography Department, Germany
[4] Université Catholique de Louvain, Earth and Life Institute, Belgium

**KEYWORDS:** AGRICULTURE MONITORING, TIME SERIES, PHENOLOGY, EARTH OBSERVATION, MACHINE LEARNING

## Abstract

Agriculture is the biggest global consumer of water, with irrigated areas constituting 40% of the total area used for agricultural production. The rate of increase in irrigated areas was approximately 2.6% per year, going from 95 million hectares (Mha) in the 1940s to 280 Mha in the early 1990s. FAO estimates that 80% of food needs in 2025 will be covered by irrigated agriculture and more than 324 million hectares are equipped for irrigation in the world. In Brazil, irrigated agriculture is responsible for 46% of withdrawals from water bodies and for 67% of consumption in relation to the total volume of water collected, representing the highest consumptive use in the country. Center pivot irrigation systems account for more than 50% of the expansion of the irrigated area in the last 20 years. Understanding how different crops use water over time is essential for planning and managing water allocation, water rights, and agricultural production. Analysing the dynamic of water use in agriculture requires information on the crop types that are planted in irrigated areas. Phenological metrics extracted from dense time series of medium-resolution satellite images have been successfully used to classify crop types since they capture variations in the agricultural calendar (Bendini et al., 2019). In addition, phenometrics allow the inference about the emergence and harvesting periods, as well as the duration of the crop cycle, which is essential for understanding the periods of high water demand. We proposed a methodology for monitoring agricultural dynamics in center pivots in Brazil, based on the use of Sentinel-2 EVI (Enhanced Vegetation Index) time series obtained from Google Earth Engine (Figure 1), and the methods developed by Bendini et al. (2019). An objective protocol was defined for visual inspection of the Sentinel-2 EVI time series for labelling the training samples. The considered crop type classes were Double cropping (summer crops and a second crop with a short cycle, usually maize) (DC), Double and long crops (summer crops and a second crop with a longer cycle, usually cotton) (DLC), Winter crops (summer crops and a second crop cultivated during the winter) (WC), Perennial crops (mostly coffee plantations) (P), Semi-perennial crops (usually sugarcane) (SP), Single crops (only one crop season during the year) (SC), and Triple cropping (more than two crop cycles during the crop year) (TC). A user-friendly web application named Earth Surface Point Inspection Application (ESPIA), hosted at https://espia.snirh.gov.br, was developed to carry out the inspection of points by trained interpreters. The ESPIA application was organized into four main components: Visual Interface, Server, Data Layer, and External APIs. Its architecture is in line with current

trends in software development based on web services and the Open Geospatial Consortium (OGC) standards, so the implementation of communication between client and server, via REST requests, allows greater performance and dynamism in the presentation of data on the system's interactive map. For assessing the robustness of the method, we did a transferability analysis using a model trained with samples collected during the 2020/2021 crop year, in order to predict the crop types for the 2021/2022 crop year, and vice-versa. The obtained overall accuracy was, respectively 90% and 88%. Major confusion was found between Winter crops and Double crops, and also between Semi-perennial crops and Single and Perennial crops, which can be related to inaccuracies during the labelling and in the detection of the second agricultural crop. The last issue is mainly due to the limitations for the pre-processing methods for interpolating and smoothing the EVI time series. Future works involve testing other methodologies for the pre-processing of the time series and for extracting the phenological metrics. We also aim to expand the application of this method for irrigated agriculture areas by other irrigation systems in other biomes, such as the Caatinga and Pampas. This work is in the context of the project "Irrigated Agriculture Based on Remote Sensing Technologies to Update and Improve ANA's Atlas Irrigation", developed by INPE and ANA (Process CNPq 423959/2021-2), which aims at developing a method for automatically mapping irrigated agricultural land and estimating water use in Brazilian irrigated agriculture. The methodology is already being used by the National Water and Basic Sanitation Agency (ANA), and the results are compiled annually in the Irrigation Atlas (ANA, 2021), available at https://www.snirh.gov.br/.

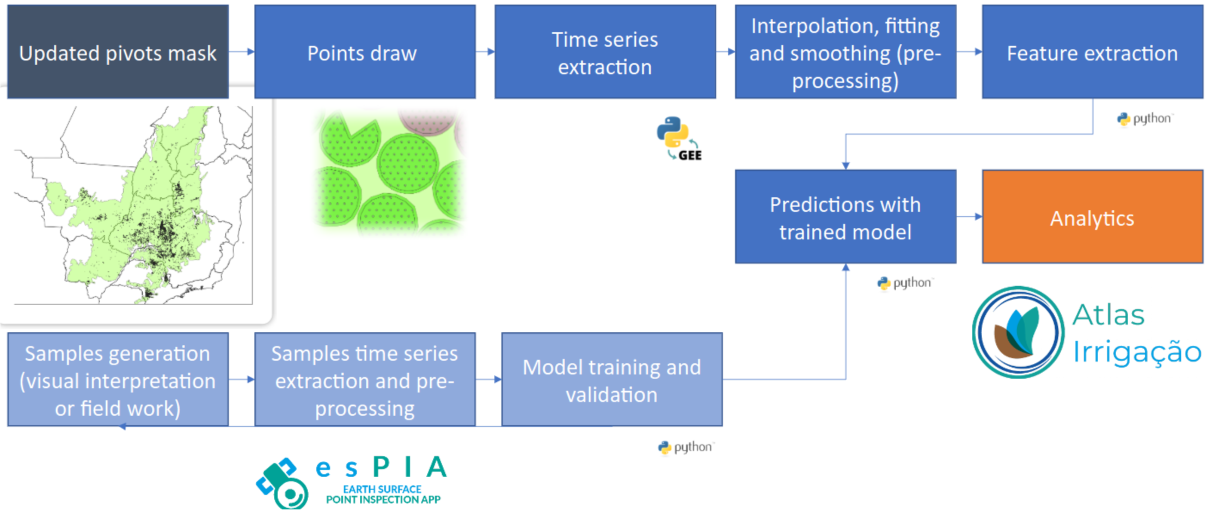

**Figure 1.** Framework for the proposed methodology for monitoring irrigated agriculture in Brazil.

EARSeL Bucharest 2023

Abstract

# Products for Monitoring of Agriculture from Earth Observation Time Series and Very High Resolution Data

Corresponding Author:
Ursula.gessner@dlr.de

Ursula Gessner[1], Sarah Asam[1], Andreas Hirner[1], Jennifer Kriese[1], Jonas Meier[1], Sophie Reinerman[2], Martina Wenzl[1]

[1] German Aerospace Center (Dlr), German Remote Sensing Data Center (Dfd), Germany
[2] Julius-Maximilians-Universität Würzburg, Germany

**Keywords:** Cropland, grassland, crop rotation, mowing, harvest dates, landscape elements, biodiversity

## Abstract

Today, agriculture faces multiple challenges, in Europe and at global scale. A growing population and changing dietary habits lead to an increasing demand for food, and agricultural products are furthermore required by the rising bioenergy market. At the same time, climate change and the global decline in biodiversity and natural assets necessitate sustainable production methods and climate adaptation measures in agriculture. Earth Observation allows contributing data and information products that can be used by a wide range of stakeholders – from farmers over scientist to public agencies – for finally supporting knowledge-based decisions.

This contribution presents a palette of earth-observation-based products for cropland and grassland that have been developed by the group ‘Agricultural and Forest Ecosystems’ at the German Remote Sensing Data Center (DFD) of the German Aerospace Center (DLR). Originating from mainly third party-funded research projects, the analyses have a regional focus on Germany and Africa. The presented products on crop type distribution, crop rotation and crop diversity are based on machine learning, integrating multi-sensor spatial-temporal time series features. Further, time series analyses are applied to detect crucial management events. Examples are the identification of harvest dates in cropland, as well as the detection of mowing events in grassland, including the timing and annual frequencies of mowing. Such information on management activities, their timing and intensity is relevant for estimating fertilizer inputs and nitrogen fluxes, for example. Additionally, grassland biomass and proxies for cropland productivity are quantified. All above mentioned information products are based on either multispectral Sentinel-2 time series, or on a combination of Sentinel-2 and Sentinel-1 SAR data. These data provide information on the complete growing cycle, even at times and in regions of high cloud coverage. According to the technical characteristics of Sentinel-2 and Sentinel-1, these datasets feature a spatial resolution of 10-20 m. Furthermore, we use very high resolution earth observation data to delineate small features in agricultural landscapes. Hedges and other linear woody features are detected based on aerial imagery and deep learning techniques, using a large in-situ reference data base. Knowledge on the distribution of small natural elements in agricultural landscapes allows assessing spatial diversity of such landscapes, and contributes to a better understanding of nutrient and water fluxes, erosion and biodiversity. Finally, for a better understanding of droughts and heat waves and of their impact on agricultural landscapes, long time series from sensors such as MODIS which span over more than two decades are used for assessing vegetation stress from a long-term perspective. These analyses are currently being complemented by time series of more recent missions such as Sentinel-3 in order to guarantee continuity also after the lifetime of MODIS. In combination with this spatially coarse (250-200m) information, higher

resolution time series of Sentinel-2 allow evaluating – for the last few years – crop type specific drought effects and vegetation stress at field scale. The datasets presented are on the one hand an important foundation for further geoscientific studies and are either analysed directly or used as input for modelling. But likewise, they serve as an information basis for actors and decision makers in the field of agriculture and can be, for example used to simplify workflows and support planning.

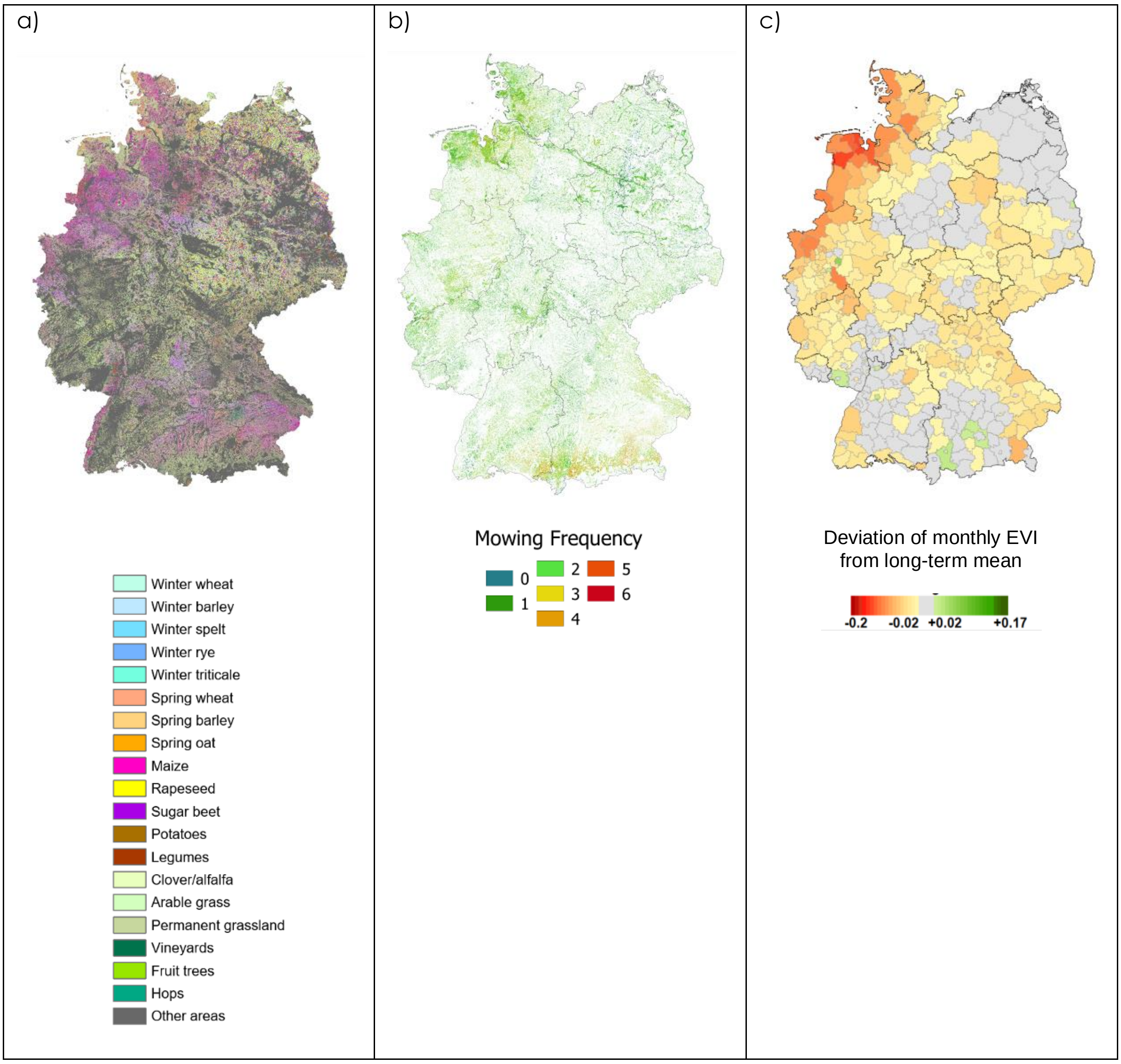

**Figure 9.** Selected earth observation based products for Germany (a) Crop type map 2018 (after Asam et al. 2022); (b) Mowing frequency map 2020 (after Reinermann et al. 2019); (c) Vegetation stress on cropland in August 2018 (after Reinermann et al. 2022)

# The Data Cube of ERATOSTHENES Centre of Excellence to empower environmental monitoring in EMMENA Region

EARSeL Bucharest 2023
Abstract

Corresponding Author: Stelios Neophytides
stelios.neophytides@eratosthenes.org.cy

Stelios Neophytides[1], Thanasis Drivas[2], Christiana Papoutsa[1], Charalambos Kontoes[2], Diofantos Hadjimitsis[1]

[1]ERATOSTHENES Centre of Excellence, Environment and Climate, Cyprus
[2]National Observatory of Athens, Greece

**Keywords:** Earth Data Cube, Big Data, Earth Observation, Remote Sensing, Agriculture

## Abstract

Over the last few years, we have been passing through the era of Big Data, and nowadays, we must deal with uninterrupted streams of large volume of data. When dealing with the Big Data challenge in Earth Sciences, the complexity of the data format is rapidly increased due to the vast number of images obtained by different sensors and satellites in combination with data from other remote sensing sources, such as aerial and terrestrial. Thus, the necessity of constructing Earth Data Cubes is rising to overcome this obstacle, not only in terms of storing the data, but also in processing the data. For a better understanding of the ecosystems and to create models as tools for decision-making, the integration of historical data into reference frameworks is essential. Therefore, an Earth Data Cube is constructed under a spatiotemporal scheme (figure 1). That accumulation of knowledge can facilitate data processing for studying the trends and the dynamic responses of the various ecosystems under stress. Furthermore, Earth Data Cubes are also easing the time series trends analysis, forecasting environmental stresses and monitoring land cover dynamics, among other, across an ecosystem (e.g., agricultural zones, forests, wetlands, etc.)

For constructing and developing the Data Cube of ERATOSTHENES Centre of Excellence to support the environmental monitoring, we used the Open Data Cube (ODC), an Open-Source Geospatial Data Management software providing engineers and researchers with tools to develop the Cube. An ODC ecosystem (figure 2) is characterized from the Satellite Data that are ingested to the Cube, alongside with ODC Core which offers a unified environment for analysing gridded data from various satellite and other data collection systems, with access to decades of earth observation satellite data that is ready for analysis. ODC Core is combined with ODC Algorithms and ODC applications. From the output, each distinct user, can manipulate the ingested satellite data for different usages such as crop type mapping, vegetation dynamics derivation, deforestation risk assessment, water resources quality and management, illegal mining and other applications. In addition to satellite imagery data, ODC can also encompassing a variety of information, including topographic models, grids based on physical characteristics of the Earth, surfaces derived from interpolated data, and output from computer models.

After the data acquisition from the different repositories, a procedure of data pre-processing to provide users with Analysis Ready Data (ARD) was implemented. Regarding pre-processing, for example Sentinel-2 imagery data are pre-processes in order to diffuse any atmospheric noises and mask areas covered from clouds. To decrease the need for storage and face the big data volume, we converted our GeoTiffs to a new format named Cloud Optimized GeoTiff.

The most important step in constructing a Cube is the description of metadata to index those different data in a PostGIS database (based on PostgreSQL). The final shape of our Data Cube will be fed with data from Sentinel-2, Sentinel-1, different NASA's MODIS (Moderate Resolution Imaging

Spectroradiometer) products (Vegetation Indices 16-Day L3 Global 250 m, Vegetation Continuous Fields Yearly L3 Global 250 m, Vegetation Indices Monthly L3 Global 1 km, Leaf Area Index/FPAR 8-Day L4 Global 500 m, Burned Area Monthly L3 Global 500 m, Land Surface Phenology (Land Cover Dynamics) Yearly L3 Global 500 m), Corine Land Cover data maps from COPERNICUS Land Services, and Digital Elevation Models (Copernicus EU DEM v1.0m which is a fusion of SRTM and ASTER GDEM), among other types of products. Open Data Cube framework characterize each type of data as product, and we also need to generate unique YAML files to describe the metadata for each product type.

The next step is the establishment of the developed Earth Data Cube to cover other countries in the EMMENA (Eastern Mediterranean, Middle East and North Africa) region and Europe, too, as an initiative of ERATOSTHENES Centre of Excellence to gather stakeholders and local authorities to provide a tool for improving management practices and creating new mitigation and planning strategies regarding different environmental threats. That will lead to a sustainable and greener ecosystem (agriculture, water resources, soil, etc) in the region by achieving a balance between ecological, social, and economic values. Among our future works, the development of a set filled with jupyter notebooks in Python for different use cases will be established, among an online exploitation platform as Web-Service in a Docker environment with Layers deployed to serve the community of researchers and citizens who are in interest of using earth data for environmental monitoring. Furthermore, one of the tasks of EXCELSIOR H2020 Teaming Project is the establishment of a Ground Receiving Station, acquiring satellite data near real- time covering the EMMENA region and data pipelines will best developed to host those data in our Data Cube.

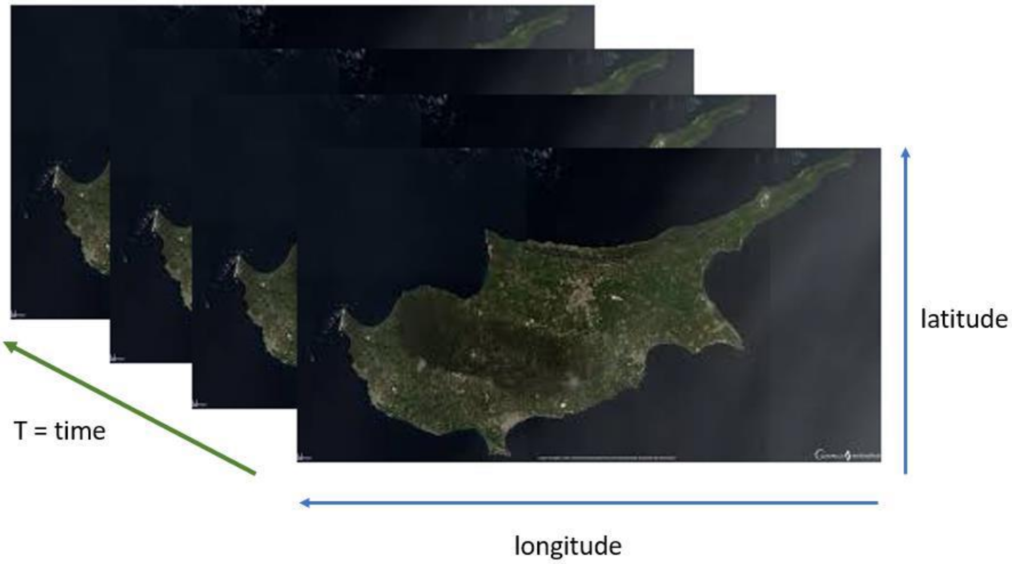

**Figure 1.** Spatiotemporal scheme of Cyprus' Data Cube

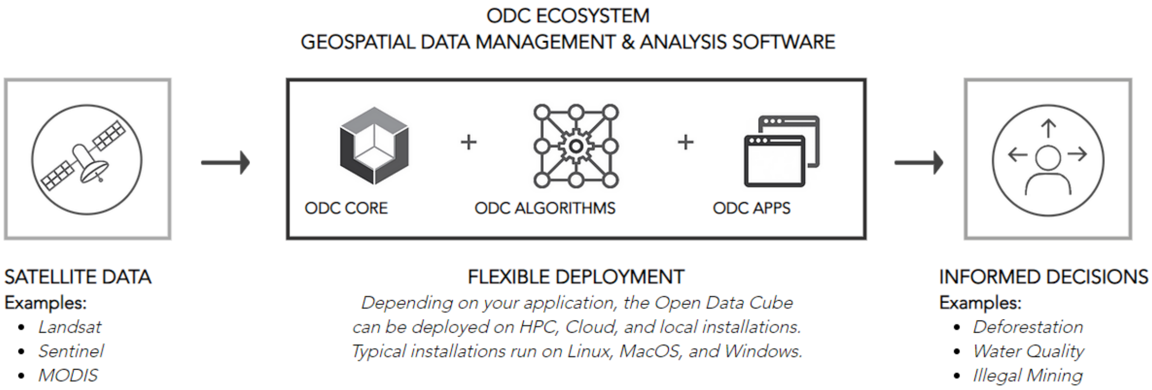

*Depending on your application, the Open Data Cube can be deployed on HPC, Cloud, and local installations. Typical installations run on Linux, MacOS, and Windows.*

**Figure 2.** ODC Ecosystem (source: https://www.opendatacube.org/overview)

# Quantification and Mapping of Non-Photosynthetic Cropland Biomass Using Laboratory Hyperspectral Data and Machine Learning

EARSeL Bucharest 2023
Abstract

Corresponding Author:
Stefanie.Steinhauser@lmu.de

Stefanie Steinhauser[1], Matthias Wocher[1], Andrej Halabuk[2], Svetlana Košánová[3] and Tobias Hank[1]

[1] Ludwig-Maximilians-Universität München (LMU), Department of Geography, Germany

[2] Slovak Academy of Sciences, Institute of Landscape Ecology, Slovakia

[3] Constantine the Philosopher University in Nitra, Department of Ecology and Environmental Science, Slovakia

**Keywords:** remote sensing, hyperspectral, NPV, SVR, agriculture, PRISMA, EnMAP

## Abstract

This study covers the development of a model quantifying non-photosynthetic vegetation (NPV) [$g/m^2$], based on hyperspectral laboratory data using a supervised machine learning algorithm. Due to its influence on nutrient, carbon and water cycles, NPV plays an essential role in both, agricultural and natural systems. For agricultural applications, two forms of NPV are of particular interest: 1) late growth stage crops, and 2) crop residues (CR). The quantification of NPV biomass has rarely been possible due to the lack of large scale and high temporal resolution hyperspectral data. With a new operating generation of spaceborne spectrometers, such as the PRecursore IperSpettrale della Missione Applicativa (PRISMA) or the Environmental Mapping and Analysis Program (EnMAP), these data now become accessible across the globe and open up new possibilities for large scale NPV-mapping. Due to similar spectral properties in the VNIR, distinguishing NPV from bare soils is difficult. However, NPV can be spectrally distinguished from bare soil in the shortwave infrared (SWIR) domain (approximately 1400- 2500 nm) due to the absorption of non-pigmented organic molecules, mainly lignin and cellulose. For example, the narrow band cellulose absorption index (CAI) measures the relative depth of the cellulose absorption near 2100 nm. Based on laboratory measured hyperspectral data, using an ASD FieldSpec4 (FS4) Standard spectrometer (350-2500 nm), six different models were developed based on support vector regression (SVR). Thereby the CAI, the SWIR domain and the full spectrum were evaluated as training input. Eleven different NPV concentrations with a maximum of 1000 [$g/m^2$] were measured in logarithmic intervals, which were summarized into four quantitative categories (0-50 [$g/m^2$], 50-150 [$g/m^2$], 150-450 [$g/m^2$], 450-1000 [$g/m^2$]) for further processing and evaluation of the model results. To assess the performance of the various models, field measurements of both, standing NPV as well as CR, were compared to the model estimations of NVP biomass. Moreover, two satellite scenes from PRISMA and EnMAP were acquired over the same test site as the field measurements in the MNI test area northeast of Munich, Germany. In addition, further validation data from 107 sampling points were collected on October 8th 2021 parallel to a PRISMA acquisition in the area around Levice (Slovak Republic). For a qualitative assessment of NPV abundancy, the land cover was differentiated into six different land categories. As the most promising model, an approach based on a scaled version of the CAI was determined, returning 0.62 $R^2$, 0.23 NRMSE and 106.88 [$g/m^2$] MAE. Applying the selected laboratory trained model to open sky satellite data from PRISMA and EnMAP demonstrates that NPV biomass can be quantitatively estimated in realistic dimensions (Fig. 1). Furthermore, the results show that bare soil and NPV can successfully be separated. Nevertheless, limitations are revealed for stronger NPV biomass above 400-500 [$g/m^2$]. None of the models perform well and misestimate the biomass for standing senescent NPV above these high weights pe ground area. Different soil and crop types, soil moisture as well as atmospheric influences can affect the

NPV detection. Moreover, spatial heterogeneity of the material can strongly influence the mixed spectrum that is observed by medium resolution spaceborne sensors. Leaf area, leaf orientation, angular distributions as well as density and spatial arrangement are also contributing to the spectral signal in the considered domain. Given the new possibilities and now vastly increased availability of hyperspectral datasets from satellites, large scale research to fully understand dynamics and effects of NPV can be conducted.

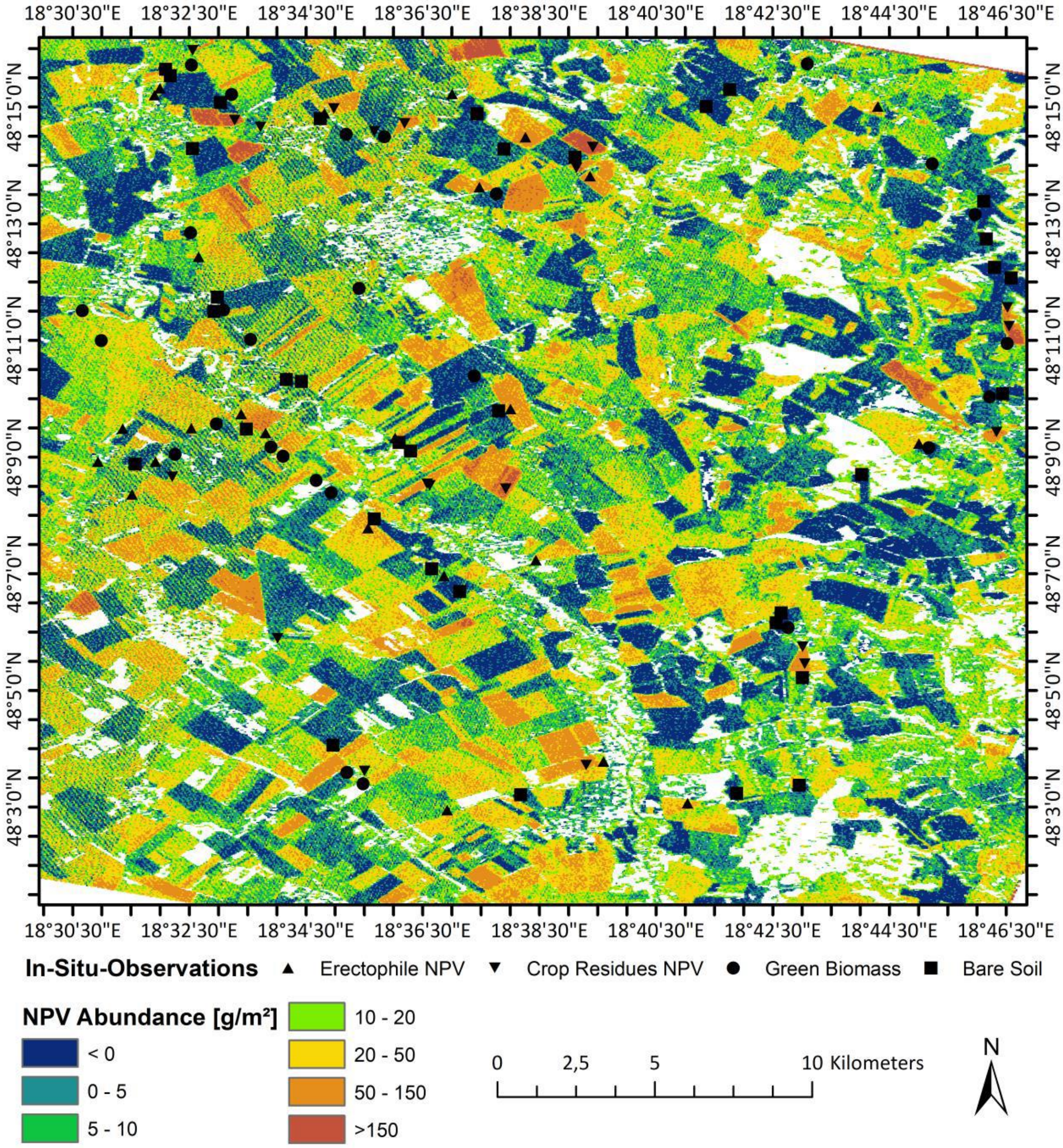

**Figure 1.**

Quantitative NPV map derived from PRISMA data acquired on October 8th 2021 in the area around Levice (Slovak Republic). The map was created using an SVR model that was pretrained in the laboratory based on destructively sampled NPV data. For a qualitative assessment, six different land categories, including 107 sampling points, were obtained and merged to four land cover classes. Due to the image classification, only crops and grasslands, as well as bare soil areas are mapped.

## Section V - Monitoring and mapping multi-hazards under climate change

# Spatiotemporal characteristics of drought and their impacts on cropland vegetation over the Lower Mekong Basin using satellite-based time-series observations

EARSeL Bucharest 2023
Abstract
Corresponding Author: Tuyen V. Ha
Email address: tuyen.havan@dlr.de

Tuyen V. Ha[1,2*], Soner Uereyen[1], Juliane Huth[1], and Claudia Kuenzer[1,2]

[1]German Remote Sensing Data Center (DFD), German Aerospace Center (DLR), Oberpfaffenhofen, 82234 Wessling, Germany

[2]University of Wuerzburg, Institute of Geography and Geology, Department of Remote Sensing, Am Hubland, 97047 Wuerzburg, Germany

**Keywords**: Drought, Remote sensing, NDVI, Lower Mekong Basin

## Abstract

Drought is a recurring slow-developing natural hazard phenomenon with a significant impact on both economy and the environment. The Lower Mekong Basin (LMB) is a major crop-producing area worldwide and is becoming more vulnerable to drought hazards. Understanding the spatiotemporal characteristics of drought and their impacts on cropland vegetation is essential for drought early warning management, mitigation efforts, and agricultural development planning. In this study, we present a recent detailed analysis of the space-time characteristics (e.g., drought onset and cessation, drought events, intensity, frequency, and inter-arrival time) over the LMB using remote sensing-based and meteorological variables (e.g. Soil Water Deficit Index and/or Vegetation Condition Index) between 2000 and 2021. In addition, we investigated the impacts of drought events on cropland vegetation during the dry and rainy growing seasons based on MODIS Normalized Difference Vegetation Index (NDVI) using linear regression. Results showed that the LMB suffered from frequent and prolonged drought conditions. Most of the prolonged drought events were recently observed in the Vietnamese Mekong Delta, eastern Thailand, and the surrounding areas of Cambodian Tonle Sap Lake. In addition, these areas are characterized by high drought intensity and inter-arrival time. Drought duration over the LMB lasts, on average, from three to four months. The onset of severe drought conditions was commonly found from January to February in the Vietnamese Mekong Delta, whereas the onset in eastern Thailand was earlier, between November and December. During the past 21 years, the cropland vegetation suffered from great variations in space and time, especially observed in the Vietnamese Mekong Delta and Cambodian lowland areas. The findings of this study could provide crucial information for regional and local drought early warning management and agricultural planning in the context of increasing climate change and human-induced impacts.

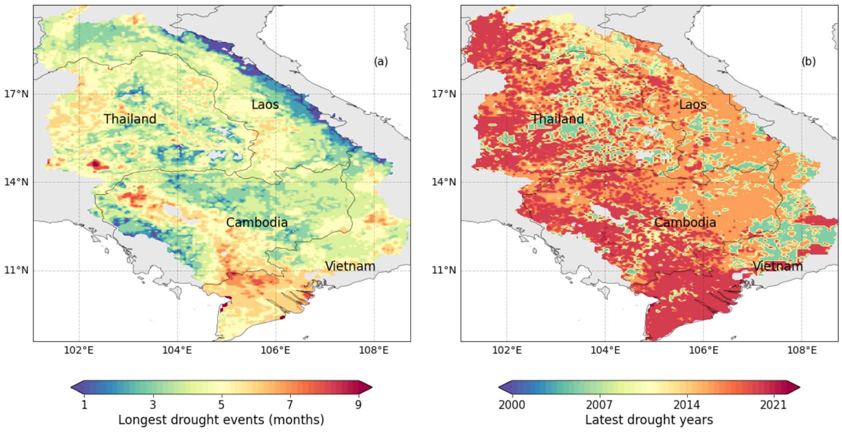

**Fig. 1.** Spatial variations of longest drought events (a) and its occurrence years (b) over the LMB from 2000 to 2021

---

# Mapping Soil Erosion Intensity Based On Multitemporal Sentinel-1 SAR and Sentinel-2 MSI Satellite Imagery. An Inter-Comparison Approach Using In-situ Measurements

EARSeL Bucharest 2023
Abstract
Corresponding Author:
marina.virghileanu@geo.unibuc.ro

Marina Vîrghileanu[1], Bogdan-Andrei Mihai[1], Ionuț Săvulescu[1]

[1]University of Bucharest, Faculty of Geography, Department of Geomorphology-Pedology-Geomatics, Romania

**Keywords:** soil erosion, satellite imagery, multi-sensor data, multitemporal images, Sentinel

## Abstract

Soil erosion by water is one of the most significant worldwide environmental problem, causing serious losses of fertile topsoil affecting the land production capacity. Therefore, mapping and monitoring the spatial distribution of areas affected by soil erosion processes is essential for environmental monitoring, land management and regional planning strategies.

Mapping soil erosion based on remotely sensed data is a difficult task, generally targeting the delineation of some features (rills, gullies), as a consequence of the higher spectral similarities between degraded areas and different land cover classes. However, the integration of multitemporal radar and optical imagery, together with in-situ measurements, can help the discrimination of the affected areas by increasing their spectral separability.

In this respect, our paper aims to compare and assess the suitability of multi-source and multitemporal input imagery, acquired by Sentinel-1 SAR and Sentinel-2 MSI sensors, as well as derived spectral and biophysical indices, integrated together with in-situ training samples for soil erosion intensity mapping. The analysis focuses on several test-sites from Romanian Carpathians and Subcarpathians, where a complex land cover with a strong anthropogenic influence (agriculture, traffic and oil industry) creates favourable conditions for the intensification of soil erosion process.

The approach is organized between three levels. First, all the satellite images are pre-processed in order to obtain geometrically and radiometrically calibrated data. The second level focuses on searching a

group of derived spectral and biophysical indices suitable for soil erosion analysis, as well as on testing different data extraction methods in order to design the most effective workflow for soil erosion intensity mapping. The third level focuses on the validation of the obtained results with in-situ measurements data, consisting in soil erosion intensity level obtained through soil sample profiles from selected locations. For each soil profile, the surface horizon is identified and measured and then compared with the reference standards for the given soil types.

The results show good overall accuracies for mapping the soil erosion intensity with three classes (low, moderate and high) for several tested indices (around 70%), with the help of in-situ measurements of soil samples. Particularly, better accuracies are obtained for the high soil erosion intensity class with the help of Soil-Adjusted Vegetation Index (SAVI) and Degraded Land Area (DAI) indices (around 83%) and for moderate soil erosion intensity class with the help of the Leaf Chlorophyll Index LCI (99%). Regarding the pixel-based classification approach, better accuracies are obtained by using multi-sensor and multi-date input imagery, with an overall accuracy of 93%, respectively of 66% for the soil erosion class.

EARSeL Bucharest 2023
Abstract

Corresponding Author:
niels.dedring@ruhr-uni-bochum.de

# HEC-RAS simulation of a Glacial Lake Outburst Flood to determine potential impacts using the example of Chamlang North Tsho (Lake 464) in the Hongu Valley, Nepal

Niels Dedring[1], Dr. Valerie Graw[1], Jun. Prof. Dr. Andreas Rienow[1]

[1] Ruhr-University Of Bochum, Department Of Geography, Germany

**Keywords:** Glacial Lake Outburst Flood, HEC-RAS, Sentinel-1

## Abstract

A so-called "Glacial Lake Outburst Flood" (GLOF) describes the sudden release of water from a glacial lake, regardless of the cause or trigger mechanism. In the event of a moraine dam failure, a GLOF occurs in which outflows of several tens of thousands of cubic metres of water per second, together with mud and debris, can flow downslope for well over 100 km in the shortest possible time. The resulting flood wave poses a major socio-economic threat to the downstream population as well as neighbouring villages and infrastructure. This problem will be illustrated in the context of this study using the example of Chamlang North Tsho (Lake 464) in the Hongu Valley, in eastern Nepal. This lake has a very high exposure for a GLOF due to the direct adjacent glacier and the steep slopes with numerous ice overhangs and gradients of up to 80°. The objective of this work was to determine the extent to which only freely available data in conjunction with HEC-RAS is sufficient to simulate a GLOF for the Chamlang North Tsho. Based on those results, it should be determined which measures and adjustments can be taken to reduce the risk of an outbreak of the lake and its impacts in the event of a GLOF. The analysis is divided into two sub-analyses. First, the determination of the current extent of the lake and its development in recent years on basis of Sentinel-1A data, and secound, a GLOF modelling and simulation of the Chamlang North Tsho using HEC-RAS. The two sub-analyses build on each other and the results of the first sub-analysis are used for the simulation in the second sub-analysis.

The radar analysis used Sentinel-1A data (IW) of each August and September from 2014 to 2021. A slightly positive growth for the lake can be derived from the data for each individual year and for the overall period. In 2014, the lake area's size was 861287.91 m² and in 2021 already 892219.09 m². This results in an absolute increase in area of 30931.18 m² or a relative increase of around 3.59 % over the considered period. Due to the small difference in height between the lake level and the terminal moraine of the glacial lake of less than one metre, the maximum size of the lake can be assumed. The data required for a GLOF simulation consists of a digital terrain model, land cover data with the respective roughness coefficients according to Manning and Strickler or Manning's n values, data on the surface, depth and volume of the lake itself, and Open Street Map data. The used digital terrain model is based on radiometrically terrain corrected ALOS PALSAR data with an interpolated resolution of 12.5 m. The ESA WorldCover 2020 was used to represent the land cover and corrected and enhanced along the adjacent

course of the Hunku Dranka and Dudhkoshi rivers. Open Street Map data with the attributes "buildings", "bridges" and "roads" were then used to roughly determine potential impacts and damages and blended with the results of the GLOF simulation. Numerical models based on other glacial lakes in the Himalayas were used to estimate the maximum and average depth as well as the volume of the lake. The most frequent trigger for GLOFs in the Himalayas are avalanches. Therefore, an avalanche was also chosen for this simulation. For this purpose, three scenarios with different sizes of avalanches were created ($5 \times 10^4$ $m^3$, $9 \times 10^5$ $m^3$, $6.6 \times 10^6$ $m^3$) and an erosion of the terminal moraine of 20 m was assumed.

Due to missing in situ data as well as high-resolution geodata (especially DEM) and the lack of references, a validation of these results is unfortunately not possible. Nevertheless, the results of the simulation, especially under the medium avalanche scenario (9 x 105 $m^3$), are very close to the results of two past studies of a GLOF simulation (one-dimensional) on Chamlang North Tsho. In this simulation, the GLOF came to a halt just before the Dudhkoshi flows into the Sunkoshi. This flood wave thus travelled almost 110 km and affected an area of approximately 12.312 $km^2$. In total 71 buildings, 7.051 km of roads and paths and 22 bridges are situated within the affected area. In summary, this study was able to show that a GLOF simulation can be created worldwide using only freely available data and software applications, and that initial statements about its course and possible impacts can be derived. For the Chamlang North Tsho, despite its remote location, a very extensive damage picture emerged. Accordingly, field research on the Chamlang North Tsho and the terminal moraine should be undertaken in the near future in order to better assess the risks and to be able to make a more valid simulation of possible impacts.

a)

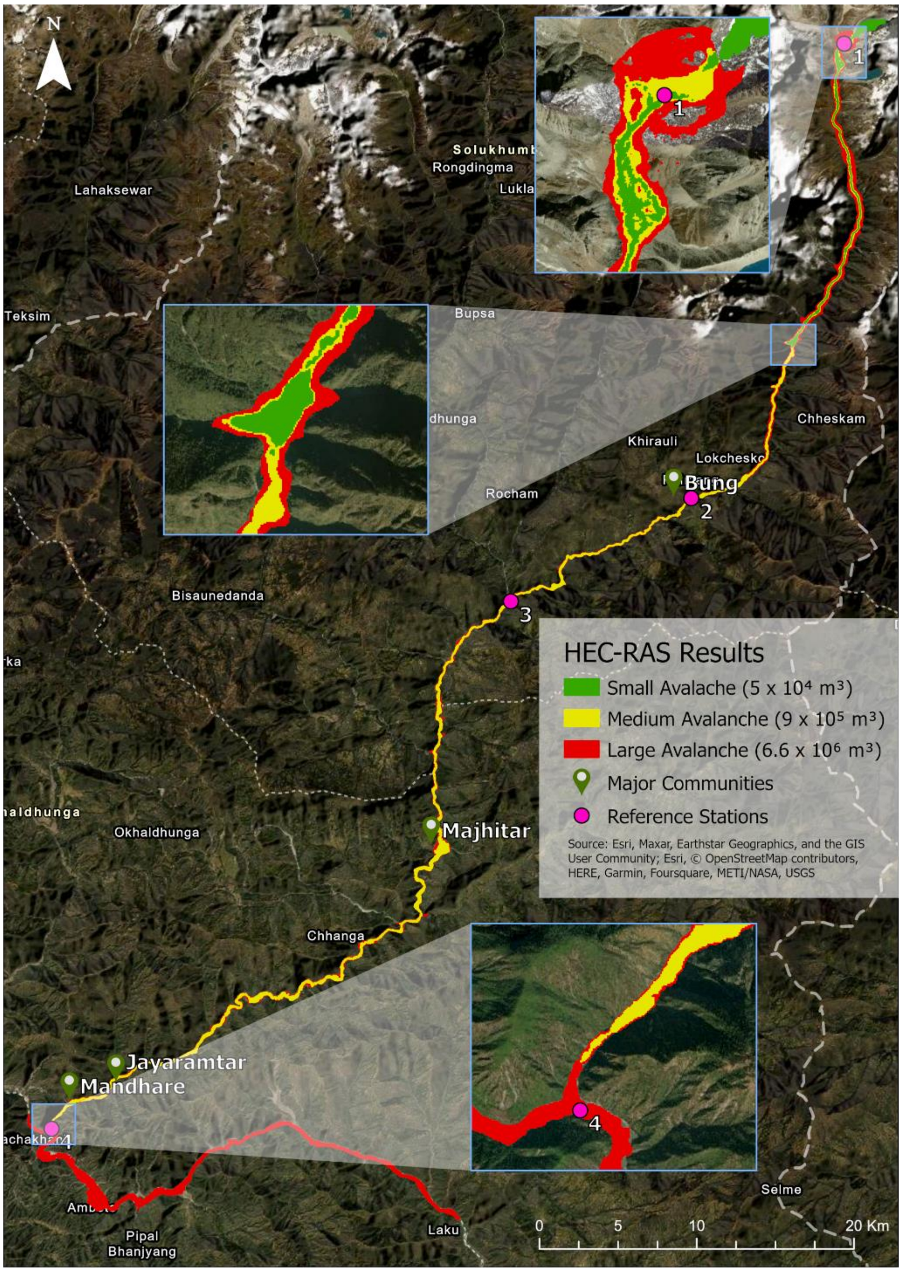
N
Solukhumbu
Rongdingma
Lukla
Lahaksewar
Teksim
Bupsa
dhunga
Chheskam
Khirauli
Lokchesko
Bung
Rocham
Bisaunedanda
ka
aldhunga
Okhaldhunga
Majhitar
Chhanga
Jayaramtar
Mandhare
achakha
Ambo
Pipal Bhanjyang
Laku
Selme
1
2
3
4
HEC-RAS Results
🟩 Small Avalache (5 x 10⁴ m³)
🟨 Medium Avalanche (9 x 10⁵ m³)
🟥 Large Avalanche (6.6 x 10⁶ m³)
Major Communities
● Reference Stations
Source: Esri, Maxar, Earthstar Geographics, and the GIS User Community; Esri, © OpenStreetMap contributors, HERE, Garmin, Foursquare, METI/NASA, USGS
0
5
10
20 Km

b)

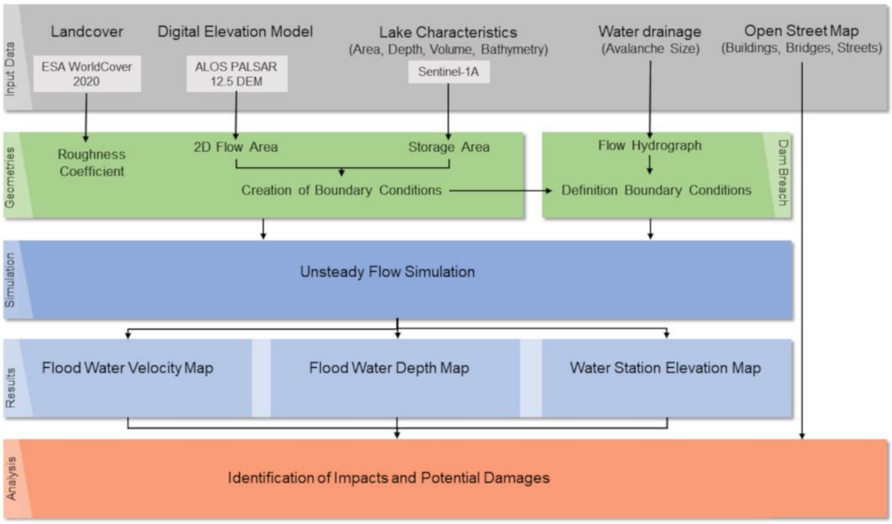
Input Data
Landcover
ESA WorldCover 2020
Digital Elevation Model
ALOS PALSAR 12.5 DEM
Lake Characteristics (Area, Depth, Volume, Bathymetry)
Sentinel-1A
Water drainage (Avalanche Size)
Open Street Map (Buildings, Bridges, Streets)
Geometries
Roughness Coefficient
2D Flow Area
Storage Area
Creation of Boundary Conditions
Flow Hydrograph
Definition Boundary Conditions
Dam Breach
Simulation
Unsteady Flow Simulation
Results
Flood Water Velocity Map
Flood Water Depth Map
Water Station Elevation Map
Analysis
Identification of Impacts and Potential Damages

**Figure 1.** Results (a) and simplified workflow (b) of the GLOF analysis with HEC-RAS

EARSeL Bucharest 2023

Abstract

# Evaluation of Sentinel-1-Based Change Detection Approaches for Regressive Erosion along the Coca River, Ecuador

Corresponding Author:
torben.dedring@rub.de

Valerie Graw[1,2,3], Torben Dedring[1], Roman Hiby[1], Jose Jara-Alvear[2,3,4], Pablo Guzman[2,3,4], Carsten Juergens[1], Andreas Rienow[1]

[1] Geomatics Research Group (Grg), Ruhr-University Bochum (Rub), Bochum, Germany
[2] Transdisciplinary Center For Coupled Socio-Ecological Systems (Traces), Universidad Del Azuay (Uda), Cuenca, Ecuador
[3] Energy Sciences Research Group (Ciener), Universidad Del Azuay (Uda), Cuenca, Ecuador
[4] La Corporación Eléctrica Del Ecuador (Celec Ep), Cuenca, Ecuador

**Keywords:** Landslide Monitoring, Sentinel-1, Regressive Erosion, Disaster Risk Management

## Abstract

Being situated within the Pacific Ring of Fire and the El Niño Southern Oscillation, Ecuador's geographical location is one of the major drivers for the country's above average damage-rate caused by natural hazards. Over 70% of the Ecuadorian people are exposed to two or more natural hazards. The combined effects of high seismic activity, the tropical mountainous environment with steep slopes, hydrological variability, as well as increasing land pressure contribute to a frequent occurrence of landslides, which are expected to increase in frequency and intensity due to climate change. On 2 February 2020, Ecuador's biggest waterfall, San Rafael, collapsed due to an unusual erosion phenomenon caused by volcanic debris avalanche deposit behind the natural lava-dam barrier of the waterfall. A following change of the Coca River's course triggered regressive erosion upstream of the waterfall resulting in damaged oil pipes (affecting the indigenous Kichwa population) and threatening the Coca Codo Sinclair Dam, which supplies 25% of the country's electricity demand.

This study investigates the spatiotemporal developments of landslides between the former San Rafael waterfall and the Coca Codo Sinclair Dam using GIS- and remote sensing-based approaches in order to contribute to ongoing disaster risk management and monitoring efforts. Being situated roughly 20 km south of the equator just between the Cayambe-Coca and the Napo-Galeras National parks, the investigation area naturally experiences a high precipitation rate and thus a high cloud cover. Thus, we used Sentinel-1 Synthetic Aperture Radar (SAR) data to investigate the spatiotemporal development of the regressive erosion using two different approaches. We compared a bi-temporal change detection (BCD) with a cloud-computing-based sequential change detection (SCD), both based on 32 Sentinel-1 Ground Range Detected images in Interferometric Wide Swath mode captured between 14 February 2020 and 16 March 2021. The presentation will focus on the latter detection method. The BCD was carried out within the Sentinel Application Platform based on 12-day interval image pairs using standard pre-processing steps, followed by a Principal Component Analysis-based comparison. We created binary change-detection maps using a threshold method and subsequent subtraction of permanent water bodies. The SCD was carried out within the recently published EESAR Docker Container, which utilises the Google Earth Engine (GEE) cloud-computing environment. On a per-pixel basis, the technique identifies whether a change occurred at a defined significance level between two SAR images taking into

consideration the full time-series starting with the first image and ending with the most recent one. With a test statistic, p values are generated for each observation and a change map is then generated based on the testing of p values against the defined significant level. By integrating the omnibus test, the identification of changes in a pixel can be conducted and updated. Besides the bands containing the changes between the intervals, the resulting raster dataset includes a band with the time of most recent changes, the time of first change and another band with the total number of registered changes.

The results show that especially the SCD can accurately track the spatiotemporal genesis of the regressive landslide. We validated the change detection approaches with high-resolution satellite images from PlanetScope, a close exchange with local experts and comparisons with local assessment reports by CELEC SUR. We conducted a detailed validation for a smaller area along the lower part of River Coca. Therefore, we combined the results of the BCD and the SCD with the digitized eroded areas derived from the high-resolution imagery and computed a confusion matrix. Figure 1 shows the spatial validation of both approaches. About 75.31% of changes detected by the SCD were identified as true positive, while only 58.54% of the BCD were identified as true positive. According to the confusion matrix, the BCD got an overall accuracy of 0.89, a sensitivity of only 0.44, and a specificity of 0.97, while the SCD has a sensitivity of 0.75, a specificity of 0.94, and an overall accuracy of 0.91.

Landslide monitoring in the study area is crucial to support national risk management. The presented results allow for near real-time monitoring with Sentinel-1 time-series with a spatial resolution of 20 m and a 12-day temporal resolution. Nevertheless, optical reference data cannot replace field validation data and might contribute to error propagation in the validation processes, especially as the acquisition times of PlanetScope do not match accurately with the revisit time of Sentinel-1. Thus, the SCD's tendency to over-prediction could be the result of uneven recording dates. Unlike the BCD, the SCD promotes a continuous analysis over the time-series and thus considers the trend over all images from the time-series.

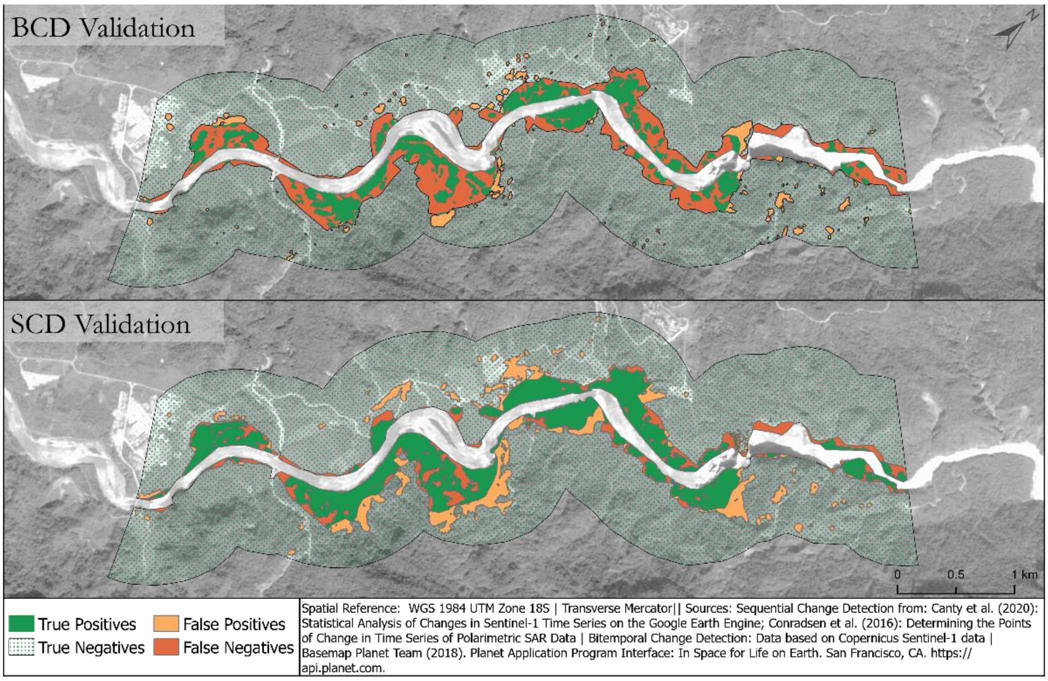

Spatial Reference: WGS 1984 UTM Zone 18S | Transverse Mercator|| Sources: Sequential Change Detection from: Canty et al. (2020): Statistical Analysis of Changes in Sentinel-1 Time Series on the Google Earth Engine; Conradsen et al. (2016): Determining the Points of Change in Time Series of Polarimetric SAR Data | Bitemporal Change Detection: Data based on Copernicus Sentinel-1 data | Basemap Planet Team (2018). Planet Application Program Interface: In Space for Life on Earth. San Francisco, CA. https://api.planet.com.

**Figure 10.** Validation results of BCD and SCD compared to PlanetScope Data

EARSeL Bucharest 2023

Abstract

Corresponding Author:

gurcanb@istanbul.edu.tr

# Potential of Planet's SkySat Collect Images for Topographic Mapping

Gurcan Buyuksalih[1], Cem Gazioglu[1], Karsten Jacobsen[2]

[1]Istanbul University, Marine Sciences and Management Institute, Turkey

[2]Leibniz University Hannover, Institute of Photogrammetry and Geoinformat., Germany

**Keywords:** SkySat, Orientation, Mapping, Economic solution

## Abstract

Currently we have a higher number of optical satellites with 0.5m up to 1m ground sampling distance (GSD) usable for mapping purposes. Not only the technical quality, but also the economic solution is important. For this reason, Planet's SkySat small satellites were analysed for their mapping potential. SkySat-4 to -15, launched in 2016 up to 2018, operating in 450km height and SkySat-16 to -21, launched in 2020 in 400km orbit elevation operating currently. Each SkySat has 3 CMOS detectors with 2560 x 2160 pixels. In flight direction, 1080 pixels are used for panchromatic and 270 pixels each for blue, green, red and near infrared (see figure below). The perspective images are recorded at 30 Hz. The up to 9 times overlapping images are used for image sharpening, allowing an improvement of the original images to 50cm GSD based on originally 81cm GSD for SkySat-4 up to -15. An analysis of the effective ground resolution by edge analysis confirmed the effective 50cm resolution for nadir view. For inclined view direction it is slightly reduced according to the increasing GSD as function of the angle of incidence.

The staggered arrangement of the sensors in the focal plane causes a time interval of the outside sensors to the central sensor, which can be seen at the SkySat Collect images generating joint ortho images of the 3 sensors and a selectable number of images in flight direction. Planet distributes the original images as Basic in addition to the joint Collect. For nadir view, the Basic images, distributed with 0.65m GSD, are covering just 2074m x 875m. The orientation information is available as rational polynomial coefficients. SkySat satellites are low cost satellites in relation to the larger satellites as used e.g. by Airbus DS and MAXAR. Due to this, the orientation accuracy is limited to approximately 60m to 100m in orbit direction and 40m across orbit, requiring an improvement by ground control points (GCP). The orientation was done by bias corrected RPC as well as by resection, leading to the same accuracy of 1m up to 2m dominated by the GCP identification. This is satisfying for mapping with 0.5m GSD images, but the limited scene size is only economical for special small projects.

SkySat Collect imagery should normally be preferred for mapping. They have a swath width for nadir view of about 5.8 km and can theoretically be up to 200 km long. The Collect images are ortho images generated by Planet. As GCP information they use other ortho-images with automatic point detection. SRTM mostly is used as height information, even if AW3D30 would be better. The bias of the DEM used does not matter, as this only causes a shift due to the small field of view, which is compensated by the orientation with a reference ortho. The standard deviation of the DEM is in the range of 3m for SRTM and 2m for AW3D30. With a 20° angle of incidence limitation, the standard deviation of SRTM would introduce an error of about 1m and for AW3D30 0.7m. An intensive analysis of 9 Collect scenes with manually identified GCPs revealed a standard deviation of the Collect scenes in the range up to 2m when the incidence angle was below 20°. For angles of incidence up to 34°, the accuracy was reduced to 4m to 5m, but even such angles of incidence should be avoided for

mapping purposes due to the displacement of building roofs compared to the ground-level location. In conclusion, the SkySat images up to an angle of incidence of 20° could be used for mapping purposes in a similar way to the images from the large satellites (see also details in the image below).

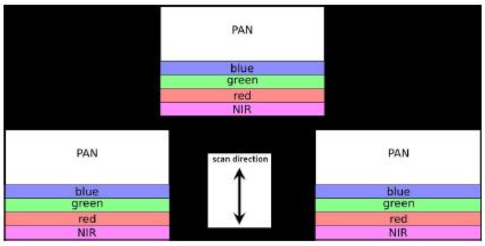

SkySat sensor constellation

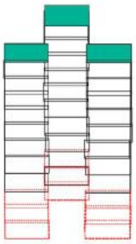

configuration

SkySat Collect

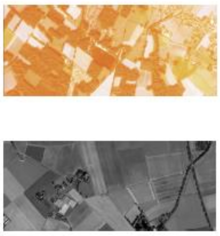

SkySat Basic

Part of a SkySat pan-sharpened Collect image

## Section VI - New methods and algorithms in EO for agriculture

# Apple fruit load estimation in multi-temporal high-resolution UAV imagery by deep learning

EARSeL Bucharest 2023

Abstract

Corresponding Author: Chenglong Zhang

Chenglong.zhang@wur.nl

Chenglong Zhang[1,3], Joao Valente[2], Wensheng Wang[3,4], Leifeng Guo[3], Lammert Kooistra[1]

[1] Wageningen University & Research, Laboratory of Geo-Information Science and Remote Sensing, The Netherlands
[2]Wageningen University & Research, Information Technology Group, The Netherlands
[3] Chinese Academy of Agriculture Science, Agriculture Information Institute, China
[4] Ministry of Agriculture and Rural Affairs, Key Laboratory of Agricultural Big Data, China

**Keywords:** apple yield, deep learning, photogrammetry, UAV

### The challenge

Harvesting period accounts for the majority of total management costs in orchards. A timely and accurate mapping of apple yield is fast becoming a key focus of the optimization during the harvesting process. Recent achievements in computer vision have advanced fruit detection in images. Yet progress in connecting the detected fruits with specific trees, to achieve a tree-level apple yield estimation, is much less. The main challenge in fruit load estimation is occlusion. Apples occluded by adjacent apples, leaves, or branches limit the performance of detection model. Another problem is assigning apples to individual trees to achieve tree-level yield estimation. Early studies based on orthomosaic or point clouds provided an initial solution. However, the pre-processing steps, e.g., structure-from-motion, cost a lot of time.

### Methodology

In this research, a novel framework that requires no conventional time-consuming pre-processing steps, e.g., structure-from-motion, was proposed for tree-level apple yield estimation using single raw UAV RGB imagery. An 'Elstar' apple orchard in Randwijk, the Netherlands, was taken as an example to examine the potential of single raw aerial images in yield mapping. In four consecutive years, starting from 2018 to 2021, ultra-fine resolution UAV images and in-field ground truth (GT) data were collected. Different UAV platforms and flying altitudes were designed for comparison purposes. While GT consists of apple counting and actual weights which were prepared for the model performance validation.

First, a lightweight YOLOv4 model was trained and validated to detect and count apples in original aerial images. Detected apples were delineated with bounding boxes and center-pixel positions of the bounding boxes in the image were treated as apple positions. Next, a resourceless photogrammetric approach was designed for the projection of detected apples into a geographic coordinate system. To assign the detected apples to individual trees, a clustering method was applied. Finally, obtained results were compared with in-situ apple counting for regression-based yield estimation.

## Outlook for the future

The use of UAVs in supporting orchard management is still in its infancy. Initial results show potential to achieve tree-level apple yield estimation with the use of single raw UAV RGB imagery. In comparison with conventional orthomosaic or point clouds-based methods, the proposed novel framework for apple orchard monitoring has a great advantage in data processing efficiency and convenience. Further research should include larger datasets for the training of deep learning models. A focus on model generalization is required, especially for the application in agriculture where a complex and changeable circumstance exists. Publicly available orchard datasets and annotated image datasets are also recommended. In addition, to enhance the use of single geotagged aerial images, a more accurate positioning system in UAV is also excepted.

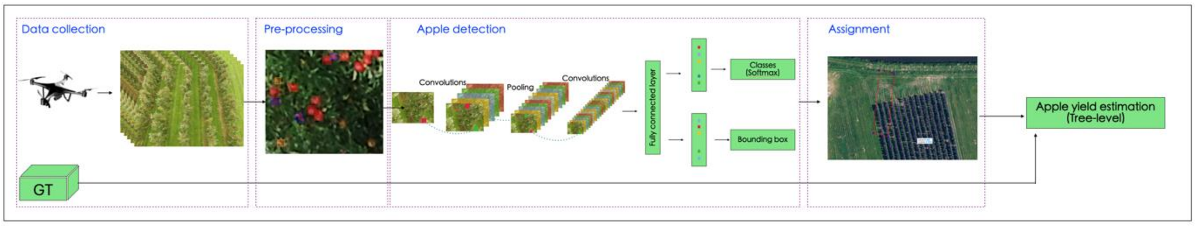

**Figure 11.** Workflow of the proposed apple yield estimation method

# Leveraging PIXXEL's Hyperspectral Imagery for Land Use and Land Cover Mapping in an Agricultural Region of Northeast Australia

EARSeL Bucharest 2023
Abstract
Corresponding Author: Spyridon E. Detsikas
email address sdetsikas@hua.gr

Spyridon E. Detsikas[1], George P. Petropoulos[1], Rahul Raj[2]

[1] Department Of Geography, Harokopio University Of Athens, El. Venizelou
70, Kallithea, 17671, Athens, Greece
[2] Pixxel.Space, Bengaluru, Karnataka, India

**Keywords:** Hyperspectral imaging, Machine Learning, Random Forest, PIXXEL MANTIS, LULC mapping

## Abstract

Accurate land use/land cover (LULC) data is required in numerous applications and research purposes, including land management, agricultural planning, and environmental monitoring. Hyperspectral remote sensing is a powerful tool for this purpose since it allows obtaining high spectral resolution data not available through traditional multispectral imagery.

Recently, there has been an unprecedented increase in spaceborne hyperspectral data with several missions launched, such as the Environmental Mapping and Analysis Program (EnMAP) satellite, resulting to an unparalleled abundance of hyperspectral data. Moreover, several private sector companies have also entered the hyperspectral data market, with PIXXEL, an Indian private entity, being a pioneering provider in this space. PIXXEL's vision to provide increased temporal and spatial resolution hyperspectral data has the potential to significantly improve the accuracy and efficiency of LULC mapping over large areas.

This study aims at investigating the capability of PIXXEL's MANTIS hyperspectral imagery coupled with Random Forests (RF) machine learning (ML) pixel-based classification algorithm in obtaining LULC mapping over an agricultural area in Northeast Australia. This area is characterized by diverse land cover types ranging from natural vegetation to irrigated crops and manmade reservoirs. The satellite imagery used in this study was acquired on 17th September 2022 (Figure 1), at a spatial resolution of 30 m and a spectral resolution of 67 bands ranging from the visible to near-infrared spectrum (490 – 950 nm). Accuracy assessment of the derived land cover map was conducted using the error matrix statistics and additional comparisons were performed against other LULC products available for the experimental site.

Results obtained, showed a high overall accuracy and Kappa statistics, evidencing the capability of PIXXEL's Mantis hyperspectral imagery when coupled with ML algorithms such as RF in mapping accurately land use/cover distribution for the study site. Our findings highlight the value of PIXXEL's hyperspectral data in mapping land use and land cover with potential applications in agriculture, land management, and environmental monitoring.

# Mowing Detection Intercomparison Exercise (MODCiX): A Cross-European Evaluation of Mowing Detection Algorithms

EARSeL Bucharest 2023
Abstract
Corresponding Authors:
marcel.schwieder@thuenen.de

Marcel Schwieder[1,2], Felix Lobert[1,2], Arnab Muhuri[3], Natascha Oppelt[3], Sarah Asam[4], Sophie Reinermann[5], Julien Morel[6], Mattia Rossi[6], Dominique Weber[7], Filippo Sarvia[8], Samuele De Petris[8], Enrico Borgogno-Mondino[8], Oliver Buck[9], Stefan Ernst[2], Patrick Hostert[2,10], Silvia Valero[11], Anatol Garioud[12], Ann-Kathrin Holtgrave[13], Clément Mallet[14], Mathilde De Vroey[15], Andreas Schaumberger[16], Iason Tsardanidis[17], Ruth Sonnenschein[18], Stefan Erasmi[1]

[1] Thünen Institute of Farm Economics, Bundesallee 63, 38116 Braunschweig, Germany
[2] Humboldt Universität zu Berlin, Geography Department, Unter den Linden 6, 10099 Berlin, Germany
[3] Earth Observation and Modelling (EOM), Christian-Albrechts-Universität zu Kiel, Geographisches Institut, Ludewig-Meyn-Straße 8, 24118 Kiel, Schleswig-Holstein, Germany
[4] German Remote Sensing Data Center (DFD), German Aerospace Center (DLR), 82234 Wessling, Germany
[5] University of Würzburg, Institute of Geography and Geology, Department of Remote Sensing, 97074 Würzburg, Germany
[6] European Commission, Joint Research Center (JRC), 21027 Ispra, Italy
[7] Swiss Federal Research Institute WSL, Zürcherstrasse 111, 8902 Birmensdorf, Switzerland
[8] Department of Agricultural, Forest and Food Sciences, University of Turin, L.go Braccini 2, 10095 Grugliasco, Italy
[9] EFTAS Fernerkundung GmbH, Oststraße 2-18, 48145 Münster
[10] Humboldt Universität zu Berlin, Integrative Research Institute on Transformations of Human-Environment Systems - IRI THESys, Unter den Linden 6, 10099 Berlin, Germany
[11] CESBIO, Université de Toulouse, CNES/CNRS/INRAE/IRD/UPS, 31400 Toulouse, France
[12] IGN – French Mapping Agency (Institut Géographique National), 94160 Saint-Mandé, France
[13] Technische Universität Berlin, Geoinformation in Environmental Planning Lab, Straße des 17 Juni 145, 10623 Berlin, Germany
[14] Université Gustave Eiffel, IGN, ENSG, LASTIG, 94160 Saint-Mandé, France
[15] Earth and Life Institute, Université Catholique De Louvain, 1348 Louvain-la-Neuve, Belgium
[16] Agricultural Research and Education Center Raumberg-Gumpenstein, 8952 Irdning-Donnersbachtal, Austria
[17] BEYOND Centre of EO Research and Satellite Remote Sensing, IAASARS, National Observatory of Athens, 15236 Penteli, Greece
[18] Institute for Earth Observation, Eurac Research, Drususallee/Viale Druso 1, 39100 Bozen/Bolzano, Italy

**Keywords:** European grasslands, land-use intensity, algorithm comparison, change detection.

## Abstract

Grasslands are a major component of Europe's agricultural landscapes and provide important ecological functions and ecosystem services within a multifunctional agriculture. Grasslands supply fodder, straw or raw biomass for energy production and provide habitat for endangered flora and fauna. They hence have a high relevance for the preservation of biodiversity and climate protection. However, grasslands are exposed to a wide spectrum of management activities and intensity, which impact grassland development and resilience. Their conservation and sustainable management directly contribute to strategies and policies at the European and national scale aimed at transitioning toward a more sustainable agriculture in the framework of the European Green Deal. Besides prohibitions on the

conversion of grasslands to croplands, those strategies also target a more extensive management. For meadows, the management intensity can be described by proxies such as the timing and frequency of mowing. A higher number of annual cuts as well as an early timing of the first cut in a year are usually associated with higher management intensities. Such information can be used as indicators for the evaluation of biodiversity or climate protection measures (e.g., in peatlands) and agri-environmental measures within the Common Agricultural Policy (CAP) such as mowing on fallow land.

Dense time series of remote sensing data were shown to be beneficial to derive information on grassland-use intensity. Several methodological approaches have been published that make use of SAR data, optical data, or a combination of both. They either built on rule-based algorithms relating to underlying biophysical principles or stem from the realm of machine learning techniques. However, most of these studies have a rather local or regional focus and are usually limited by the availability of reference data against which they are developed and evaluated. Tests on model transferability in time and space are usually lacking due to the unavailability of consistent reference data sets. In addition, different validation strategies inhibit direct comparisons of individual studies.

To overcome these limitations, we established a network of more than 30 researchers from 8 European countries that brought together a unique reference data set that is representative for several grasslands in Europe with varying climatic and environmental conditions. The aim of the network is to evaluate existing mowing detection algorithms based on openly accessible satellite data across Europe using a consistent validation framework. The reference data set comprises management information such as timing or number of mowing events for more than 4,000 grassland parcels covering six years, stretching from Sweden and Estonia in the North to Southern France in the Southwest (Figure 1). We harmonized the reference data and assigned a label of accuracy to each parcel depending on how the information was collected. We pre-processed satellite data from Landsat, Sentinel-1 and Sentinel-2 for each region and year for which reference data were available. Based on this data set we run and evaluate a total of around 20 algorithms that were developed to estimate grassland-use intensity using mowing events as a proxy.

By the time of writing this abstract, we finalized the pre-processing of the satellite data which will be used by the individual groups to run their algorithms. The results will be independently validated using unseen validation data in a way that the spatial and temporal transferability of the different approaches can be assessed. We expect to identify strengths and limitations of the individual approaches aiming to formulate specific user recommendations to choose the optimal combination of data and algorithm for the application and region of interest. Results will inform the growing user community interested in grassland use intensity and its impact on the whole breadth of related ecosystem services.

**Figure 12.** Distribution of regions in Europe for which reference data are available. Red dots indicate the general countries / regions, the blue dots indicate that reference data for several regions in the country are available.

# Convolutional neural network hardware implementation for oil roughness estimation

EARSeL Bucharest 2023
Abstract
Corresponding Author:
stefan.popa@unitbv.ro

Stefan Popa[1], Kamal Marandskiy[1], George Feldioreanu[1], Mihai Ivanovici[1]

[1]Transilvania University of Brasov, Department of Electronics and Computers, Romania

**Keywords:** VGG, convolutional neural network, soil roughness estimation

## Abstract

In the Agriculture 5.0 context, computer vision and artificial intelligence are two key technologies for the automatic agricultural field and crop monitoring and management. For enabling the usage of both technologies on portable or mobile devices, including unmanned aerial vehicles, hardware implementations are required, for real-time performance, high-precision running and low power consumption. We implemented a Very Deep Convolutional Neural Network (VGG-11) for Soil Surface Roughness's (SSR) Random Roughness (RR) parameter estimation from digital images of a line laser beam projection on the analyzed surface. We used the Python PyTorch framework for modelling the VGG-11 in software. We compare the results against the classical contact measurement pinboard method on both artificial and real soil surfaces. SSR is defined as the irregularities of the soil surface, as a consequence of various factors including soil texture, aggregate size, rock fragments, vegetation cover and land management. SSR is directly related to soil water storage, infiltration and overland flow. Our VGG-11 is trained for 120 epochs and provides a 99.42% accuracy on the test set. This software model for SSR's RR estimation is intended as a golden model for the validation of a hardware implementation using the Verilog hardware description language. The hardware implementation is mainly targeted at Field Programmable Gate Array (FPGA) devices and can easily be interfaced with a microprocessor system. A similar hardware implementation of a VGG-11 is presented in [1].

### Soil Roughness

The SSR quantifies the unevenness of soil surface caused by a plethora of factors such as soil texture, tillage operations, land management, rock fragments, vegetation, etc. The SSR influences the wind and water erosion, infiltration and surface storage level [2], [3]. It contains several separate indices that express distinct soil characteristics. The focus of the presented work is on the RR SSR parameter which is linked to the stability of the soil aggregate. RR expresses height variations at random locations on the soil surface [4] and can be measured through contact or sensor measures. The pinboard [5] and chain methods [6] are two popular contact methods while terrestrial laser scanning [7] is a non-destructive, non-contact sensor method. The chain contact method employs a bicycle chain being placed on the surface and measuring the Euclidian distance between its ends with a ruler. In this case RR is calculated as $RR = \left(1 - \frac{L_2}{L_1}\right) \times 100$ [6], where $L_2$ measured distance between the chain ends while on the surface and $L_1$ is the length of the stretched chain. In our measurements $L_2$ = 1 m and the chain link pitch is 13 mm. The pinboard contact method assumes multiple elevation measurements using a set of equidistant identical pins as depicted in Figure1. RR is the standard deviation (SD) of the measurements after the elimination of slope effects [8]. Our pinboard covers 73 cm with 53 aluminum pins 33 cm in height.

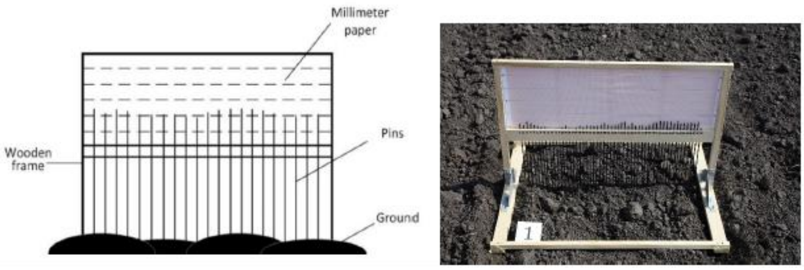

**Figure 1.** Diagram of pinboard setup (left) and in situ usage (right).

## Measurements

We performed measurements on four artificial surfaces and one soil surface, depicted in Figure 2. The flat artificial surface (i.e. painted wood plank) represents a corner case since its RR has a value close to 0 for both classical contact methods and the laser line beam results in an approximately straight projected line. The regular artificial surface (plastic) contains regularly-placed humps of identical shape. The cvasi- regular artificial surface (painted cardboard for holding eggs) contains regularly-placed humps and dimples larger in scale and with small elevation random variations. The irregular artificial surface (uneven concrete) contains random relatively small elevation variations. For the real soil surface more measurements were performed due to its anisotropic nature.

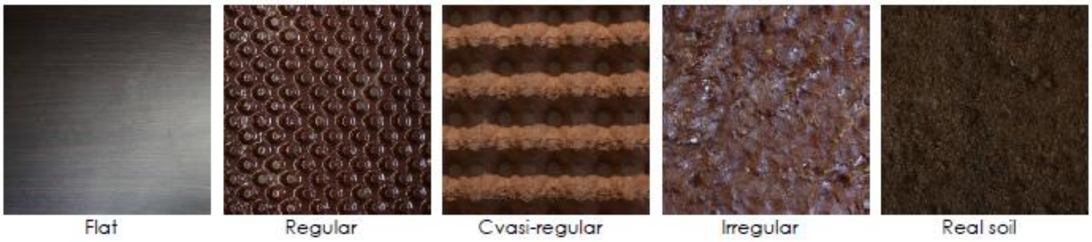

In addition to the chain and pinboard contact methods we also used a line laser as a sensor method. The line laser was placed above the targeted surface so that the geometric plane of its beam was perpendicular to the surface geometric plane. A Canon 5D Mark II digital camera was placed on the same horizontal plane as the laser with its lens's center axis pointing towards the laser projection on the targeted surface and making a 30˚ angle with the surface horizontal plane. Thus the laser projections in the resulting images spanned from left to right. The number of images taken for each surface type is listed in Table 1. From each image a 100 × 200 pixels area of interest was cropped. Such samples are depicted in Figure 3, one per each surface type. Each sample was then binarized resulting in black and white images as depicted in Figure 4. To augment the data set of 28 binarized images we added noise of various types (i.e. Gaussian, speckle, salt and paper) with various parameters (i.e. mean, SD) resulting in a data set of 168 grayscale 100 × 200 pixels images. Samples of such images with noise are depicted in Figure 5.

**Table 1.** The number of RGB laser images taken for each surface type.

| Surface | Number of RGB laser images |
|---|---|
| Flat | 1 |
| Regular | 4 |
| Cvasi-regular | 3 |
| Irregular | 10 |
| Real soil | 10 |

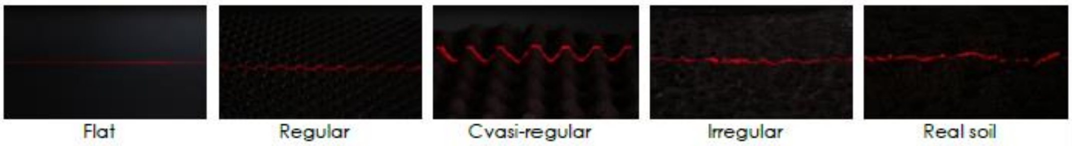

**Figure 3.** Sample 100 × 200 pixels areas of interest cropped from RGB images of the projections of a red laser line beam on the surface samples from Figure 2.

**Figure 4.** Sample binarized (black and white) images resulted from the RGB area of interest crops.

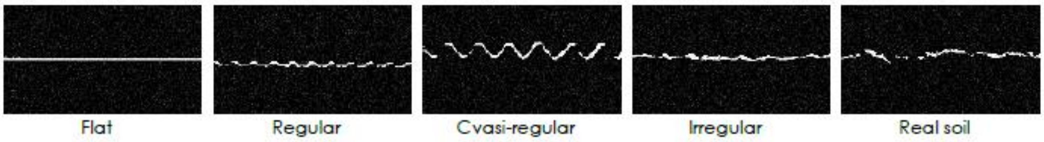

**Figure 5.** Sample grayscale images de ived from the binarized ones by adding Gaussian noise of 0 mean nd 1% variance.

## Convolutional Neural Network for SSR RR Pinboard Estimation

Our CNN model is based on the VGG-11 model architecture proposed in [9] with several modifications such as the modified input layer size and the sizes of the 3 fully connected layers at the output. Its detailed architecture is depicted in Figure 6.

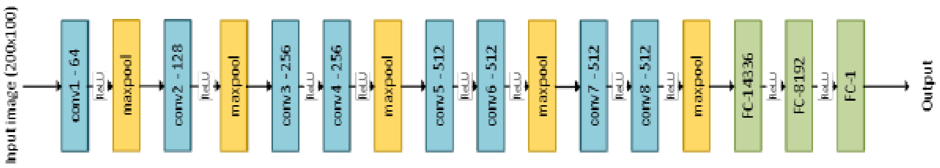

**Figure 6.** The architecture diagram of our VGG-11 model.

The data set of 168 grayscale images was divided in 66.7% training, 16.6% validation and 16.6% test. We trained the network for 120 epochs using the Stochastic Gradient Descent (SGD) optimizer with a Mean Square Error (MSE) loss function, a momentum of 0.9 and an initial learning rate of 0.01. We used the ReduceLROnPlateau [10] learning rate scheduler with a factor of 0.1 and a patience of 20. The training and validation loss per each epoch are depicted in Figure 7.

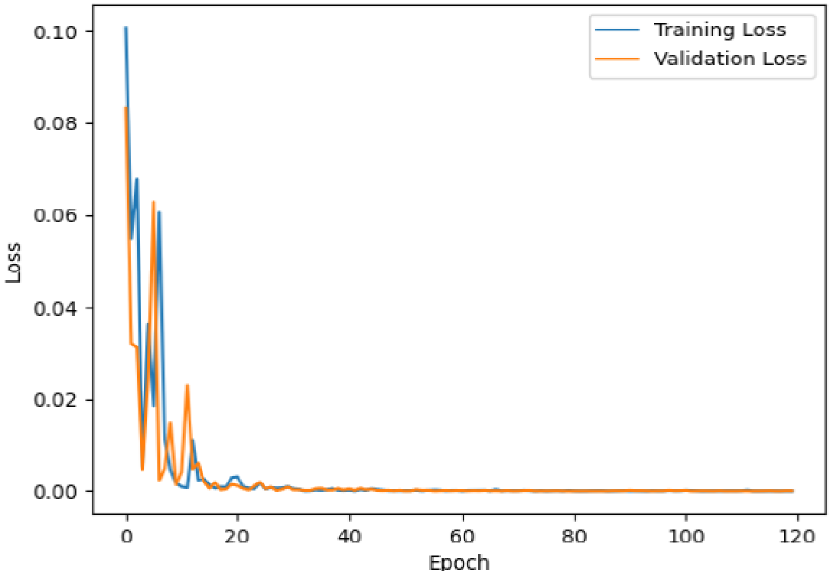

**Figure 7.** Training and validation loss per epoch

On the test set, the network yields a MSE of 0.00003146, and an average pinboard RR prediction error of 0.58%, thus, an accuracy of 99.42%. The prediction error for each output RR value has been calculated as $e = \frac{\text{predicted} - \text{expected}}{\text{expected}} \times 100[\%]$.

## Future work

For future work, we plan to implement a similar VGG-11 software model for the estimation of SSR RR obtained with the chain contact method. Once the two models achieve sufficient accuracy we plan to fully implement them as hardware Intellectual Property cores for integration in microprocessor systems.

## Acknowledgment

This work was funded by the AI4AGRI project entitled "Romanian Excellence Center on Artificial Intelligence on Earth Observation Data for Agriculture". The AI4AGRI project received funding from the European Union's Horizon Europe research and innovation program under grant GA no. 101079136.

## References

[1] S. P. a. M. I. George Feldioreanu, "Convolutional Neural Network implemented on FPGA for trajectory classification," in *submitted for publication to International Symposium on Signals, Circuits and Systems - ISSCS*, Iasi. Romania, 2023.

[2] J. V. M. a. A. P. G. E. V. V´azquez, "Characterizing anisotropy and heterogeneity of soil surface microtopography using fractal models," *Ecological Modelling, Elsevier,* pp. 337--353, 2005.

[3] D. M. A. a. S. N. J. K. Amoah, "Quantifying watershed surface depression storage: determination and application in a hydrologic model," *Hydrological Processes,* vol. 274, no. Wiley Online Library, pp. 2401-2413, 2013.

[4] R. A. a. M. A. R. Burwell, "A field measurement of total porosity and surface microrelief of soils," *Soil Science Society of America Journal,* vol. 27, no. Wiley Online Library, pp. 697-700, 1963.

[5] R. E. B. W. E. L. R. F. H. e. a. R. Allmaras, "Total porosity and random roughness of the interrow zone as influenced by tillage," *Agricultural Research Service, US Dept. of Agriculture,* 1966.

[6] A. Saleh, "Soil roughness measurement: chain method," *Journal of soil and water conservation,* vol. 48, no. Soil and Water Conservation Society, pp. 527-529, 1993.

[7] M. S. a. I. M.-J. R. J. Barneveld, "Assessment of terrestrial laser scanning technology for obtaining high-resolution DEMs of soils," *Earth Surface Processes and Landforms,* vol. 38, no. Wiley Online Library, pp. 90-94, 2013.

[8] P. V. D. A. D. R. a. M. V. N. Cremers, "Spatial and temporal variability of soil surface roughness and the application in hydrological and soil erosion modelling," *Hydrological processes,* vol. 10, no. Wiley Online Library, pp. 1035-1047, 1996.

[9] K. S. a. A. Zisserman, "Very deep convolutional networks for large-scale image recognition," *arXiv preprint arXiv:1409.1556,* 2014.

[10] "ReduceLROnPlateau - PyTorch 2.0 Documentation," [Online]. Available: https://pytorch.org/docs/stable/generated/torch.optim.lr_scheduler.ReduceLROnPlateau.html . [Accessed 27 04 2023].

# Quantification of nitrogen uptake in cover crops from UAV-based multispectral images

EARSeL Bucharest 2023

Abstract

Corresponding Author: Lammert Kooistra

Lammert.kooistra@wur.nl

Paolo Dal Lago [1], Nikos Vavlas[1], Lammert Kooistra[2], Gerlinde de Deyn[1]
(presenting author underlined)

[1] Soil Biology Group, Environmental Sciences, Wageningen University, The Netherlands
[2] Laboratory of Geo-Information Science and Remote Sensing, Wageningen University, The Netherlands

**Keywords:** agriculture, plant traits, vegetation indices, machine learning, UAV

## The challenge

Efficient nitrogen (N) use is a main target for achieving sustainable agriculture. Planting of cover crops (CC) is an important management strategy to prevent N losses to the environment by immobilizing soil N in their biomass over the crop rotation intervals. N is released for the next main crop in the crop rotation by integrating the CC biomass into the soil where it is decomposed by the soil biota. However, CC effects vary because the rate of N mineralisation and amount of N released is dependent on the CC traits. To support sustainable nutrient management, modelling and monitoring the processes of N uptake and release can assist growers in their long-term nutrient management. Traditional measurements are based on destructive small-scale sampling and analysis of N quantity and quality of the CC biomass in laboratory. This approach is laborious and incapable of capturing spatial and temporal variability. Earlier studies have shown the applicability of spectral remote sensing to quantify N uptake in arable crops and grasslands. Studies for monoculture cover crops and especially for mixtures of CC species are limited.

## Methodology

To fill this gap, a statistical model to estimate CC traits was calibrated in this study, by establishing relationships between UAV-based high-resolution multispectral data and ground truth data. Three CC species were planted in monoculture, bi-, and tri- species mixtures: common vetch (Vicia sativa), black oat (Avena strigosa), and fodder radish (Raphanus sativus) in a long-term field experiment. The CC species showed distinct variation in traits (biomass, %N), whereas CC mixtures were more similar. A combination of photogrammetry derived Canopy Surface Model (CSM) features, vegetation indices and textural features were used as predictors to estimate above ground biomass (AGB), N concentration, N uptake, C:N ratio of CC monocultures and mixtures with promising results. Based on ground measurements, no effect in the quantity of N uptake was found but when compared to monocultures, the CC species traits changed significantly when intercropped. We adopted specific prediction models including a feature selection approach to quantify cover crop AGB (R2: 0.71, RMSE: 28.71 g/m2, NRMSE: 11.74 %), N concentration (R2: 0.80, RMSE: 1.77 gN /kg, NRMSE: 6.96 %), N uptake (R2: 0.56, RMSE: 9.38 kgN /ha, NRMSE: 15.08 %), and C:N ratio (R2: 0.62, RMSE: 1.86, NRMSE: 10.98 %).

### Outlook for the future

Features derived from optical remote sensing proved successful to model strategic CC traits in an economical and spatial explicit way for both CC monocultures and mixtures. This study develops strategies in the application of UAV-based optical remote sensing in agriculture to monitor and optimize nutrient management.

## Section VII - Remote sensing solutions for a sustainable forest management

# Sentinel-2, PlanetScope 2 And Airborne Hyspex Hyperspectral Imagery For Mountain Woody Species Mapping

EARSeL Bucharest 2023

Abstract

Corresponding Author:

m.kluczek@uw.edu.pl

Marcin Kluczek[1], Bogdan Zagajewski[1], Tomasz Zwijacz-Kozica[2]

[1] Department of Geoinformatics, Cartography and Remote Sensing, Chair of Geomatics and Information Systems, Faculty of Geography and Regional Studies, University of Warsaw, Poland
[2] Tatra National Park, Poland

**Keywords:** vegetation mapping, mountain ecosystem, woody tree species, the Tatras, classification, biodiversity

## Abstract

Monitoring of forest stands is now extremely important as a consequence of anthropopressure and climate change which speeds up transformation processes taking place in tree species. Especially in the case of mountain areas, which are habitats for valuable flora, biodiversity and endemics species that are extremely sensitive to climate change. It's a demanding challenge so it is necessary to develop methods that can prove large scale and repeatable monitoring of forest communities. The main interest of work is to investigate the potential use of Sentinel-2 and PlanetScope images for woody species mapping and measure statistically the differences with hyperspectral images.

The study area covers the Tatra Transboundary Biosphere Reserve located between Polish and Slovak border. The northern slopes are different from the southern parts. Also, research is important because there is a need-to-know what types of processes are taking place on the other side, and cooperation between border parks is often difficult. That way we can observe the processes taking place in the forest communities as a whole. The research object is 13 forest species (7 conifer, 6 broadleaf) from all plant altitudes. Most of the work focuses on using one source of remote sensing data (such as hyperspectral). Here we want to extend our research with LiDAR and SRTM topographic derivatives data, thermal imagery, Sentinel-2 and PlanetScope multi-temporal data. The high altitudes and steep slopes make conducting surveys challenging. During field campaign we have collected nearly 1000 verification samples with GNSS location of tree species on large homogeneous areas. We have tried to distribute the samples regularly over the area and at different altitudes in order to avoid spatial autocorrelation in the assessment of classification accuracy.

Three datasets were used for classification: PlanetScope, Sentinel-2 and HySpex. To which additional data (LiDAR, SRTM and thermal data) were then appended and the effect on classification accuracy was tested. The classification procedures were conducted using the open-source R programming language. The algorithms learning parameters were optimized using the grid search method, where each combination of the parameters is checked from the pool of parameters. The bias of classifications was reduced using an iterative accuracy assessment, which was repeated 100 times. Training and testing datasets were randomly selected in the 50:50 ratio; it was ensured that they were divided according to their belonging to a polygon in order to meet the condition of their independence. Then training of Random Forest and Support Vector Machines classifiers and classification accuracy results were saved

for each classification. For the final map production, models with the highest average F1-score for all scenario classes were selected. The ease of the implementation of the used algorithms makes reproducing the results possible and comparable.

The average F1-score accuracies ranged from 86-97%; relating this to the individual datasets: Sentinel-2 (86% RF; 82% SVM), PlanetScope (83% RF; 84% SVM) and HySpex (84% RF; 77% SVM). The Random Forest algorithm performs better for Sentinel-2 (by 4%) and HySpex (by 7%) data, while SVM is better for PlanetScope images (by 1%). Detailed results will be presented during the Symposium.

# Exploring Characteristics Of National Forest Inventories For Integration With Global Space-Based Forest Biomass Data

EARSeL Bucharest 2023
Abstract
Corresponding Author:
karimon.nesha@wur.nl

Karimon Nesha[1], Martin Herold[1], Veronique De Sy[1], Sytze De Bruin[1], Arnan Araza[1], Natalia Málaga[1], Javier GP Gamarra[2], Kristell Hergoualc'h[3], Anssi Pekkarinen[2], Carla Ramirez[2], David Morales-Hidalgo[2], Rebecca Tavani[2]

[1]Wageningen University and Research, Netherlands

[2]Food and Agriculture Organization of the United Nations

[3]Center for International Forestry Research (CIFOR)

**Keywords:** National Forest Inventory (NFI), NFI plot design, CCI biomass, Forest Resources Assessment (FRA), NFI and space-based data integration

## Abstract

National forest inventories (NFIs) are a reliable source for national forest measurements. However, they are usually not developed for linking with remotely sensed (RS) biomass information. There are increasing needs and opportunities to facilitate this link towards better global and national biomass estimation. Thus, it is important to study and understand NFI characteristics relating to their integration with space-based products; in particular for the tropics where NFIs are quite recent, less frequent, and partially incomplete in several countries. Here, we (1) assessed NFIs in terms of their availability, temporal distribution, and extent in 236 countries from FAO's Global Forest Resources Assessment (FRA) 2020; (2) compared national forest biomass estimates in 2018 from FRA and global space-based Climate Change Initiative (CCI) product in 182 countries considering NFI availability and temporality; and (3) analyzed the latest NFI design characteristics in 46 tropical countries relating to their integration with space-based biomass datasets. We observed significant NFI availability globally and multiple NFIs were mostly found in temperate and boreal countries while most of the single NFI countries (94 %) were in the tropics. The latest NFIs were more recent in the tropics and many countries (35) implemented NFIs from 2016 onwards. The increasing availability and update of NFIs create new opportunities for integration with space-based data at the national level. This is supported by the agreement we found between country biomass estimates for 2018 from FRA and CCI product, with a significantly higher correlation in countries with recent NFIs. We observed that NFI designs varied greatly in tropical countries. For example, the size of the plots ranged from 0.01 to 1 ha and more than three-quarters of the countries had smaller plots of ≤0.25 ha. The existing NFI designs could pose specific challenges for statistical integration with RS data in the tropics. Future NFI and space-based efforts should aim towards a more integrated approach taking advantage of both data streams to improve national estimates and help future data harmonization efforts. Regular NFI efforts can be expanded with the inclusion of some super-site plots to enhance data integration with currently available space-based applications. Issues related to cost implications versus improvements in the accuracy, timeliness, and sustainability of national forest biomass estimation should be further explored.

# Automatic detection of tree species in heterogeneous forests using RGB imagery and deep learning

EARSeL Bucharest 2023
Abstract

Corresponding Author: Mirela Beloiu
email address: mirela.beloiu@usys.ethz.ch

Mirela Beloiu[1], Nataliia Rehush[2], Verena Griess[1]

[1] ETH Zurich, Department of Environmental Systems Science, Switzerland
[2] Swiss Federal Institute for Forest, Snow and Landscape Research WSL

**Keywords:** forest monitoring, Convolutional Neural Network (CNN), conifer and deciduous species, temperate forest, tree species geolocation

## Abstract

Forests provide a myriad of ecological, economic, and climatic benefits, yet they are highly vulnerable to climate extremes. Active management of forest ecosystems for resilience and adaptation is crucial to ensure that forests can continue to provide their many services today and for centuries to come. Forest monitoring and in particular tree species identification, is a fundamental building block to achieving these goals and enabling sustainable forest management. Yet species monitoring is a challenging task that typically requires extensive field surveys that are time-consuming and costly. In addressing these challenges, remote sensing can contribute significantly.

Among Deep Learning algorithms, convolutional neural networks (CNNs) are proving promising tools for efficient tree species detection and identification. Object detection algorithms have not yet been assessed for their suitability to detect and map multiple tree species in a heterogenous forest setting. Yet, they offer essential information over existing classification approaches, such as identifying and locating single tree species. The object detection algorithm can incorporate data from a range of tree species and be applied on a broader scale, thus having the potential to become a universal tree species detection algorithm. Here, we aim to address this challenge by developing an automatic, affordable, and simple approach using Convolutional Neural Networks (CNN) and open-source RGB imagery that can identify and geolocate tree species in heterogeneous forests. Over 10'000 individual tree points for coniferous and deciduous tree species were gathered from existing research and forest inventories for model training.

The results showed that multi-species models detecting a combination of coniferous species reached higher accuracies (F1-score of 0.80) than multi-species models detecting a coniferous-deciduous species mixture (0.76) (Fig. 1). While *Pinus sylvestris* was most accurately detected in multi-species models (Fig. 1b), *Picea abies* was detected with the highest accuracy in single-species models. Compared with single-species models, multi-species models had improved precision but decreased recall. Further, when more species were added to the models, the number of misclassified tree species decreased. Generally, the performance of the CNN models was influenced by site conditions, such as forest stand structure, and less by illumination.

This work advances our current understanding of forest inventory by providing an automatic and accessible approach for detecting both individual tree crowns and tree species in heterogenous forests using the available CNN framework. This approach has the advantage of being applicable to other regions where the studied species are widespread and RGB imagery is available. Thus, the presented CNNs models and approach are compatible with low-cost UAV systems that are easy to operate and thus applicable to a wide range of users. Such automatic species identification can serve as a basis for improved inventory planning, forestry operations planning, and targeted management actions for more resilient forests.

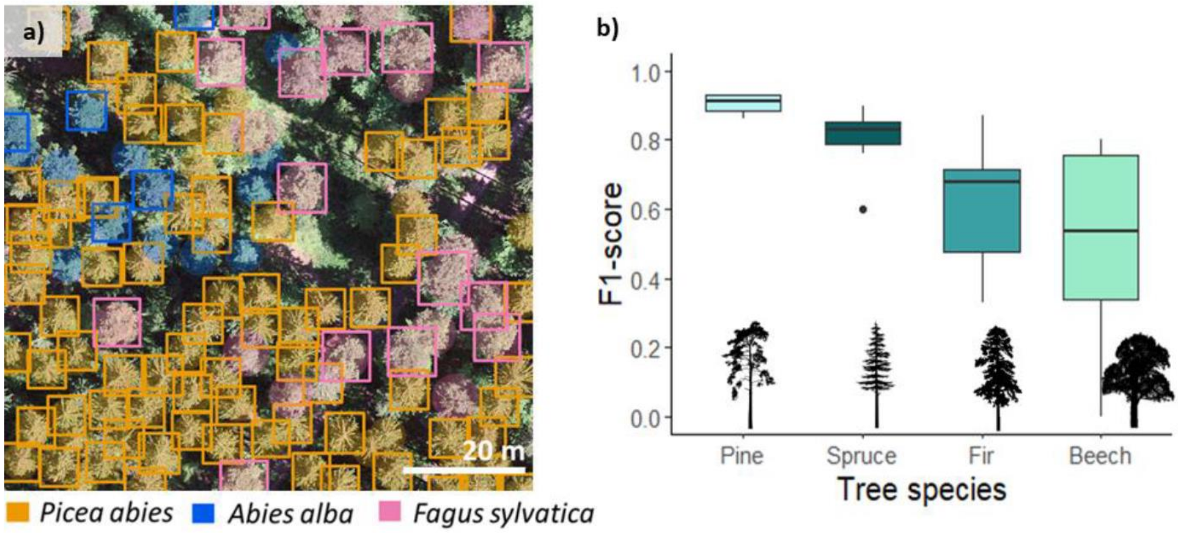

**Figure 1.** Model performance of multi-species detection in heterogeneous forests. (a) Tree species detection in a (1-ha) test site and (b) F1-score for each species, with values closer to 1 indicating higher accuracy. Bounding boxes = detected trees, circles = ground-truth data.

# Identification, mapping, and assessment of windthrow effects using remote sensing methods

EARSeL Bucharest 2023
Abstract
Ionel BAN
banionell@yahoo.com

Constantin-Cosmin LOGHIN[1], Flaviu POPESCU[1], Florin ACHIM[1], Ionel BAN[1], Mihai FURDUI[1], Robert-Ştefan CIOBANU[1], Răzvan RĂDUCU[1], Virgil ZAMFIRA[2], Aurelian VLĂDOIU[2],

[1]National Institute for Research and Development in Forestry „Marin Drăcea”, Romania;
[2]Curtea de Argeș Forest District, Romania

**KEYWORDS:** WINDTHROW, DRONE, WOOD VOLUME, REMOTE SENSING, SPRUCE STAND

## Abstract

The integration of precision photogrammetry into forestry management is subject to some aspects related to the prevention and reduction of risks associated with the forest health (pest attacks and other phytopathological vectors), in the prevention and reduction of personnel injury risks during the management of natural hazards of windfall.

Therefore, the purpose of this paper is to present, in the context of the forestry management of a disruptive event, how is a managed a windfall that occurs in a high-altitude stand.

The photograms were obtained with the help of a eBee RTK drone, equipped with a camera with standard sensors, type RGB, 12Mp, by making a flight at a height of 400 m above the crown of the trees. The forest stand subject to evaluation is located in the upper mountainous area of the Făgăraș Mountains, in the Vâlsan river basin, at altitudes ranging between 1500 and 1700m and which was affected by windthrow in December 2019.

The flight to assess the damage caused by the wind throw was carried out in June 2020, for the assessment of the impact, the most representative management units (UP I Vâlsan, - 29B, 30B, 32A and 33A) were selected. The preliminary results, obtained immediately after the flight, consisted of orthophoto plans (referenced and assembled frames), these being used for the administrator of the forest in order to identify the affected areas and to evaluate the wood volume that needs to be harvested.

The results obtained after the complete inventory of the wood volume were correlated with the data obtained from the photo interpretations, in order to identify expeditious methods of quantitative evaluation of the impact of the windthrow.

The use of local aerial photograms in forestry proves to be a quick and effective way to identify the disruptive natural events (wind throws, snow breaks, insect attacks), allowing decisions making process to be efficient in order to reduce of the impact of negative effects on the forest environment. The improvement of aerospace technologies, through the development of new methods, will allow in the short future to make more accurate quantitative assessments regarding the impact of disturbing factors on the forests.

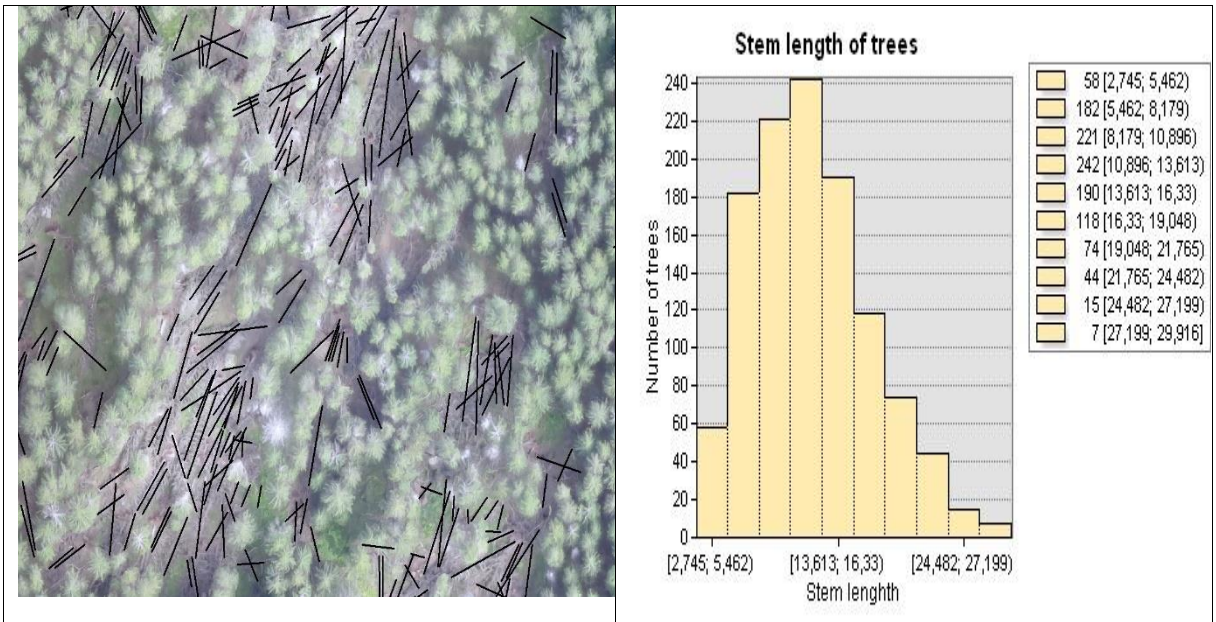

(a) (b)

**Figure 13.** Spruce main stems were identified on orthophoto maps (a) sample image from the analysis set – management unit 33A (b) graph showing stem length distribution over management unit 32A

## Section VIII - Risk detection and management in agriculture - climate

# A web tool for irrigation management to support local authorities and farmers in Cyprus from ERATOSTHENES Centre of Excellence

EARSeL Bucharest 2023

Abstract

Corresponding Author:
stelios.neophytides@eratosthenes.org.cy

Stelios P. Neophytides[1,3], Marinos Eliades[1], Georgios Papadavid[2], Christiana Papoutsa[1,3], Diofantos Hadjimitsis[1,3]

[1] ERATOSTHENES Centre of Excellence, Cyprus
[2]Agriculture Research Institute, Cyprus
[3]Cyprus University of Technology, Cyprus

**Keywords:** agriculture, agricultural meteorology, web-app, crop evapotranspiration, irrigation management

The EMMENA area encompasses various climate regions, including desert and semi-arid areas in the south and subtropical and temperate regions in the north. Over the past 40 years, the region has seen accelerated warming at a rate that is almost double the global average and faster than other regions such as Europe and North America. Changes in the water cycle and rainfall patterns have also been observed, leading to droughts in some areas that are unparalleled in the recorded history. Cyprus is an area in this region which means that it is affected by hot summer and long dry periods. All these phaenomena are expected to increase their intensity due to Climate Crisis as has been projected in many future climate projections.

These extreme weather events are affecting various ecosystems such as agriculture, forestry, and wetlands. Agriculture is one of the main industries of Cyprus and it needs different resources to survive among them, the irrigated water. In order to support the industry, ERATOSTHENES Centre of Excellence in collaboration with Agriculture Research Institute of Cyprus (ARI) is developing a web tool, which is an online web application, which at the first phase is integrating an agricultural meteorology tool, forecasting and mapping the daily reference crop evapotranspiration ($ET_o$) and crop evapotranspiration under standard conditions ($ET_c$) using meteorological measurements daily acquired from the 45 meteorological stations of Department of Meteorology network. Evapotranspiration is the occurrence of two physical events at the same time, evaporation, and transpiration. It is difficult to differentiate between evaporation and transpiration as they both occur at the same time. The amount of evaporation from a cropped soil is largely influenced by the amount of sunlight that reaches the soil surface and the availability of water in the topsoil. As the crop grows and covers more of the ground, the amount of solar radiation reaching the soil decreases, and transpiration becomes the dominant process, while evaporation becomes less important. At the beginning of the growing period, nearly all the water loss is due to evaporation, but by the time the crop is fully developed and covers the entire soil surface, over 90% of the water loss is through transpiration.

To calculate the daily evapotranspiration, we set up an interface between our server and the Department of Meteorology, and we are feeding with the measurements the Penman-Monteith (FAO 56) mathematical equation (1) which results to the reference crop evapotranspiration. Standard conditions crop reference evapotranspiration is a result of the multiplication (2) of $ET_o$ with Crop Coefficient (Table

1) factor ($K_c$). The values of $K_c$ represent the crop type and the development of the crop. There may be several $K_c$ values for a single crop depending on the crop's stage of development. During the crop's germination and establishment most of the evaporation occurs as evaporation from the soil surface.

Table 1. Crop coefficient factor ($K_c$)

Reference crop evapotranspiration and crop evapotranspiration under standard conditions is calculated as described in the following equations responsively:

$$(1)\ ETo = \frac{0.408\Delta(R_n - G) + \gamma \frac{900}{T+273} u_2 (e_s - e_a)}{\Delta + \gamma\left(1_{0.34u_2}\right)}$$

where:

Rn = net radiation at the crop surface

G = soil heat flux density

T = mean daily temperature at 2 m height

$u_2$ = wind speed at 2 m height

$e_s$ = saturation vapour pressure

$e_a$ = actual vapour pressure

$e_s - e_a$ = vapour pressure deficit

Δ = slope vapour pressure curve

γ = psychrometric constant

$$(2)\ ET_c = ET_o\ x\ K_c$$

where:

$ET_o$ = Reference evapotranspiration

$K_c$ = Crop coefficient factor

In order to calculate an approximation of the water losses in litres per day we are using the following equation (3):

$$(3)\ Water\ Losses = ET_o\ x\ A$$

Where:

$ET_o$ = Reference evapotranspiration

A = Crop covered area

Furthermore, as our measurements are local on different points representing the meteorological stations of meteorological network, around Cyprus, and in order to provide users with an evapotranspiration forecasting covering all the different agricultural and forest areas of Cyprus we deployed an interpolation model, utilizing Inverse Weighted Distance (IDW) interpolation method which is a kind of multivariate interpolation estimates the values between the different meteorological stations (points). The closer a pixel/cell is to a meteorological station, there is an increased likelihood have similar value.

This web application will be serving the community such as farmers, local authorities, stakeholders in order to adapt better irrigation management accordingly to the irrigation demands and water losses. Another service to the community of our hub will be the calculation of daily reference crop evapotranspiration over the afforested areas in Cyprus. The list of support crop categories will be updated in a regular basis. Our major scope is to enlarge this web tool and be a completed suite of tools by combining in the future with the Cyprus national Data Cube for environmental monitoring built by our team, in-situ measurements (soil moisture, soil temperature, electrical conductivity, etc.) of LoRa Wide Area Network (LoRaWAN) Internet of Things (IoT) sensors network that we are willing to establish in important agricultural zones of Cyprus and offer more tools.

**Work still under development, it will be online soon. Contact the corresponding author for more information if needed.*

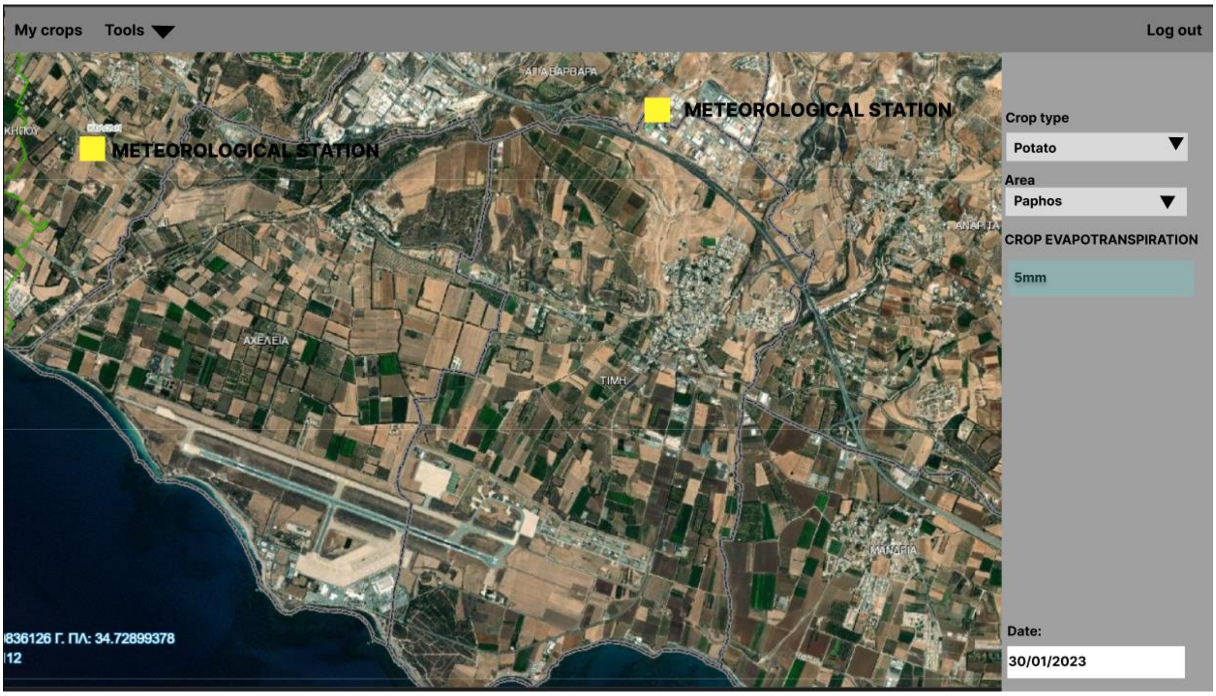

Crop type: Potato

Area: Paphos

CROP EVAPOTRANSPIRATION: 5mm

Date: 30/01/2023

**Figure 14.** Platform graphical user interface mock up

# Agricultural drought monitoring in the Danubian lowland using vegetations indices derived from MODIS time series

EARSeL Bucharest 2023
Abstract
Corresponding Author:
tomas.rusnak@savba.sk

Tomáš Rusňák[1]

[1] Institute of Landscape Ecology, Slovak Academy of Sciences v.v.i., Slovakia

**Keywords:** Danubian lowland, Drought indices, MODIS, NDVI, VHI

## Abstract

To identify drought risk during the growing season and reducing possible agricultural losses, effective drought monitoring is necessary. Knowing when and where vegetation growth is predominantly water-limited in this setting. Remote sensing as an important tool has been widely used for drought managing and monitoring. Remote sensing-based drought indices can identify agricultural dry zones. In our study we focused on maize crops in Danubian lowland in growing season (April to August) from 2019 to 2022. In our analysis we used Vegetation Health Index (VHI) and NDVI anomaly, which are ones of the most used remote sensing indices for drought monitoring and can be used to monitor the areas where vegetation may be stressed, as proxy to detect potential drought. VHI can be derived based on both the Land Temperature Surface (LST) and Normalized Differenced Vegetation Index (NDVI) from MODIS (MOD13Q1.061 Terra Vegetation Indices 16-Day Global 250m). We calculate monthly average of indices of crops for particular months. Monthly indices of crops were aggregate to hexagonal grids (5,1 km2) based on area weighted interpolation. VHI represent overall vegetation health in percentage (0 – 100). Based on the NDVI anomaly we classified 5 classification classes: mild drought, moderate drought, severe drought, and a very severe drought in descending order of severity. We found that overall, the most vulnerable month for maize are April and May (54.83 and 52.52 % of area). However, August of 2022 were very specific because 94,64 % of all area were affected by long term drought.

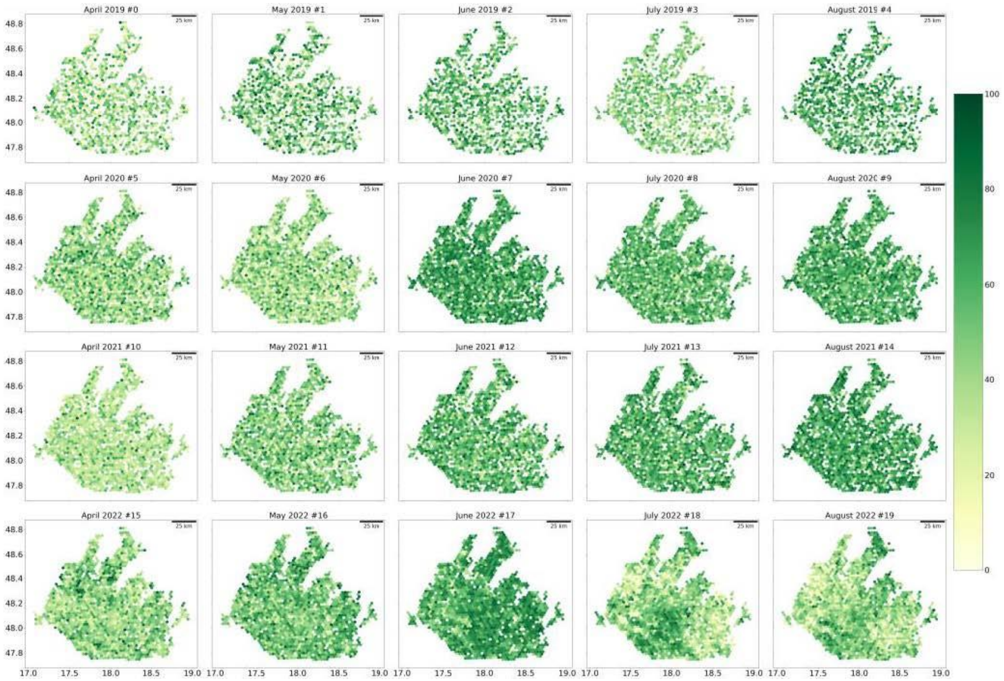

**Figure 1.** (a) Drought mapping in Danubian lownlad using VHI index during growing season (April to August) from 2019 to 2022.

# Evaluating Sentinel-1's ability to identify bare soil on tillage parcels in winter in the Republic of Ireland using Random Forest Model

EARSeL Bucharest 2023
Abstract
Mohana Priya Logakrishnan:
MohanaPriya.Logakrishnan@teagasc.ie

Mohana Priya Logakrishnan[1&2], Jesko Zimmermann[1] Stuart Green[1&2]

[1] TEAGASC-REDP, Ashtown, Dublin, Ireland
[2] TERRAIN-AI, Ireland

**Keywords:** Winter Cover crop, Sentinel-1, RVI

## Abstract

Establishing winter cover crops on tilled ground is an important management process to mitigate GHG emissions. Winter cover crops are also an effective way to reduce nitrate leaching into water bodies. On-site farm surveys may not be practical to determine which farms comply with the obligations to plant such crops because the costs are significant and require periodic monitoring. Many high spatial, spectral, and temporal resolution satellite images are now freely available and have proven to be a valuable resource in monitoring agriculture activities on the ground. The use of vegetation indices from optical sensors is a well-established technique to distinguish vegetation types and determine their quality and quantity. However, the persistent cloud cover in northern Europe limits the use of time-series optical sensor images to monitor the changes. Synthetic-Aperture Radar (SAR) can penetrate clouds, and its capability of monitoring vegetation is proven; hence, we explored the capability of SAR in this study.

This study evaluated the potential of Sentinel-1 in identifying farms that do not have winter green cover crops in the Republic of Ireland using a Random Forest (RF) model. A preliminary analysis, exploring simple ratios and backscatter thresholds, using a panel data approach (five acquisitions of SAR both on rainy and non-rainy days between November and December 2019 for the same parcels) indicates that an increase in rainfall (2 days cumulative) has a negative effect on VH backscatter (on both bare and vegetated fields). A significant positive effect is observed on VV backscatter (vegetation), reducing the effectiveness of a backscatter threshold approach to detecting bare soil.

Three RF models were trained, tested, and validated in this study on two sites in ROI, Lullymore and Gorey. The first two models were created using images from two distinct time periods at the Lullymore site (Model-A, 16 December 2019, 2-day cumulative rain – 0 mm, and Model-B, 2 December 2019, 2-day cumulative rain - 0.2 mm). The third model (Model-C) is the difference between the two periods. To train the model classes (bare and vegetation), the corresponding time period of Sentinel-2 and high resolution Google Earth imagery were available. The input parameters to the RF model are RVI, the normalized ratio procedure between bands (NRPB), VH, VV, and their quotient and product in decibels. The trained model (546 parcels) was applied to the testing dataset (234 land parcels). The performance of the model was also validated on a different site (389 land parcels at the Gorey site) using images from November 3, 2020, and December 3, 2020. On the tested data set, the overall accuracy of the three models is 90.17%, 85.47%, and 88.03%, with kappa coefficients of 0.80, 0.76, and 0.71, respectively. The overall accuracy of the three models on the validation data set is 84.6%, 73%, and 82.12%, respectively, with a kappa coefficient of 0.56, 0.40, and 0.51, respectively. The majority of completely bare and vegetation parcels are classified accurately, whereas crop residues and scattered low vegetation parcels pose a challenge, as does the absence of a definition of "bare soil" within relevant agri-environment policies.

# From the Lab to the Farm: Quantifying Factors Influencing Temperature Measurements from Miniaturized Thermal Cameras to Benefit Crop Water Stress Detection at Different Crop Growth Stages

EARSeL Bucharest 2023
Abstract
Corresponding Author:
quanxing.wan@wur.nl

Quanxing Wan [1], Magdalena Smigaj [1], Benjamin Brede [2], and Lammert Kooistra [1]

[1] Laboratory of Geo-Information Science and Remote Sensing, Wageningen University & Research, Droevendaalsesteeg 3, 6708 PB Wageningen, The Netherlands; magdalena.smigaj@wur.nl (M.S.); lammert.kooistra@wur.nl (L.K.)

[2] Helmholtz Center Potsdam GFZ German Research Centre for Geosciences, Section 1.4 Remote Sensing and Geoinformatics, Telegrafenberg, 14473 Potsdam, Germany; benjamin.brede@gfz-potsdam.de (B.B.)

**Keywords:** UAV; thermal imaging; FLIR; WIRIS; emissivity; calibration; non-uniformity correction; drift compensation; ambient environment; canopy temperature; maize; water stress

## Abstract

The detection of crop water stress requires detecting subtle temperature changes, which might not be as crucial for other applications. The capability of capturing subtle changes needs a good understanding of the structure and work process of thermal cameras and error sources. However, it is challenging to derive accurate temperature observations from uncooled thermal cameras on Unmanned Aerial Vehicles (UAV) in a field setting due to sensors' intrinsic characteristics and continuously changing ambient environmental conditions that can affect temperature readings. In this study, we aimed to delineate the spatial distribution of crop water stress at different crop growth stages of maize for explaining its effect on biomass accumulation. To address this, we undertook multiple field campaigns at different crop phenological stages of maize using two UAV-based thermal sensors (FLIR Tau 2 and WIRIS 2nd GEN) that previously underwent laboratory characterisation of their performance. Among these campaigns, we accomplished pre-flights with self-prepared temperature reference materials aiming at gaining experience by using these materials for calibrating uncooled thermal sensors in the early vigour stage of maize. Flights have been executed at different flying heights (5 m, 10 m, 20 m, and 40 m) under varying meteorological conditions (e.g., air temperature, solar radiation, wind speed, etc.). The setup was based on quantifying the effect of a combination of factors on temperature measurements from uncooled thermal cameras during flights.

For calibration and evaluation purposes, multiple temperature reference materials were placed on the ground during flights. These materials included several types of panels with fixed-emissivity thermographic paints on the surface, different soil samples, a box of cold water, and warm water at a fixed temperature of 50 Celsius degrees in a slow cooker. The temperature range of these materials covered the conditions that might be experienced during the growth period of maize locally, allowing the application of the empirical line method for thermal imagery calibration. For comparison, contact-type thermocouples with a data logger were attached to the materials to record reference temperature data.

Before thermal imagery calibrations, preliminary results showed that the observation accuracy decreased significantly at higher flight heights under all ambient environmental conditions because of atmospheric attenuation of thermal radiation. With the inclusion of non-factory calibration models, the overall error in thermal-based temperature readings could be reduced. More importantly, as a major source of error when deriving temperatures from thermal cameras, emissivity values of ground targets could be adjusted conveniently referring not only to that of the adopted fixed-emissivity panels but also the well-documented spectral emissivity libraries. Therefore, higher final accuracy of in-field temperature measurements was achieved by treating multiple sources of error properly throughout the process from conducting fieldwork to post-processing steps.

During crop-sensitive periods, we joined the above-mentioned temperature reference materials in the field campaigns to test whether they could help correctly characterise the spatial variability (heterogeneity) of crop water stress without using any handheld thermal imager synchronously with UAV flights. The UAV-mounted thermal sensors flew above the reference materials multiple times (specifically, after take-off, in the middle of the flight, and before landing) to make the most use of temperature reference information. By this means, the spatial distribution of crop canopy temperature could be closer to the ground truth. The realization was enabled together with the correction of pre-tested error sources, which included applying non-uniformity corrections to individual images and solving the problem of thermal drifts in orthomosaics. In the post-processing procedure, we explored optimizing the photogrammetry processing workflow to assess how different practices in producing orthomosaics (e.g., different blending modes) could improve the absolute accuracy of temperature measurements outdoors as well. Further, the stress distribution could be delineated more properly and used to explain the yield loss by also joining auxiliary ground-based data.

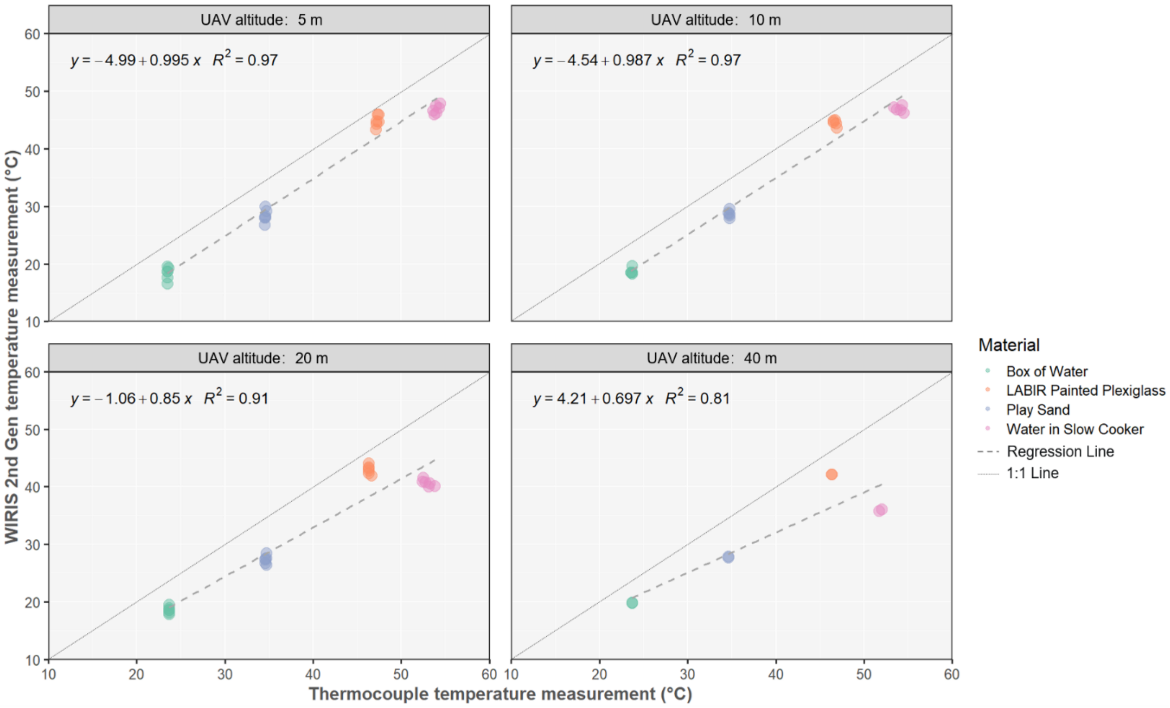

**Figure 15.** An example of validation of surface temperature recorded at varying flying heights by the UAV-mounted WIRIS 2nd Gen thermal camera with surface temperature recorded by the type-K thermocouples for temperature reference materials during a field campaign in Nergena, Wageningen on 11th May 2022.

# Comparing Multispectral RPAS And Satellite Data For Rice Crop Multitemporal Characterisation

EARSeL Bucharest 2023
Abstract Corresponding Author:
enrico.chiesa814@edu.unito.it

Enrico Chiesa[1], Samuele de Petris[1], Alessandro Farbo[1], Filippo Sarvia[1], Enrico Borgogno-Mondino[1]

[1]University of Turin, Department of Agricultural, Forest and Food Sciences, Grugliasco L.go Braccini 10095, Turin, Italy

**Keywords:** UAV, Mapir Survey 2, Sentinel-2, NDVI, Precision Farming, Rice

## Abstract

Rice is one of the most important crops in the world. In Italy, it is mainly cultivated in flooded paddy fields in the North-West as a highly demanding crop inputs. Precision agriculture (PA) has been found as a valuable tool to improve pesticides, water and fertilizers management through the combination of new technologies comprising Geographic Information Systems (GIS), Global Navigation Satellite System (GNSS) and Remote Sensing (RS) data. Specifically, RS can provide multispectral information from satellite and aerial platforms. Sentinel-2 (S2) satellite mission provides free data every five days with good spectral and spatial resolution (10-20 m). However, S2 geometric resolution may be inadequate in monitoring small fields typical of the Italian agricultural context. Thus, the introduction of UAV (Unmanned Aerial Vehicle or drones) has enriched the survey of vegetated surfaces. Especially in the agricultural context, the drones, equipped with appropriate sensors, can provide information about the surfaces investigated with a high geometric resolution. Moreover, the actual availability of low-cost multispectral sensors allows to map crops conditions and improve crop management following the PA approach. Despite market provided a huge number of multispectral sensors for UAV, their spectral measures reliability is poorly assessed by research community. Especially, for agricultural purposes, spectral measures inaccuracy can lead to misleading deductions and uneffective treatments. In this work spectral information from MAPIR Survey2 (MP) sensor was compared to one derived by S2. In particular, the comparison involved red and near infrared (NIR) bands (664 nm and 842 nm respectively). Study area (AOI, Fig. 1) is in Langosco municipality (NW-Italy), where a rice field sizing 8 ha was selected as test site. MP was equipped on the DJI Phantom 4 and four UAV flights performed. Sensing period was from 12/05/2022 to 06/09/2022 and somehow representative of 4 main rice phenological phases. Each flight was performed setting a relative height of 90 m and an average side- forward overlap between images of about 70% and 80% respectively. About 200 captures per image block were collected and processed in Agisoft PhotoScan vs 1.2.4. For each image block, 7 ground control points (GCPs) were surveyed in correspondence of target panels (markers) distributed over the area before the flight. GCPs survey was achieved by VRS-NRTK (Virtual Reference Station - Network Real Time Kinematic) GNSS mode using a Leica 1200 receiver (3D positioning accuracy was ~ 25 cm). After the block bundle adjustment, multispectral orthomosaics (OMs) were generated having a geometric resolution of 200 cm and a 3D positional accuracy of 50 cm. Finally, each OM were downsampled over S2 grid (geometric resolution 10m) using the average method. Normalized difference vegetation index (NDVI) was computed from both sensors. Resampled OM red, NIR and NDVI bands were compared at- the-pixel level to correspondent S2 ones (Fig. 2). Comparisons between S2 and MP spectral bands show variable correlation values depending on the phenological phase and the considered spectral bands. Specifically, NIR bands appear to be generally poor correlated while red bands highlight better correlation values. Finally, NDVI measures show in most cases the highest correlation values over the entire phenological season. Nevertheless,

after fitting an ordinary linear regression between NDVI maps from two sensors, a significant variability in regression gain and offset values exist alerting about the reliability of this correlation. To give practical implications of these results, for each sensing phase we finally computed a k-means unsupervised classification looking for 3 clusters somehow related to high, medium and low vigor conditions within AOI. Considering these preliminary findings and cost related issues of UAV data, it appears to be desirable a further deepening concerning the reliability of spectral measures from UAV low-cost sensors.

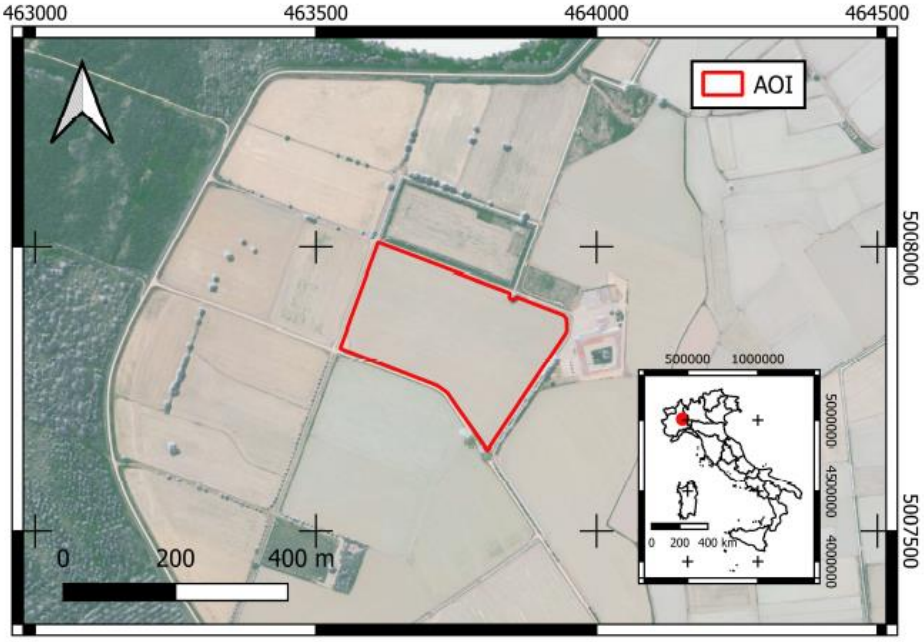

**Figure 1.** Study area (AOI) in Langosco, NW Italy. Reference System: WGS 84 / UTM 32 N, EPSG 32632.

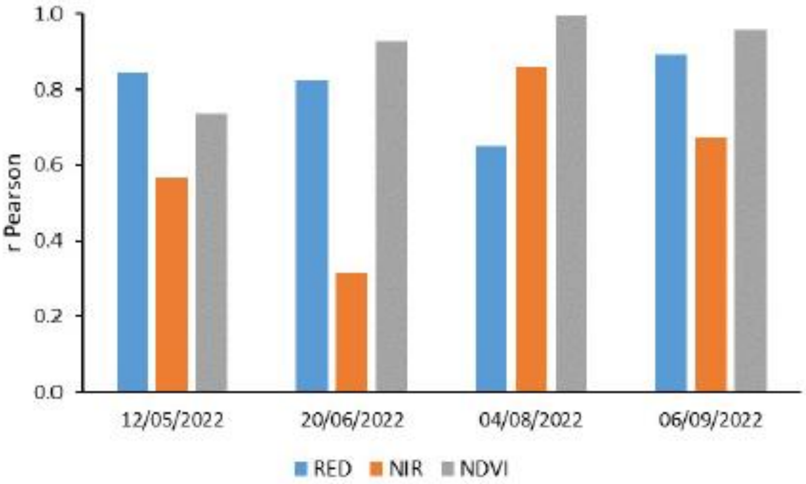

**Figure 2.** Correlations between S2 and MP red NIR and NDVI along phenological season.

## Section IX - Recent Earth Observation technology applications in natural hazards research

EARSeL Bucharest 2023
Abstract

Corresponding Author:
Ales Létal
ales.letal@upol.cz

# Automatic mapping of landslides by deep learning and high-resolution LiDAR products

Ales Létal[1], Ionuț Șandric[2], Jan Klimes[3],

[1]Palacký University Olomouc, Faculty of Science, Department of Geography, Czech Republic
[2]University of Bucharest, Faculty of Geography, Romania
[3]Institute Of Rock Structure And Mechanics Of The Czech Academy Of Sciences, Czech Republic

**Keywords:** landslides inventory, LiDAR, deep learning, U-NET

## Abstract

The present era is marked by the widespread use of advanced data collection methods, cloud technologies for efficient processing and sharing, and artificial intelligence with machine learning. These technological advancements have opened up new possibilities in the research and knowledge of Earth processes and landforms. Using these novel methods and data sources has enriched the field of geosciences in several ways: it has facilitated the acquisition of new knowledge, providing more detailed and comprehensive views of landforms and processes and has extended our knowledge in time from the past to the future, from the local to the planetary level; it has promoted the development of multidisciplinary approaches to research activities, enriching and expanding geoscience disciplines; it has facilitated more efficient transfer and sharing of acquired skills and data in the geoscience community and beyond, including other scientific fields such as archaeology, technical fields, and public administration.

Better knowledge of hazards and appropriate measures to eliminate associated risks can transform acquired scientific knowledge into specific societal needs for sustainable life on Earth. Moreover, using modern approaches and technologies in mapping, analysing, and predicting natural hazards is highly desirable. In research activities, there is a growing trend to use a data-based approach (statistical approach) instead of a heuristic approach (knowledge-based). This approach eliminates subjectivity in the weight assignment process, quantifies the relative importance of various causative factors using objective techniques, and reduces bias. However, the quantitative methods are limited by data availability, quality, and reliability.

In the Czech Republic, the combination of morphological, lithological, and climatic properties has created three regions that are more susceptible to landslides, covering around 34% of the country. The lithology in these regions is similar, with the northwest region consisting of Cretaceous sediments containing claystone, sandstones, siltstones, and marlstones. In addition, Neoidic volcanic intrusions layered on Perm and Cretaceous bedrocks have made slope instability complex in this area. The eastern region is comprised of Carpathians flysh rock layers, which also contribute to the higher risk of landslides in this region. Although the conditions for the occurrence of slope instabilities can be found in other areas of the country, they do not pose such a significant risk. These areas have also been mapped and included in the slope instability register.

In Czechia, the systematic registration of landslides was started in 1962 based on the results of nationwide registration of these phenomena in former Czechoslovakia ordered by Government Resolution No. 103/1961. The current study used the Slope Instability Register, which contains raw data on registered and verified slope instabilities in the Czech Republic. The register contains a map at 1: 25,000 scale and processed record cards with basic topographic, documentation, geological, geomorphological, geotechnical and economic - technical data. In 1976 it was transferred into database form. The database is now accessible as INSPIRE download service provided by the Czech Geological Survey Institute (https://app.geology.cz/atom/datalist2.xml). The database was verified over

high-resolution LiDAR data. User classification of the recorded landslides according to the current status and development was performed. Such a modified spatial database was an essential input for advanced analyses and deep-learning methods utilisation.

U-NET architecture was applied to LiDAR high-resolution digital surface and elevation models, available nationwide for the current study case. U-Net is a deep learning architecture that has been used in various image segmentation tasks, including those related to landslides. Originally developed for biomedical image processing, U-Net has been adopted in geosciences for its ability to accurately segment and classify landslide features from satellite imagery and other remote sensing data. The U-Net architecture is well-suited for landslide segmentation because it can effectively capture the complex patterns and morphological features of landslides, such as their shape, size, and location. The use of U- Net for landslide mapping can help improve our understanding of landslide hazards and facilitate better decision-making for disaster risk reduction and management.

Overall, the U-Net architecture has proven to be a powerful tool in landslide research, offering improved accuracy and efficiency in landslide mapping and monitoring. As U-Net and other deep learning methods continue to expand in the geosciences, their potential for improving landslide hazard assessment and management will only increase.

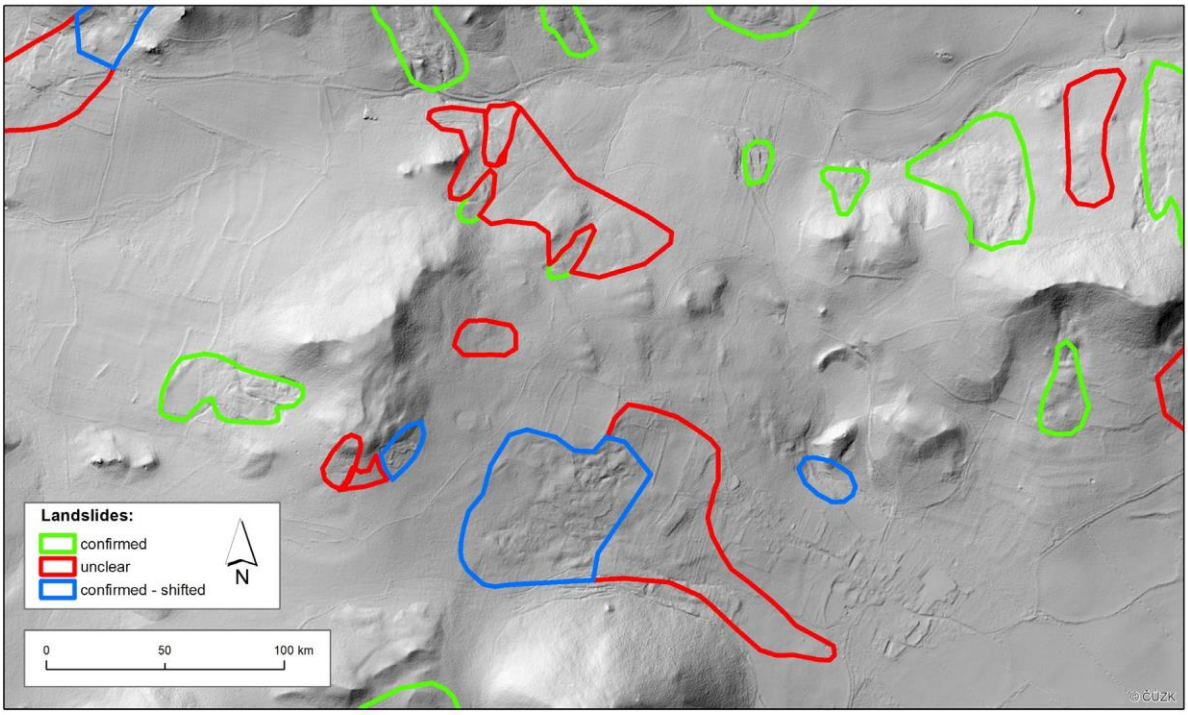

**Figure 1.** Example of verified landslide inventory under LiDAR high-resolution DEM used in research process

# Satellite analysis of the impact of severe meteorological phenomena on the vulnerable sandy lands of the Baragan Plain

EARSeL Bucharest 2023
Abstract

Corresponding Author:
claudiu.angearu@meteoromania.ro

Claudiu-Valeriu Angearu[1], Anişoara Irimescu[1], Denis Mihăilescu[1], Irina Onțel[1], Argentina Nerțan[1], Vasile Crăciunescu[1]
[1] National Meteorological Administration, Department of Remote Sensing and Meteorological Satellite, Romania

**Keywords:** Baragan Plain, blizzard, wind erosion, Copernicus, Sentinel-2, Landsat

## Abstract

This paper is about the importance of using satellite images for monitoring and analyzing natural hazards in the Baragan Plain caused by the action of the wind, namely blizzard and wind erosion. In Baragan Plain, the vulnerability to destructuring processes through wind erosion manifests itself differently, the soil texture having a special role, so that soils with a loamy, sandy texture or in combinations between clay and sand represent surfaces at risk of degradation. An area of about 110.000 ha within the studied plain presents soils with a high and very high risk of manifestation of degradation processes caused by wind erosion. The process of deflation in the Baragan Plain (a form of wind erosion in which fine, dry soil particles are blown away, removing the top layer of soil) is clearly visible since 1987 from the multitemporal analysis of Landsat-5 satellite images (30 m spatial resolution) in natural color combinations. In recent years (e.g., 2019-2020), the deflation produced by wind erosion was much more pronounced throughout the spring, Sentinel-2 images (10 m spatial resolution) capturing this fact very well. At the level of soils vulnerable to wind erosion, the processes arising from changes in land use in the period 1990-2018 represent about 15%. In the case of the blizzard phenomenon of January 2017 (the blizzard episodes from 6, 10-11 and 17-18 January), the satellite analysis of its effects was performed only for the available satellite images unaffected by cloud cover, namely the Sentinel-2 data from 13 and 26 January. The vulnerable lands between the localities of Însurăței and Zăvoaia (south of Lake Traian), respectively the lands south of the localities of Săveni, Lăcusteni and Platonești were noted based on the comparison of the two temporal false-color images, and the threshold of 0.4 of the Normalized Difference Snow Index (NDSI), computed from Sentinel-2 images. By correlating the areas bare of snow and the types of land use (extracted from the Corine Land Cover 2018 database) it was found that an area of 24.353 ha was affected by the blizzard, of which 22.202 ha was arable land, 1.655 ha was pasture, 277.41 ha of vineyards and 205.12 ha of orchards. In the case of sandy lands vulnerable to wind erosion in the localities of Zăvoaia and Insurației, the blizzard affected an area of 2.086 ha, with arable land being the most affected (2.024 ha), followed by pastures (60 ha) and vineyards (2 ha).

At the level of soils vulnerable to wind erosion, the processes arising from land use changes in the period 1990-2018 represent about 15%, occupying an area of 19.086,98 ha out of the total vulnerable area of 130.450 ha. Extensification is the main process (73.26% of the total area), followed by intensification (17.51). In the case of the afforestation process, the third in weight of the total changes that occurred (6.75%), the beneficial role of the resulting conversion can be emphasized, because the presence of the forest in the region vulnerable to wind erosion determines the reduction of the impact of the wind erosion and deflation processes, respectively the restoration soil quality.

Therefore, high-resolution spatial satellite images and products such as Sentinel-2 and Landsat-5 and 8 represent a very useful tool in the case of identifying and monitoring the effects produced by dangerous phenomena generated by the action of the wind (example: blizzard, wind erosion/deflation).

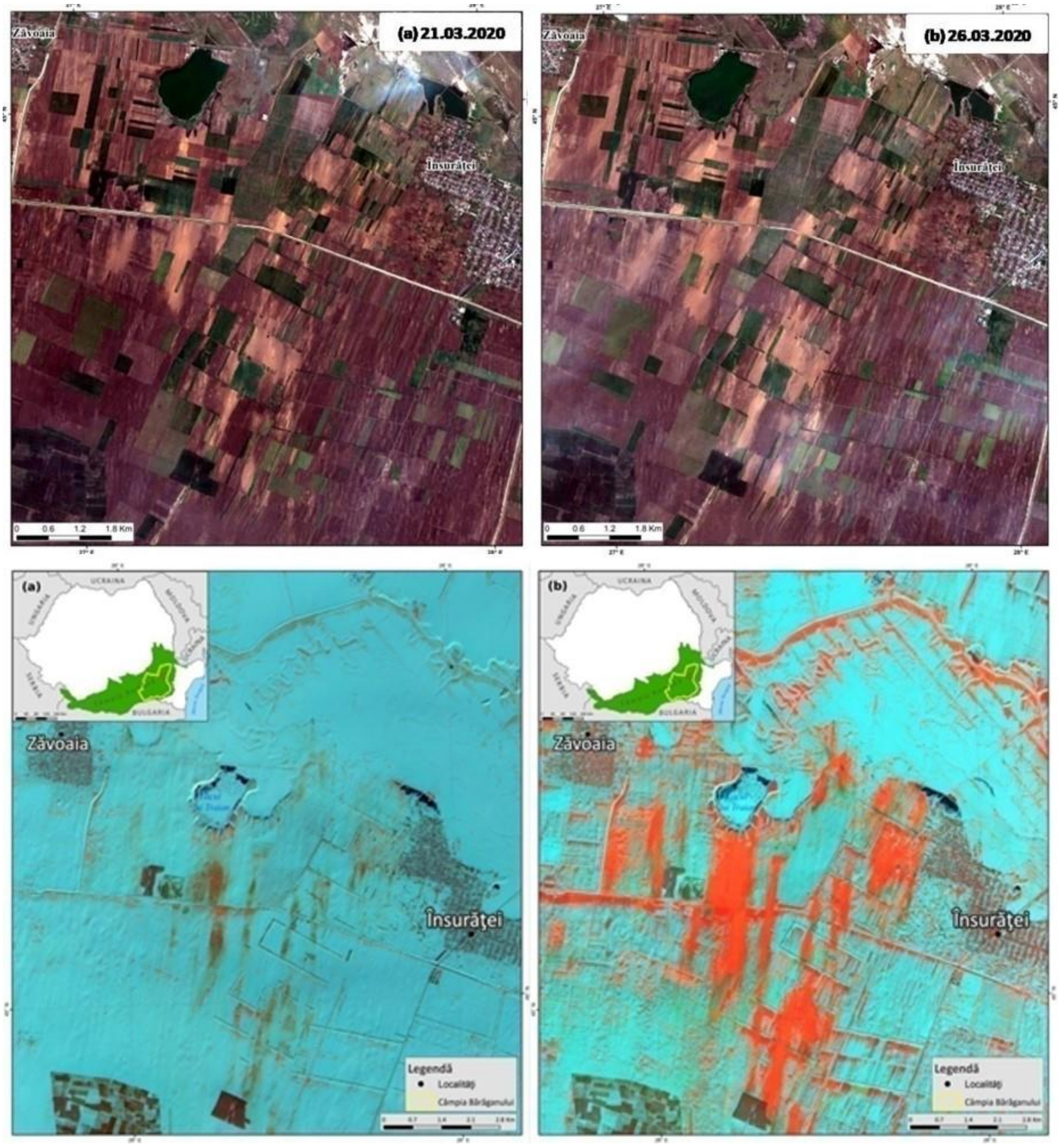

**Figure 16.** Wind erosion (the images above) from Sentinel-2: (a) 21 and (b) 26 March 2020;
The effects of the blizzard (Sentinel-2 data) between the Însurăței and Zăvoaia: (a) 13 and (b) 26 January 2017

# Mapping active slow-moving landslides using Persistent Scatters Interferometry in Romania

EARSeL Bucharest 2023
Abstract
Corresponding Author:
email address
ionut.sandric@geo.unibuc.ro

Ionuț Șandric[1], Viorel Ilinca[2], Zenaida Chițu[3,4], Radu Irimia[1], Ion Gheuca[2]

[1] University of Bucharest, Faculty of Geography, Romania
[2] Geological Institute of Romania, Romania
[3] National Meteorological Administration, Romania
[4] National Institute of Hydrology and Water Management, Romania

**Keywords:** persistent scatters, interferometry, landslides, space-time patterns

## Abstract

Persistent Scatterers Interferometry (PSI) is a remote sensing technique that has proven useful in mapping landslides. Landslides are natural hazards that are caused by geological, meteorological, and anthropogenic factors. They can have disastrous effects on human lives, infrastructure, and the environment. Therefore, their early detection and monitoring are critical for mitigating the risks associated with them. PSI has been found to be effective in mapping and monitoring landslides due to its ability to detect ground movements with high precision and over large areas. The principle of PSI is based on the interferometric phase differences between radar images acquired from a Synthetic Aperture Radar (SAR) sensor. The distance causes the phase difference between two radar images travelled by the radar signal between the satellite and the ground surface. This distance is affected by the topography and any changes in the ground surface, including landslides. By analysing the interferometric phase differences of a series of SAR images, PSI can detect and measure the magnitude of ground movements that occur between the acquisitions of the images. PSI works by analysing the radar images of an area acquired over a long period, typically several years. The images are processed to generate a coherence matrix, which is a measure of the similarity between two images. The coherence matrix is then analysed to identify stable points on the ground surface, known as Persistent Scatterers (PS). These points have a high coherence over the entire period of image acquisition, indicating that they have not undergone significant ground movements during this period. The PS points are then used as reference points to calculate the interferometric phase differences between subsequent radar images. Any changes in the phase differences are interpreted as ground movements, which are then mapped and monitored over time. PSI has several advantages over other remote sensing techniques for mapping landslides. Firstly, it can detect ground movements with high precision, typically within a few millimetres. This level of precision is critical for detecting small-scale ground movements that may indicate the early stages of a landslide. Secondly, PSI can map large areas over long periods, allowing for the identification of temporal patterns in ground movements. This information can predict the likelihood of a landslide and monitor its progress over time. Finally, PSI is insensitive to atmospheric conditions, making it a reliable technique for mapping landslides in areas with frequent cloud cover or precipitation.

For the current study, the data provided by the European Ground Motion Service (EGMS) was used. EGMS is a European Union (EU) funded initiative that provides information on ground motion and deformation across Europe. The EGMS data products are available free of charge to registered users through a web-based portal. The portal allows users to access a range of data products, including ground motion velocity maps, time series of ground motion, and displacement maps. The data products are presented in a user-friendly format, allowing users to visualise and download the data for further analysis easily.

The analysed area is located in the Subcarpathians and the Curbura Carpathians in Romania, an area heavily affected by landslides. The current study aims to create a current inventory of active slow-moving landslides, unlike similar studies that generated inventories of landslides regardless of the state of

the landslides. The spatial identification of a landslide was achieved by using the Getis-Ord Gi spatial clustering algorithm to identify areas, where persistent scatters are grouped. The algorithm, implemented in ArcGIS Pro software, was run on the mean velocity values extracted from the Ortho product offered by EGMS. Only the clusters formed for a confidence interval of at least 90% were retained. The state of the landslide was determined by applying the algorithms for identifying trends from a time series. Thus, only those points with a clear subsidence tendency were retained as active deformations. The spatial distribution of landslides located in areas without forest vegetation was obtained from the intersection of the spatial clusters with the points with a semi-significant trend. The automatically mapped landslides were validated by intersecting the points with an existing inventory, achieved through the interpretation of high-resolution aerial images. If at least one persistent point intersected a landslide, then it was considered a valid detection. Thus, more than 80% of the persistent points considered to be active landslides were validated.

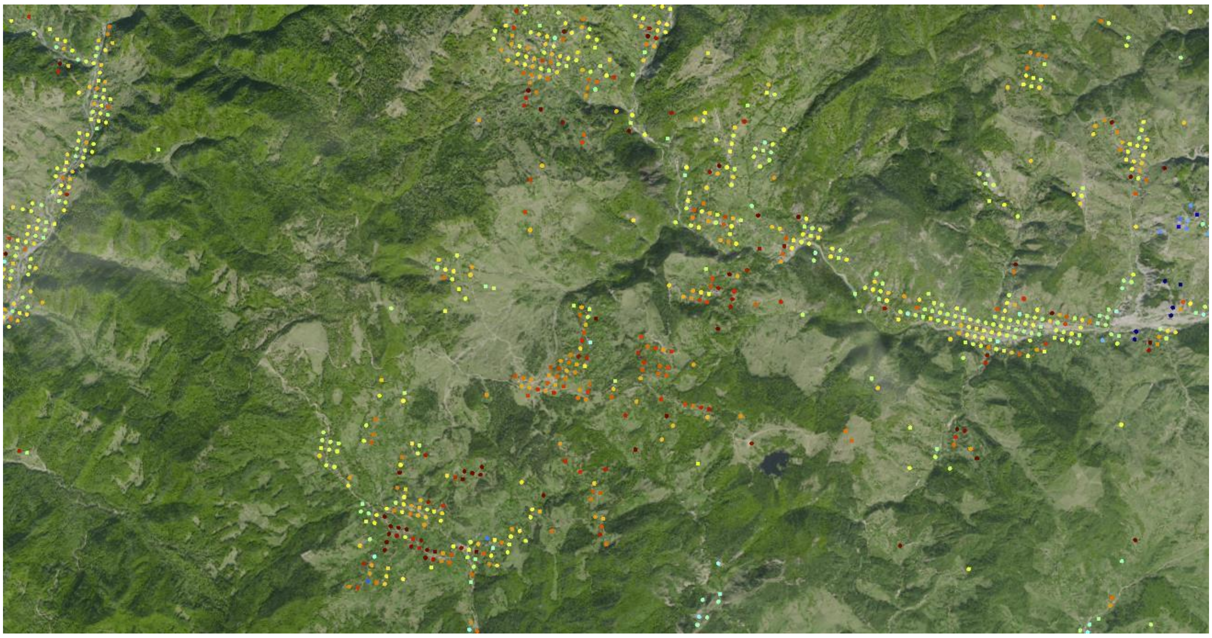

**Figure 1.** Persistent Scatters showing surface deformations in mm over Bent Subcarpathians.

EARSeL Bucharest 2023
Abstract

Corresponding Author: Mohammad Amin Khalili
Mohammadamin.khalili@unina.it

# Enhancing Landslide Deformation Prediction in Southern Italy Using a CNN-LSTM Algorithm with Spatio-Temporal Dependency

Mohammad Amin Khalili[1], Luigi Guerriero[2], Domenico Calcaterra[2], Diego Di Martire[2]

[1] Federico II University of Naples, Department of Earth, Environmental and Resource Sciences, Italy
[2]Federico II University of Naples, Italy

**Keywords:** Landslide prediction, CNN-LSTM algorithm, Spatio-Temporal dependency, Deep learning, Machine learning, Moio della Civitella, PSI technique

## Abstract

Landslides are a significant natural hazard that can cause severe damage to infrastructure and impact local communities' safety and prosperity. Accurate and reliable prediction of deformation caused by landslides is crucial to implementing effective disaster management strategies that can mitigate the risk of landslides and their impact on communities. This study proposes a comprehensive approach to landslide prediction in the Moio della Civitella region of southern Italy, a critical area that has experienced significant landslides that have impacted settlements and infrastructure. The study uses a CNN-LSTM algorithm with Spatio-Temporal dependency to predict cumulative deformation caused by landslides, employing geological, geomorphological, and geospatial data as predisposing factors. These factors include elevation, slope, Topographic Wetness Index (TWI), Stream Power Index (SPI), geology, flow direction, curvature, Normalized Difference Vegetation Index (NDVI), and land use. The Permanent Scatterer Interferometry (PSI) technique was used to obtain cumulative deformation data as labels, providing an extensive data set that allowed for accurate and reliable prediction of landslide deformation. The proposed CNN-LSTM algorithm integrates convolutional neural networks (CNNs) and long short-term memory (LSTM) networks to learn the spatio-temporal dependencies between landslides' predisposing factors and their cumulative deformation. This approach allows the algorithm to capture the complex relationships between the predisposing factors and the occurrence of landslides, resulting in a more accurate and reliable understanding of landslide dynamics. In comparing the proposed CNN-LSTM algorithm with other deep learning architectures and machine learning algorithm, we found that these models were less effective in predicting cumulative deformation caused by landslides based on the evaluation metrics. For example, the Support Vector Machine (SVM) model was found to be less effective as it cannot model spatio-temporal dependencies and is limited to linear decision boundaries. Similarly, other deep learning architectures, such as Recurrent Neural Networks, Gated Recurrent Units, and LSTM, were outperformed by the CNN-LSTM model. While these models are effective in modeling temporal dependencies, they do not consider spatial information, which can limit their ability to capture the complex relationships between predisposing factors and the occurrence of landslides. Table 1 compares the advantages and disadvantages of the proposed CNN-LSTM algorithm with Spatio-Temporal dependency to other deep learning architectures and machine learning algorithms. The table highlights the advantages of the proposed algorithm in learning spatio-temporal dependencies and integrating geological and geospatial data while acknowledging its potential limitations due to its complex architecture. In table 2, we compare the RMSE (root mean squared error), MAE (mean absolute error), R2 (coefficient of determination) and explained variance metrics for the proposed CNN-LSTM algorithm with Spatio-Temporal dependency and other deep learning architectures and machine learning algorithms, which illustrates that the proposed CNN-LSTM algorithm with Spatio-Temporal dependency has the lowest RMSE and MAE, indicating that it has the highest accuracy in predicting cumulative deformation caused by landslides. The CNN-LSTM algorithm also has the highest R2 and explained variance metrics, indicating that it can explain a more significant proportion of the variance in landslide deformation. Overall, the proposed algorithm's superior performance in predicting cumulative deformation caused by landslides highlights the potential of deep learning algorithms to enhance landslide prediction and disaster management strategies. The

proposed algorithm can support effective decision-making, provide valuable insights for disaster management, and help mitigate the impact of landslides on local communities and infrastructure.

Table 1. Comparing the advantages and disadvantages of the proposed CNN-LSTM algorithm with RNN, GRU, LSTM, and SVM

| Algorithm | Advantages | Disadvantages |
|---|---|---|
| CNN-LSTM | Learns spatio-temporal dependencies | Complex architecture may require more computation resources |
| RNN | Good for modeling temporal dependencies | Cannot model spatio-temporal dependencies |
| LSTM | Good for modeling temporal dependencies | Cannot model spatio-temporal dependencies |
| SVM | Good for lineling temporal | Cannot model spatio-temporal dependencies |

Table 2. Comparing four evaluation metrics between the proposed CNN-LSTM algorithm with RNN, GRU, LSTM, and SVM

| Algorithm | RMSE | MAE | R2 | Explained Variance |
|---|---|---|---|---|
| CNN-LSTM | 0.1879 | 0.1763 | 0.8956 | 0.8972 |
| RNN | 0.8734 | 0.9378 | 0.7387 | 0.7391 |
| GRU | 0.6259 | 0.8572 | 0.7756 | 0.7775 |
| LSTM | 0.4719 | 0.5020 | 0.7571 | 0.7583 |
| SVM | 1.1087 | 1.0861 | 0.4389 | 0.4422 |

# Desertification Mitigation policies in the Face of Climate Change in Kenya: Exploring the potential of Remote Sensing for supporting stakeholder involvement

EARSeL Bucharest 2023

Abstract

Corresponding Author:

martinchegee@gmail.com,

angeline.asangire.oprong@uni-oldenburg.de

Martin W. Chege [1], Angeline Asangire Oprong [2]

[1] Remote Sensing Research Group (RSRG), Institute of Geomatics GIS & Remote sensing (IGGReS), Dedan Kimathi University of Technology (DeKUT), Kenya.

[2] Adjunct Lecturer, School of Computing Science, Business Administration, Economics and Law Carl von Ossietzky Universität Oldenburg, Germany

**Keywords:** DESERTIFICATION, CLIMATE CHANGE, REMOTE SENSING, MITIGATION POLICIES STAKEHOLDERS, KENYA

## Abstract

Desertification, a kind of land deterioration attributed to both natural processes and anthropogenic activity, is becoming an increasingly pressing issue in Kenya. The process is exacerbated by climate change, which in turn leads to a decrease in agricultural output and an increase in the susceptibility of the local people to a myriad of other problems. The purpose of this study is to investigate and discuss the challenges that prevent Kenya from successfully adopting remote sensing policies particularly for use in early warning in order to combat desertification attributed to climate change. It also explores the possibilities that exist and the way forward for incorporation of remote sensing in early warning systems.

The use of remote sensing technology has the potential to make a substantial contribution to the fight against desertification by delivering information that is both timely and accurate on the condition of the areas in question. This information may be used to involve stakeholders and improve their engagement in the execution of policies. This study investigates the feasibility of utilizing remote sensing to facilitate stakeholder participation in the development of desertification prevention policies in Kenya. Remote sensing data and information can be utilized to provide stakeholders with visual representations of the effects of desertification and facilitate assessment of the efficacy of desertification mitigation initiatives. Both climate change and remote sensing are overarching in nature and have an interdisciplinary characteristic that attract multiple stakeholders. The aforementioned attributes, are instrumental in combating desertification. However, in order to fully harness the promise of remote sensing, there are a number of challenges that need to be addressed. These constraints include weak policies, unavailability and inaccessibility of data, limited technological capability, and the requirement for inter-disciplinary collaboration. The findings of this study show the necessity for ongoing research and investments in remote sensing technology as a means to promote successful stakeholder participation in efforts to mitigate desertification in Kenya.

## Section X - Risk detection and management in agriculture - pests and weeds

# Leveraging Multimodality For Disease Detection In Seed Potatoes

EARSeL Bucharest 2023

Abstract

Corresponding Author:

magdalena.smigaj@wur.nl

Magdalena Smigaj[1], Harm Bartholomeus[1], Lammert Kooistra[1]

[1] Laboratory of Geo-Information Science and Remote Sensing, Wageningen University & Research, Droevendaalsesteeg 3, 6708 PB Wageningen, The Netherlands

**Keywords:** precision agriculture, disease detection, hyperspectral, thermal, LiDAR

## Abstract

As biotic and abiotic stresses can have adverse effects on yield and quality, information on their presence and severity is vital for effective crop management. The applicability of various remote sensing technologies (spectroscopy, thermography, LiDAR, fluorescence sensing) for detecting stress responses has been widely demonstrated. Each of these sensors can provide information on different physiological responses, i.e. hyperspectral imagery is sensitive to changes in leaf biochemical properties, thermography to alterations in transpiration, LiDAR to structural changes, and chlorophyll fluorescence to changes in photosynthesis. Combining information from such a range of sensors could therefore enhance the ability to quantify the stress level and diagnose its cause. However, most remote sensing research still focuses on utilisation of a single modality, predominantly focusing on spectral responses with the main limiting factor so far being data availability. The emergence of miniaturised multi-sensor arrays deployable on Uncrewed Aerial Vehicles (UAVs) has opened new possibilities. Over the last decade, UAVs have become a ubiquitous tool for environmental monitoring, providing a cost-effective alternative for surveys at local scale for applications which simultaneously require high spatial level of detail, such as precision agriculture. Yet explorations into multi-modal approaches and how they can contribute to detailed monitoring of stress levels and their causes has so far been limited.

We aimed to address this gap by exploring how different modalities can complement each other, focusing on improved detection of two commercially important diseases in seed potatoes, which produce a range of different infection symptoms: (i) late blight caused by bacterial infection with Erwinia spp. and (ii) the Potato virus Y (PVY). Further variability was added through incorporation of multiple potato varieties, which have shown varying levels of resistance to infection, within our trial. Throughout the growing season the condition of each plant was monitored on a weekly basis by a certified disease expert; exact locations of each diseased plant were recorded using a GNSS receiver. Following these visits we collected UAV-borne VNIR hyperspectral (Headwall Nano-Hyperspec), thermal (FLIR Tau 2) and LiDAR (Velodyne Puck) data, capturing symptoms development over time. In the analysis, we focused on derivation of plant-specific responses for which individual plants were segmented through point cloud clustering based on initial planting locations – these were mapped using a UAV RGB dataset collected soon after potato plant emergence. In this contribution, we will present preliminary results of investigations into (i) the disease diagnostic capabilities of the used modalities, (ii) how the importance of key plant-level metrics changes throughout the growing season, and (ii) the potential of multimodal remote sensing for differentiation between different diseases.

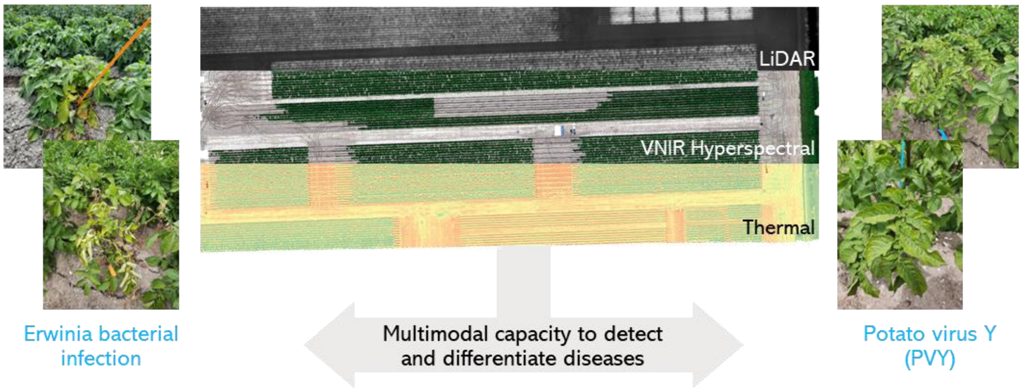

**Figure 17.** Simplified conceptual diagram of the study.

# Mapping vineyards pathogens using convolutional neural networks

EARSeL Bucharest 2023
Abstract
Corresponding Author:
Diana Petre

Diana Petre[1], Diana Vizitiu[2], Ionela Sărdărescu[2], Marian Dârdală[1], Cristian Ioniță[1], Ionuț Șandric[3]

[1] The Bucharest University of Economic Studies, Department of Economic Informatics and Cybernetics, Romania
[2] INCDBH Ştefăneşti, Romania
[3] University of Bucharest, Faculty of Geography, Romania

**Keywords:** convolutional neural networks, vineyards pathogens, object detection

## Abstract

Pathogens pose a significant threat to the health and productivity of vineyards worldwide. One of the most common and destructive pathogens affecting vineyards is Uncinula necator (U. necator), commonly known as grapevine powdery mildew. This fungal pathogen can infect all parts of the grapevine, including leaves, shoots, flowers, and fruit, causing significant damage to grape crops and reducing their quality and yield. The spread of this pathogen can also lead to a decline in vineyard health and productivity over time. Therefore, understanding the biology, ecology, and management strategies for grapevine powdery mildew and other pathogens is critical for maintaining the sustainability and profitability of vineyards. The study is focused on mapping several pathogens that can affect vineyards and compromise the annual yield by using object detection techniques based on convolutional neural network.

The study site is located in Ştefăneşti, a town located in Pitești county from Romania in the vineyard of the INCDBH Ştefăneşti. During a period between 2021 and 2022 images with several pathogens were collected with the Samsung phone (connected to a Flir device). The temporal and spatial distribution of the pathogen U. necator was monitored using a local meteorological station and the microclimate conditions of the study area were recorded. To map the U. necator distribution, images in both the visible spectrum and images in the thermal infrared spectrum were collected. The images from the thermal infrared spectrum were used to identify the thermal stress determined by the presence of the pathogen and based on that to detect the pathogen only on thermal stress. Also, the fusion between the thermal infrared spectrum and the visible spectrum was achieved, at the level of the Flir sensor. These images, RGB, thermal and false-color RGB-thermal, were used for sampling using the labelImg program. The samples were collected in PascalVOC format.

For the detection of the pathogen U. necator, the convolutional neural model Single Shot Detector was tested and trained. Single Shot Detector has two components: backbone and head. The backbone component is an image classification network pre-trained to recognize certain features. This is usually a network like ResNet, Inception V3 etc trained on ImageNet from which the final fully connected classification layer has been removed. SSD head is just one or more convolutional layers added to the backbone, and the outputs are interpreted as spatially localized object classes. Several training sessions with different sizes were run for the collected samples. Because the size of the images taken with the phone were very large and introduced noise in the training process, the images were cropped to smaller tiles. Several tests were made with different tile sizes and only the tiles with sizes of 128 pixels and 256 pixels were retained. Models with samples larger than 256 pixels gave unsatisfactory results and were abandoned. The algorithm used for cropping the images is based on ArcGIS Pro. To enhance and increase the number of images, several transformations were applied automatically by the ArcGIS Pro tool. For each tile size, a stride of half of the tile size was used, thus increasing the number of tiles generated for the training process. In this context, several models were used, including

EfficientNet0 with TensorFlow Lite object detector, RetinaNet with backbone ResNet50 and ResNet152, and Single Shot Detector with backbone ResNet50 and ResNet152, utilizing PyTorch and OpenAI. The use of pre-processed images helps to improve the accuracy of the models by reducing noise and unwanted features, allowing them to focus on the specific patterns and features indicative of vineyard pathogens. Successful deployment of these models could help growers and winemakers detect and respond to disease outbreaks quickly, leading to improved crop yields and the quality of the wine produced.

Using the previously mentioned models we have been able to obtain the following results, where the percentage refers to the Average Precision Score:

1) For the images with the tile of 256x256 pixels:
    - SingleShotDetector with resnet50 backbone: UN: 52%, PV: 18%, T: 55%;
    - SingleShotDetector with rasnet152 backbone: UN: 52%, PV: 19%, T: 57%;
    - RetinaNet with rasnet50 backbone: UN: 22%, PV: 18%, T: 26%;
    - RetinaNet with rasnet152 backbone: UN: 2%, PV: 1%, T: 19%;
    - Tensorflow Lite EffiecentNet0: UN: 23%, PV: 0%, T: 9%.
2) For the images with the tile of 126x126 pixels:
    - SingleShotDetector with resnet50 backbone: UN: 47%, PV: 26%, T: 55%;
    - SingleShotDetector with rasnet152 backbone: UN: 46%, PV: 26%, T: 57%;
    - RetinaNet with rasnet50 backbone: UN: 40%, PV: 25%, T: 42%;
    - RetinaNet with rasnet152 backbone: UN: 41%, PV: 33%, T: 42%;
    - Tensorflow Lite EffiecentNet0: UN: 25%, PV: 0%, T: 12%.

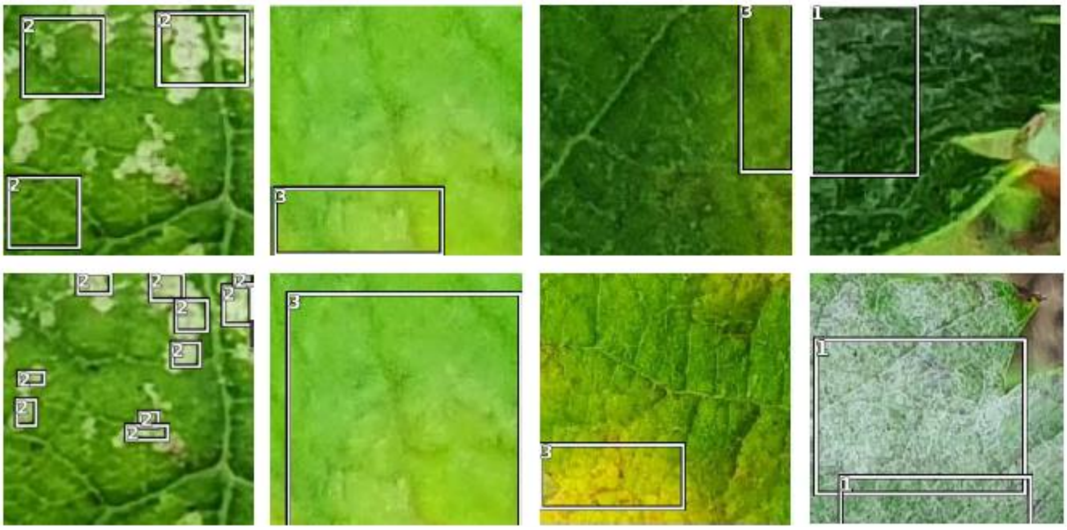

**Figure 1.** Vineyards pathogens detection using Single Shot Detector

# Sentinel-2 and PlanetScope data for alien invasive species of goldenrod (*Solidago* spp.) mapping

EARSeL Bucharest 2023
Abstract
Karolina B. Zdunek:
kb.zdunek@student.uw.edu.pl

Karolina Barbara Zdunek[1], Marcin Kluczek[1], Bogdan Zagajewski[1]

[1] University of Warsaw, Faculty of Geography and Regional Studies, Department of Geoinformatics, Cartography and Remote Sensing, Poland

**Keywords:** biodiversity, invasion, flora, Natura 2000, Random Forest, Support Vector Machine, F1-score.

## Abstract

Climate change, anthropopression and the process of occupying new habitats by invasive species are the greatest threats to biodiversity (Perera et al., 2021). The research problem remains an implementation of effective monitoring methods and protection of native flora. The task is regulated by both national and international law, e.g., the European Union Regulation issued in 2014 (No. 1143/2014), introducing, among others, list of invasive alien species, which should be monitored in the scale of the EU countries. Due to the regulations, interest in the use of satellite techniques for mapping invasive plants has increased in recent years, but so far the research has been carried out locally, using hyperspectral airborne data or high-resolution UAV or satellite data. Sabat-Tomala et al. (2020) based on hyperspectral HySpex images, the Radom Forest (RF) and Support Vector Machine (SVM) algorithms, classified three species of invasive plants, achieving high accuracy oscillating around 0.90 of the F1- score. Akandil et al. (2021) for the detection of goldenrod (*Solidago gigantea*) used an approach using multispectral images obtained with a drone, which, using the Maximum Likelihood algorithm, allowed to achieve 95% of the producer (PA) and user (UA) accuracies.

Our research focusses on *Solidago* spp. mapping based on multi-temporal Sentinel-2, RF and SVM classifications. For this purpose, based on field research, we created training and verification polygons from the Silesian-Cracow Upland, which is characterized by a large share of agricultural and industrial areas, which allow for intensive invasions of *Solidago* spp.

**Figure 1**. Long and intensively blooming goldenrod is a valuable source of nutrients for numerous insects that contribute to the intensive spread of the alien invasive plant species.

We created two classification scenarios, including only polygons with homogeneous goldenrod patterns, and the second case based on a mix of goldenrod with other plants, e.g., bushes. We used an iterative classification method (100-fold classification randomized selecting training and verification pixels each time to capture the varying patterns of invasion outposts and the core surfaces). In both cases and for the tested algorithms, high accuracy results were obtained, amounting to: 0.85 of the median F1-score value for the mix class for both RF and SVM, from 0.94 to 0.96 for goldenrod in the classification variant with the mix class, and 0.93-0.94 for homogeneous patterns.

The presented results are satisfactory and comparable with those of other authors; Nkhwanna et all (2022) classified the invasive shrub *Serephium plumosum* on the Senitnel-2 data with 97% overall accuracy for Random Forest and 95% for Support Vector Machine, also Ade et all (2022) obtained 79% PA and 91% UA for two invasive aquatic macrophytes identified in the Sentinel-2 images.

The developed methodology confirms the usefulness of Sentinel-2 data for effective monitoring of the tested plant, which sets a new direction in preventing its invasion of other areas. The right solution seems to be the adoption of a variant that identifies the places of homogeneous patches of goldenrod and heterogeneous communities, as they are the next outposts of the invasion, key to distinguishing in order to quickly implement preventive measures.

Detailed research results will be presented during the conference.

**Funding:** This research received funding (including publishing costs) from the European Union's Horizon 2020 research and innovation program under the Marie Skłodowska-Curie grant agreement No. 734687 (H2020-MSCA-RISE-2016: innoVation in geospatial and 3D data—VOLTA) and the Polish Ministry of Education and Science (Ministerstwo Edukacji i Nauki—MEiN) in the framework of H2020 co-financed projects No. 3934/H2020/2018/2 and 379067/PnH/2017 for the period 2017–2022.

**References**

Ade, C., Khanna, S., Lay, M., Ustin, S. L., & Hestir, E. L. (2022). Genus-Level Mapping of Invasive Floating Aquatic Vegetation Using Sentinel-2 Satellite Remote Sensing. Remote Sensing, 14(13), 1–20. https://doi.org/10.3390/rs14133013

Akandil, C., Meier, P., Otaru, O., & Joshi, J. (2021). Mapping invasive giant goldenrod (Solidago gigantea) with multispectral images acquired by unmanned aerial vehicle. Journal of Digital Landscape Architecture, 2021(6), 245–256. https://doi.org/10.14627/537705021

Nkhwanana, N., Adam, E., & Ramoelo, A. (2022). Assessing the utility of Sentinel-2 MSI in mapping an encroaching Serephium plumosum in South African rangeland. Applied Geomatics, 14(3), 435–449. https://doi.org/10.1007/s12518-022-00423-5

Perera, P. C. D., Szymura, T. H., Zając, A., Chmolowska, D., & Szymura, M. (2021). Drivers of Solidago species invasion in Central Europe—Case study in the landscape of the Carpathian Mountains and their foreground. Ecology and Evolution, 11, 12429– 12444. https://doi.org/10.1002/ece3.7989

Sabat-Tomala, A., Raczko, E., & Zagajewski, B. (2020). Comparison of support vector machine and random forest algorithms for invasive and expansive species classification using airborne hyperspectral data. Remote Sensing, 12(3). https://doi.org/10.3390/rs12030516

# Spatialization of Japanese knotweed colonies: from local drone scale to regional airborne application

EARSeL Bucharest 2023

Abstract

Corresponding Author:

c.wyard@issep.be

Coraline Wyard[1], Florian Bueno[1,2], Benjamin Beaumont[1], Yasmina Loozen[1], Eric Hallot[1]

[1] Remote Sensing and Geodata Unit, Institut Scientifique de Service Public (ISSeP), Liège, Belgium
[2] Ecole Nationale des Sciences Géographiques (ENSG), Paris, France

**Keywords:** Invasive Plants, Japanese Knotweed, Drone, Airborne, Multispectral

## Abstract

Japanese knotweed (*Fallopia japonica*) is a species of fast growing herbaceous perennial plant considered as an invasive alien species in many European countries. The rapid proliferation of this plant, by rhizomes, is strongly accelerated by human activities and climatic events, such as the July 2021 floods that occurred in Wallonia, southern Belgium. Movement of contaminated land and transport of rhizome fragments by waterways are indeed the primary pathways of expansion for this species in this geographical context. This makes the dynamic inventory of the resource in the field complex. To this end, this research studies the opportunities offered by Earth observation (EO) by focusing on two aspects: (1) the site-specific characterization of a large knotweed colony using multispectral data (RedEdge MX Dual Camera System – 10 spectral bands) acquired by drone (DJI M600 Pro) and (2) the replicability of the classification scheme on regional EO datasets.

In (1), this research analyses a monthly time series of 11 drone coverages (from September 2020 to July 2021) over a known colony located on a brownfield in the municipality of Beyne-Heusay, suburb of Liège. Compared to the surrounding vegetation, the Japanese knotweed shows atypical growth profiles and spectral signature. Indeed, the knotweed grows up to 3-4 meters high in summer and falls back to ground level in late winter. During winter, knotweed presents itself as a dry homogeneous vegetation cover due to its inhibiting properties completely crowning out any other species. We implemented a solution exploiting Python, Jupyter Notebook and ArcGIS Pro to derive 14 spectral and bi-temporal indices, performed pixel-based classification approaches. Our first conclusions highlight the need for very high spatial (<10cm) and spectral resolution (RGB-RedEdge-NIR). The complementarity of seasonal spectral and altimetry (digital surface models) data is demonstrated by obtaining the highest F1-score (0.87). Combining early fall and early spring coverages seems the most relevant to discriminate Japanese knotweed from other vegetation species.

Regarding (2), such conclusion limits the regional replicability of the approach at this time given the currently existing regional datasets. The lack of available earth observation dataset with both sufficiently high spectral and spatial resolution seems difficult to fill. The size of knotweed colonies prevails the use of Sentinel-2 satellite imagery, even though its spectral and temporal properties could have been promising. However, the short-term prospects are much more promising. Indeed, Wallonia is reinforcing its airborne data acquisition strategy by aiming at two annual acquisitions (spring and autumn) of RGB-NIR orthophotos and digital surface models starting 2022, and is studying the refinement of these acquisitions, currently at 25 cm spatial resolution, towards 5 cm data.

Another use of regional datasets is demonstrated: the historical orthophotos time-series date back to 1971, with annual coverages starting in the 2000s. This allows tracking the initial appearance, and so possibly the responsible landowner at that time, and growth of inventoried knotweed colonies. As an example, the previously mentioned colony in Beyne-Heusay appeared on the site around 1994, with a

calculated mean growth of 150 m² per year. The climax was reached in 2018. Since then the colony has not been growing significantly more, as it colonized all of the available open spaces in the area.

Future research will aim to transpose the drone approach to other study sites, for a fine quantification of land stocks to be treated, and to exploit the new regional airborne data to assess the regional resource. A scientific watch will be carried out to follow the evolution of satellite sensors, whose constant evolution in resolution will contribute to an improvement of the classification potential.

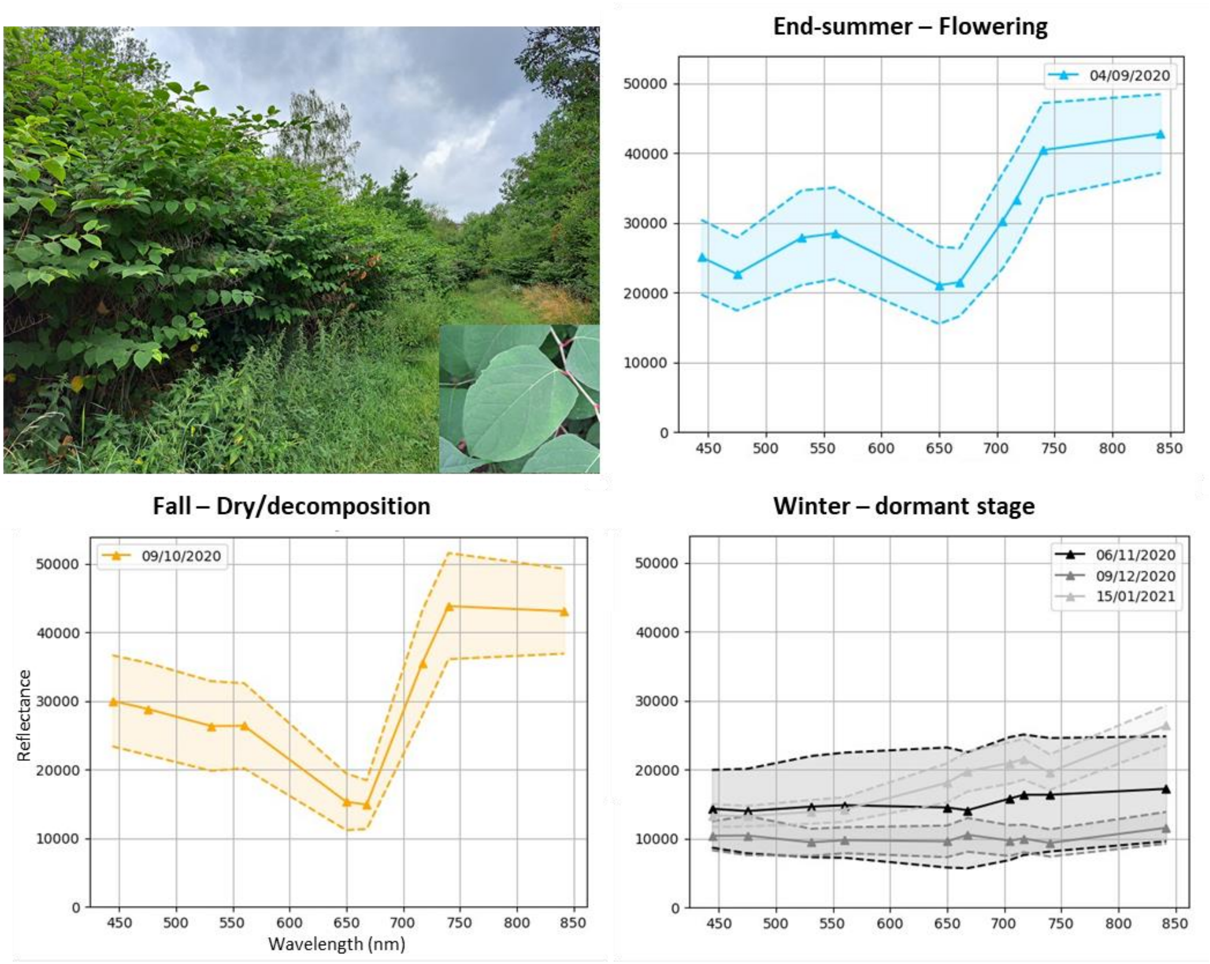

**Figure 18.** Summer phenology and spectral profiles of 3 phenological stages of Japanese knotweed.

# Assessing the Impact of Ozone on Crop Health and Productivity Using Open-Source Remote Sensing Data and Machine Learning

EARSeL Bucharest 2023
Abstract

Corresponding Author: Luka Mamic
luka.mamic@uniroma1.it

Luka Mamic[1], Francesco Pirotti[2,3]

[1] Sapienza University of Rome, Department of Civil, Building and Environmental Engineering, Italy
[2] University of Padova, Department of Land and Agroforestry Systems (TESAF), Italy
[3] University of Padova, Interdepartmental Research Centre in Geomatics (CIRGEO), Italy

**Keywords:** ozone, crops, Sentinel-5P, Sentinel-2, machine learning

## Abstract

The relationship between ozone levels and crop health is complex and multifaceted. In low concentrations, ozone can act as a natural pesticide and provide a mild stress that can increase the plant's resistance to diseases and pests. However, at high concentrations, ozone can cause significant damage to crops, reducing their growth, altering their physiology, and decreasing their yield and quality. The consequences of exposure to high levels of ozone include damage to the leaves of crops, resulting in visible symptoms such as chlorosis, necrosis, and stunted growth. This can lead to reduced photosynthetic efficiency, which in turn affects the plant's overall growth and productivity. In some cases, exposure to high levels of ozone can also increase the plant's susceptibility to other stress factors, such as drought, disease, and pests. To maintain the health and productivity of crops, it is important to keep ozone levels within a certain range.

The use of remote sensing data and machine learning techniques has the potential to revolutionize the way we assess the impact of ozone on crops. Using the vast amounts of data generated by remote sensing satellites and using advanced machine learning algorithms, it is possible to develop models that accurately predict the impact of ozone on crops and provide valuable insights into the relationship between ozone emissions and crop health.

The Sentinel-5P and Sentinel-2 satellite missions provide an opportunity to study the impact of ozone on crops using remote sensing data and machine learning. This study aims to assess the impact of ozone on crop health and productivity using data from these missions and assimilated open-source remote sensing data from the Google Earth Engine platform. One of the challenges in studying the impact of ozone on crops is the interaction between multiple factors that affect crop health and productivity. This study will address the aforementioned challenge by incorporating an integrated approach that investigates the relationship between the Normalized Difference Vegetation Index (NDVI), precipitation, soil pH, and ozone emissions in crop monitoring using a machine learning approach. This will be done by analyzing the spectral properties of crops in the study area, including the reflectance and thermal properties, and comparing them to the ozone concentrations measured by Sentinel-5P's TROPOMI. Additionally, other parameters such as crop type, crop stage, and surrounding land use will be considered to gain a comprehensive understanding of the impact of ozone on crops.

The results of this study will provide valuable insights into the impact of ozone on crops and contribute to the development of strategies to mitigate the negative effects of ozone on crop health and productivity. Furthermore, this study will demonstrate the potential of using open-source remote sensing data and machine learning techniques to assess the impact of environmental stressors on crops and support informed decision-making in agriculture.

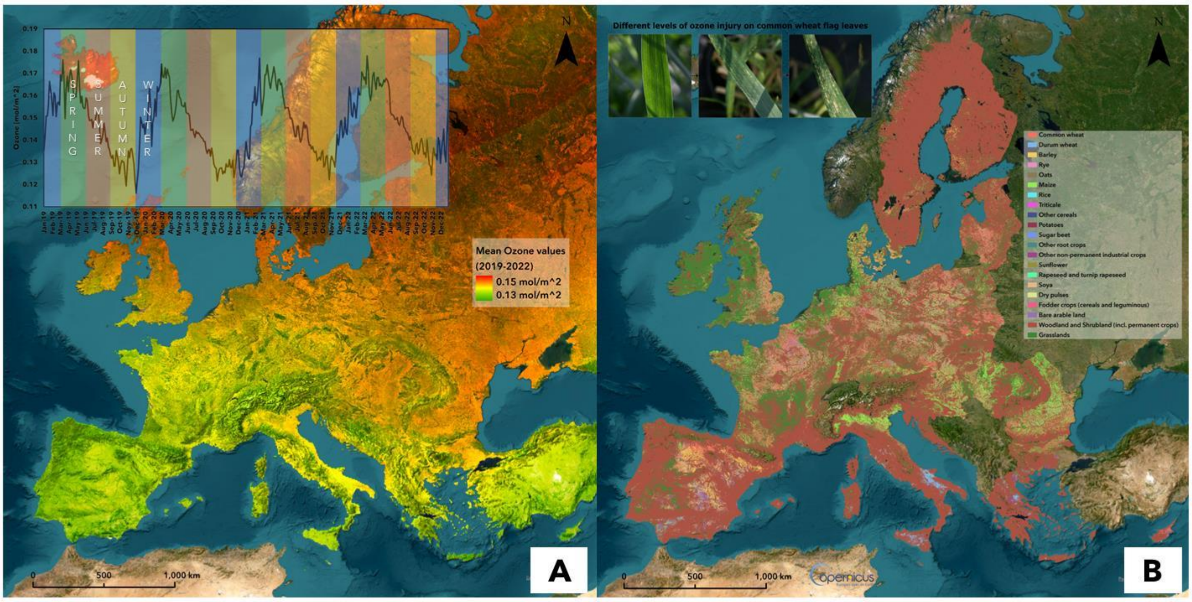

**Figure 1.** (a) Mean Ozone concentrations over Europe and their seasonal variations derived from Sentinel-5P for period 2019-2022 (b) European crop type map based on Sentinel-1 and LUCAS Copernicus in-situ observations for 2018. and (b) example of ozone injury on common wheat [2]

1) d'Andrimont, R. Verhegghen, A., Lemoine, G., Kempeneers, P., Meroni, M. & van der Velde, M. (2021). From parcel to continental scale – A first European crop type map based on Sentinel-1 and LUCAS Copernicus in-situ observations, Remote Sensing of Environment, 266, https://doi.org/10.1016/j.rse.2021.112708.

2) Harmens, H., Mills, G., Hayes, F., Sharps, K., & Frontasyeva, M. (2014). Air pollution and vegetation: ICP Vegetation annual report 2013/2014.

This study was carried out within the funding of the National Research Center for Agricultural Technologies (AGRITECH) from the European Union Next-GenerationEU Piano Nazionale di Ripresa e Resilienza (PNRR)–M4C2 Investimento 1.4–D.D. 1032 17/06/2022, CN00000022–CUP HUB B63D21015240004.

## Section XI - Land use and land cover - remote sensing

# Comparison of Machine Learning Algorithms For Land Cover Mapping According to Corine Land Cover Nomenclature

EARSeL Bucharest 2023

Abstract

Corresponding Author:

m.kluczek@uw.edu.pl

Marcin Kluczek[1], Bogdan Zagajewski[1], Edwin Raczko[1], Marlena Kycko[1], Anca Dabija[1], Ahmed H. Al-Sulttani[1], Anna Tardà[2], Lydia Pineda[2] and Jordi Corbera[2]

[1] Department of Geoinformatics, Cartography and Remote Sensing, Chair of Geomatics and Information Systems, Faculty of Geography and Regional Studies, University of Warsaw, Poland
[2] Catalan Earth Observation Centre, Cartographic and Geological Institute of Catalonia, E-08038 Barcelona, Spain;

**Keywords:** land cover classification, machine learning, Random Forest, Support Vector Machines, classification accuracy

## Abstract

Land cover information is essential in European Union spatial management, particularly invasive species, natural habitats, urbanization, and deforestation; therefore, the need for accurate and objective data and tools is critical. For this purpose, the Corine Land Cover (CLC) was created. Intensive works are currently being carried out to prepare a new version of CLC+ by 2024. The geographical, climatic, and economic diversity of the European Union raises the challenge to verify various test areas methods and algorithms. In the frame of this presentation, multitemporal (spring, summer, autumn) Sentinel-2 and Landsat 8 satellite images were tested to assess classification accuracy and regional and spatial development in three varied areas of Catalonia, Poland, and Romania keeping all Corine LC program's precise guidelines. The proposed method is based on two machine learning algorithms, Random Forest and Support Vector Machines, with four different kernels functions (linear, polynomial, radial kernel function, and sigmoid). The classification procedures were conducted using the open-source R programming language. The algorithms learning parameters were optimized using the grid search method, where each combination of the parameters is checked from the pool of parameters. The bias of classifications was reduced using an iterative accuracy assessment, which was repeated 100 times. Training and testing datasets were randomly selected in the 50:50 ratio; it was ensured that they were divided according to their belonging to a polygon in order to meet the condition of their independence. Then training of Random Forest and Support Vector Machines classifiers and classification accuracy results were saved for each classification. For the final map production, models with the highest average F1-score for all scenario classes were selected. The ease of the implementation of the used algorithms makes reproducing the results possible and comparable. The results show that Sentinel-2 satellite images allowed to classify land cover with better overall accuracy (8–10%) than the Landsat 8 data. Support Vector Machines algorithm with an RBF kernel function achieved the best results and obtained higher overall accuracy results (6–7%) than Random Forest. The best classification results were achieved for classes: sea and ocean (F1-score: 100%), water courses (F1-score: 98%), water bodies (F1-score: 97%), rice fields (F1-score: 96%), beaches, dunes, sands (F1-score: 95%), vineyards (F1-score: 94%), coniferous forests (F1-score: 94%). The classes characterized by discontinuity and fragmentation obtained lower accuracy results than compact homogeneous large-area classes. The difficulties in classification were found in heterogeneous classes, containing many elements of coverage simultaneously, e.g., principally occupied by agriculture, with significant areas of natural vegetation (F1-score: 67%), transitional

woodland/shrubs (F1-score: 65%), and olive groves (F1-score: 32%). The high accuracy classes that can be updated and classes that should be redefined are specified. The methodology's potential can be used by developers of CLC+ products as a guideline for algorithms, sensors, possibilities, and difficulties of classifying different CLC classes.

Acknowledgments: This research has received funding from the European Union's Horizon 2020 research and innovation programme under the Marie Skłodowska-Curie grant agreement No. 734687 (H2020-MSCA-RISE-2016: innoVation in geospatial and 3D data—VOLTA) and the Polish Ministry of Science and Higher Education (Ministerstwo Nauki i Szkolnictwa Wyższego—MNiSW) in the frame of H2020 co-financed projects No. 3934/H2020/2018/2 and 379067/PnH/2017 in the period 2017–2021.

# Can we improve the accuracy of the land cover classification by pre-selection of the reference samples and applying DEM in the mountain area in Norway?

EARSeL Bucharest 2023
Abstract

Corresponding Author:
adam.wasniewski@igik.edu.pl

Adam Waśniewski[1], Agata Hościło[1], Linda Aune-Lundberg[2]

[1] Institute of Geodesy and Cartography, Centre of Applied Geomatics, Poland
[2] Norwegian Institute of Bioeconomy Research, Division of Survey and Statistics, Norway

**Keywords:** reference samples, random forest, land cover classification, digital elevation model, Sentinel-2

## Abstract

Up to date maps and reliable information on land cover and land use status is important in many aspects of human activities, such as urban planning, management of natural resources, environmental protection and sustainable development. The open data policies and increasing number of reference datasets available on national geoportals popularized the land cover classifications and results in the increasing number of global land cover products. The selection of appropriate and reliable database, knowledge and understanding of the process of reference data collection is crucial for land cover classification accuracy. Selection of reference data and appropriate pre-processing can be a challenging task in the process of preparation of reference samples. Reference samples are quite often selected based on the existing land cover products, which may result in the error propagation. Furthermore, collection of in situ data on the ground is expensive, time-consuming and often difficult in particular over a large area. On the other hand, creating reference samples manually based on, for example, aerial orthophotos is time consuming and subjective. Therefore, it is very important to apply the automated method for assessing of thematic and geometric accuracy of the reference samples. In this study, we examined the impact of the selection of the reference samples for the classification accuracy. The land cover classification was carried out using the Random Forest algorithm based on satellite Sentinel-2 data for the Viken county in Norway. The following ten land cover classes were mapped: sealed surfaces, woodland coniferous, woodland broadleaved, low vegetation, permanent herbaceous, periodically herbaceous, mosses, non- and sparse vegetation, water, snow and ice.

The main aims of this study are i) to examine how the selection of the reference samples may affect the classification accuracy, ii) to derived the best possible land cover classification, iii) to examine whether the use of detailed Digital Elevation Model (DEM) can improve the classification accuracy. Firstly, we performed the classification using the automatically selected reference sampling points derived directly from the national databases. Secondly, we focused on automated approach of creating and filtering reference samples to achieve the most reliable set of reference points. We carried out the detailed analysis of the spectral signatures through the analysis of the histogram for the main land cover classes. Due to the definition of classes in the national databases or methodological issues, some of the sampling points had to be removed, for example points assigned to woodland classes, which overlaid on the clearcuts. Histograms were analysed especially for woodland broadleaved, woodland coniferous, sealed surfaces, mosses and wetland classes, because for these classes obtaining the most reliable set of reference samples seem to be the most difficult without filtering. The difficulty arises from the scale and level of generalization of the reference data. Then, the pre-selected reference sampling points were used

to perform the classification. The comparison of both classification results revealed that the accuracy of selected classes has increased after the pre-selection of reference samples. Figure 1 show the change of the accuracy of woodland broadleaved and woodland coniferous, after filtration of reference samples the overall accuracy increase from 50.6% to 72.5%, and from 88.4% to 93.2%, respectively. The highest increase by 40.7 percentage points (from 33,3% to 74,0%) was achieved for non- and sparse vegetation class. This shows the significance of control of automatically created samples.

The set of pre-selected reference samples was used to classify the land cover over the entire study area. Then, we examined, whether including the DEM in the classification process can improve the classification accuracy. Using the DEM improved the user's (UA) and producer's (PA) accuracy for nine out of ten land cover classes. The highest improvement of PA was observed for classes located at higher altitudes: low vegetation (from 75.9% to 84.7%) and non- and sparse vegetation (from 81.3% to 85.8%). DEM was also the most informative variable in the classification.

The research leading to these results has received funding from the Norway Grants 2014-2021 via the Polish National Center for Research and Development - project InCoNaDa "Enhancing the user uptake of Land Cover / Land Use information derived from the integration of Copernicus services and national databases".

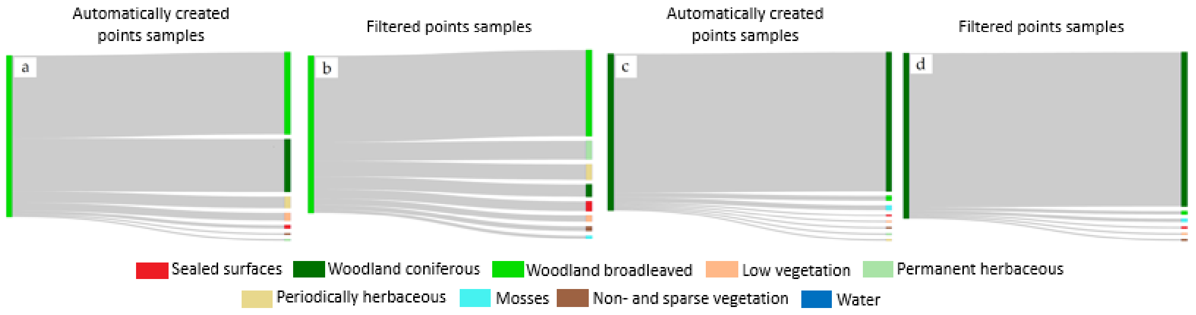

**Figure 19.** Effect of filtration of reference samples points on misclassification between classes, (a, c) misclassification of automatically created points samples, (b, d) misclassification of filtered points samples.

# ST_LUCAS: Easy Access System for Harmonized LUCAS Dataset

EARSeL Bucharest 2023

Abstract

Tomáš Bouček:

tomas.boucek@fsv.cvut.cz

Tomáš Bouček[1], Martin Landa[1], Lukáš Brodský[1], Lena Halounová[1], Ondřej Pešek[1]

[1]Czech Technical University in Prague, Faculty of Civil Engineering, Department of Geomatics, Czech Republic

**Keywords:** LUCAS, in situ, data harmonization, data distribution, web services, QGIS plugin

## Abstract

The LUCAS (Land Use and Coverage Area frame Survey) dataset is a unique source of in-situ data covering almost the entire European continent. It consists of points distributed in a regular grid providing a range of information, including mainly land cover and land use information. The LUCAS dataset is provided and maintained by Eurostat. The dataset has been updated every three years since 2006, with the latest version released in 2018 (2022 data are under preparation). However, the limitation of the original data is its distribution. From the official website (Eurostat 2023) the LUCAS dataset can only be downloaded in CSV (Comma Separated Values) table format, either country by country or all points at once. This way of distribution is not the most suitable from the point of view of the potential user, because it forces the user to preprocess the data first in order to be able to use the dataset for GIS (Geographic Information System) analysis, land cover product validation or classification model calibration as for instance. Another problem is the inconsistency of the data across years. The LUCAS dataset currently contains nearly 100 attributes for each point. These attributes have been successively evolved (new added, removed, renamed, changed coding) during the years. This fact limits the ability to work with the original LUCAS dataset for possible multitemporal analyses or other applications where the user would like to use data from more than one year, and therefore harmonization was necessary to apply.

Therefore, we decided to create an open-source system ST_LUCAS (SpaceTime_LUCAS) for harmonization and distribution of the LUCAS dataset (https://geoforall.fsv.cvut.cz/st_lucas/). It provides data through an OGC (Open Geospatial Consortium) compliant interface. The full architecture of the system and the LUCAS data harmonization process is described in Landa et al. 2022. A user accessing the harmonized data has two options. One is to access it using the Python API (Application Programming Interface), which allows easy implementation into automated workflows (https://geoforall.fsv.cvut.cz/st_lucas/api). Interested users can use the developed ST_LUCAS tutorials (https://geoforall.fsv.cvut.cz/st_lucas/api/tutorials.html). The second option is to use the QGIS plugin (https://geoforall.fsv.cvut.cz/st_lucas/qgis_plugin/) serving as the ST_LUCAS GUI (Graphical User Interface) integrated into open source QGIS platform.

Unlike the official distribution, the user can download a predefined subset using spatial (country, map canvas, user-defined polygon), temporal, and thematic filters, eliminating the need to download the entire LUCAS dataset. The data is received in GPKG (OGC GeoPackage) format, which allows easy work with it in both GIS and Python environments. In addition to these improvements regarding the accessibility of the LUCAS dataset, we also addressed the aforementioned harmonization, which included both attribute and coordinate harmonization. We considered the 2018 version of the dataset, which is currently the most recent and therefore the most developed, as the reference and the other years were therefore harmonized according to it. However, the system is also ready to process the forthcoming 2022 version of the dataset, which, according to the first research, should not differ substantially from 2018. In case of work with multi-temporal data, i.e. work with LUCAS data from multiple years, the function of the so-called space-time aggregation was implemented, which aggregates multiple measured points over the years into one record in the attribute table. Further on, analytical functions for aggregation and translation of LUCAS nomenclature have been added to the system. Besides information on individual points, Eurostat also provides photographs showing the location of a particular point and views in the four cardinal directions. Therefore, we have added the ability to easily view the photos for individual points, either again using the Python API or using the QGIS plugin.

The source code of the ST_LUCAS software components is available from Gitlab repositories ([https://gitlab.com/geoharmonizer_inea/st_lucas](https://gitlab.com/geoharmonizer_inea/st_lucas)).

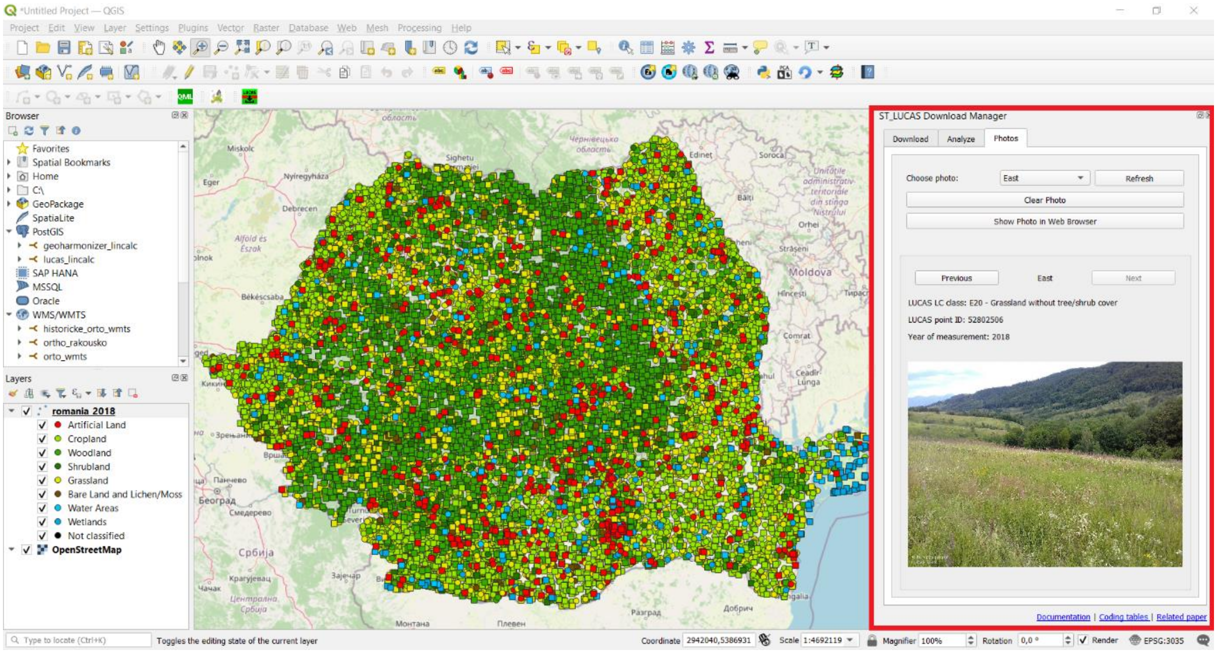

Choose photo: East

LUCAS LC class: E20 - Grassland without tree/shrub cover

LUCAS point ID: 52802506

Year of measurement: 2018

Coordinate 2942040,5386931

Scale 1:4692119

**Figure 20.** ST_LUCAS QGIS plugin (highlighted by a red box) retrieving harmonized LUCAS data for the selected Area of Interest (background basemap: OpenStreetMap—public WMS view service). The LUCAS point symbology indicates the first level of the LUCAS land cover nomenclature (8 basic classes).

# Exploring the Use of Orthophotos in Google Earth Engine for High-Resolution Mapping of Impervious Surfaces: A Data Fusion Approach in Wuppertal, Germany

EARSeL Bucharest 2023
Abstract

Corresponding Author:
jan-philipp.langenkamp@rub.de

Jan-Philipp Langenkamp[1], Andreas Rienow[1]

[1] Ruhr-University of Bochum, Geomatics Research Group, Institute of Geography, Germany

**Keywords:** impervious surfaces, data fusion, Google Earth Engine (GEE), orthophotos, random forest

## Abstract

Germany aims to reduce the rate of soil sealing to less than 30 hectares per day by 2030. However, despite this goal, the rate of soil sealing remains well above this target. This expansion of impervious surfaces, such as roads, parking lots, and buildings, has negative impacts on the environment, including loss of biodiversity, increased runoff, flooding, and altered water cycles. As cities adapt to a changing climate, high-resolution information about the distribution of impervious surfaces is becoming increasingly important for urban planners and decision-makers. Currently, Germany's soil sealing rate is measured on ground-based land use information provided by the Official Real Estate Cadastre Information System (ALKIS). However, due to changes in the data model and data collection in 2016, there are inconsistencies and breaks in the time series, making it difficult to accurately assess the distribution and changes of impervious surfaces. Moreover, ALKIS land use data does not specifically provide information on impervious surfaces as land cover, requiring the use of statistical methods to approximate this information. Therefore, there is a lack of sufficient high-resolution spatially explicit datasets about the distribution of impervious surfaces.

This study aims to address the need for sufficient datasets to support urban planning processes on a local to regional scale. The objective of this study is to develop a methodology that 1) enables meter- precise mapping of impervious surfaces, 2) is easily transferrable, and 3) considers both freely available data and free computing. The study area is located in the city of Wuppertal in the federal state of North Rhine-Westphalia (NRW), Germany. Wuppertal was chosen due to its heterogeneous land cover, including a steep gradient of rural and urban areas. This study proposes a method based on free and official remote sensing data such as high-resolution colour-infrared orthophotos (0,9 m), digital elevation models, and vector data from 2021. The free cloud-processing platform Google Earth Engine (GEE) is used to provide fast computation. In the first step, a remote sensing-based mapping approach is conducted, using a pixel-based random forest (RF) classification process that utilizes a combination of spectral indices, such as the Perpendicular Impervious Surface Index (PISI), Gray-Level Co-occurrence (GLCM) texture features, and topographic features (elevation and slope). This provides a straightforward and effective method for mapping impervious surfaces. To reduce problems of high- resolution images such as shadow or high intra-class spectral variability, the RF classification result is subsequently superimposed with selected ALKIS ground-based vector data. To ensure that only relevant ALKIS data is utilized, an examination of misclassified validation points from the RF classification result is conducted, resulting in the selection of only those ALKIS data that contribute to the development of a robust impervious surface map.

The results show that the proposed method allows for meter-precise mapping of impervious surfaces in the study area. According to the results, 43,49 km² of Wuppertal's total area is impervious. Corresponding to a proportion of impervious surfaces of 25,82%. The RF classification results showed an overall accuracy (OA) of 92.31% and a Kappa-Coefficient (KC) of 84.62%. The superimposition of ALKIS land use data led to an increase in OA of 4% and in KC of 8%. While problems caused by the high spatial resolution of the orthophotos still persist, the use of ALKIS road network data effectively reduced deficits of shaded and obscured impervious surfaces, especially in settlement and traffic areas, which increased the robustness of the created map to a certain extent. The proposed method generated the

recent most detailed remote sensing-based map of impervious surfaces for the city of Wuppertal, providing improved knowledge of the distribution of impervious surfaces for urban and rural areas.

Mapping impervious surfaces, particularly using high-resolution imagery, is a challenging task that requires ongoing research and approaches to solutions. An opportunity for future research could be to introduce different types of impervious surfaces to better differentiate their impact and severity in a spatial context. Additionally, the methodology could be improved, for example, by using object-based image analysis in GEE to effectively face intra-class spectral variability, as well as the integration of additional ground-based data sources such as green cadastre data to optimize the ALKIS road network.

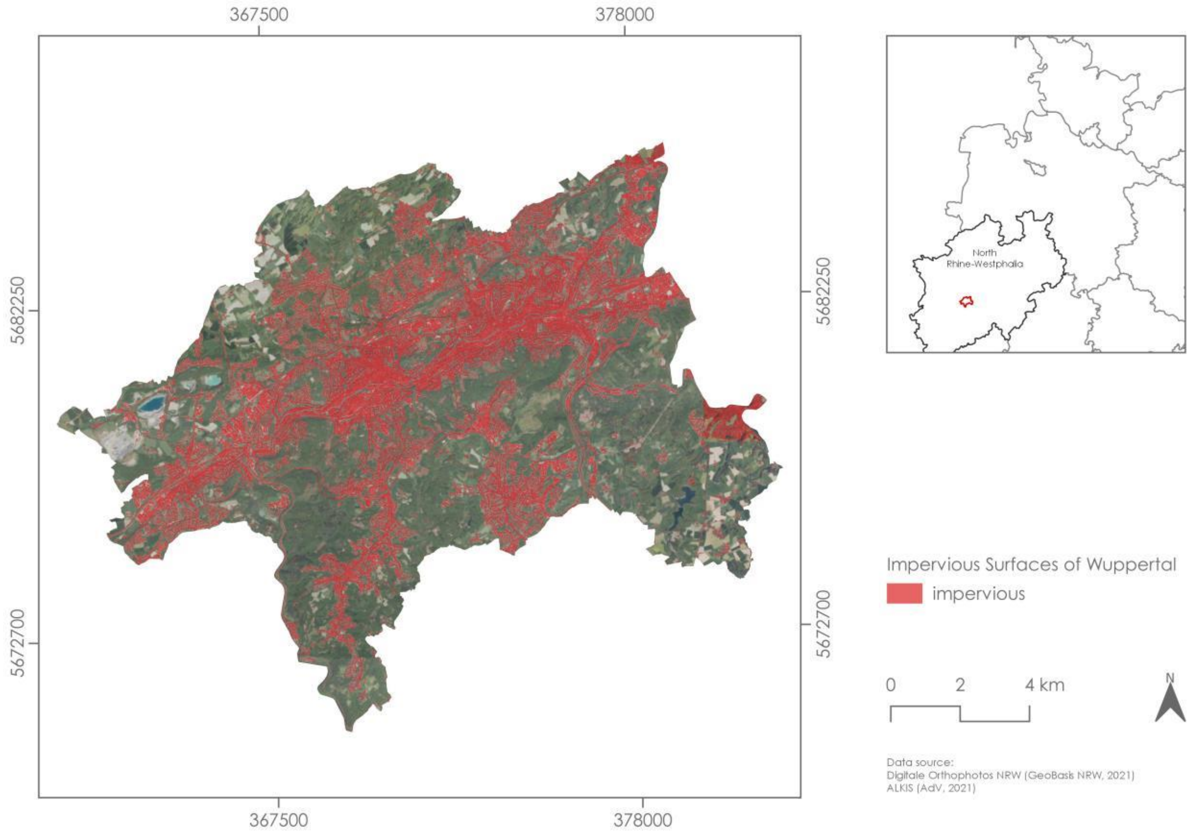

**Figure 1.** High-resolution map of impervious surfaces in the city of Wuppertal in 2021

# Regional Modeling of Future Urban Growth based on Global Settlement Products – Comparing the Performances of OSM with the Global Human Settlement Layer and the World Settlement Footprint

EARSeL Bucharest 2023
Abstract
Corresponding Author:
andreas.rienow@rub.de

Andreas Rienow[1]

[1] Ruhr-University of Bochum, Geomatics Research Group, Institute of Geography, Germany

**Keywords:** Ohsome API; World Settlement Footprint; Global Human Settlement Layer; SLEUTH

## Abstract

By 2050, two-thirds of the population is expected to live in cities. With this continuously increasing urban population and its footprint, sustainable urban development requires the assessment, mapping, and modelling of urban environments with high spatial detail. This is particularly true since the impacts of progressing anthropogenically induced climate change also affect an increasing number of cities and agglomerations in temperate climate zones. Machine learning-based urban models are recognized as one of the main tools for urban monitoring in terms of description, explanation, planning, and future prospects of urban growth. These models rely on accessible, accurate, and temporally and spatially detailed input data on settlement patterns. Recently, satellite-based global urban datasets have emerged, providing researchers with human settlement footprints with associated historical development, such as the Global Human Settlement Layer (GHSL) and the World Settlement Footprint Evolution (WSF Evo). Furthermore, the Ohsome Application Programming Interface enables scientists to access historic OpenStreetMap (OSM) data, making it the most used volunteered geographic information system worldwide. However, studies which focus on spatially explicit geosimulation of future urban growth based on OSM data are lacking. This is also true for studies comparing the geosimulation potential of open global urban land cover or land use products and their applicability at the regional level. Therefore, the objective of this contribution was to carry out a regional study on future settlement developments in the context of environmental effects. This was executed through the calibration, validation, implementation of WSF, GHSL, and OSM data for simulation of urban growth. Global Earth observation-based settlement datasets were utilized for regional planning purposes, which had vast temporal extensions (1975–2015 GHSL), the highest temporal resolution (annually from to 1985–2015, WSF), and most up-to-date data (OSM). The CA used in this study was the SLEUTH Urban Growth Model (UGM), which is one of the most recognized urban growth models in the world. The study area is the metropolitan area of Ruhr in Western Germany and was chosen for its challenging polycentric structure for bottom-up machine learning models. The three global datasets were compared with a national- administrative dataset, assuming a higher accuracy of settlement information than the global datasets. The Digital Land Cover Model (DLM) for Germany (German "Digitales Landbedeckungsmodell für Deutschland", LBM-DE, until 2012 DLM-DE) was based on selected areal object types of the authoritative ATKIS® Basis-DLM including areas of settlement, traffic, vegetation, and water bodies, which were adapted as a modified form to tailor for the specific requirements of CORINE Land Cover nomenclature. The minimum mapping area of the dataset was 1 ha. The spatial simulation results for 2030 were combined with two maps of environmental phenomena: frequent flood risk and less favorable/ unfavorable thermal conditions.

The results show, that all models reach very high accuracy levels in terms of quantity and allocation, while the area of new settlements range from 40.77 km2 to 477.91 km2. The OSM-based CA was calibrated with the most recent datasets. The WSF-based CA showed a higher certainty than the other three CAs which were tested (Fig. 1a). The older the OSM data, the higher the probability of type-I errors

(false positives). The global WSF-Evo dataset outperformed the national LBM-DE dataset. The latter met the null resolution only at a level where one pixel was approximately the same size as the entire study area. All models showed a similar relative portion of new settlement areas affected by floods; however, they varied in terms of areas affected by unfavorable thermal conditions (Fig 1b).

In conclusion, the study demonstrates that historic OSM data can be utilized for training cellular automata to geosimulate future settlement growth. In addition, it also shows the applicability of global Earth observation-based urban data sets for regional geosimulation purposes and the effects of different input data on the accuracy, certainty, quantity, and allocation performances of model simulations of future conditions. Future research needs to focus on the definition of “urban” in global products. The global earth observation-based datasets (GHSL and WSF Evolution) used in this study focused on urban land cover (i.e., primarily impervious surfaces). The administrative data (LBM-DE) and OSM-derived data also considered urban land uses, such as urban recreational areas and leisure facilities. Open spaces within an urban area were the first to experience edge expansion, which is the most dominant growth type of CA.

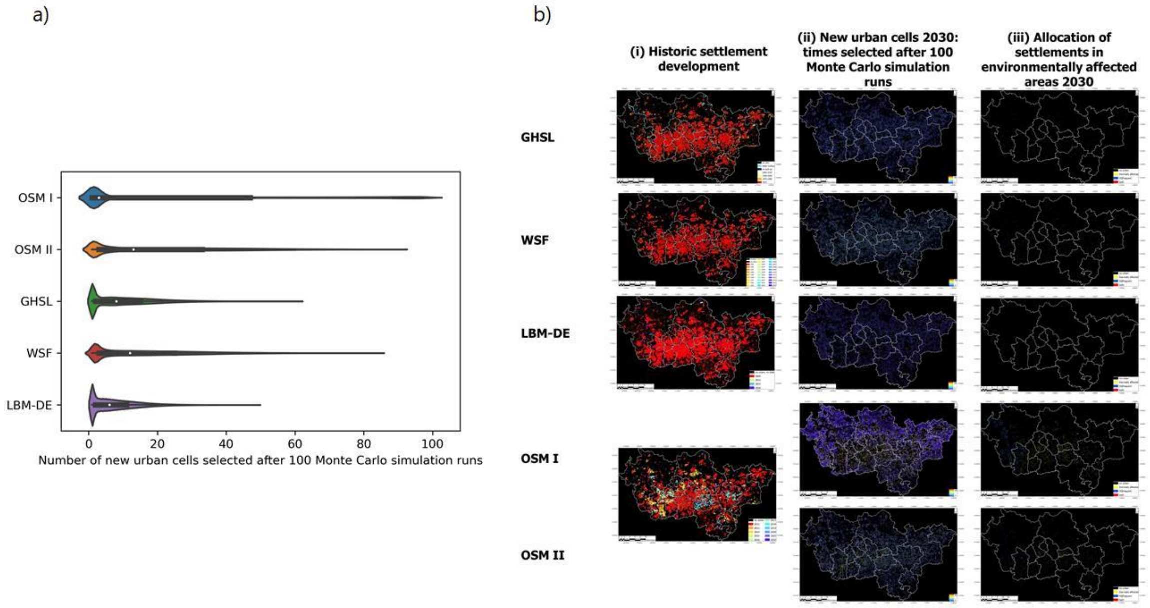

**Figure 1.** a) Violin plot depicting the outcome 100 Monte Carlo simulation runs of the five implemented CA. b) The historic settlement development (i), the probability of future settlement allocations after 100 Monte Carlo simulation runs (ii), and the allocation of new settlement areas in regions of HQfrequent areas (i.e., flood affected areas), in areas with a less favorable/ unfavorable thermal situation, and both HQfrequent and less favorable/ unfavorable thermal conditions (iii).

## Section XII - Urban climate and green infrastructure applications with remote sensing

# Investigating extreme temperature variabilities in deprived urban areas in Sub-Saharan African cities

EARSeL Bucharest 2023
Abstract

Corresponding Author: Stefanos Georganos
email address:stefanos.georganos@kau.se

Stefanos Georganos[1], Sabine Vanhuysse[2], Angela Abascal[3], Jon Wang[4], Monika Kuffer[4]

[1] Geomatics Unit, Department of Environmental and Life Sciences, Karlstad University, Sweden
[2] Department of Geosciences, Environment & Society, Université libre De Bruxelles (ULB), 1050 Bruxelles, Belgium
[3] Navarra Center for International Development, Instituto de Cultura y Sociedad (ICS), University of Navarra, Pamplona, Spain
[4] Faculty of Geo-Information Science & Earth Observation (ITC), University of Twente, Enschede, The Netherlands

**Keywords:** land surface temperature, population mapping, urban sustainability, deep learning, earth observation, deprived urban areas

## Abstract

### The challenge

In recent years, urbanization has been rapidly accelerating, particularly in Low- and Middle-income countries (LMICs). Cities are rapidly transforming in order to provide housing, infrastructure and services for an increasing number of urban dwellers. The urban population growth and the consequent intensification of urbanization, has led to the proliferation of the so-called ‘slums’ or ‘deprived urban areas’ (DUAs). In Sub-Saharan African cities, current estimates place the number of DUA inhabitants at just over 50% and in absolute terms, over 238 million people. DUA dwellers, reside in settlements that often lack fundamental amenities, such as electricity, clean water, sanitation, adequate housing materials, access to healthcare and educational opportunities as well as open recreational areas. In addition, DUA communities are more vulnerable than any other urbanized urban area to climate change adaptation. They tend to suffer most from extreme weather events, such as floods and heat variations, as they are located in risk areas and the materials and morphology pattern do not facilitate their resilience. Furthermore, in order to quantify the vulnerability of DUAs to extreme temperatures, it is vital to estimate their exposure (i.e. the population living in them). This has been extremely challenging as census data in several regions of LMICs are outdated, or heavily under sampled in DUAs, producing severely underestimated measurements. One way to monitor the vulnerability in DUAs and mitigate these bottlenecks, is through the use of remote sensing techniques, coupled with machine learning methods. In this research, our overall objective is to explore the potential of remote sensing, survey data and machine learning to better understand the vulnerability of DUA residents to extreme temperature variations in data resource-limited settings in sub-Saharan Africa cities.

### Methodology

As proof of concept, we investigate 4 cities, Khartoum (Sudan), Nairobi and Kisumu (Kenya) and Ouagadougou (Burkina Faso). We start with deriving RS-based land surface temperature (LST) from MODIS and Landsat. Following, we perform a temporal analysis to identify LST trends in DUAs and non-DUA neighbourhood in the cities and identify potential cold/hot spots. We retrieve DUAs from publicly available databases, which include spatial information on their extent and location. To identify the exposed population in the DUAs, we use both, existing products (such as WorldPoP) and survey data carried out by community-dwellers. Following the reliability of the reference data, we develop deep learning models to mitigate the census dependency as they are bottom-up methods.

The deep learning models will make use of publicly available satellite imagery (such as Sentinel-2) and datasets such as Google's and Microsoft's building footprint products.

## Results

The results are presented in a gridded format (i.e., 100m spatial resolution) and focus on i) investigating the hypothesised differences in temperature extremes between DUAs and non-DUAs in the four cities, and ii) comparing the population modelling approaches (bottom-up and top-down) to retrieve the exposed population. The example of Nairobi (Kenya) Figure 1 and Table 1 show a moderate positive and significant correlation between the location of the DUAs and the highest LST. The results indicate that more deprived grid cells have higher LST temperatures. Similar positive associations are demonstrated between DUAs population density and LST. The percentage of grid cells with a deprivation probability of more than 75% makes up only 10% of all grid cells in Nairobi. However, more than 70% of the population in Nairobi lives in these areas. On average, the most deprived quartile has a 3-degree Celsius higher temperature, as compared to the least deprived quartile.

## Outlook for the future

This work aims to provide tangible evidence, highlighting the climate vulnerability of DUAs in a rigorous manner. We hope that this will work will pave the road for formalized vulnerability frameworks for the most vulnerable communities, addressing the needs of the citizens of the countries of the Global South and meaningfully contribute to the monitoring of the Sustainable Development Goals and evidence-based decision making.

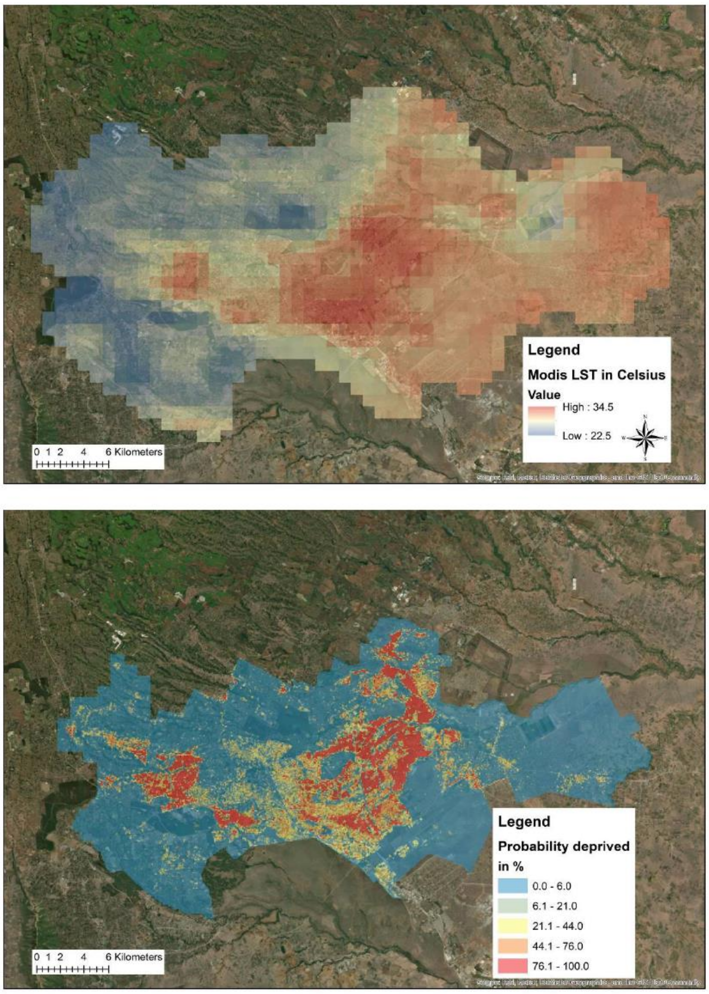

**Figure 1:** top panel) Land surface temperature (LST) deprived of Modis annual average, bottom panel) model of deprivation probability based on EO data (S1/2) for Nairobi, Kenya.

Table 1: Correlation between LST, Deprivation probability, Built-up density and Population density in Nairobi, Kenya.

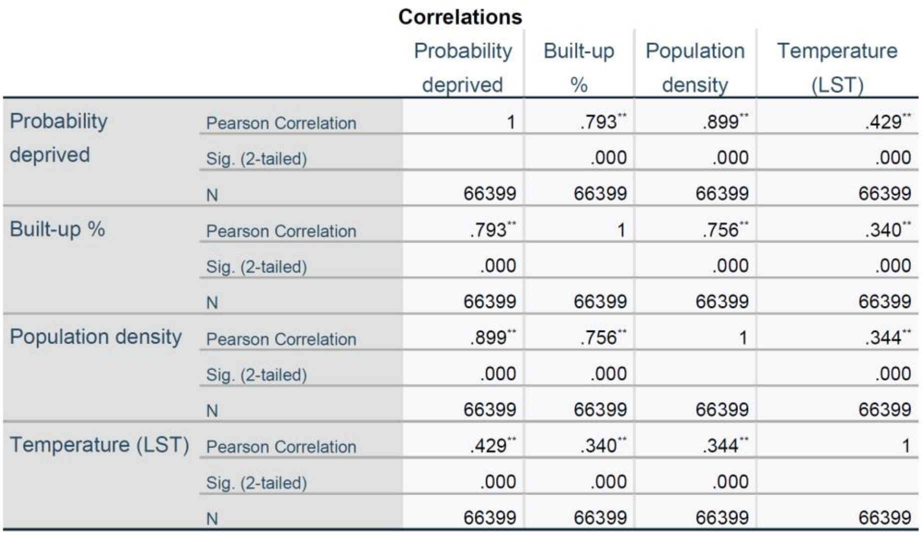

**Correlations**

| | | Probability deprived | Built-up % | Population density | Temperature (LST) |
|---|---|---|---|---|---|
| Probability deprived | Pearson Correlation | 1 | .793** | .899** | .429** |
| | Sig. (2-tailed) | | .000 | .000 | .000 |
| | N | 66399 | 66399 | 66399 | 66399 |
| Built-up % | Pearson Correlation | .793** | 1 | .756** | .340** |
| | Sig. (2-tailed) | .000 | | .000 | .000 |
| | N | 66399 | 66399 | 66399 | 66399 |
| Population density | Pearson Correlation | .899** | .756** | 1 | .344** |
| | Sig. (2-tailed) | .000 | .000 | | .000 |
| | N | 66399 | 66399 | 66399 | 66399 |
| Temperature (LST) | Pearson Correlation | .429** | .340** | .344** | 1 |
| | Sig. (2-tailed) | .000 | .000 | .000 | |
| | N | 66399 | 66399 | 66399 | 66399 |

# Comparative Study of Urban Heat and its Vulnerability in Nashville and Portland, USA

EARSeL Bucharest 2023
Abstract
Sunhui Sim:
ssim@una.edu

Sunhui Sim[1]

[1] University of North Alabama, Department of Geoscience, USA

**Keywords:** Social Vulnerability to Heat, NDVI, surface temperature, Spatial Autocorrelation, Landsat OLI/TIRS

## Abstract

This Extreme heat is one major weather hazard accounting for nearly 8000 heat-related deaths since 1979 in the US. Measurement of the Urban Heat Island (UHI) effect has been captured using basic temperate loggers as well as satellite imagery such as NOAA AVHRR, Landsat Thematic Mapper, and MODIS. When satellite imagery is utilized, it is analysed using an index such as Normalized Difference Vegetation Index (NDVI), Difference Vegetation Index (DVI), Enhanced Vegetation Index (EVI) and Perpendicular Vegetation Index (PVI), all of which have been used in studies across the globe. Spatial pattern of UHI has been studied in physical geography and remote sensing. Spatial Interaction between the geographic locations of social vulnerability to heat is important to understand urban heat environment. Some studies showed that there is the relationship between heat-related death and social variables including socioeconomic status and neighbourhood characteristics.

The primary goal of this research is to examine the variation of heat vulnerability in Nashville and Portland, USA. The socio-economic vulnerability to heat is an index of socioeconomic status, household composition, land surface temperature (LST), and normalized differential vegetation index (NDVI). We then performed a case study of the socio-economic vulnerability to heat in Portland and Nashville on three research objectives: deriving NDVI and land surface temperature, building socio-economic vulnerability index of heat, and characterizing the patterns of heat vulnerability. Land surface temperature and NDVI were derived from the red, NIR and thermal infrared (TIR) of a Landsat OLI/TIRS images collected on August of 2020. The study built a composite heat vulnerability index from these four measures (LST, NDVI, socioeconomic status and household condition). LST and NDVI were summarized by US census track. Social, economic and household variables were downloaded from Agency for Toxic Substances and Disease Registry – the social vulnerability index (SVI) in 2018. The socioeconomic variables include poverty, unemployment rate, income, and education levels. Household composition includes percentage of people older than 65 and people younger than 16, civilian with a disability and single-parent households. Raw vulnerability measures for each tract were normalized against the entire study area. Then, four normalized measure scores for each tract varied from 0 to 1, with higher magnitudes indicating more vulnerability. Lastly, global spatial autocorrelation was examined to characterize spatial pattern of heat vulnerability.

The study found that heat vulnerability is highly clustered spatially, resulting in “hot spots” and “cool spots”. The results show significant health disparities. The hotspots of social vulnerability to heat occurred in neighbourhoods with lower socioeconomic status as measured by low education, low income and more poverty, greater proportion of elderly people and young children. The high temperature and low NDVI occurred in inner city and low temperature in outer city. The findings of this study are important for

identifying clusters of heat vulnerability and the relationships with social factors. These significant results provide a basis for heat intervention services.

---

# Semantic Identification of Urban Green Spaces: Urban Gardens

EARSeL Bucharest 2023

Abstract

Corresponding Author:

irada.ismayilova@geo.uni-augsburg.de

Irada Ismayilova[1], Sabine Timpf[1],

[1] University of Augsburg, Geoinformatics Group, Germany

**Keywords:** urban green spaces, urban gardens, semantic classification

## Abstract

The connection of Urban Green Spaces (UGS) to reduction of environmental pressure in densely populated urban areas is intensively studied. However, decision-making process in the context of planning and managing UGSs is still challenged by several factors, such as definition and typology of UGSs. Existing Land Use and Land Cover (LULC) maps both on national and European level employs UGS typology that misclassifies small and heterogeneous UGSs into different LULC categories. This is mainly due to the minimum mapping unit of the LULC maps. Consequently, these data sources are not sufficient to depict actual green space status of urban areas.

In this work, we look into a mostly misclassified UGS type: urban gardening areas. Typically, LULC maps assign gardening areas to “sport and leisure facilities” class. Yet, these areas store considerable amount of vegetation and substantially contribute to ecosystem services as well as human well-being. Identification of gardening areas is challenging due to their size and heterogeneity. Currently, existing methods to map similar areas heavily rely on very high-resolution satellite images and Deep Learning techniques. Deep Learning models implement semantic segmentation as a part of their classification procedure. Yet, it is nearly impossible to extract human understandable semantic information that is characteristic to the classified green space type. Therefore, in this work, we perform a semantics driven urban garden identification workflow in Augsburg, Germany. We take into consideration the following semantic information: in urban areas, gardens are low-rise areas; they accommodate garden huts that are limited in size; they are covered with narrow and unpaved paths; and are usually close to railroads or riversides. We perform analysis using very high-resolution aerial imagery (20cm), a digital surface model (DSM, 40cm) as well as a digital elevation model (DEM, 1m).

As a first step, we calculate the normalised digital surface model (NDSM). NDSM is a derivative elevation product, calculated by subtracting DEM values from DSM, thus indicating the above ground height of objects. We test several height thresholds and establish that the height of three meters adequately masks out buildings (that are higher than garden huts) and other high objects while separating gardening areas from the remaining scene. Furthermore, we implement geo object based image analysis (OBIA) using aerial imagery as well as NDSM layer as input. This way we can distinguish between similar looking objects, e.g. roofs and roads. Segmentation is an obligatory step in OBIA, which creates super pixels/objects by combining raster cells with similar reflectance values as well as other characteristics (e.g. shape descriptors). As a segmentation method, we utilize the Segment Mean Shift algorithm in ArcGIS Pro. By adjusting spatial and spectral detail as well as minimum segment size, we achieve very well separated

surface objects. Subsequently, using Random Forest classification method, we assign objects to LU classes such as roads, vegetation, buildings. We further make distinction between unpaved narrow paths and paved wider roads. As the spectral resolution of aerial imagery is limited and does not differentiate these two classes, we calculate width of road/path objects using minimum enclosing bounding boxes. The combination of narrow path and lower height areas limits the scene to only urban gardens and thus eliminates the need to add proximity to railroads and rivers parameters. Finally, we calculate the area of vegetation coverage in the identified gardening plots.

We conclude that semantics derived classification proves to be suitable to precisely identify and map gardening areas. However, it is time intensive and requires manual adjustment at every step in the workflow. Furthermore, due to the nature of gardening areas, very high-resolution imagery is a must criterion, which is usually not free of charge. High-resolution orthophotos, due to their limited spectral resolution, remain incapable to precisely separate between similar spectras in urban areas. In future work we will focus on refining the semantic characteristics of UGSs and derive rules from them that can be used for rule-based classification of UGSs.

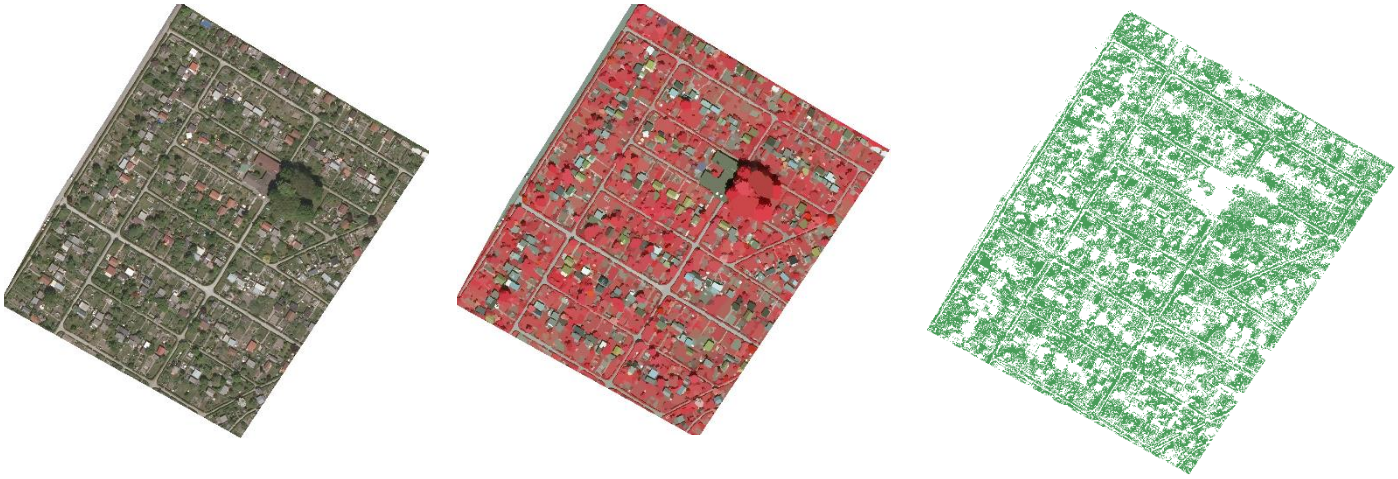

**Figure 1.** Excerpt of the aerial imagery (left) segmented imagery (middle) as well as the classified green space imagery (right) of a sample urban gardening area.

# Using GEOBIA and vegetation indices to assess small urban green areas in two climatic regions

EARSeL Bucharest 2023
Abstract
Corresponding Author: Ana-Maria Popa
email address: anamaria.popa@geo.unibuc.ro

Ana-Maria Popa[1,2], Diana-Andreea Onose[1,2], Ionut-Cosmin Sandric[2], Evangelos A. Dosiadis[3], George P. Petropoulos[3], Athanasios-Alexandru Gavrilidis[1,2], Antigoni Faka[3]

[1]University of Bucharest, Centre for Environmental Research and Impact Studies, Romania
[2]University of Bucharest, Faculty of Geography, Romania
[3]Harokopio University of Athens, Department of Geography, Greece

**Keywords:** small urban green areas, GEOBIA, NDVI, MSAVI2, Planet

## Abstract

The importance of small urban green areas has increased in the context of rapid urbanization and densification of the urban tissue. The analysis of these areas through remote sensing has been limited due to the low spatial resolution of freely available satellite images. We propose a timeseries analysis on 3 m resolution Planet images, using GEOBIA and vegetation indices, with the aim of extracting and assessing the quality of small urban green areas in two different climatic and biogeographical regions – temperate (Bucharest, Romania) and mediterranean (Athens, Greece). Our results have shown high accuracy (over 91%) regarding the extraction of small urban green areas in both cities, across all analysed images. The timeseries analysis showed consistency in location for around 55% of the identified surfaces throughout the entire period. The vegetation indices registered higher values in the temperate region, due to the vegetation characteristics and the planning of the two cities. For the same reasons, the increase in vegetation density and quality, as a result of the distance from the city centre and the decrease in the density of built-up areas is more obvious in Athens. The proposed method provides valuable insights in the distribution and quality of small urban green areas at city level and can represent the ground basis for many analyses, currently limited by poor spatial resolution.

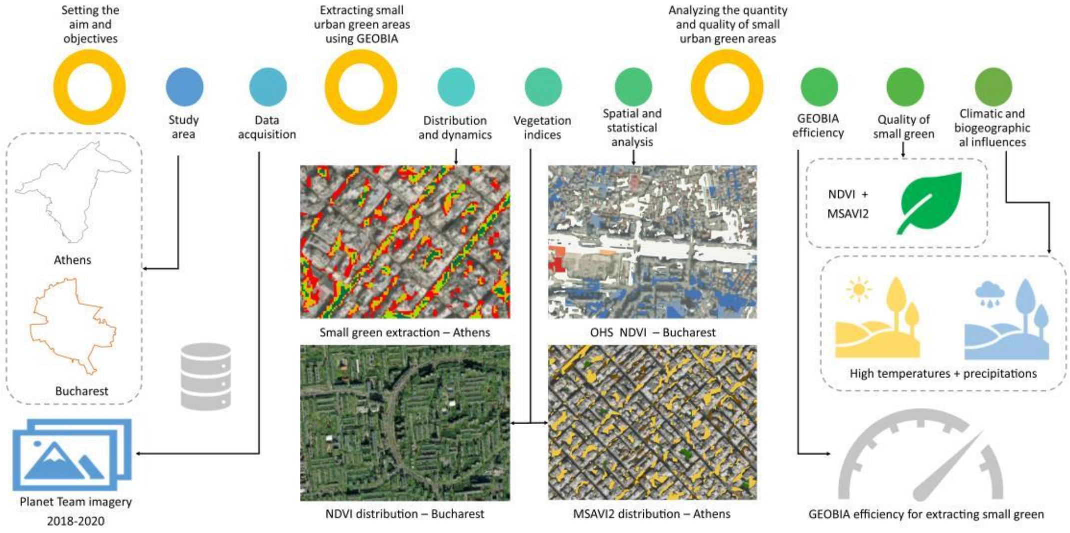

**Figure 1.** Workflow of the research

# Monitoring urban traffic impact in urban environments using Yolo7

EARSeL Bucharest 2023
Abstract

Corresponding Author:
marian.puie@s.unibuc.ro

Marian Puie[1], Mihai Bogdan-Andrei[2], Ionuţ Şandric[3]

[1] University of Bucharest, Department of Geography, Romania
[2] University of Bucharest, Faculty of Geography, Department of Geomorphology-Pedology-Geomatics, Romania
[3] University of Bucharest, Faculty of Geography, Department of Regional Geography and Environment, Romania

**Keywords:** Urban Traffic Monitoring, Yolo7, Deep Learning

## Abstract

Urban transport is a pressing issue in Romania, with a greater number of vehicles leading to congestion and traffic-related problems such as pollution, time-wasting and the need to prevent accidents. In response, traffic optimization programs have been implemented, but their effectiveness remains limited. However, traffic monitoring cameras can be an effective solution, because their positioning and orientation at a fixed point facing the roadway can collect and retrieve the real positions of traffic participants.

To address this challenge, innovative solutions are being sought using deep learning technology to increase road traffic flow and reduce congestion in large cities such as Bucharest and Oradea. One such technology is YOLO (You Only Look Once), which can analyse traffic events in real time by detecting and recognizing elements in video or still images. Object detection is a technique used to identify and locate objects in an image or video. Image localization is the process of identifying the correct location of one or more objects using bounding boxes, which correspond to the rectangular shapes around the objects. Sometimes the two processes are confused with image classification or image recognition, which aims to predict the class of an image or an object within an image into one of the categories or classes. This process, known as one-step detection, provides two crucial benefits: speed of processing and accuracy of the final product, by using intelligent optimization algorithms that then enable the possibility of a forecast of the state of the traffic and the formulation of solutions to the problems encountered.

By extracting valuable information from the environment, such as the number of pollutants emitted into the atmosphere at each video surveillance intersection, YOLO can help optimize traffic flow and reduce the negative impact of traffic congestion on the environment and public health. The positioning of the area of interest is the key in maximizing the effectiveness of this technology, especially in high traffic areas such as the central area of Oradea and the surrounding intersections. In the drawn area of interest, there are 38 traffic monitoring cameras that provide constant data regarding the road activity in their visual field. Thus, over 300 cars and pedestrians pass through the central area daily under normal traffic conditions. At the same time, the intersections are crossed by more than 200 cars and pedestrians, on normal traffic days. Approximately 35% of the city's traffic is concentrated in the 3 major intersections of the city, and approximately 43% of the traffic is concentrated in the central area, which in both cases also involves the emission of a large number of suspension gases that leaves its mark both on air quality but also on the health of the population living in the central area or in the neighbourhood.

Overall, deep learning technology such as YOLO provides an effective solution to the challenge of urban transportation by enabling pre-computed and applied traffic mitigation programs and strategies to optimally control traffic conditions. Due to continuous research and development in terms of processing speed, which refers to the low duration of the time of processing, detection accuracy, which refers to the accuracy of object recognition, the much better generalization that is made suitable for the domains where it detects brings an important contribution and the fact that it is an open-source service, which means that all programmers can contribute to the development of this

technology voluntarily. These technologies can ultimately lead to more efficient and sustainable urban transport systems, benefiting both the environment and the public.

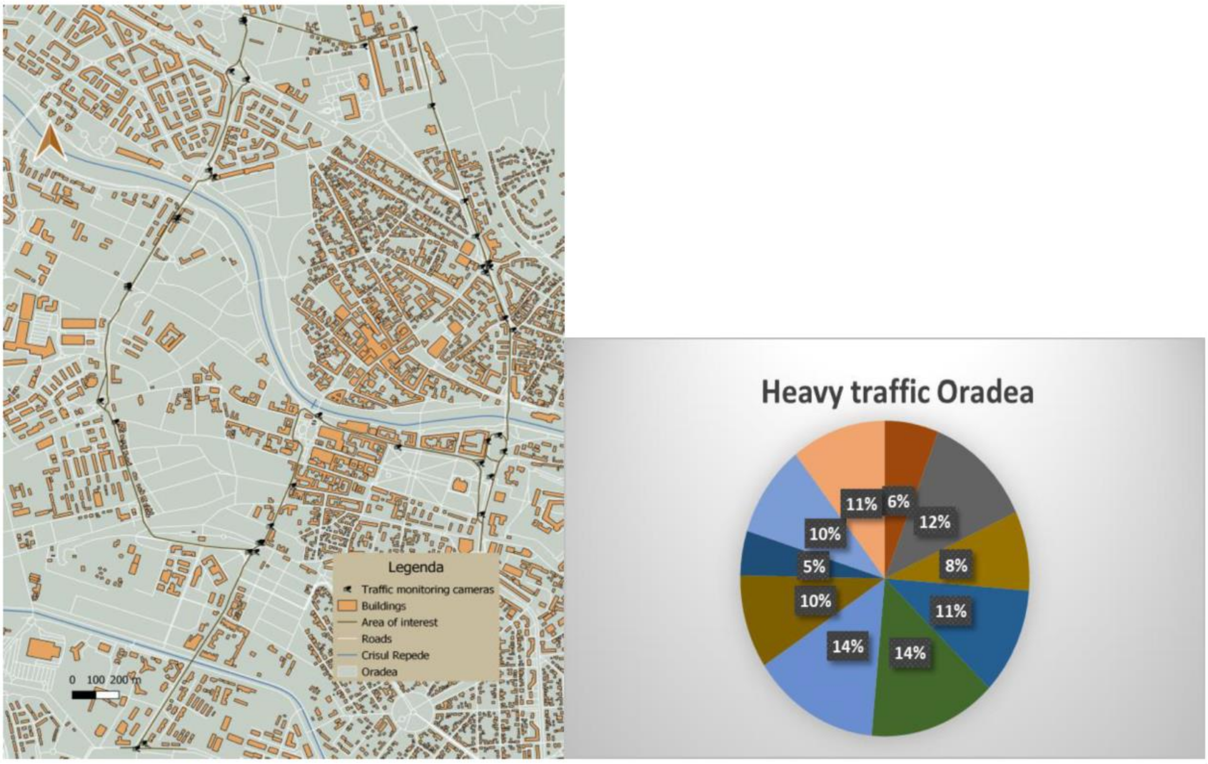

**Figure 1**. On the left side is an example of a map of the area of interest with the positioning of the traffic control cameras in Oradea. On the right side is an analysis of the number of cars that pass through the sights of those cameras on a normal day.

## Section XIII - Hyperspectral and multispectral applications of remote sensing

# Assessment Of The Novel Watersat Imaging Spectrometer Enhanced (WISE) Sensor For The Mapping Of Optically Shallow Inland And Coastal Waters

EARSeL Bucharest 2023
Abstract

Corresponding Author: Gabriela Ifimov
gabriela.ifimov@nrc-cnrc.gc.ca

Gabriela Ifimov[1], Raymond Soffer[1], Raphaël Mabit[2], Simon Bélanger[2]

[1]Aerospace, National Research Council Canada, Ontario, Canada
[2] Université du Québec à Rimouski, Québec, Canada

**Keywords:** hyperspectral, radiometric correction, aquatic environment, mapping macro-algae

## Abstract

The primary objective of the presented work was to acquire and assess the spectroradiometric quality of airborne hyperspectral imagery from the WaterSAT Imaging Spectrometer Enhanced (WISE) sensor. The WISE sensor was developed for monitoring aquatic environments. This on-going study is part of the "Hyperspectral assessment of marine algae and their importance for blue-carbon sequestration using the WaterSat Imaging Spectrometer Enhanced (WISE): Algae-WISE project", led by the Université du Québec à Rimouski (UQAR). The project's long-term goal is to demonstrate the potential of hyperspectral imagery for the detection and quantification of the three types of marine algal biomass that are the foundation of the marine ecosystem productivity and vitality: phytoplankton, submerged macro-algae and floating algae.

The WISE instrument is a prototype Visible and Near Infrared (360 - 980 nm) airborne hyperspectral system designed for the Canadian Space Agency in preparation for the development of a satellite sensor system focused on the study of coastal and inland waters. The instrument, based upon the heritage of the Compact Airborne Spectrographic Imager (CASI-1500) sensor, incorporates a novel spectrometer and fore-optics designed to enhance sensitivity to low signal levels, particularly those encountered in the blue wavelength region. Data was recorded using a 144 channels configuration and a 32 ms integration time. The airborne campaign was planned in coordination with multiple in-situ terrestrial and aquatic measurements required for the development and validation of higher-level data products.

In total 11 flight lines were acquired covering the southwestern coastal area of Anticosti Island, Québec, Canada, on July 5th, 2022. The recorded sensor altitude was 3054 ± 180 m MSL with a ground speed of 45 ± 2.5 m/s yielding a ground resampled spatial resolution of approximately 1.5 m in both the along and cross-track directions. Calibration targets were not deployed within the WISE imagery acquired on Anticosti Island. In its place, WISE imagery of the National Research Council (NRC)'s cal/val site in Ottawa, Ontario, Canada, was acquired the day prior with near-coincidental SVC HR-1024i field spectroscopy measurements (340 nm – 2522 nm wavelength range) of four targets (i.e., black tarp, asphalt, concrete, and grey tarp). For validation purposes, UQAR acquired field measurements of typical ground targets in Port Menier, Anticosti Island, using an SVC HR-512i spectrometer measuring the 339 nm – 1074 nm wavelength range.

An assessment of the surface reflectance (SR) spectra generated from the WISE imagery following atmospheric correction was performed. Significant errors were found across all wavelengths with low signal strength necessitating the application of an in-flight radiometric calibration (IFRC) correction. Application of a traditional linear IFRC, based upon the black tarp and concrete calibration targets, was found to produce anticipated results in agreement with the field measurements for moderate levels targets (i.e., black tarp around 4% through concrete levels at 30 – 40 %). Dark targets (i.e., most aquatic targets), however, resulted in the generations of negative reflectance levels, while higher level targets (i.e., grey tarp around 50%) were found to be several percent higher than anticipated. When the field spectrometer data of all four calibration targets was applied to the production of the IFRC correction, a single, second order polynomial curve was found to fit the various data points. Application of this IFRC

curve to the original imagery prior to atmospheric correction resulted in SR spectra that was found to be closely aligned with the validation spectra over the entire wavelength range at all signal levels. When compared with the ground spectra of the validation targets taken in Port Menier, absolute differences in SR were on average between 1.2% (grass) and 2.8% (mixed vegetation) with observed discrepancies of up to 7.7% for the water and vegetation spectra (Figure 1). Given the differences in the surface composition of the average field spectra with that contributing to the compared airborne hyperspectral image pixel, these results are considered to be more than reasonable. The paving stone surface (Figure 1c) composition represents the most homogenous of the targets making it the most suitable for direct comparison. The application of IFRC, based upon NRC calibration targets, provided a refinement to the original spectroradiometric calibration. This was necessary to generate at-sensor radiance and reflectance for surface targets with anticipated spectral shapes and intensity levels.

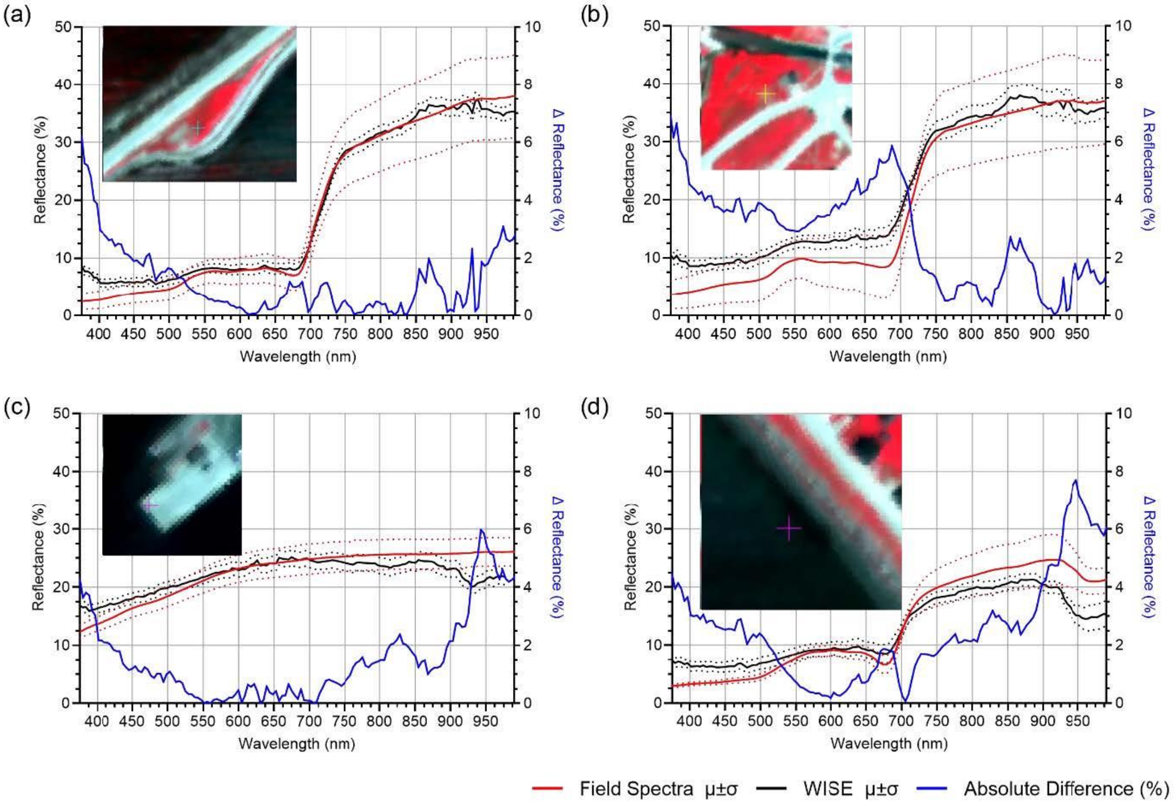

**Figure 1.** Comparison in average (μ) ± standard deviation (σ) surface reflectance of validation points for (a) grass, (b) mixed vegetation, (c) paving stone, and (d) mix of water and vegetation between WISE imagery and field spectra, and their respective absolute differences. Spectral averages are based on 13 samples for the field measurements and on 25 pixels for the WISE imagery. Airborne imagery data acquired off the north shoreline of Port Menier, Anticosti Island, Québec, Canada. Imagery is displayed in the inset colour infrared images (R: 860 nm, G: 650 nm, B: 550 nm).

# Detection of geothermal anomalies using pre-dawn thermal remote sensing data from ECOSTRESS sensor

EARSeL Bucharest 2023
Abstract

Corresponding Author: Agnieszka Soszynska
a.soszynska@utwente.nl

Agnieszka Soszynska[1], Thomas Groen[1], Harald van der Werff[1], Eunice Bonyo[2], Robert Hewson[3], Robert Reeves[4], Christoph Hecker[1]

[1] University of Twente, the Netherlands
[2] KenGen, Kenya
[3] Independent researcher, Australia
[4] GNS Science, New Zealand

**Keywords:** Thermal remote sensing, geothermal anomalies, ECOSTRESS, pre-dawn imagery, automated detection

## Abstract

As energy transition becomes increasingly urgent, remote sensing technologies can contribute by delivering maps of sustainable energy sources. One example of such source are volcanic geothermal systems. Energy from geothermal systems can be produced constantly, regardless of weather conditions, and some countries like Kenya already make use of this advantage, by producing a large proportion of their energy demands from geothermal resources. Using space-borne thermal imagery allows automated mapping of terrains suitable for energy production from geothermal systems, by detecting thermal anomalies associated with presence of a geothermal system.

Detection of geothermal anomalies is a challenging task, because such anomalies are only slightly warmer than their surroundings, and typically rather small. Additional difficulty lies in thermal properties of surfaces, which are being warmed-up by solar radiation. It is therefore advantageous to use nighttime thermal imagery, but early in the night the surfaces are still cooling down which can falsify detections. It would by optimal to use pre-dawn imagery only, because the contrast between geothermal anomalies and their surroundings should be the highest in that moment. However, most available sensors image the areas of interest shortly after sunset.

The launch of ECOSTRESS sensor in 2018 provided new opportunities for global geothermal system exploration from space. ECOSTRESS has a precessing orbit of International Space Station, where it is installed, so data can be acquired at different times of day and night for the same location. Thus, ECOSTRESS can acquire imagery pre-dawn, which opens promising opportunities for global mapping of geothermal anomalies.

ECOSTRESS uses three spectral bands to create Land Surface Temperature and Emissivity datasets, which are provided in spatial resolution of 70 m. Its high spatial resolution provides additional advantage in using ECOSTRESS data for preliminary exploration of geothermal systems.

In our research, we decided to test the feasibility of using pre-dawn ECOSTRESS data for detection of geothermal surface temperature anomalies. The study was conducted in Olkaria region, Kenya, which is administered by KenGen, a company owning geothermal power plants in this area. We compared the results obtained from nighttime imagery (all the acquisition times) to the results obtained from pre-dawn imagery only. We validated both results against auxiliary data which was produced during field work conducted in March 2022. Thus, detection overall accuracy, producer's- and user's accuracy, as well as omission and commission error could be calculated.

The main differences between pre-dawn and all-night imagery lays in edges of the anomalies. The geothermally active areas receive heat from solar radiation as well as from the geothermal motor, but the edges of the anomalies seem to cool down during the night. The true size of anomalies is, therefore,

visible much more clearly in the pre-dawn imagery. Another interesting result is visible in several locations classified as commission errors in all-night imagery. These areas do not appear as detections in the pre-dawn imagery. These places are areas with a lot of bare rocks, which possibly warm up significantly over the daytime and require long time to cool down due to higher heat capacity and thermal inertia.

The presented results prove that using pre-dawn imagery for geothermal anomaly detection delivers more accurate results than the imagery from different times of day and night. ECOSTRESS pre-dawn imagery prove potential for global mapping of geothermal anomalies and thus contributing to energy transition.

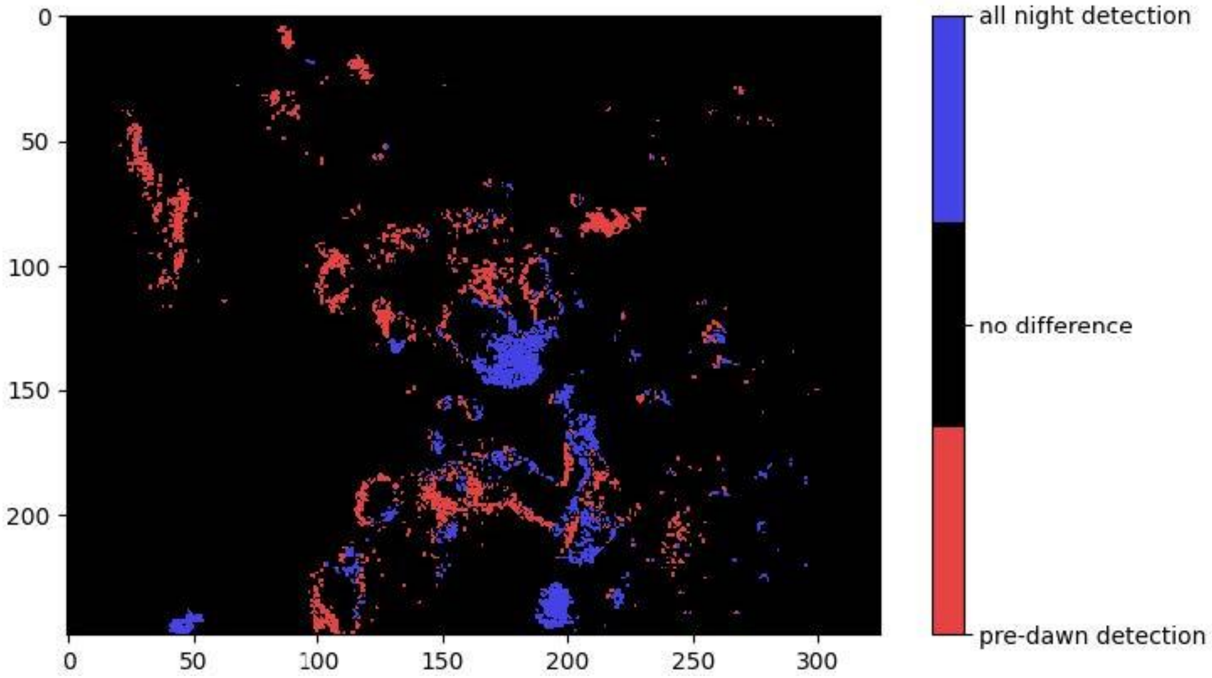

**Figure 1.** Comparison between geothermal anomalies detected in nighttime imagery and in pre-dawn imagery only.

# Initial Validation of Sentinel-2 Collection-1 L2A-Products

EARSeL Bucharest 2023
Abstract
Corresponding Author:
Bringfried.pflug@dlr.de

Bringfried Pflug[1], Jérôme Louis[2], Avi Putri Pertiwi[1], Raquel de los Reyes[1], Francesco C. Pignatale[3], Silvia Enache[4], Rosario Quirino Iannone[5], Valentina Boccia[6], Ferran Gascon[6]

[1]German Aerospace Centre, Remote Sensing Technology Institute, Germany
[2]Telespazio France - A Leonardo / Thales Company, France
[3] Telespazio Germany GmbH – A Leonardo / Thales Company, Germany
[4] CS Group, France
[5] Rhea spa, Italy
[6] European Space Agency (ESA), European Space Research Institute (ESRIN), Italy

**Keywords:** Sentinel-2, Collection-1, Level-2A, Validation

## Abstract

The Copernicus Sentinel-2 mission provides data since the launch of the Sentinle-2A unit in 2015. With the launch of the Sentinel-2B in 2017 it is a constellation of two polar orbiting satellite units. Both Sentinel-2A and Sentinel-2B are equipped with an optical imaging sensor MSI (Multi-Spectral Instrument) which acquires high spatial resolution optical data products. The Sentinel-2 mission serves for observation of land-cover change and deriving biophysical variables related to agriculture and forestry, monitors coastal and inland waters and is useful for risk and disaster mapping.

Atmospheric correction processor Sen2Cor was developed to remove the effect of the atmosphere from Sentinel-2 data. Sen2Cor is designed for mono-temporal processing of Sentinel-2 L1C data products providing Level-2A Bottom-of-Atmosphere (BOA) surface reflectance product together with Aerosol Optical Thickness (AOT), Integrated Water Vapour (WV) and Scene Classification (SCL) maps.

Since June 2017, ESA uses Sen2Cor for systematic, operational Level-2A processing of Sentinel-2 acquisitions. Products are available on the Copernicus Open Access Hub. However, several evolutions of Sen2Cor and L2A-products since 2017 resulted in a quite inhomogeneous time series. Therefore, ESA started a reprocessing campaign of the complete Sentinel-2 data archive. The resulting Collection-1 of Sentinel data archive provides a real homogeneous time series based on the recent Sen2Cor processor version.

The presentation provides initial validation results for AOT, WV and (BOA) surface reflectance retrieval together with quality assessment of cloud screening. Accuracy and uncertainty of AOT and WV retrieval is assessed with reference measurements from AERONET stations. BOA reflectance retrieval can be estimated on a limited number of reference data only from RadCalNet-sites and in-situ campaigns. Reference data for cloud screening are generated by manual labelling of test images.

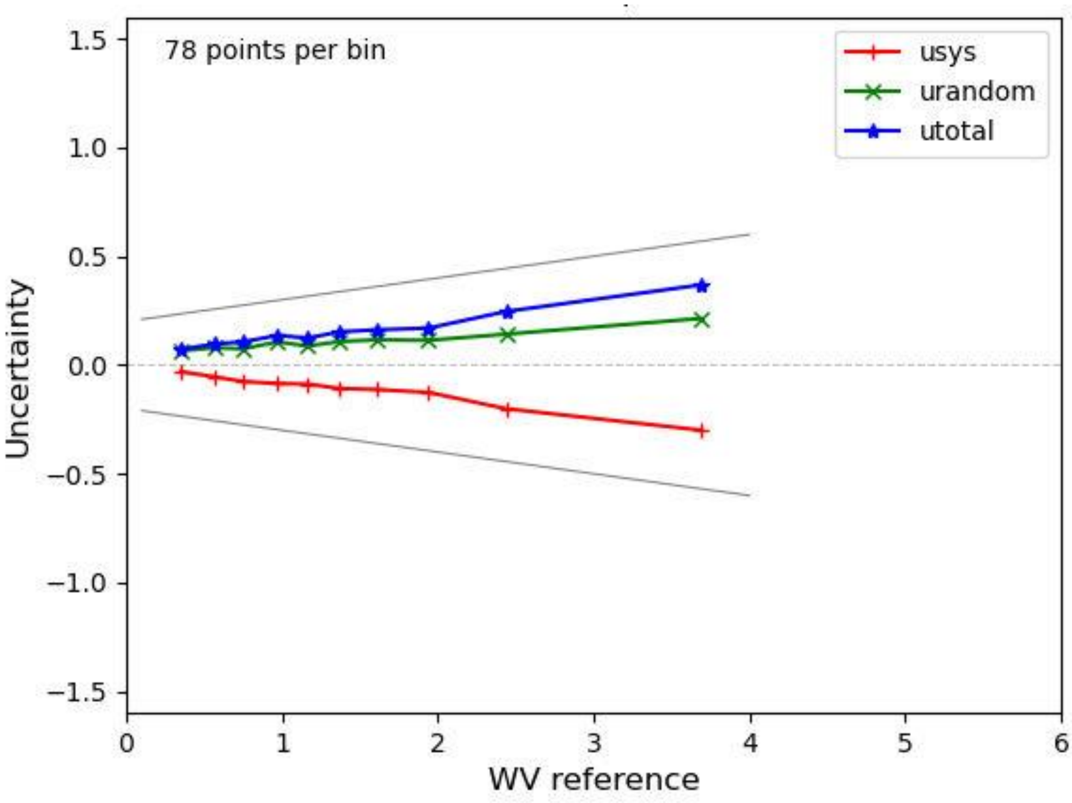

**Figure 1.** Example of uncertainty of WV retrieval with Sen2cor per WV bin

# Monitoring high-resolution LST in woody crops from the synergy of Sentinel-2 and Sentinel-3

EARSeL Bucharest 2023
Abstract

Corresponding Author:
Juanmanuel.sanchez@uclm.es

Juan M. Sánchez[1], Joan M. Galve[1], Alejandro M. Simón-Sánchez[1], José González-Piqueras[1], Ramón López-Urrea[2]

[1] University of Castilla-La Mancha, Remote Sensing and GIS group, IDR, Campus Universitario s/n, 02071 Albacete, Spain.
[2] Instituto Técnico Agronómico Provincial, Parque empresarial Campollano, 2ª Avda. Nº 61, 02007 Albacete, Spain.

**Keywords:** Disaggregation, land surface temperature, downscaling, Copernicus

## Abstract

Woody crops such as vineyards traditionally occupy large areas in arid and semi-arid agricultural regions, and other such as almond and pistachio orchards are proliferating very fast. The shortage of water resources and the low rainfall during the crop growing season under these conditions, makes it necessary to conduct efficient use of irrigation water in order to improve the sustainability of these crops. Land Surface Temperature (LST) is a valuable source of information for estimating water stress and actual evapotranspiration ($ET_a$) in crops. For this reason, temporal series of LST with fine spatial and temporal resolution are essential in agricultural applications, water resources management or irrigation scheduling. These requirements cannot be fully satisfied by the currently operational TIR satellite sensors since the revisit time is too poor or the spatial resolution is too coarse. Disaggregation techniques offer a solution to this lack of high-resolution satellite Thermal InfraRed (TIR) data and can bridge the gap until operational TIR missions accomplishing spatio-temporal requirements are available. In this work, we adopt a downscaling method that has already shown good results in previous research, and integrate the necessary adjustments to be applied to the tandem Sentinel-2 (S2)/Sentinel-3 (S3). Maps of Land Surface Temperature (LST) with 10-m spatial resolution are obtained as output from the synergy S2-S3 images.

An assessment experiment was conducted in an agricultural area located in the Barrax test site, Spain (39º 03' 35'' N, 2º 06' W), for the summers of 2018-2019. Ground measurements of LST transects collocated with overpasses of the Sea and Land Surface Temperature Radiometer (SLSTR) on board Sentinel-3 were used for a ground validation of the disaggregation approach. A dataset of more than 70 points from 15 different dates were available, covering a variety of croplands and surface conditions, and including 20 samples in vineyard and almond trees. Despite the large range of temperatures registered (295-330 K), an average RMSE of ±2.7K and a negligible systematic deviation were obtained for the full ground dataset. Focusing on the woody crops, good agreement was also observed between modelled and observed LST with a similar RMSE of ±2.7K, and a slight overestimation of 0.6 K.

A cross-validation of the LST products was also conducted using an additional set of Landsat-8/TIRS images. Using a land use classification map and focusing on almond orchards, both drip-irrigated and rainfed plots, an average estimation error of ±3.0 K was obtained, with no appreciable differences between both water regimens. These results are promising for rainfed, but also drip-irrigated, woody crops such as almonds or pistachio orchards, since S3-S2 disaggregated LST can help in increasing the

frequency of daily $ET_a$ estimates through surface energy balance modeling in these crops. However, some limitations associated with extreme LST, or irrigated fields using sprinklers, claim the necessity to explore the implementation of soil moisture or vegetation indices more sensitive to soil water content as inputs in the disaggregation approach for a better performance in highly vegetated fields, particularly in small plots.

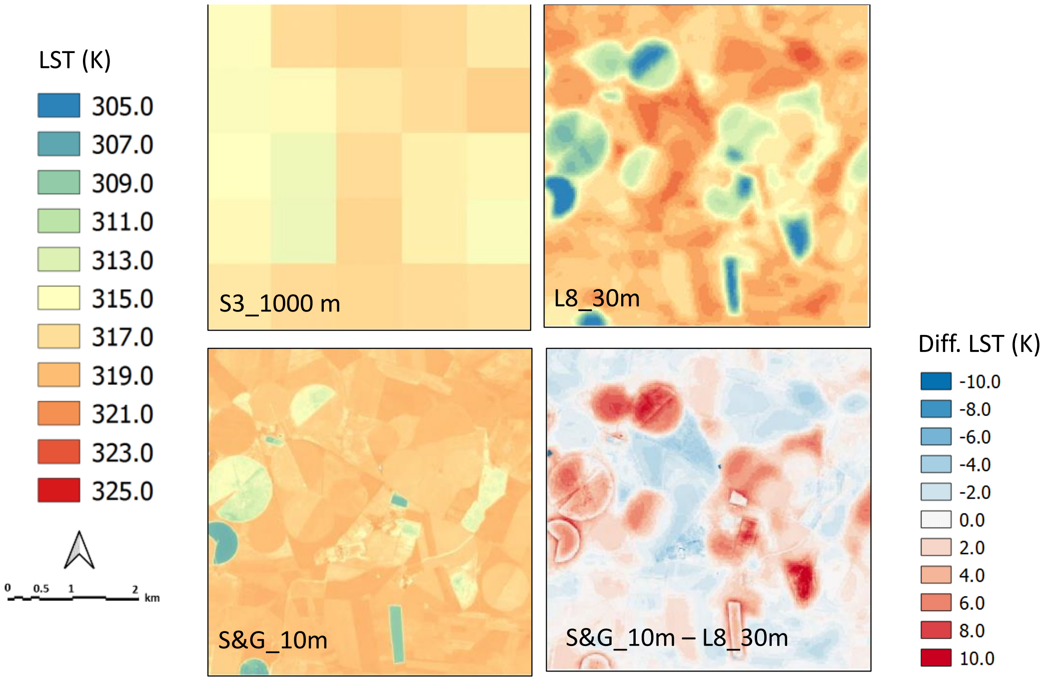

**Figure 21.** Disaggregated LST (S&G_10m), together with the original S3_1000m and L8_30m products. Differences between disaggregated LST and L8 LST product are also included. This example corresponds to a subset of 5x5 km$^2$ covering our study site, and date 07/17/2018.

# Assessment of fractional woody vegetation cover change in an African savannah region

EARSeL Bucharest 2023

Abstract

Corresponding Author:

e.symeonakis@mmu.ac.uk

Elias Symeonakis[1], Christina Karakizi[1], Arnau-Rosalen, E.[1], Antonis Korkofigkas[2]

[1] Manchester Metropolitan University, Department of Natural Sciences, United Kingdom
[2] National Technical University of Athens, Greece

**Keywords:** Woody vegetation, savannah, encroachment, land degradation, Landsat, multitemporal, time-series

## Abstract

There is growing concern over the sustainability of savannahs. Increases in the woody cover at the expense of grasslands have been reported globally. The cause and dynamics of this process remain unclear, with $CO_2$ enrichment, increased nitrogen deposition, altered fire regimes and grazing pressure all suggested as causative agents. Such alterations of savannah composition can have a major impact on rangeland productivity and biodiversity, the livelihoods of millions of African pastoralists, and often lead to severe poverty and famine of in rural communities. Monitoring woody savannah vegetation is, therefore, essential for identifying areas where land degradation mitigation measures are a priority.

For large sections of sub-Saharan Africa, there are considerable methodological challenges that limit the choice of methods for monitoring the fraction of woody vegetation. For example, southern Africa suffers from a scarce Landsat archive for the 1980s and 1990s, which poses a real obstacle for historic dense time series analysis. In such areas, vegetation trajectories derived from multi-date imagery with regular or even irregular observation intervals spanning two years or more have instead been used. Such multi-year intervals can indeed limit the level of temporal detail in which land cover trajectories can be captured; however, this is more of a hurdle for monitoring fast-growing biomes, such as the wet tropics, than drylands. Moreover, spectral variability metrics (e.g., min, max, percentiles) that capture the temporal variation of surface reflectance can be employed as they have the potential to distinguish spectrally similar land cover classes in heterogeneous landscapes, such as savannahs.

To date, mapping and monitoring the extent of large-scale woody encroachment over South Africa remains unresolved. The overarching aim of our study was to develop and test a methodological framework for the assessment of the spatiotemporal distribution of the fraction of woody vegetation in a South African savannah region: the Northwest Province (~105,000km$^2$). We employed Google Earth Engine to calculate dry-season (June-September) spectral variability metrics of Landsat imagery spanning more than three decades. We also used aerial imagery and a combination of shallow and deep learning models in order to map the fraction of savannah woody vegetation and assess the evolution of the fractional woody cover through time using a combination of a linear trend analysis and the BFAST break detection algorithm. The most recent estimates of fractional woody vegetation cover in the Northwest Province (2022) range from 0% to 87%, with the vast majority (80%) being less than 30%. The lowest woody cover values can be seen in the Molopo region in the west (Figure 1: areas “a” and “b”) and in the more intensively managed central and eastern agricultural regions, while the highest values are mostly found in the northeast of the Province (Figure 1, areas “c” and “d”). Our time series analysis results showed a widespread increasing trend in woody vegetation throughout the Province, with many areas demonstrating a doubling in their fractional cover over the last three decades. Our results can be used for identifying hot-spots where woody suppression measures should be prioritised and assist in the regional efforts for controlling this process which is causing significant hardship in the local pastoralist and farming communities.

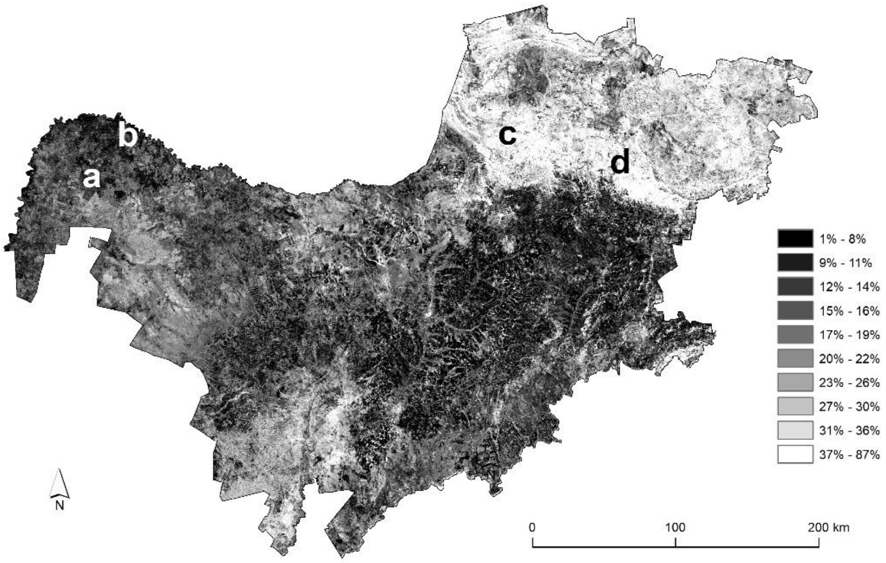

**Figure 22.** Fractional woody cover for Northwest Province, South Africa, for the dry season of 2022

## Section XIV - Using UAS for natural hazards and environmental studies

# Self-calibration still an underestimated tool

EARSeL Bucharest 2023
Abstract
Corresponding Author: Karsten Jacobsen
jacobsen@ipi.uni-hannover.de

Karsten Jacobsen

Leibniz University Hannover, Institute Of Photogrammetry And Geoinformation

**Keywords:** image orientation, pose, bundle block adjustment, calibration, additional parameters

## Abstract

Optical 3D measurement techniques have reached enormous market potential due to the wide spread use of unmanned aerial vehicles (UAV), 3D city mapping and the increasing use of classical photogrammetric applications. With the influence of machine learning, new terms for photogrammetry came such as pose determination for sensor orientation. The geometric characteristic of sensor orientation is now also known as aleatoric and epistemic uncertainty, where aleatoric corresponds to the random part treated by least squares adjustment, while the epistemic part (lack of knowledge) corresponds to the determination of systematic errors.

The required camera calibration today often is expressed by the Brown-Conrady parameters, introduced in 1971, which are almost identical to the Australis parameters. The development of self calibration is ignored by several newer bundle block adjustment programs such as Agisoft Metashape or Australis. The camera geometry is influenced by the flight conditions, especially changing temperature and the lack of flatness of the digital sensor. This requires self calibration in addition to camera calibration information that comes with the camera. Also, the set of additional parameters used must be able to express the difference of the perspective model (collinearity equation) and the real camera geometry. The Brown-parameters have some limitations, they use the following terms: k1, k2, k3 and k4 for the radial symmetric distortion corresponding to $r^3$, $r^5$, $r^7$ and $r^9$ with r being the radial distance from the principal point; p1, p2 as decentering distortion (tangential distortion); and b1 and b2 for affinity and angular affinity in addition to principal point location and the focal length. The Brown and Australis parameters do not respect the correlations between the unknowns. The radial symmetric k2 and k3 usually correlate higher than 0.998 and the correlation between k3 and k4 is listed as 1.000. Such high correlations are close to a linear dependency and this must be avoided. Unlike Metashape, Australis does not include the useless k4. In addition, the classical k1 up to k3 do not have a zero crossing, which has a direct influence on the focal length. In both sets, b1 and b2 affect only the x' image coordinates and not with equal effect 50% for the x'- and 50% with opposite sign the y'- coordinate. This causes a direct correlation to the projection centres X0 and Y0. Not all all systematic image errors can be determined with these additional parameters (Figure 1d). The not covered systematic image errors can be determined by superimposing all image points in an image and averaging over 15 x 15 sub-areas in this case. Reliable determination is possible with 401 000 image points. In this case, a standard UAV-camera was used. The UAV-cameras do not have the geometric quality of the mid- and large-format photogrammetric cameras, which explains the non-negligible remaining systematic image errors with a size of up to 5.4 pixels.

The given calibration, expressed by Australis-parameters, as usual also for large format cameras, which has to be corrected by self-calibration, leading to the corrections shown in Figure 1c). The given calibration is dominated by the radial symmetric component (Figure 1B). The radial symmetric distortion could also be reduced linear line from the centre to an adjusting line, which would also reduce the distortion from 84µm at the largest radial distance to around 30 µm with a correction of the focal length also to around 30µm. In general, a proper handling of the systematic image errors in this case improved the results of the block adjustment up to 10 pixels.

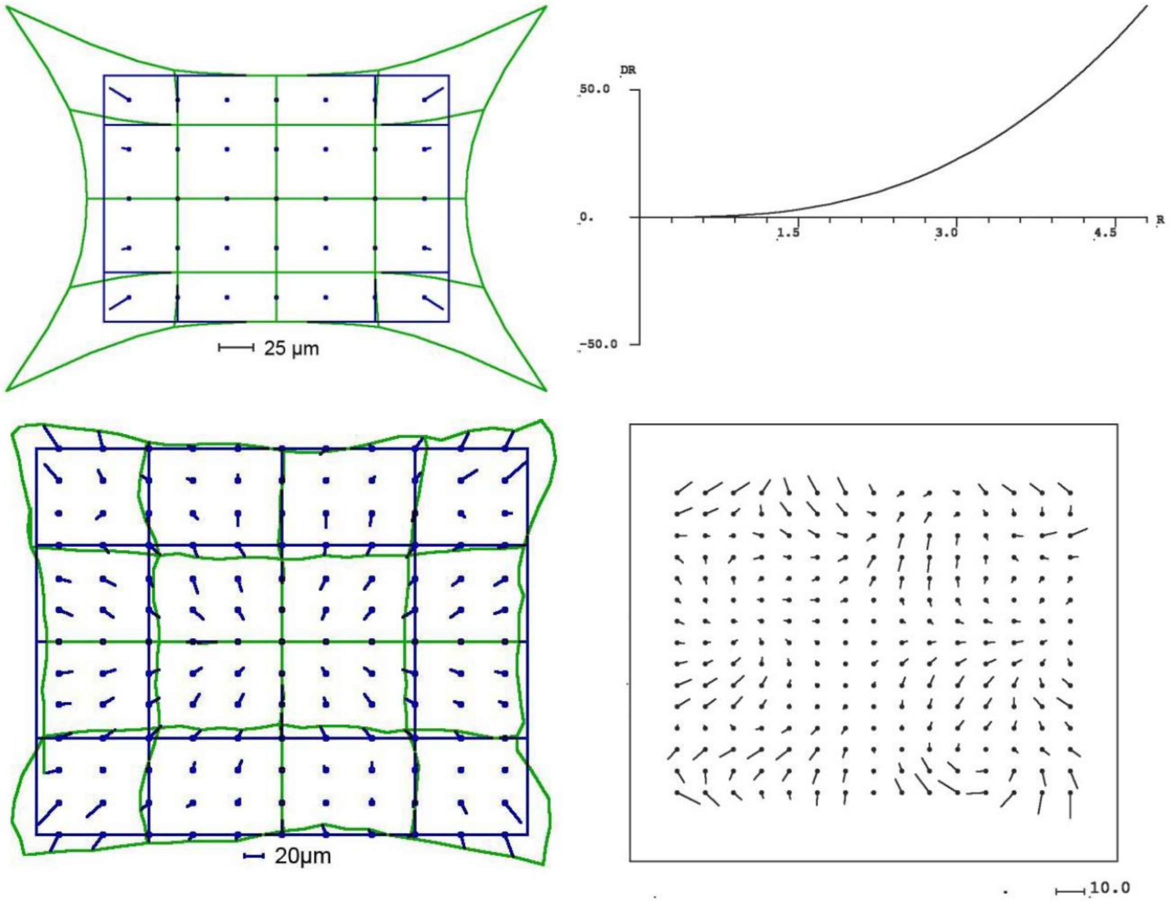

1a (upper left) = given distortion

1b (upper right) = given radial symmetric distortion

1c (lower left) = additional correction by self-calibration

1d (lower right) = remaining systematic image errors

# Geo-monitoring of tree species, vitality and maintenance condition of fruit trees in meadow orchards using UAV technology

EARSeL Bucharest 2023

Abstract

Corresponding Author:

siegmund@ph-heidelberg.de
communication@africanremotesensing.org

Sarah Pflüger[1], Mario Blersch[1], Maike Petersen[1], Alexander Siegmund[1,2]

[1] Department of Geography – Research Group for Earth Observation (rgeo), Heidelberg University of Education, Germany
[2] Heidelberg Center for the Environment (HCE) & Institute of Geography, Heidelberg University, Germany

**Keywords:** meadow orchards, unmanned aerial vehicles, biodiversity, cultural landscapes

## Abstract

Traditional orchards comprised of extensively cultivated fruit trees and meadows are hotspots of biodiversity in Central Europe, providing a habitat for more than 5,000 different plant and animal species. Meadow orchards contribute to soil and ground water conservation by forgoing the use of pesticides and are important areas for local recreation and tourism, therefore providing a wide range of ecosystem services. However, in the second half of the 20th century, many orchards were cleared due to policy changes and low economic profitability. Despite recent efforts of nature conservation initiatives, orchard areas are still declining, quantitatively as well as qualitatively concerning vitality and maintenance condition of stands. In order to preserve the remaining orchards, comprehensive data on the current number, spatial distribution and state of trees is needed for directed measures of pruning untended trees and replacing dying individuals.

The feasibility of assessing the current state of orchards using unmanned aerial vehicles (UAVs) was tested near Bad Schönborn in southwestern Germany. Images were taken with a high-resolution RGB camera and additional red-edge and near-infrared channels were added from a WorldView-3 scene. Selected test areas comprising a total of approx. 40 ha were flown at a height of 30 m above ground three to four times during the vegetation period. Subsequently, the complete, ca. 500 ha large area was flown at a height of 80 m above ground. The resulting orthomosaics and digital elevation models had a spatial resolution in the sub-centimeter range and of several centimeters, respectively. A total of 4,995 fruit trees were detected by segmentation of the digital elevation model. Using the size of the trees, the normalized difference vegetation index (NDVI) and texture measures applied to each spectral band in combination with ground-truthing data, a model was created to determine the tree species, vitality and maintenance condition of the fruit trees based on the UAV images.

The majority of all classified trees was apple trees (68 %, figure 1.) followed by pear (16 %) and walnut (5 %). While almost all trees were classified to have a high vitality (99 %), only 28 % were considered well maintained. 53 % were found to have a low and 19 % an urgent need for maintenance measures. This reflects on the discrepancy between a vital plant and an agriculturally used plant where pruning is required to improve yields. The overall accuracies of the classifications rage between 56 % and 85 % which indicates a need to improve the workflow, by adjusting acquisition time of the UAV imagery.

The classifications results were implemented in an interactive web-based map (Web-GIS) to inform decision makers and the local public but also to foster an adoption program. Through this Web-GIS owners of fruit trees can find people who are interested in taking care of their trees in exchange for the yields.

This will help to maintain the meadow orchards in Bad Schönborn and can be used as a model for other regions which struggle to preserve and improve this cultural landscape.

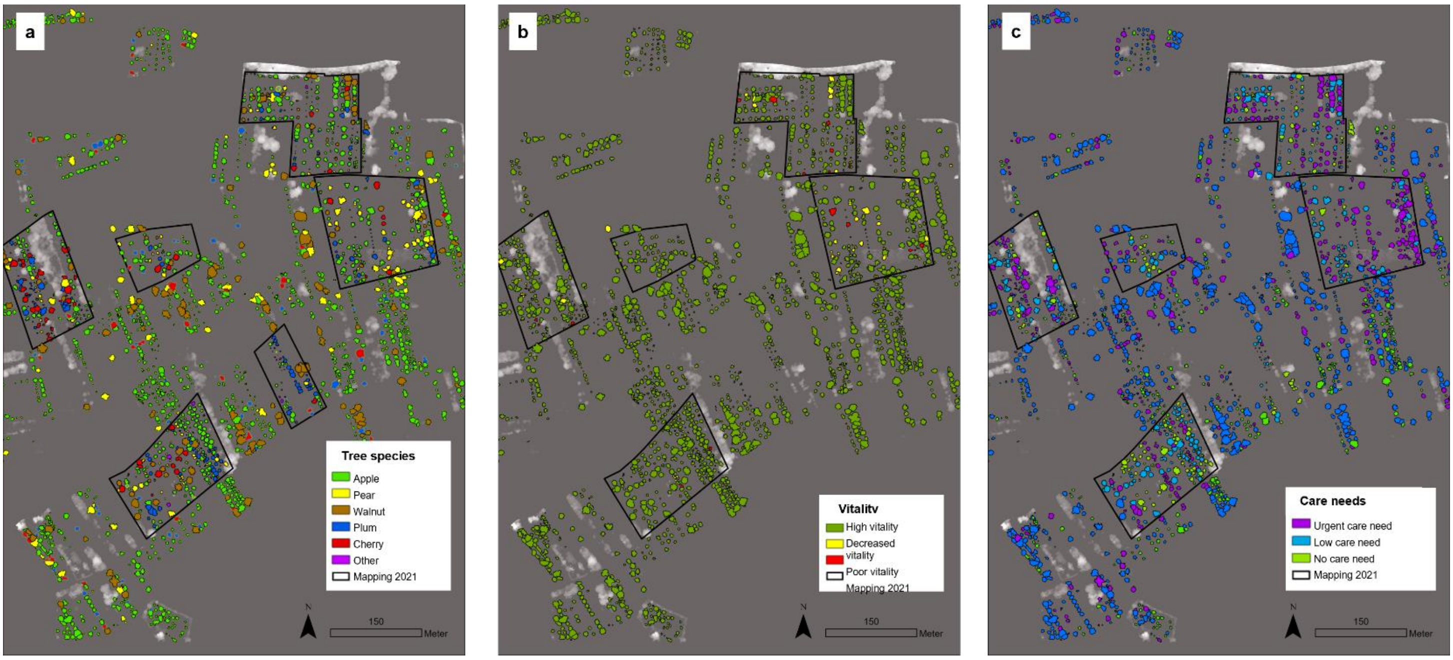

**Figure 23.** Classification results of tree species (a) the trees' vitality (b) and their care needs (c) and the location and extent of the areas mapped for training and validation

EARSeL Bucharest 2023

Abstract

Corresponding Author:

razvan_doru@yahoo.com

# The support of the UAV imagery in complementarity of the satellite high resolution remote sensing imagery for the Romanian shore monitoring

Razvan Mateescu[1], Liliana Rusu[2], Elena Vlasceanu[1], Dragos Niculescu[1]

[1] National Institute For Marine Research And Development “Grigore Antipa”, Department Of Physical Oceanography And Coastal Engineering, Romania
[2] Faculty Of Engineering, “Dunarea De Jos” University Of Department Of Mechanical Engineering, Romania

**Keywords:** UAV shoreline monitoring, satellite imagery, EO data analysis, coastal vulnerability, coastal management

## Abstract

High resolution remote sensing/Earth Observation (EO) provide a routine monitoring of coastal areas at the global scale, thus delivering a big amount of data. The aerial monitoring, refining the data in the definite vulnerable areas, it has now become one of the main instruments in support of the satellite remote sensing applicability, with the help of drones in specific monitoring activities for the shoreline in lagoon/low lands, but also in cliffs areas.

The work presents the technologies used to develop a rapid platform that can use high resolution UAV data, including data extraction and fusion, by comparing imagery products against high precision (D)GPS measurements collected in the field. In the present study, special software was used to process satellite images, such as ERDAS, and respectively digital mapping program, ArcGIS / ArcMap for vector data / GPS. The applicability of UAV monitoring in the field data collection methods depends on their effectiveness in different situations, in the context of climate change, related to the influence of the normal or exceptional coastal and/or deltaic hydrological regime over the Romanian coastal system. The results show different types analysis of the field data that are complementarity with remote sensing data which are provided by several EO services, including IKONOS, Deimos and Pleiades satellites.

The obtained results support coastal management implementations issues related to specific setbacks delineation in areas of the natural cliffs and arranged beaches, in the Romanian southern shore unit, but also rapid assessment of shore vulnerability in the northern part of the Romanian coast, respectively the marine lagoons associated with the Danube Delta.

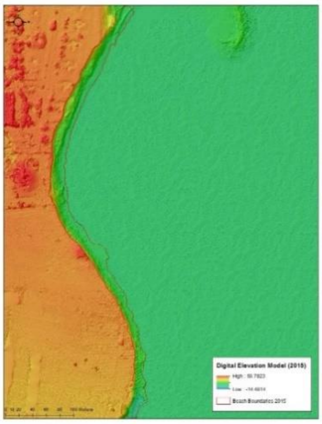

**Figure 24.** Shore sector of 2Mai - cliff apex/foot position

# The relation between tree above-ground biomass and crown height model using a high-resolution camera on UAV: a case study in Sessile Oak stand.

EARSeL Bucharest 2023

Abstract

Corresponding Author:

email address
CUCUALEXANDRU27@GMAIL.COM

Cucu Alexandru-Bogdan[1], Radu Gheorghe Raul[1], Petrea Ștefan[1], Șerban Tibor[1]

[1] National Institute for Research and Development in Forestry "Marin Drăcea", Department of Biometrics and Forest Management, Romania.

**Keywords:** crown height model (CHM), aerial imagery, UAV, above-ground biomass (AGB).

## Abstract

The global climate system has been negatively affected by the increasing concentration of greenhouse gasses (GHGs) in the atmosphere. This is considered a significant risk to human beings and other life forms, as it disrupts the natural balance of ecosystems. To mitigate the adverse effects of climate change, forests are being recognized as a sustainable solution that can help reduce CO2 emissions and enhance carbon sinks. Trees absorb carbon dioxide from the atmosphere through photosynthesis and store it in their biomass. However, estimating the biomass of forest stands using traditional methods, which require intensive field inventory and data analysis, can be costly and time-intensive and may have limited applicability in less accessible stands.

Remote sensing techniques have emerged as an efficient and economical way to monitor above-ground biomass. These techniques typically focus on determining forest stand characteristics such as the number of trees per area, height, and the relationship between crown area and tree breast height diameter. At the same time, each factor is estimated with a degree of uncertainty. This study explores the relationship between tree groups' above-ground biomass (AGB) and pixel statistics of overstory crown cover and height. To conduct our study, we measured the diameter at breast height (dbh), height (h), and precise coordinates of 177 trees in mature stands near the Brasov region covering an area of 3.6 ha. The forest stand is described as a group of even-aged Sessile Oak mature trees, with specific variations in dbh, height distribution, and crown cover of 70%. High-resolution images were collected from the study site using a precision RTK UAV with a Red Green Blue (RGB) band camera. We applied the same flight parameters to obtain a ground sample distance (GSD) of 10 cm/px for Vulcan location. A crown height model (CHM) was produced using a digital surface model (DSM) obtained from the collected UAV images and a digital terrain model (DTM) obtained from ground point measurements. In each forest stand, groups of trees were mapped using automated and manual tools based on the CHM. We assessed AGB for 51 groups of trees using multiple linear models and statistics of pixel values based on the CHM.

The results of this study indicate a strong positive correlation between the above-ground biomass (AGB) of tree groups and various pixel statistics, including the number of pixels, mean pixel elevation, and maximum pixel elevation. A multilinear regression analysis was conducted on the tree groups, randomly divided into training and testing datasets to investigate this relationship further. The performance of the regression model was evaluated by computing the

root mean squared error (RMSE) and the coefficient of determination ($r^2$) between predicted and observed AGB values. The analysis showed an average RMSE error of 2.2 $m^3$ and a strong $r^2$ value of 0.91, indicating that the model performed well predicting AGB for the test data. Overall, these findings suggest that pixel statistics derived from high-resolution imagery can be effectively used to estimate the AGB of tree groups.

Our study provides new insights into the potential of remote sensing techniques to estimate above-ground biomass, which can help improve our understanding of forest carbon stocks and contribute to developing more effective forest management strategies.

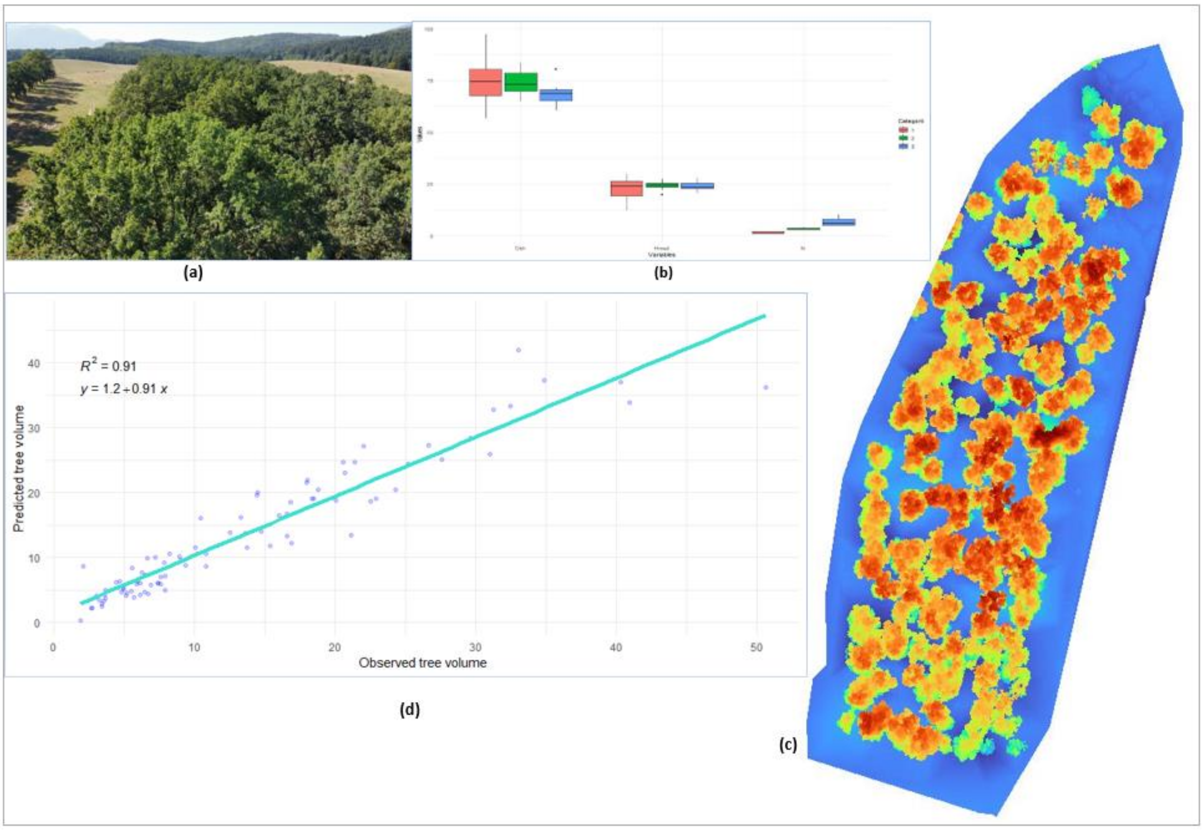

**Figure 25.** (a) overview of the sessile oak study plot (Vulcan area); (b) stand structure of dbh, h and number of trees in a tree group (divided into three frequency classes); (c) crown height model of the studied area obtained between digital surface model and digital terrain model; (d) scatterplot of the observed and predicted volume represented by a linear model equation, where number of pixels is the independent variable.

# Identification of the driving factors for the occurrence of forest fires and the zoning of forest fire hazard through Logistic Regression and Random Forest in Romania

EARSeL Bucharest 2023

Abstract

Corresponding Author:

adrian.lorent@icas.ro

Adrian Lorenţ[1,2], Marius Petrila[1], Bogdan Apostol[1], Florinel Capalb[1,2], Cristiana Marcu[1], Ovidiu Badea[1,2]

[1]National Institute for Research and Development in Forestry (INCDS), "Marin Drăcea", Romania
[2]"Transilvania" University of Braşov, Faculty of Silviculture and Forest Engineering, Brașov, Romania

**Keywords:** forest fires, fire hazard, forest fires driving factors, random forest, logistic regression

## Abstract

Forest fires have increased in occurrence and intensity in Romania since the year 2000 due to increasing periods of droughts, changes in land ownership and human practices like agricultural burnings. In order to determine the main factors that influence forest fires occurrence and map the hazard zones, we tested a parametric (Logistic Regression - LR) and a non-parametric method (Random Forest – RF). Ignition points for the 2006-2018 period were used as dependent variable to run and train the models. The points were used to generate a kernel density raster in the case of RF method while in the case of LR there were generated a number of 4220 presumably non-ignition points firstly by generating a 3 km buffer around the real ignition points and randomly placing 4220 points in the forested area where no forest fires had occurred. As independent variables were used 42 geo-spatial strata comprising topographic, anthropic and bio-climatic features. In case of the RF model the most important predictive variables were seasonal precipitation (coefficient of variation), NDVI - Normalized Differential Vegetation Index, distance from localities, maximum temperature of the warmest month and CLC 243 - proportion of agricultural land (from Corine Land Cover), altitude and precipitation in the driest month while LG model found as most important fire determinants topographical variables (altitude, slope, TRASP - topographical index for quantifying solar radiation), climatic variables (average temperature of the warmest quarter, precipitation of the driest month, precipitation of the coldest quarter, precipitation of the driest quarter), anthropogenic variables (livestock, population density, proportion of agricultural land, proportion of secondary pastures) or calculated according to the type of vegetation cover forest or scrubland (NDVI, proportion of shrub areas). The fire hazard maps were generated for a 5 scale classes (low, low-medium, medium, medium – high and high) and were validated against the fire incidents recorded by the Visible Infrared Imaging Radiometer Suite sensor. Both the LR and RF hazard map (Fig.1 ) showed that the most fire prone areas are in the South Western part of the country, in the Mehedinți and Gorj counties and mostly in the sub-Carpathian region, in hills and plains where the forest is fragmented and interspersed with agricultural lands or pastures and where practices of burning plant residues are frequent, the population density is high and the climate is dry. The large and compact forest massifs in the mountain areas are less prone to fires in normal conditions. The LR map gave however a higher risk hazard in the low lands in the South and East part of the country and the Danube corridor was placed in the maximum hazard class, which is rather debatable, given that this area is not generally affected by forest fires. We found that by using RF and LR methods may be obtained reliable forest fires hazards map which highlighted where forest fires are most likely to occur, while the LR method indicated a greater area with increased level of fire hazard than the RF method. In terms of the fire driving factors, we found less agreement between the two methods, different variables being chosen as relevant, but nevertheless it

revealed that the topographic, climatic and human related factors play a conjugate role in forest fire occurrence.

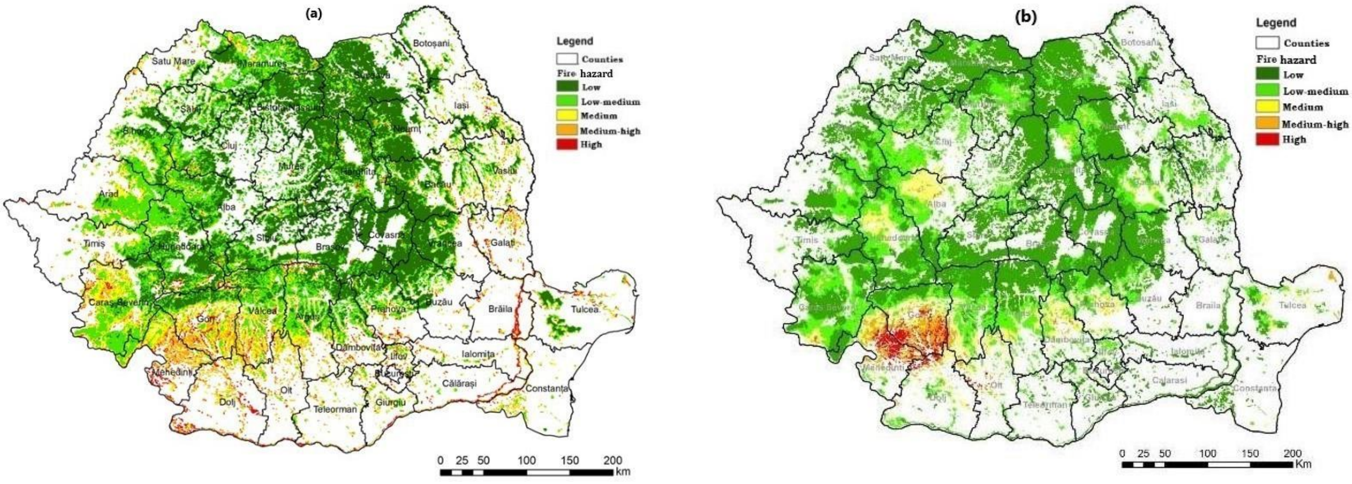

**Figure 26.** (a) forest fires hazard map obtained through the LR method, (b) forest fires hazard map obtained through the RF method

## POSTERS:

### Crop dynamics monitoring using earth observation

# Exploring Sentinel-2 dense image time series to identify cover crop emergence and destruction dates in France: Towards the development of an approach for biomass estimation

EARSeL Bucharest 2023

Abstract

Corresponding Author:

hugo.do-nascimentobendini@univ-tlse3.fr

Hugo do Nascimento Bendini[1], Rémy Fieuzal[1], Pierre Carrere[2], Aubin Allies[2], Aurélie Galvani[2], Éric Ceschia[1]

[1]CESBIO, Université de Toulouse, CNES/CNRS/INRAE/IRD/UT3, Toulouse, France
[2]EarthDaily Agro, Balma, France

**KEYWORDS:** LOW-CARBON AGRICULTURE, RED-EDGE, CLIMATE CHANGE, REMOTE SENSING, PHENOLOGY

## Abstract

Mitigating climate change is an unavoidable challenge for the coming years. Agriculture is an activity that presents a great opportunity to reduce the impacts of climate change, particularly through the implementation of agricultural practices that promote the sequestration of carbon in the soil. The implementation of crops such as oat, rye, phacelia, crimson clover, vetch seed, and/or niger between cash crops, aims to limit the disadvantages observed in periods of bare soil (e.g., risk of drainage and nitrate leaching) while offering a set of direct and indirect benefits (e.g., soil C storage, albedo effects, increase biodiversity, ...). In France, many farmers are implementing such practices, either voluntarily or in response to territorial regulations. In this context, the monitoring of cover crops requires the estimation of key vegetation descriptors in order to quantify their actual benefits. The project EASY4AG, developed as a partnership between EarthDaily Agro and CESBIO (Centre d'Etudes Spatiales de la Biosphère), aims to create a methodology for estimating the biomass of cover crops in France, using remotely sensed data and a ground-based observation network. More than 100 fields distributed over various agricultural regions in France are thus being monitored since the end of the crop summer season in 2022 (Fig. 1a). Data collected are sowing and destruction dates, percentage of each cover crop species, and measurements of biomass before destruction. To develop a robust and scalable methodology for estimating cover crops biomass over the whole country, it is first necessary to discriminate between the different main cropping practices. For doing so, it is important to derive the phenology of cover crops, and consequently properly determine the beginning and the end of the cover crops cycle, which is comprised between the emergence and destruction of the cover crops, as cover crops can be destroyed before the senescence. Dense optical satellite image time series have already been successfully used for identifying such phenological events in agriculture for main crops, and for classifying different cropping practices, but there´s still the need to develop a robust method focusing on cover crops. In this first assessment, we aim to investigate the possibility of using Sentinel-2 vegetation indices time series to determine the beginning and end of the cycle and to determine the optimal period for biomass estimation, which corresponds to the period of higher vegetative development. We selected 78 fields distributed representative of the different regions in France and analyzed the Normalized Difference Red Edge Index (NDREI). This index was derived from the Sentinel-2 images, obtained from Google Earth Engine (GEE), between June 2022 to the present, when the cover crops are starting to be destroyed. We used the QGIS Plugin GEE Time Series

Explorer to extract the time series, for the cloud and shadow masking. Pre-processing methods for interpolating and smoothing the time series were implemented, in order to correct for the residual noisy observations caused by cloud and shadow cover. Then, from the smoothed time series we tested two different simple approaches based on the detection of valleys and moving averages in the time series to estimate the emergence date (Fig. 1b). We compared the detected dates to the ground truth data as informed by the farmers to evaluate the results' accuracy. The average difference between the ground truth dates and the detected dates was of 16 days. Although the results are promising, some outliers were observed. Those outliers occurred mainly when there were overlaps within the crop calendar, with a full cycle of cash crops still observed while cover crops starts, and when frost events happened, leading to false valleys in the time series. Additional results will also be presented regarding the detection of the date of destruction, a practice that is currently underway in the monitored plots.

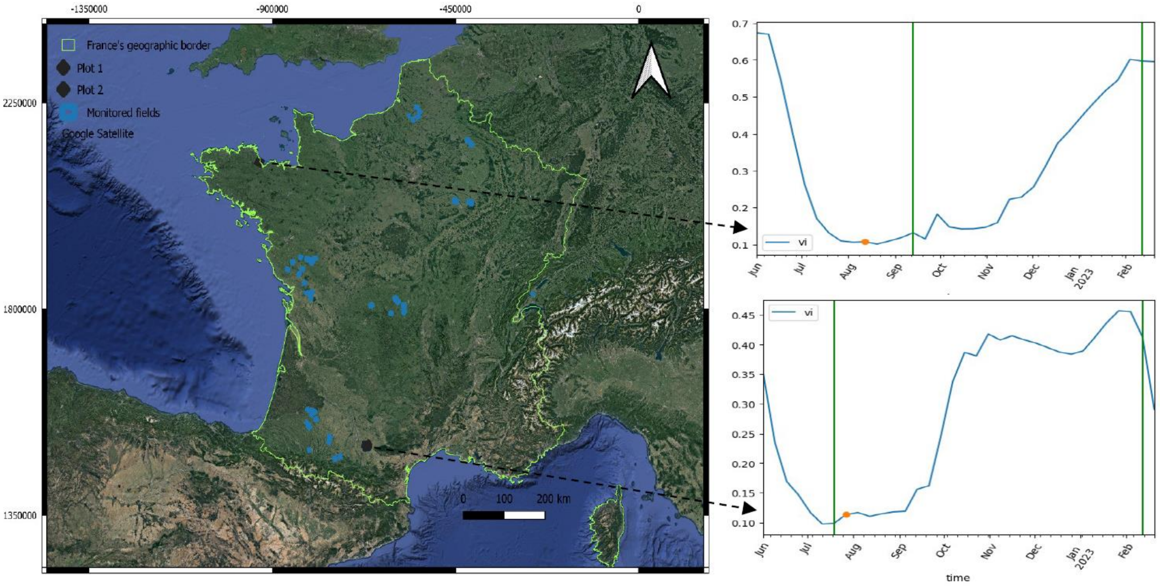

**Figure 1.** (a) Distribution of the monitored fields in France (Europe Albers Equal Area Conic Projection, ESRI: 102013) and (b) examples of NDREI time series with the detected emergence dates and the ground thruth dates of both sowing and destruction of the cover crops.

# Deriving Winter Wheat Phenology From Combined Optical And SAR Time Series With Deep Learning

EARSeL Bucharest 2023

Abstract

Corresponding Author:

felix.lobert@thuenen.de

Felix Lobert[1,2], Johannes Löw[3], Marcel Schwieder[1,2], Alexander Gocht[1], Michael Schlund[4], Patrick Hostert[2,5], Stefan Erasmi[1]

[1] Thünen Earth Observation, Thünen Institue of Farm Economics, Germany
[2]Earth Observation Lab, Geography Department, Humboldt-Universität zu Berlin, Germany
[3]Department of Geoecology, Institute of Geosciences and Geography, University of Halle-Wittenberg, Germany
[4]Faculty of Geo-Information Science and Earth Observation (ITC), University of Twente, the Netherlands
[5]Integrative Research Institute of Transformations of Human-Environment Systems (IRI THESys), Humboldt-Universität zu Berlin, Germany

**Keywords:** agriculture, crop monitoring, convolutional neural networks, U-Net, multisensor, data fusion

## Abstract

Understanding the effects of climate, climate change, and different management techniques on crop production requires information of crop phenology. There has never been a greater opportunity to provide such information thanks to the data base of optical and SAR satellite data that are available today. However, the current state of research largely lacks comprehensively validated methods that make use of these data base to provide highly detailed crop phenology information at the field level that directly relates to phenological phases that can be described from a biological perspective. Here, we suggest a method using dense satellite image time series acquired by Sentinel-1 (S1), Sentinel-2 (S2), and Landsat 8 (L8) to identify the beginning of winter wheat's main phenological stages from seeding to harvest. This approach extends the widely used concept of Land Surface Phenology (LSP) where general descriptors of the vegetation phenology such as the start and end of the growing season are targeted.

From the satellite data, we derived raw band measurements for S2 & L8 and $\gamma^0$ backscatter coefficient for S1. In addition, we calculated the Enhanced Vegetation Index (EVI) and backscatter cross-ratio (VH/VV) as input features. We further complemented the remote sensing imagery with daily precipitation measurements from a national precipitation radar network and mean temperature measurements from weather stations from the German Weather Service (DWD). From these input data, we formed several input feature sets and assessed their suitability to train a one-dimensional temporal U-Net, that we developed inspired by phenology-like problems in medical applications. We used an extensive reference data set consisting of 16,000 field observations from a national phenology monitoring network in Germany between 2017 and 2020 that we related to winter wheat fields derived from a German-wide crop type map to evaluate our method and assess the model performance.

Our findings demonstrate that optical and SAR data differ in their suitability for the detection of the different phenological stages due to the specific sensor characteristics. While SAR data performed better for detecting the earlier stages from seeding to heading, optical data is superior for later stages like milk ripeness and harvest. However, combining data from both sensor types has shown that our model is able to synergize their complementary information and improve the overall model performance. The input feature set based on optical and SAR data showed the best predictions with 50.1% to 65.5% of all

phenological stages derived with less than 6 days of absolute error. Especially late stages like harvest were well predicted with a coefficient of determination ($R^2$) between 0.51 and 0.62. Early stages like stem elongation still showed difficulties ($R^2$ between 0.06 and 0.28). Adding meteorological data to the input feature set did not improve the model performance, suggesting that small-scale phenological developments in winter wheat can only be partially explained by meteorological data of the used resolution.

In conclusion, our findings show the potential of dense EO satellite time series from the Sentinel and Landsat missions combined with the high versatility of deep learning models to leverage the synergies of optical and SAR data and derive phenological information.

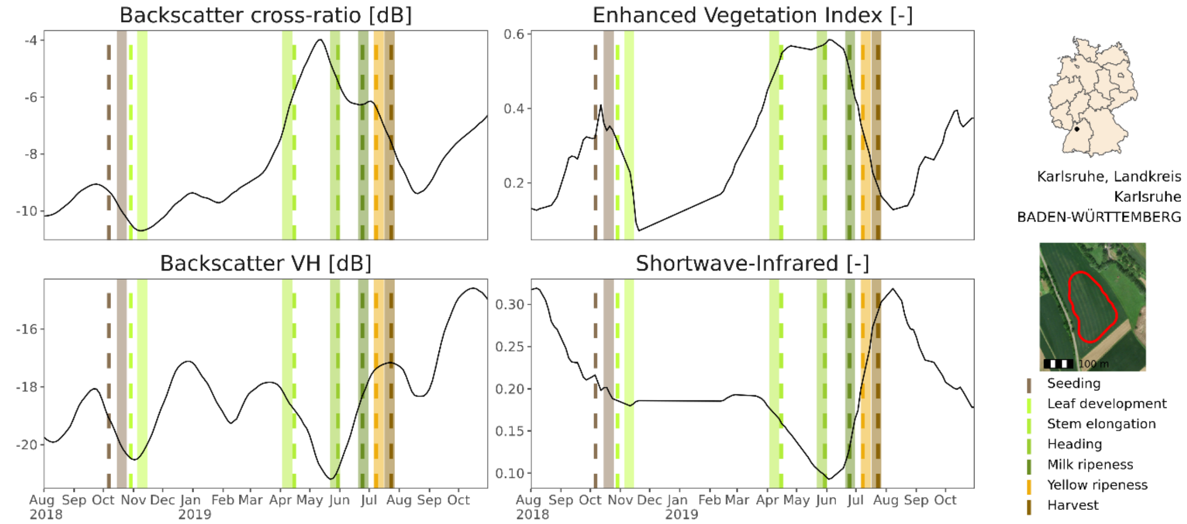

**Figure 27.** Predicted entry dates for the different phenological stages for a winter wheat field with a selection of optical and SAR-based input features. Dashed vertical lines show the prediction, segments in the background give the reference date including a buffer of 6 days.

# Derivation of crop parameters using Sentinel-1 SAR data: A case study for winter wheat in northern Germany

EARSeL Bucharest 2023

Abstract

Corresponding Author: Karlmarx Thangamani

email address: Karlmarx.thangamani@julius-kuehn.de

Karlmarx Thangamani[1], Tanja Riedel[2], Jennifer McLelland[2], Markus Möller[1], Heike Gerighausen[1]

[1] Julius Kuehn Institute (JKI) - Federal Research Centre for Cultivated Plants, Institute of Crop and Soil Science, Research Center for Remote Sensing in Agriculture, Braunschweig, Germany

[2] Julius Kuehn Institute (JKI) - Federal Research Centre for Cultivated Plants, Institute for Strategies and Technology Assessment, Research Center for Remote Sensing in Agriculture, Kleinmachnow, Germany

**Keywords:** Crop monitoring, Leaf Area Index (LAI), Biomass, Sentinel-1.

## Abstract

Early identification of potential problems such as nutrient deficiencies, pest infestation, heterogeneity and yield loss of the crop fields is essential for a crop field management. Crop monitoring is the systematic way of observation, measurement and analysis of the crop growth management and development, which is most important for the farmers to make future agricultural strategic decision. Biomass and green leaf area are important biophysical indicators for crop growth monitoring. Accurate, area wide and frequent estimation of these parameters may be helpful for decision making on improved fertilizer application and management of the diseases and weeds. However, conventional approaches such as ground surveys are time consuming and limited to field scale. On the other hand, optical remote sensing is often affected by cloud cover and available only during day time. These limitations are overcome by using Synthetic Aperture Radar (SAR), which can provide images independent from day light and weather conditions at large scales. Moreover, SAR data is already successful and common in monitoring crops due to its sensitivity to crop parameters. Open and freely available Sentinel-1 SAR data are used here. Two test sites at Demmin for 2021 and 2022 and at Braunschweig for 2022 in Germany were selected as study area. Figure 1a represents time series of Dual Pol Radar Vegetation Index (DpRVI) curves over the mean Elementary Sampling Units of the two fields in 2022 along with the mean LAI measurement values.

The data for the analysis involves the Ground Range Detected (GRD) and the Single Look Complex (SLC) products of Sentinel-1, from which backscatter coefficients $\gamma^0$ (VV polarisation and VH polarisation), backscatter coefficient ratio ($\gamma^0_{VH}/\gamma^0_{VV}$), Dual Pol Radar Vegetation Index (DpRVI) were calculated. Additionally, the soil water Index (SWI) from Copernicus Global Land Service is deployed in this study as soil moisture, tend to have great influence on LAI and biomass. SWI was obtained from the fusion of Surface Soil Moisture (SSM) observations from Sentinel-1 C-band and Metop ASCAT satellite sensors. The temporal profile of extracted SAR parameters were compared with crop parameters at various growth stages for analysing the phenology of winter wheat crop. For deriving the target crop parameters, machine learning techniques such as Partial Least Square regression (PLSR), Support Vector Regression (SVR) and Random Forest (RF) were applied. Therefore, we split the in-situ data by 5-fold of 20 times with the different randomization in each repetition based on repeated K-fold cross validation method. As a result, 80% of data points were used for training the model and 20% for validating the model. Here, we used indicators such as Root Mean Square Error (RMSE) and coefficient of determination ($R^2$) for evaluating the model performance.

Among all extracted parameters, $\gamma_{VV}^0$ was found to have significant influence on LAI and biomass in all models. Soil moisture ranks second in the variable importance with high importance in SVR and RF models. Considering the model outputs, the $R^2$ values of PLSR (0.466), SVR (0.666) and RF (0.757) and the RMSE values of PLSR (1.255), SVR (0.992) and RF (0.845), indicate that RF model outperforms other models for retrieving crop parameters of winter wheat crops. Figure 1b represents scatter plot of predicted LAI versus observed LAI by Random Forest model. Single fields reach more than 0.9 $R^2$ value with the backscatter coefficient $\gamma_{VV}^0$ for the most prominent model. The results of the predicted model as well as the accuracy of the other aforementioned regression models are presented.

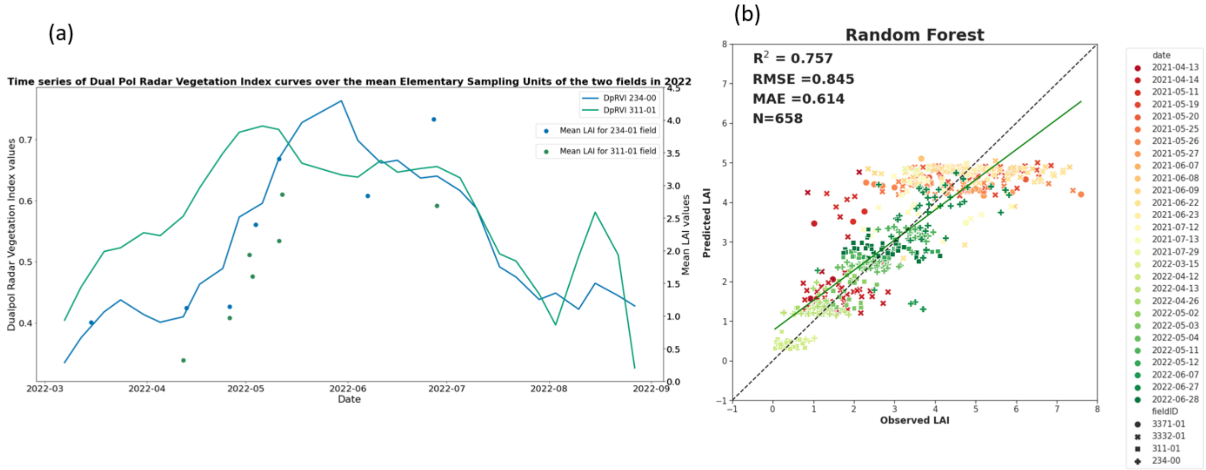

**Figure 28.** (a) Time series of Dual Pol Radar Vegetation Index curves over the mean Elementary Sampling Units of the two fields in 2022 (b) Scatter plot of predicted versus observed LAI by Random Forest model

# Monitoring irrigated areas by applying Convolutional Neural Networks to Sentinel-2 and meteorological time series

EARSeL Bucharest 2023

Abstract

Corresponding Author:
alejandro.simon@uclm.es

Alejandro-Martín Simón-Sánchez[1], José González-Piqueras[1], Luis de la Ossa[2], Juan Manuel Sánchez[1]

[1]Remote Sensing and GIS Group, Regional Development Institute, University of Castilla-La Mancha, Campus Universitario s/n, 02071 Albacete, Spain
[2]Computing Systems Department, University of Castilla-La Mancha, Campus Universitario s/n, 02071 Albacete, Spain

**Keywords:** deep learning, remote sensing, land use classification, sentinel, time series

## Abstract

Water usage is an essential aspect of our daily lives, and it encompasses direct use in households, recreation or industry, although agriculture is the major consumer of this precious resource. Water management becomes critical in arid and semiarid areas, where the driven increase in crop yields, and then food production, competes with the necessity for a sustainable use of both surface and groundwater resources. The sustainable management of water resources is a crucial challenge faced by policymakers at all levels, from local to international, due to its enormous social, environmental, and economic impacts. This requires the development and implementation of innovative strategies that promote water conservation, its efficient use, and sustainable agricultural practices, such as the control and declaration of water abstractions that minimize the environmental impact of agricultural activities.

Land use classification plays a key role in these actions by providing information on land cover and the types of human activity involved in land use. Nevertheless, gathering information on the crops harvested and their management has a high cost when it requires fieldwork. Remote sensing observation becomes an attractive solution at this point. Earth observation satellites provide high-resolution imagery of land use patterns, crop growth, and water use that can help to identify areas of high water demand and areas under risk of water scarcity. Satellite imagery can be also used to monitor the implementation of sustainable agricultural practices and identify areas where interventions are needed to promote water conservation or a more efficient use. The real-time information provided by the combination of remote sensing data with other innovative technologies such as precision irrigation, soil moisture sensors, and water accounting systems, can help farmers and policymakers to manage water resources in a sustainable way.

Multispectral sequential data from satellites provide information about crop behaviour and growth patterns. Traditionally, experts on the field have calculated Normalized Difference Vegetation Index (NDVI) from it due to its reduced complexity on the interpretation and processing. Combining this information with meteorological inputs allows to derive models for a more detailed monitoring of the water use in agriculture.

In this study, we introduce a methodology to obtain land use classification (LUC) maps by applying Machine Learning to sequences of multispectral reflectance Sentinel-2 images, soil characteristics and time-series of meteorological data. Some existing models process data at a pixel level, generating LUC successfully with a reduced number of images. Part of the pixel information corresponds to multispectral temporal patterns within the multispectral reflectance series that, despite not being especially complex, might remain undetected by models such as random forests or multilayer perceptrons. Thus, we propose to arrange this pixel information as 2D yearly fingerprints to render such patterns explicit and make use of a convolutional neural network (CNN) to model and capture them. The preliminary results (sample in Figure 1) in the semiarid agricultural area of Albacete, south-eastern Spain, show that our proposal reaches a 97% global accuracy in discerning irrigated, non-irrigated and bare soil fields compared to our rules-based expert system that achieved an 88% global accuracy. We can conclude this is a promising operational tool to automate monitoring water use over large areas.

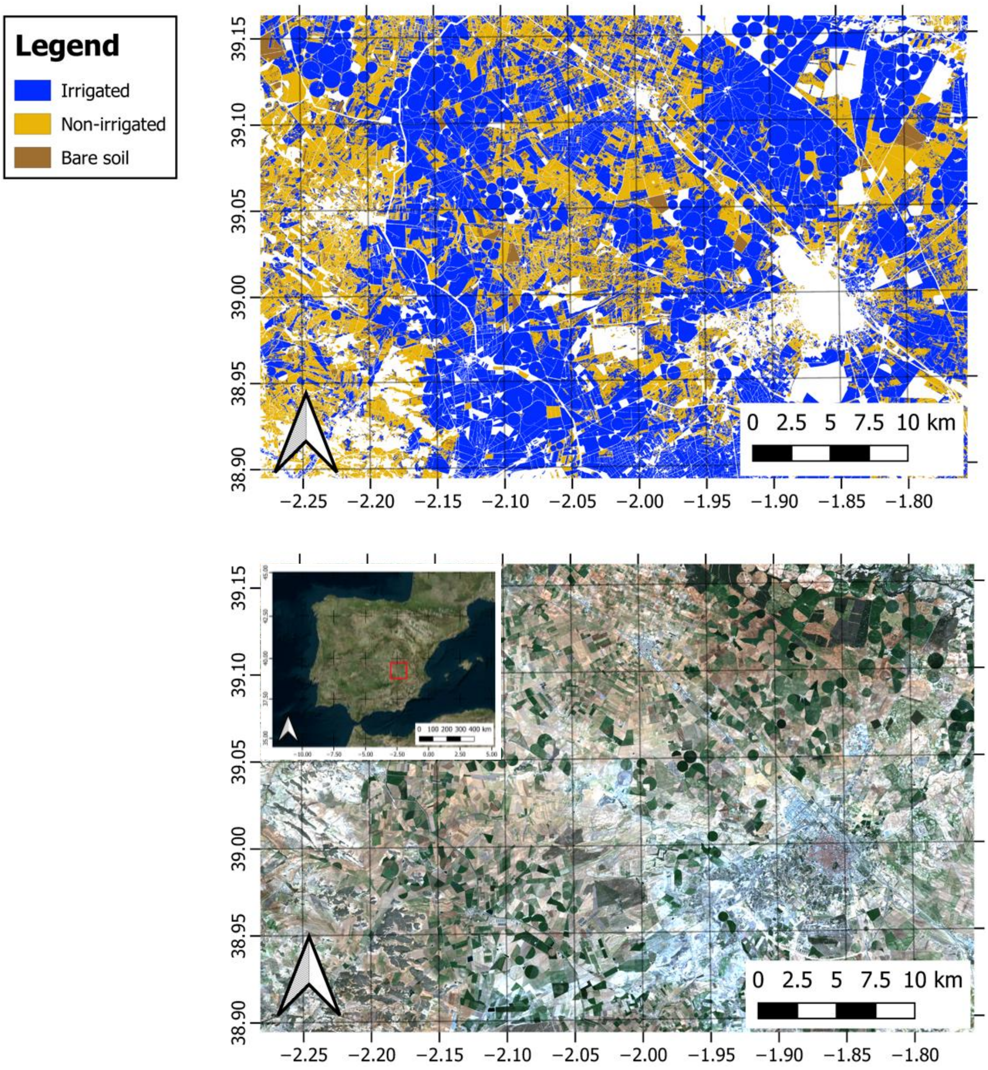

**Figure 29.** Map of land use classification per irrigation management for the year 2018 (top). RGB false colour composition from Sentinel-2 image corresponding to 27/03/2018 in Albacete-Spain (bottom). *Coordinates in EPSG:4326.

## Trends in Remote Sensing applications

# ESTIMATING PHENOLOGY METRICS FROM SENTINEL-2 TIME SERIES IN FOREST SITES

EARSeL Bucharest 2023
Abstract
Corresponding Author: Lorenzo Parigi
parigi.l@irea.cnr.it

Lorenzo Parigi[1], Mirco Boschetti[1], Francesco Nutini[1], Filippo Bussotti[2], Martina Pollastrini[2], Daniela Stroppiana[1]

[1] Institute for Electromagnetic Sensing of the Environment, National Research Council, Milan, 20133, Italy
[2] University of Florence, Dipartimento di Scienze e Tecnologie Agrarie, Alimentari, Ambientali e Forestali (DAGRI), Florence, Italy

**Keywords:** REMOTE SENSING, PHENOLOGY, MULTI-SPECTRAL DATA, GEE, NEC DIRECTIVE, FOREST HEALTH

## Abstract

Air pollution is a big treat to human health and ecosystems, it is crucial to monitor the levels of pollutant emissions and how they affect forest ecosystem. The Life MODERn NEC project has been created thanks to the directive "NEC" (National Emission Ceiling, 2016/2284) of the European Union. The objective of the project is to monitor the emissions of atmospheric pollutants and to assess the impact on water and terrestrial ecosystems. Monitoring of terrestrial ecosystems (namely forests) is carried out on 31 Italian permanent Level II plots (intensive monitoring) belonging to the ICP Forests (International Co-operative Programme on Assessment and Monitoring of Air Pollution Effects on Forests) and 6 of these sites are surveyed periodically by the Life MODERn NEC project.

Phenological metrics (PM) are very important parameters to determine the forest health status and to identify changes induced by pollutants and climatic fluctuations. But monitoring vegetation phenology with field surveys can be time and manpower consuming because the operator must visit the sites several times during the year to collect data. The use of remote sensing technologies could reduce the effort involved in field measurements and the synergy between remote and field data could increase the accuracy of the metrics. In this work, all the Italian Level II plots (31) were analysed with earth observation data. We exploited time series of Copernicus Sentinel-2 (S2) multi-spectral satellite images to estimate PM of the forest stands in the investigated sites.

The S2 constellations provide multi-spectral images with high spatial resolution (decametric) and short revisit time (up to 5 days with the two satellite constellation) which is very important to identify occurrence of the phenological stages like leaf green-up and senescence. We perform our analysis by generating time series of spectral indices (SI) from S2 imagery for the period 2016-2022. Since sites are distributed at national level, downloading and processing all S2 tiles, 28 tiles for the 7 years investigated period, to extract SI time series could be quite a resource-intensive process. To reduce processing time, SI were extracted from S2 images in Google Earth Engine (GEE) by selecting the coordinates of the central point of the forest area.

Methods to identify the PM (leaf green-up, maturity, senescence, and tree dormancy for deciduos species, corresponding to the absence of leaves in the canopies in the winter months) are based on a double sigmoid function that was fitted to the time series of the daily interpolated SI. From the sigmoid, the metrics were calculated identifying the inflection points using the derivatives of the curve. Processing has been done using the R package "sen2rts" (Ranghetti, 2012). This package takes as input S2 time series, it consider the noise that could be present in the time series, then fits a double logistic curve and extracts metrics. In the data preparation phase, the pixels under cloud or shadow condition have been removed based on quality layer of the S2 Level 2A product, and then the smoothing parameter must be regulated based on the considered SI and the annual oscillation.

The first SI we tested was the Normalized Difference Vegetation Index (NDVI) which is widely recognized as a suitable indicators of the vegetative annual cycle of plants. Thanks to the red and near infrared bands, it is possible to track the photosynthetic activity of trees, which can be translated into their vegetative activity. This is more evident for deciduous broadleaved species, that are characterized by a clear intra-annual seasonality of NDVI. Instead, the seasonal cycles of evergreen species might be more problematic to identify. These species retain their leaves for more than one year and their photosynthetic activity is continuous during the year, so different SI have been explored to identify their phenology.

The result of this work is a dataset of PM (expressed as Day of the Year) for the analysed forest sites, it has been validated with available database and/or photointerpretation. The estimated metrics and their change through the years, could be used to evaluate the difference in the annual cycle of the forest stands eventually attributable to pollutants or other environmental factors. The tested methodology and tools could be exploited to expand to the Italian Level I sites (extensive survey) of the ICP Forest programme. The Level I sites are more than 250, thus this remote sensing-based approach could allow an affordable and fast way to monitor a large number of sites through time.

The processing time and memory usage on local machines are limited thanks to the download of NDVI time series from GEE, however, the double logistic fitting steps is still quite demanding, for this reason we foresee the full implementation of the process chain in GEE, to make feasible processing of a large number of points/sites thanks to cloud computing resources.

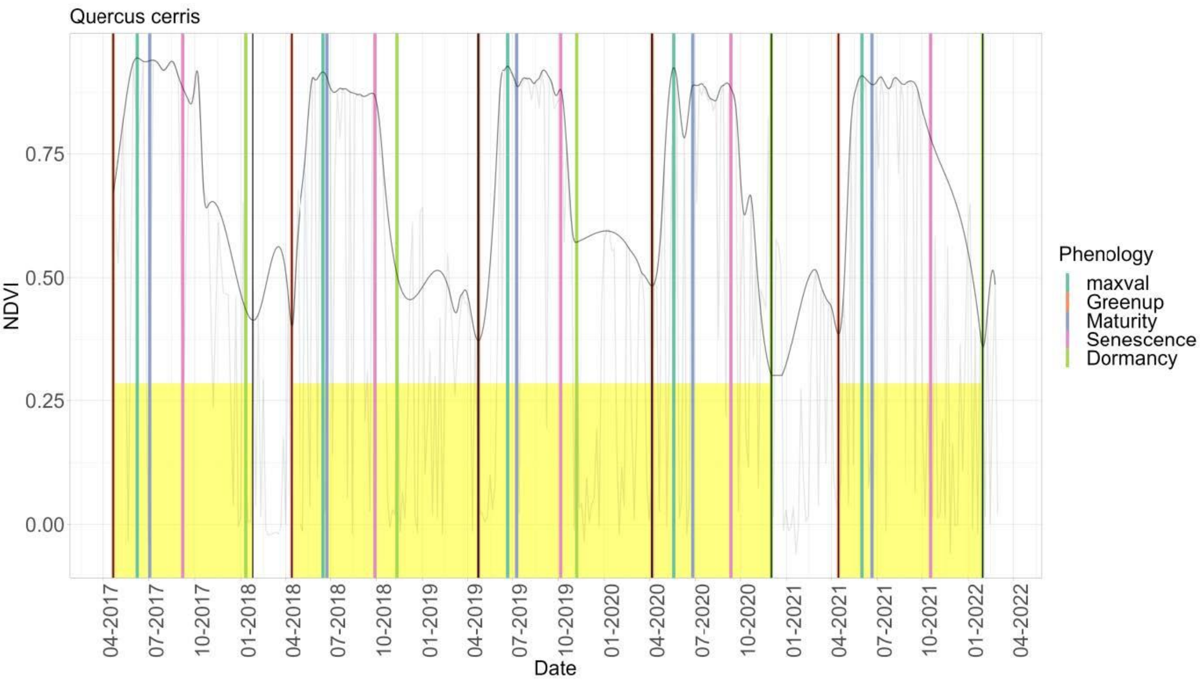

**Figure 1.** The output of the sen2rts tool for one of the sites analysed. Grey line shows the NDVI over time and coloured vertical lines the estimated dates for the phenological metrics. The black vertical line and the yellow band at the base identify the vegetative phases of the site.

EARSeL Bucharest 2023
Abstract

Corresponding Author:

martinchegee@gmail.com
Kuria.thiongo@dkut.ac.ke

# Development of a geospatial telemetric water quality monitoring

Martin W. Chege [1,2], Kuria B. Thiong'o [1,2], Arthur W. Sichangi [2], Stefanie Steinbach [3,4], Andreas Rienow [4]

[1] Remote Sensing Research Group (RSRG).
[2] Institute of Geomatics GIS & Remote sensing (IGGReS), Dedan Kimathi University of Technology (DeKUT), Kenya.

[3] Faculty of Geo-Information Science and Earth Observation (ITC). University of Twente, Netherlands.

[4] Interdisciplinary Geographic Information Science, Institute of Geography, Ruhr-University Bochum, Bochum, Germany.

**Keywords:** Geographic Information System (GIS), pH, Electrical Conductivity (EC), Turbidity, Temperature, and Long Range Radio (LoRa).

## Abstract

The sustainable utilization of natural resources ensures their perpetual existence. However, their continued uncontrolled use, coupled with population, economic and social pressures, places the very existence of these natural resources at risk. The lack of cost-effective, near-real-time monitoring tools and methods continues to hamper the management of these natural resources. The objective of this study, therefore, was to develop a low-cost and effective GIS- based telemetric water quality monitoring system for the Muringato basin in Nyeri county, Kenya. This would complement the already existing environmental monitoring efforts. The parameters considered were pH, Electrical Conductivity and Turbidity. A temperature sensor was included to be used as a secondary measure to check for any changes that would suggest the introduction of substances of varying temperatures to the water. A Long-Range telemetry Module was also included for real-time transmission of the data. A schematic was then designed and etched into a copper board to produce the printed circuit board (PCB). The identified electrical components were then soldered, tested, and calibrated. The system was then deployed along the river profile (figure 1, a) and set to collect data at five minutes intervals. From the results, the pH ranged between 2.85 and 11.35 while the electrical conductivity ranged between 0.10 and 0.47. The turbidity on the other hand ranged between 10 and 3000 NTUs. The temperature ranged between 18.10 and 21.50. The pH, EC, turbidity, and temperature sensors data was validated using laboratory-based techniques. The findings of the correlation study showed that pH and temperature had a high positive correlation of 0.81 and 0.92 respectively whereas EC and turbidity had a low positive correlation of 0.67 and 0.65 respectively (figure 1, b). Additionally, the results showed that the low-cost sensors were advantageous in terms of acquiring all the data sets at a single epoch and in real time. The performance of the low-cost sensors demonstrated that they were a reliable and cost-effective way of obtaining water quality data in real-time. Due to the high-power consumption by the sensors, power management proved to be a significant challenge. The incorporation of an

intelligent power management system into the prototype in order to cut back on any unnecessary downtime was recommended. In addition, on the basis of the various parameter ranges, regular monitoring of river's water quality was recommended, as it was of concern.

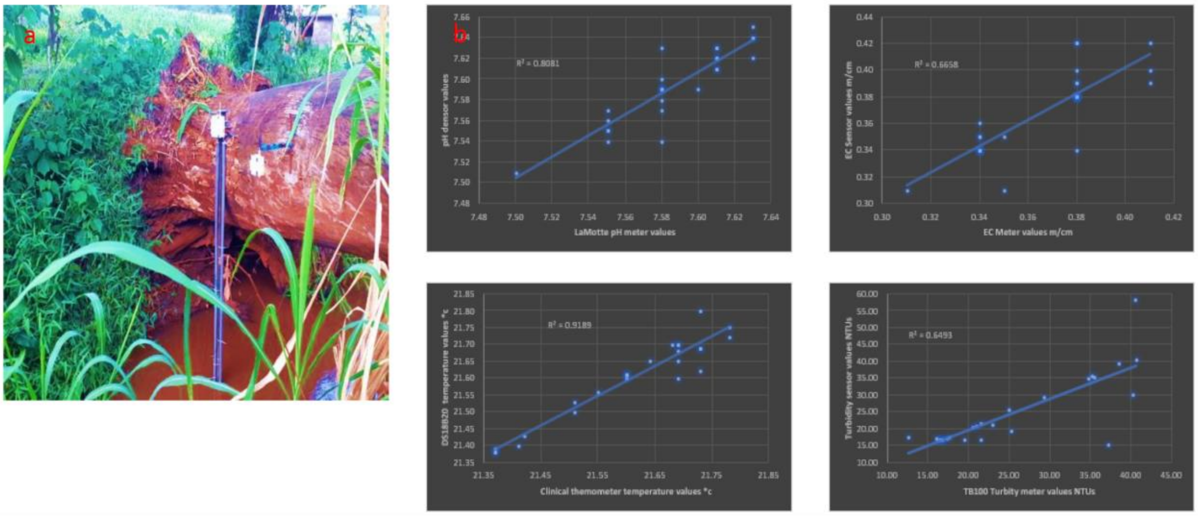

**Figure 1.** (a)The Deployed Prototype for telemetry acquisition of water quality datasets, and (b) The validation results of pH, EC, Temperature, and Turbidity.

## Integrated remote sensing methods for improving agricultural practices

# On-board Data Processing for real time inference using Edge-AI: An application on Weed Detection

EARSeL Bucharest 2023
Abstract
Corresponding Author:

Sarathchandrakumar Thottuchirayil Sasidharan[1], Daniele Latini[2], Mihai Ivanovici[3], Giovanni Schiavon[1], Kathiravan Thangavel[4], Fabio Del Frate[1]â

[1]University of Rome, "Tor Vergata",Rome, Italy

[2]GEO-k srl, Rome, Italy

[3]University of Brasov, Brașov, Romania

[4]RMIT UNIVERSITY,Melbourne, Australia

**Keywords:** Agriculture, AI4AGRI, Astrionics, Artificial Intelligence, Deep Learning, Drone, Edge AI, Neural Network, Remote sensing, Unmanned Aerial Vehicles, Weed management.

Weed control is critical in agriculture since weeds compete with croplands for nutrients, water, and light, resulting in lower crop yields and quality. Uncontrolled weeds can also harbour pests and diseases that can infect crops and cause further damage. Furthermore, some weeds are toxic to livestock and can endanger grazing animals. Effective weed management practices are required to maintain healthy and productive agricultural land. This includes a combination of cultural, mechanical, and chemical methods for weed control and prevention. The field of agriculture is a prime candidate for being revolutionized by computer vision. The use of cameras that are installed on unmanned aerial vehicles (UAVs) may provide a precise view of the fields, and object recognition that is powered by deep neural networks (DNNs) can assist us in better comprehending the condition of the field. However, in order to fully exploit the capabilities of computer vision, the processing must first take place directly on the UAVs themselves. This would make it possible for UAVs to provide information, which could then be utilized for location-specific actioning that takes place in real-time. For instance, a UAV may identify weeds, which could then be eradicated instantly by a robot operating on the ground. In agriculture, on-board data processing for real-time weed detection using Edge AI can improve weed control efficiency and accuracy. Edge AI is the use of AI algorithms on network edge devices to enable real-time data processing and decision-making without relying on a remote server. The use of Edge AI in weed detection entails taking images of crops and weeds, processing them on the device to detect the presence of weeds, and making a real-time decision on the appropriate action to take. Edge AI for weed detection can reduce reliance on manual labour, increase overall productivity, and reduce the use of harmful chemicals in weed control. In regard to the same, a workflow is outlined, and also some preliminary results are presented. The on-board processing is carried out with the help of state-of-the-art astrionics, i.e., hardware accelerators. This work is carried out as part of the AgriAdapt, which project focuses on mitigation strategies that preserve or enhance farm competitiveness, address other environmental issues, and improve farm resilience to climate change, and Ai4agri, which is a digital innovation hub that assists farmers and farm advisors in enhancing sustainable farming practises through the use of on-farm advanced technologies and farm management software.

# Fertilization of maize (*Zea mays*, L.) crops using remote sensors of an autonomous field robot

EARSeL Bucharest 2023

Abstract

Corresponding Author:

jan.kotlarz@ilot.lukasiewicz.gov.pl

Kubiak Katarzyna, Kotlarz Jan[1]

[1] Lukasiewicz Research Network – Institute of Aviation, Al. Krakowska 110/114, Warsaw, Poland

**Keywords:** precise agriculture, fertilization, vegetation indices

## Abstract

Nitrogen is an important macronutrient of biomass because it plays an important role in metabolic processes, protein production, amino acid synthesis, enzymes, hormones and is a component of chlorophyll. The assessment of its deficiencies in maize crops is the subject of scientific research. The article presents the results of measurements in controlled laboratory conditions of remote sensing indices of maize cultivated in fertilization variants of 0 - 150 kg N/ha.

In our experiment, we used controlled laboratory conditions, avoiding uncertainties resulting from uneven illumination of seedlings, varying conditions resulting from access to water, soil type variability, etc. In such conditions, the separation of indicators measured by the sensor by differentiating soil fertilization allowed to associate NDVI and NDRE with a specific fertilization variant. The Pearson's correlation coefficient between NDVI and NDRE was +0.984. The exception was the fertilization range of 125 - 150 kg N/ha. The NDVI index reached its maximum already for the fertilization level of 125 kg N/ha (NDVI = 0.685), while the NDRE index, after increasing to 0.493 - 0.496 for the fertilization level of 100 - 125 kg N/ha, increased again for the fertilization level of 150 kg N/ha up to +0.596. This result shows that for the correct estimation of the lack of fertilization in the range of up to 50 kg N/ha, measurements of both indicators are required. For deficiencies up to 25 kg N/ha, the decisive value is the NDRE indicator, for deficiencies 25-50 kg N/ha, the NDVI value is decisive, for deficiencies above 50 kg N/ha, the indications of both indicators reflect this deficiency. The obtained result allows for the development of a preliminary version of the matrix of precise fertilizer dosing by a field robot.

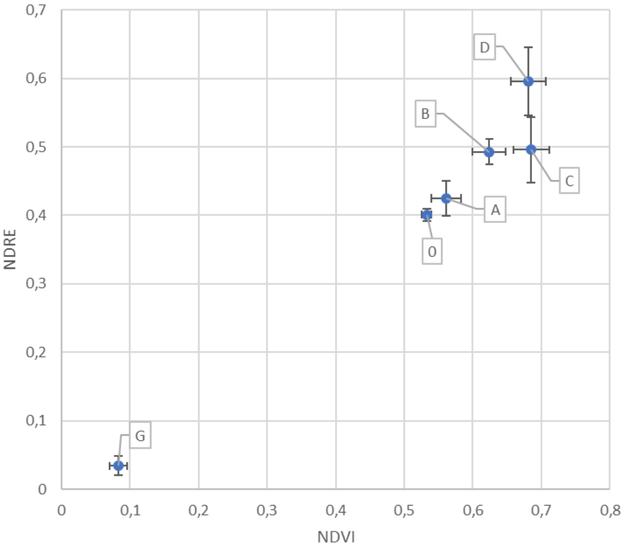

**Figure 1.** Average values of NDVI and NDRE indicators with standard deviations for individual classes of fertilization: G – soil, 0 – 0 kg/ha, A – 50 kg/ha, B – 100 kg/ha, C – 125 kg/ha, D – 150 kg/ha.

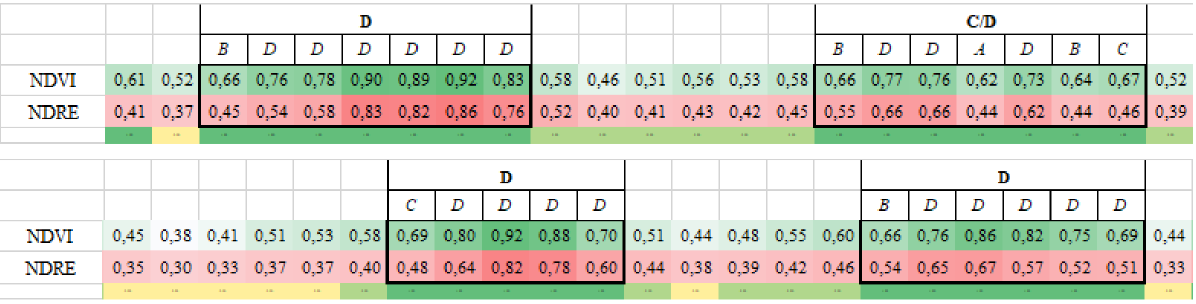

| | | | **D** | | | | | | | | | | | | | | **C/D** | | | | | | |
|---|---|---|---|---|---|---|---|---|---|---|---|---|---|---|---|---|---|---|---|---|---|---|---|
| | | | *B* | *D* | *D* | *D* | *D* | *D* | *D* | | | | | | | *B* | *D* | *D* | *A* | *D* | *B* | *C* | |
| NDVI | 0,61 | 0,52 | 0,66 | 0,76 | 0,78 | 0,90 | 0,89 | 0,92 | 0,83 | 0,58 | 0,46 | 0,51 | 0,56 | 0,53 | 0,58 | 0,66 | 0,77 | 0,76 | 0,62 | 0,73 | 0,64 | 0,67 | 0,52 |
| NDRE | 0,41 | 0,37 | 0,45 | 0,54 | 0,58 | 0,83 | 0,82 | 0,86 | 0,76 | 0,52 | 0,40 | 0,41 | 0,43 | 0,42 | 0,45 | 0,55 | 0,66 | 0,66 | 0,44 | 0,62 | 0,44 | 0,46 | 0,39 |
| | 🟩 | 🟨 | 🟩 | 🟩 | 🟩 | 🟩 | 🟩 | 🟩 | 🟩 | 🟩 | 🟩 | 🟩 | 🟩 | 🟩 | 🟩 | 🟩 | 🟩 | 🟩 | 🟩 | 🟩 | 🟩 | 🟩 | 🟩 |

| | | | | | | | **D** | | | | | | | | | | **D** | | | | | | |
|---|---|---|---|---|---|---|---|---|---|---|---|---|---|---|---|---|---|---|---|---|---|---|---|
| | | | | | | | *C* | *D* | *D* | *D* | *D* | | | | | | *B* | *D* | *D* | *D* | *D* | *D* | |
| NDVI | 0,45 | 0,38 | 0,41 | 0,51 | 0,53 | 0,58 | 0,69 | 0,80 | 0,92 | 0,88 | 0,70 | 0,51 | 0,44 | 0,48 | 0,55 | 0,60 | 0,66 | 0,76 | 0,86 | 0,82 | 0,75 | 0,69 | 0,44 |
| NDRE | 0,35 | 0,30 | 0,33 | 0,37 | 0,37 | 0,40 | 0,48 | 0,64 | 0,82 | 0,78 | 0,60 | 0,44 | 0,38 | 0,39 | 0,42 | 0,46 | 0,54 | 0,65 | 0,67 | 0,57 | 0,52 | 0,51 | 0,33 |
| | 🟨 | 🟨 | 🟨 | 🟨 | 🟨 | 🟩 | 🟩 | 🟩 | 🟩 | 🟩 | 🟩 | 🟩 | 🟨 | 🟩 | 🟩 | 🟩 | 🟩 | 🟩 | 🟩 | 🟩 | 🟩 | 🟩 | 🟨 |

**Figure 2.** Crop Circle sensor raw data for pots with fertilization of 150 kg N/ha. Fragments of data corresponding to individual maize seedlings are marked with black frames. The interpretation of the fertilization class for individual measurements was marked with a letter above the measurement, the interpretation of the fertilization class for the entire seedling was marked with a letter above the entire data fragment. The letters correspond to the group names in figure 1.

# Assessment of grassland forage quality in the context of northern Europe agriculture using Sentinel-2

EARSeL Bucharest 2023

Abstract

Corresponding Author:

julianne.oliveira@slu.se

Julianne Oliveira[1], Julien Morel[2], Junxiang Peng[1], Bengt-Ove Rustas[3], David Parsons[1]

[1]Swedish University of Agricultural Sciences, Department of Crop Production Ecology, Sweden
[2]European Commission, Joint Research Center, Ispra, Italy
[3]Swedish University of Agricultural Sciences, Department of Animal Nutrition and Management, Sweden

**Keywords:** grasslands, leys, optical satellite, nutritive value, multivariate regression models

## Abstract

Grasslands play important roles worldwide, providing many ecosystem services while being the main source of feed for livestock. In northern Europe, grasslands have great importance for dairy and meat production, predominantly as leys, a system where forages are typically harvested 3 to 4 times per year, in rotation with crops. The amount produced and the nutritive value of these forages are of crucial importance for farmers and, consequently, directly impact the economic strategies of the food industry. This means that appropriate ley management demands precise information on the quantity and quality of the forage. This is usually done by time-consuming and spatially non-comprehensive solutions such as field walks (for biomass estimation) or laboratory analysis (for nutritive value). Modelling solutions based on ecophysiological knowledge can also be used. In Sweden, the Vallprognos tool (vallprognos.se) uses a temperature-based approach to spatially estimate the start of growth and dynamics of nutritive traits of ley fields across Sweden. Forecast values are supported each year by field data collection on agricultural fields across the country, and samples are sent to laboratories for analysis. This method is usable for all harvests; however it is seldom used for later harvests, because the results for later harvests are not as generalizable. Since 2019, the coordinates of monitored fields started to be recorded, making it possible to link field measurements with remote sensing data. Indeed, satellite remote sensing is widely used to monitor vegetation in general and could be a complement to Vallprognos to assess the nutritive value of grasslands over large areas at low cost. We aim to estimate the forage quality of leys in Sweden using Sentinel-2 datasets and multivariate regression models using the dataset collected by the Vallprognos project. Ley samples were collected in 50 farm fields located across Sweden from 2019 to 2021(Figure 1). On five spots, blindly chosen on a diagonal across each field, forage samples were collected from an area of 0.25 m$^2$ by cutting to a stubble height of 8 cm, and field coordinates recorded. Representative samples were weighed and sent to laboratories where they were dried and the forage quality determined by NIRS. Bottom of atmosphere (BOA) reflectance Sentinel-2 images were selected to cover the growing season (approximately from April to October), and further filtered for clouds and shadows using the Google Earth Engine (GEE) platform. For each field, the averaged spectral signature was extracted according to the location of the samples from the cloud- and shadow-free image that was nearest in time to the field sampling date. We plan to use the reflectance of each Sentinel-2 band along with selected vegetation indices (VIs) as explanatory variables for multivariate regressions models, including machine learning algorithms. The models will be built to estimate nutritive value of the samples, including crude protein and fibre concentrations, and digestibility. Results will be discussed in the context of a transfer toward (i) an operational system as a complement to Vallprognos and (ii) to a larger geographical extent. We expect these results to provide useful information to monitor forage quality utilizing ready-to-use and open-source optical satellite images.

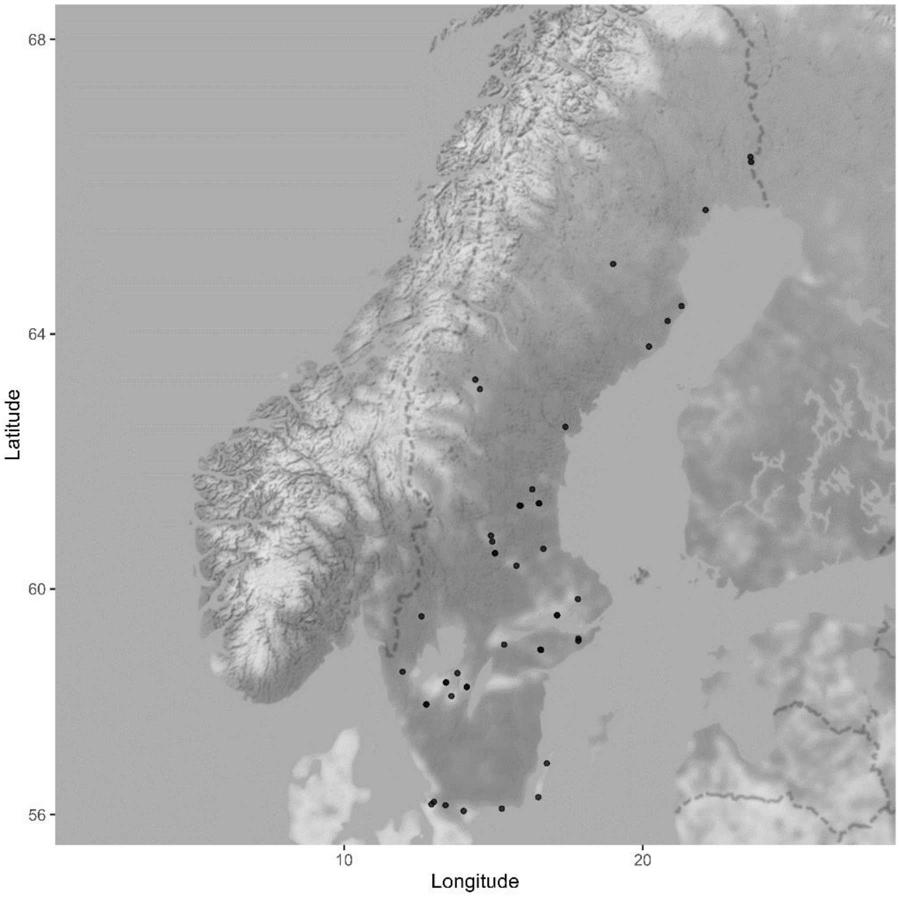

**Figure 30.** Locations of the collected ley samples

# Mowing detection based on Sentinel-1 & -2 data for supporting CAP in Wallonia

EARSeL Bucharest 2023
Abstract
Corresponding Author:
f.godechal@cra.wallonie.be

Godechal F[1], Beriaux E[1], Jago A[1], Cassiers A[1], Lucau-Danila C[1], Curnel Y[1], Planchon V[1]

[1]Walloon Agricultural Research Centre, Agricultural Productions Department, Belgium

**Keywords:** mowing, grassland, monitoring, Sentinel

## Abstract

Grasslands account for about one third of the EU's utilised agricultural area. They provide several services such as wildlife habitat, carbon sequestration, water storage and food production. Identifying mowing frequency contributes to defining grassland use intensity and its subsequent impacts on fodder production and the environment. Moreover, considering the current CAP objectives, the European Commission requires its member states to set up an operational monitoring of agricultural activities on their territory. One of these applications is the mowing detection on grasslands. Our research is embedded in this context and leverages Sentinel-1 (S1) and -2 (S2) data. Indeed, most of the time, both satellites offer sufficient space-time resolution compared to parcels size and mowing frequency.

Our objective is to develop an algorithm meeting the CAP monitoring constraints for the Walloon Paying Agency. More specifically, the mowing detection method should be efficient over several years without any recalibration for a new season. Moreover, it has to limit the number of incorrect mowing detections. The second objective is to evaluate the relevance of S1 data compared to S2 data in this context.

This study is located in Wallonia, the southern part of Belgium. There are almost 175,000 grasslands, covering 375,000 ha, with an average of 2 ha on a slightly undulating landscape. Mowing is a common agricultural practice encountered between April 1st and September 30th in the Walloon grasslands. It may be observed more than once a year on the same parcel.

Our datasets include NDVI (from S2) and 12-days coherence (from S1) time series computed at the parcel level from March 1st to October 30th 2021 and 2022. NDVI tends to sharply fall when a mowing event occurs, while coherence shows an increase a few days later. Another dataset is made of ground truth observations on more than 2,500 parcels. It includes grasslands where a mowing event has been observed (one event per year per parcel), as well as grasslands where no mowing happened during a long known period. The mowing events collection is used to evaluate the correct detection rate (an example is shown for a single parcel on Figure 1 (a)). The unmown grasslands are the reference to assess the false detection rate (Figure 1 (b) represents an example for a single parcel). Those 2,500 observations were collected during the 2021 and 2022 seasons. To assess the robustness of the model over years, it is calibrated and validated respectively on the 2021 and 2022 datasets.

The method based on S2 data uses several conditions on the NDVI time series to trigger a mowing detection on a given parcel at a given time. These conditions take the form of thresholds applied on the value of NDVI at the given time, the value of NDVI at the previous time, the slope between those values and finally, the NDVI of all permanent grasslands at that time. The S1 detection is based on two criteria only: the value of 12-days coherence for a parcel at a given time and its slope with the previous value of the same polarization.

The validation process for NDVI claims adequate results. Indeed, it presents a low number of incorrect detections (3 %) while allowing to correctly identify at least one mowing in around 60 % of all the mown grasslands during the season. Furthermore, the method seems robust from one year to another as it achieves roughly the same performance in 2021. On the other hand, the coherence-based method yields worse results already during calibration: a higher false detection rate (12 %) for only a few true detections (10 %). Also, the performances on the validation dataset are quite different, which makes the model unreliable across years.

In conclusion, using S2 NDVI data, it is possible to calibrate a mowing detection algorithm for one year and apply it to another year. The number of incorrect detections stays low while allowing for a useful number of correct detections. In contrast, the 12-days coherence gives many false detections and was not robust from one year to another, which is inadequate to the CAP operational context.

Further studies could be carried out on the sub-parcel management and on the impact of the grassland size. In connection with this, we wish to explore the potential of working at the pixel level to detect partial mowing and the potential of Planet Fusion to benefit from its better spatial resolution.

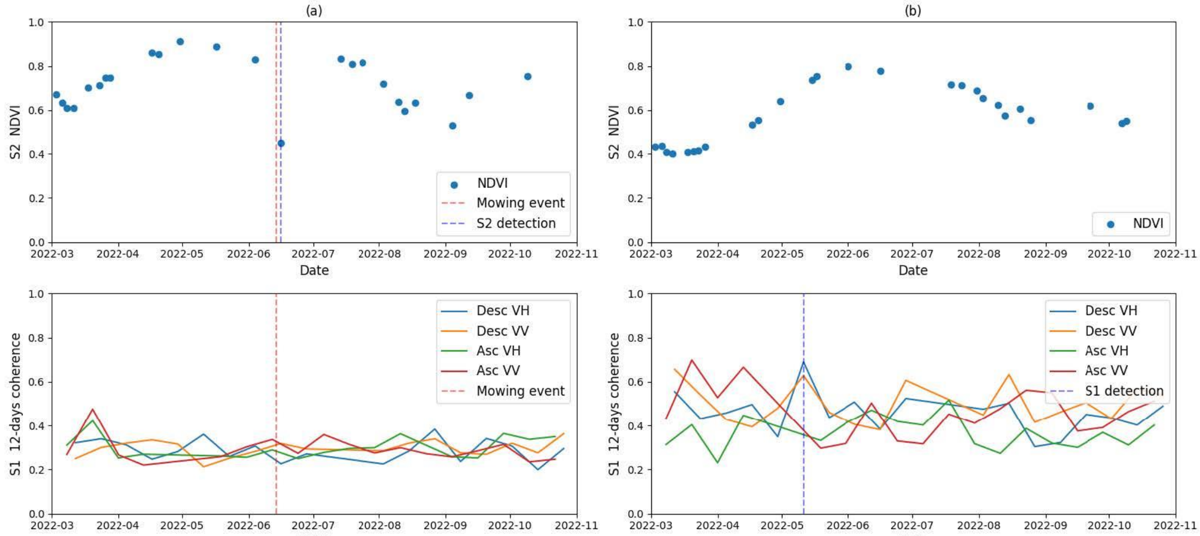

**Figure 1.** (a) A mowing event correctly identified by the NDVI method (up) but not by the coherence one (bottom). (b) Unmown grassland profile with a wrong detection from the coherence method.

# Mapping And Characterization of Hedges In Agricultural Landscapes For Ecological Assessments In Bavaria, Germany

EARSeL Bucharest 2023

Abstract

Corresponding Author:

Ursula.gessner@dlr.de

Jennifer Kriese[1], Sarah Asam[1], Mariel Dierscherl[1], Michael Stellmach[2], Kristel Kerler[2], Johanna Buchner[2], Ursula Gessner[1]

[1] German Aerospace Center (DLR), German Remote Sensing Data Center (DFD), Germany
[2] Bayerisches Landesamt für Umwelt, Germany

**Keywords:** hedgerows, ecology, small woody features, deep learning, aerial imagery, Convolutional Neural Network, Sentinel-2

## Abstract

Hedges play an important role in agricultural landscapes and support various ecosystem functions and services. They affect microclimate as well as fluxes of nutrients, carbon and water, they stabilize soils and can reduce erosion and flooding. Furthermore, they have a positive effect on biodiversity. Hedges are an important feature in the agricultural landscape for both flora and fauna, but are often missing in intensively used landscapes. They further constitute important habitats, e.g. for birds, insects, amphibians and reptiles. In addition, linear, near-natural hedge structures also fulfil biotope network functions by providing important links for animals to migrate, disperse and forage between habitats. Several European countries have explicitly included hedgerow protection into their Good Agricultural and Environmental Conditions (GAEC) standards programs that acknowledge the importance of hedges and promote their preservation. Additionally, hedgerows play an important role in the EU 2020 Biodiversity Strategy as well as in the Natura 2000 program, both of which aim to promote habitat connectivity across landscapes.

In Germany, the monitoring of biotopes is organized at the level of Federal Environmental Agencies. In our study region, the German Federal State of Bavaria, hedges are mapped on a regular basis in the context of the biotope mapping by the *Landesamt für Umwelt* (LfU). The current practise is to map hedges during in-situ campaigns. This time and resource consuming approach is repeated only every 20-30 years for an individual district (*Landkreis*). Here, remote sensing offers the possibility to support and accelerate in-situ mapping and thus to increase regular updates. The Copernicus Land Monitoring Product Small Woody Features (SWF) is a pan-European dataset at 5 m spatial resolution. However, a detailed comparison of the SWF layer with the in-situ data of the LfU's biotope mapping has shown general agreements but likewise revealed that it is not sufficient to fulfil the needs of biotope type mapping.

This contribution presents a detailed study on mapping and characterizing hedges in Bavaria, southern Germany. For this, aerial imagery, a large database of in-situ reference data and a Convolutional Neural Network (CNN), as well as Sentinel-2 time series analyses were used. In recent years, deep learning has become an important tool in earth observation with CNNs being the most popular architecture for remote sensing applications. Here, aerial RGB images with 20 cm spatial resolution were used. The 18,297 images for the whole of Bavaria, were taken between April and September in 2019, 2020 and 2021. In the first phase of the presented study, we focused on 5 districts (Freyung-Grafenau, Miltenberg, Dillingen a. d. Donau, Weilheim-Schongau, and Hassberge). We trained and evaluated a DeepLabV3 architecture on 340 aerial images and corresponding ground-truth masks derived from the biotope mapping in order to perform a semantic segmentation of hedgerows. For the division of the images into a training and a test

set, a geographically stratified split was made, since this allows a more realistic assessment with regard to a Bavaria-wide application of the model. The results for the focus districts showed a general good agreement with the visible hedgerow structures in the aerial imagery, however, with a tendency to classify also other woody features as hedges.

After the identification of the hedges, phenological information contained in Sentinel-2 time series was used for a further sub-differentiation of the landscape elements. For this purpose, NDVI time series were generated, smoothed using a Savitzky Golay filter, and phenological metrics such as start, end, length of season, and seasonal integral were extracted. Using these metrics, we conducted a clustering to identify different types of hedges.

The second stage of the project currently focuses on the expansion of mapping the whole state of Bavaria. Such a spatially comprehensive product will be a support for the Bavarian LfU. Even though it might not replace biologists conducting on-site investigations, it has great potential to facilitate the campaign planning, speed up the mapping process and enable regular reporting on statistical metrics such as hedgerow loss rates, biotope connectivity and landscape heterogeneity.

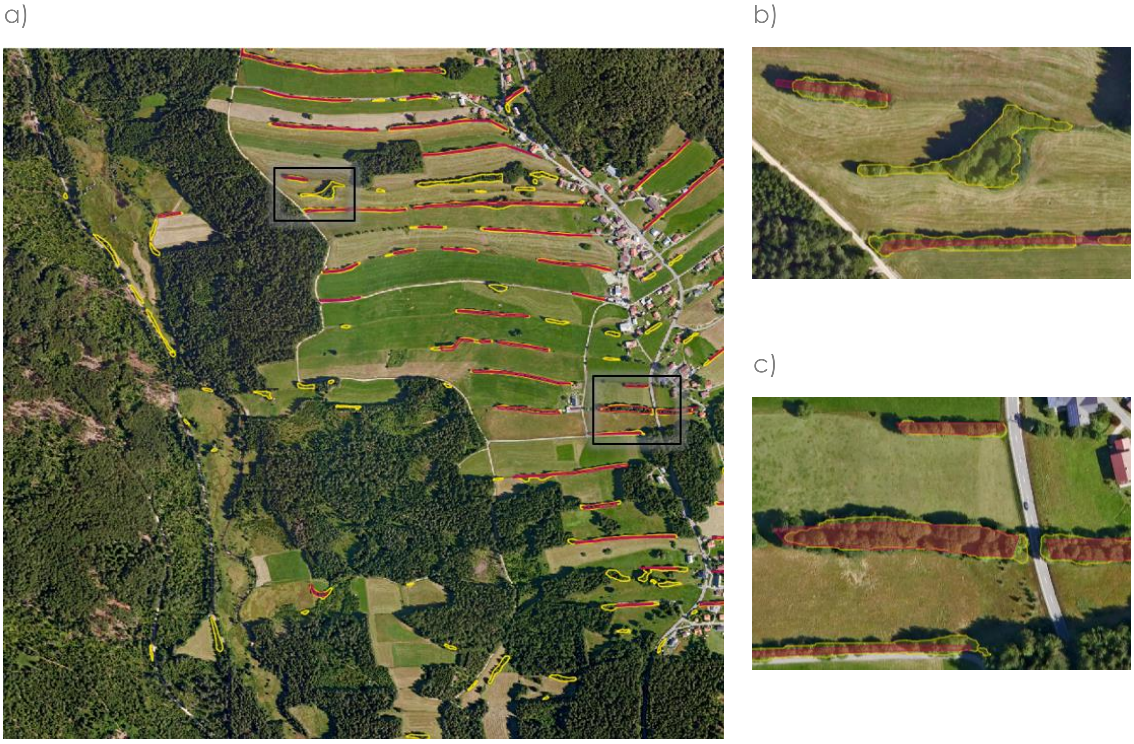

**Figure 31.** (a) Hedgerow mapping results in the Bavarian district Freyung-Grafenau with b) & c) zoom-ins for a more detailed view of the results. The location of the zoom-ins is marked by black boxes in a). In-situ reference data of LfU is shown as red polygons, remote sensing mapping results are shown in yellow.

## Remote sensing applications for natural hazards

# A semiautomated mapping of landslide volume displacements using UAV aerial imagery

EARSeL Bucharest 2023

Abstract

Corresponding Author:

radu.irimia@geo.unibuc.ro

Radu Irimia[1,2], Ionut Sandric[1,2], Viorel Ilinca[3,1], Zenaida Chitu[2,4,5], Ion Gheuca[3]

[1] University of Bucharest, Faculty of Geography, Nicolae Bălcescu, no. 1, Bucharest, Romania
[2] University of Bucharest, Institute for Research (ICUB)
[3] Geological Institute of Romania, Caransebeş Street, no. 1, Bucharest, Romania
[4] National Meteorological Administration, 013686 Bucharest, Romania
[5] National Institute of Hydrology and Water Management, 013686 Bucharest, Romania

**Keywords:** volume estimation, landslide mapping, UAV

## Abstract

The current study is focused on assessing the spatial and temporal patterns of landslide volume displacements using a semiautomated method and Unmanned Aerial Vehicle (UAV) aerial imagery. The case study is located in the Livadea village from Teleajen Subcarpathians, Curvature Subcarpathians, Romania, where a landslide was triggered on 3 May 2021. Teleajen Subcarpathians are a subunit of the Curvature Subcarpathians, a region characterised by a heterogeneous lithological constitution (clay - marl - sandy facies) and slopes with moderate declivity and rounded interfluves. These geological and geomorphological conditions favoured terrain modelling through slope processes, especially landslides and ravines.

The Livadea landslide is oriented predominantly from south to north (850 m long and about 90 m wide), and is primarily rotational, located on an old landslide covered by dense forest vegetation. It spreads over an area of 75ha, an area with dense vegetation cover, and has a detachment scarp that stretches for about 80 m in length and between 10 to 15 m in height. Most of the slopes are affected by old landslides partially stabilised by the presence of forest vegetation. According to the local community, the last known landslides are from the 60s. Even though the landslides were not recorded in the last 60 years, their presence is easily seen on the old topographical maps.

Mapping landslide volume gives a good insight into the landslide dynamics and magnitude and is one of the first steps in landslide hazard assessment. While landslide volume mapping is relatively straightforward when there is no vegetation, as in most cases of earthflows, in areas with a medium to dense vegetation cover, the landslide volume estimates are prone to high uncertainties. The task becomes more complicated when no LiDAR sensors are available. Thus, no accurate ground information can be retrieved from above when cameras from the visible spectrum are used. The main challenge arises from blocking the visible and near-infrared spectrum by vegetation. Knowing where vegetation is present and removing it is essential in mapping the landslide volume changes between sequentially UAV flights. In general, the volume of a pixel (voxel) is estimated by multiplying the area by its height. The current case study evaluated the volume of the earth moved between two stages of the landslide dynamics, as recorded by the UAV flights. The landslide volume displacement has been assessed by multiplying the difference in height between two DEMs (MDoD) with the area of one pixel. The changes in landslide surface and volume were assessed by

pairing two consecutive flights. Thus, three landslide volume changes were obtained. The maxim differences were evaluated by pairing the first and last flight.

Four separate flights were flown on 6 May, 23 May, 25 May, and 10 July using DJI Phantom 4, Mavic 2 Dual Enterprise and Phantom 4 RTK drones. Even though there is a difference in camera resolution, each flight plan was created to correspond to an approximately 4cm/pixel spatial resolution, meaning that the constant height above ground differed between the first two flights and the next ones. For the first flight, because the UAV equipped with the RTK receiver was not available, a graded consumer UAV fitted with a non-RTK receiver was used. A maximum overlap with the minor errors possible between all the flights was obtained by applying an orthorectification, using the Structure from Motion (SfM) technique, of the first, second and fourth flights with GCPs collected from the third flight. The results show volume displacement rates of 0.005 cubic meters/meter between the first and second flights and 0.05 cubic meters/meter for the period between the second and third flights. The overall displaced volume was approximately 406000 cubic meters, roughly 41000 cubic meters between the first and second flights and approximately 365000 cubic meters between the second and third flights. This approach proved quick and efficient for assessing landslide volume displacement when fast response and measures are necessary to reduce landslide consequences.

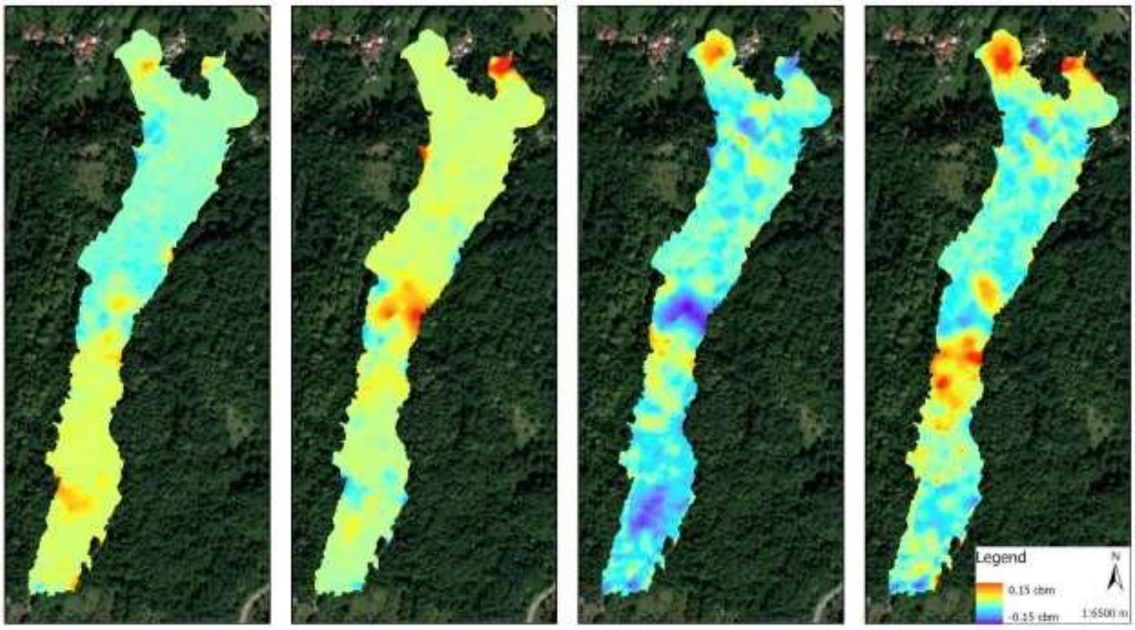

**Figure 1.** Landslide volume dynamics. From left to right: 6 May to 23 May; 25 May to 23 May; 10 July to 25 May; 10 July to 6 May

# EO-PERSIST: A cloud-based remote sensing data system for promoting research and socioeconomic studies in arctic environments

EARSeL Bucharest 2023
Abstract
George P. Petropoulos
gpetropoulos@hua.gr

George P. Petropoulos[1], Vassilia Karathanassi[2], Ionut Sandric[3], Dimitris Sykas[4], Marko Scholtze[5], Łukasz Kubowicz[6], Giuseppe Di Caprio[7], Juha Lemmetyinen[8], Massimiliano Chersich[9], Manfred Krischke[10], Spyridon E. Detsikas[1]

[1] Department of Geography, Harokopio University of Athens, El. Venizelou 70, Kallithea, 17671, Athens, Greece
[2] Remote Sensing Laboratory, School of Rural, Surveying and Geoinformatics Engineering, National Technical University of Athens, 9 Heroon Polytechniou St., Zographou, Athens, 157 80, Greece
[3] Faculty of Geography, University of Bucharest, Bd. N. Balcescu, 1, 010041 Bucharest, Romania
[4] CloudEO Hellas,
[5] Department of Physical Geography and Ecosystem Science, Lund University, Se-22362 Lund, Sweden
[6] Cloudferro Sp Z.O.O,
[7] PlanetGIS-SKY,
[8] Arctic Space Center, Finnish Meteorological Institute, P.O. Box 503, 00101 Helsinki, Finland
[9] YETITMOVES SRL, Via Ferrata 1, 27020, Pavia, Italy
[10] CloudEO AG,

**Keywords:** Cloud computing, Big data, Cryosphere, permafrost, remote sensing, social economics

## Abstract

In today's changing climate it is of key importance to understand the adverse impacts of climate change to the local and regional Arctic natural environments, infrastructures and industries. To this end, Earth Observation (EO) is the way forward, as it is extremely challenging to obtain long-term continuous ground observations. Recent advances in EO sensors, cloud-computing, geographical information systems (GIS) and in the field of socioeconomics provide unique opportunities to promote research and socioeconomic studies in the Arctic. Yet, despite their plethora, EO data are provided in a dispersed and unconnected way through several web platforms and in diverse formats, making their use difficult.

In this presentation we introduce EO-PERSIST, an EU-funded project under the MSCA Staff Exchanges scheme, providing a detailed overview of the research aims and objectives for its 4 years duration. EO- PERSIST proposes the development of a single cloud-based system that will allow in a unique way the availability of the collection, management and exploitation of the available EO data suitable to permafrost studies. The system leverages existing services, datasets and novel technologies to: a)create a continuously updated ecosystem with EO datasets suitable for permafrost studies, b)promote methodological advances in permafrost studies by exploiting the huge volume of EO datasets and c)provide indicators directly connected with socioeconomic effects to permafrost dynamics. Experimental analysis will also be carried with the system to showcase its use via five carefully selected and innovative Use Cases, that will serve as Key Performance Indicators of the system.

EO-PERSIST brings together a strong inter-sectoral experienced research team of 5 academic and 5 industrial partners, establishing a unique fertile collaborative research and innovation environment to promote pioneering research and socioeconomic studies implementation in the Arctic.

EO-PERSIST

A CLOUD-BASED REMOTE SENSING DATA SYSTEM FOR PROMOTING RESEARCH AND SOCIO-ECONOMIC STUDIES IN ARCTIC ENVIRONMENTS

# Integration of multi-sensor remote sensing data for monitoring illegal open pit mines

EARSeL Bucharest 2023
Abstract

Corresponding Author:
krystyna.michalowska@pg.edu.pl

Krystyna Michałowska[1], Ewa Głowienkar[3,2], Tomasz Pirowski [3,2]

[1] Gdańsk University of Technology, Department of Geodesy, Faculty of Civil and Environmental Engineering, Poland
[2] University of Agriculture in Krakow, Faculty of Environmental Engineering and Geodesy, Poland
[3] AGH University of Science and Technology, Faculty of Mining Surveying and Environmental Engineering

**Keywords:** Sentinel - 1, Sentinel -2, multi-temporal images, machine learning classification, spectral indices, remote sensing, illegal pit-mines

## Abstract

The research project, titled "Intelligent System for Detection and Monitoring of Mining Excavations Using Satellite and GIS Systems", aims to develop and test a prototype analytical platform that enables the implementation and integration of a wide range of spatial information sources. The target platform will process and analyze satellite radar, multispectral, and vector spatial data related to objects represented in both 2D and 3D space.

The research objective is to develop algorithms for processing and analyzing satellite data to determine spectral indices for identifying areas where mining activities are taking place. The biggest challenge in identifying mining areas using multispectral imagery is the problem of over-identification. Soils temporarily exposed as a result of agricultural activities and built-up areas are often misclassified as mining areas. To address this problem, we have proposed to use of reference spectral curves or machine learning classification methods. The research aimed to investigate different approaches to multispectral image classification to develop an optimal method for identifying and monitoring changes in open-cast mining areas that can be implemented in the system. Procedures and algorithms for processing and analyzing satellite data have been developed to determine indices that can be used to identify and locate areas where mining activities have occurred or are occurring. The indices have been calculated based on spectral characteristics that can clearly distinguish mined minerals from non-mined areas, such as agricultural land. Selected spectral characteristics of mining areas have been used to build spectral libraries, which will be used as training data for classification when extracting thematic information from satellite data.

The research focused on testing different approaches to select the simplest, fastest, most repeatable, stable, and reliable algorithm. The processing of the satellite images was divided into two phases. In the first phase, the images were subjected to quality control and atmospheric correction. The second phase aimed to produce the best possible image product to identify potential illegal mining sites. Each phase concluded with the preparation of a set of algorithms to be implemented in the target MineSens system.

The integrated multitemporal spatial database (including multispectral and radar images, UAV data, and reference data) enables the monitoring of large areas for selected periods. The developed solution, integrating a wide range of available spatial data (radar and multispectral satellite imagery, vector data), enables multi-criteria analysis for monitoring and identifying pits and open-pit mines. As a result of the research, the developed system solutions will enable the implementation of services for identifying illegally mined pits, managing mineral deposits, protecting against unauthorized use, and monitoring the intensity of open-pit mining activities.

The proposed solution is primarily dedicated to local and national administrations and business entities for conducting specialized analyses in a uniform analytical environment, integrating all necessary and up-to-date data.